THE PREDICTION OF CHF IN CROSS FLOW

by

RA-MIN TAIN

A thesis
presented to the University of Ottawa
on December, 1989
in partial fulfillment of the
requirements for the degree of
MASTER of APPLIED SCIENCE
in
MECHANICAL ENGINEERING

Ottawa-Carleton Institute for
Mechanical and Aeronautical Engineering

ISBN 0-315-60073-X

Abstract

A semi-empirical model to predict the Critical Heat Flux (CHF) in cross-flow boiling is presented in this work. This model, using an empirical correlation to calculate the vapor sheet thickness, is able to predict the CHF in subcooled or saturated region. The empirical correlation presented by Ungar and Eichhorn (1988) to calculate the vapor sheet thickness is modified by this work to include the quality effect. The RMS error for this semi-empirical correlation against the 271 experimental data obtained from various investigations is around 22%.

A correction factor resulting from the investigation of the relationship for CHF's between cross-flow and axial-flow boiling is obtained from this work. During this investigation, an empirical correlation to predict the cross-flow CHF is also discovered. The correction factor method and the empirical correlation have wider ranges of mass flux effect than the semi-empirical correlation does. The RMS error for the correction factor method and the empirical correlation against the 177 experimental data are 16.2% and 13.4%, respectively. Because these prediction methods are in dimensionless forms, they can be applied to water as well as the non-aqueous fluids.

ACKNOWLEDGEMENT

The author wish to express his thanks to his advisor, Professor S.C. Cheng, for his many valuable suggestions and advises during the course of this investigation. The author is also greatly indebted to Dr. D.C. Groeneveld, adjunct professor, for his assistance and technical advice.

Assistance and encouragement given by Mr. A. Vasic and Mr. C. Nguyen are sincerely appreciated. Financial support provided by Atomic Energy of Canada Limited and NSERC is also deeply appreciated.

Contents

List of Tables

List of Figures

Nomenclature

a	Empirical value as defined in Eq. (4.27)	
A_1^*	Coefficient used in Eq. (5.1)	
A_2^*	Coefficient used in Eq. (5.1)	
A_3^*	Coefficient used in Eq. (5.1)	
A_h	Area of heated surface,	m^2
A_j	Cross-sectional area of the vapor jets leaving the cylinder,	m^2
A_m	Mean flow area as defined in Eq. (5.4),	m^2
A_v	Cross-sectional area of the vapor stems,	m^2
A_∞	Cross-sectional area of control volume or flow channel,	m^2
b	Empirical value as defined in Eq. (4.28)	
Bo	Boiling number, or $Bo = q_{max}/(Gh_{fg})$.	
Bo_{axial}	Boiling number for axial flow	
Bo_{cross}	Boiling number for cross flow	
c	Empirical value as defined in Eq. (4.21) or Eq. (4.29)	
C_2	Empirical constant used in Eq. (3.31)	
D	Outside diameter for cross flow; inside diameter for axial flow,	m
D'	Length of control volume as shown in Fig. 5.3,	m
E_c	Eckert number	
f	Frequency of vapor departure or bubble break-off,	Hz
$\overline{f}$	Fraction of heat transferred directly to vapor	
Fr	Froude number, $U_\infty/(gD)^{1/2}$ or $U/(gD)^{1/2}$	
g	Acceleration due to gravity,	$m \cdot s^{-2}$
G	Mass flux,	$kg.m^{-2} \cdot s^{-1}$
G_c	Gravity influence parameter as defined in Eq. (3.27)	
G_D	Mass flow rate of deposition of entrained liquid droplets,	$kg \cdot s^{-1}$
G_E	Mass flow rate of the entrainment of liquid droplets,	$kg \cdot s^{-1}$
G_{LF}	Liquid film flow rate along the heated tube,	$kg \cdot s^{-1}$

h_f	Enthalpy of saturated liquid,	$J \cdot kg^{-1}$
h_g	Enthalpy of saturated vapor,	$J \cdot kg^{-1}$
h_{fg}	Enthalpy of vaporization,	$J \cdot kg^{-1}$
h_l	Enthalpy other than at saturated condition,	$J \cdot kg^{-1}$
K	Empirical constant as defined in Eq. (3.29)	
$KCHF$	Correction factor as defined in Eq. (7.1)	
K_q	Blockage factor,	D/w
L	Length of heated cylinder in cross flow,	m
L_h	Length of heated tube in axial flow,	m
m	Empirical constant as defined Eq. (3.30)	
$MESC$	Mechanical energy stability criterion	
$\dot{m}_g$	Mass flow rate of vapor at the outlet of control volume,	$kg \cdot s^{-1}$
$\dot{m}_l$	Mass flow rate of liquid at the outlet of control volume,	$kg \cdot s^{-1}$
$\dot{m}_\infty$	Mass flow rate of liquid at the inlet of control volume,	$kg \cdot s-1$
q	Heat flow rate,	W
$\ddot{q}$	Heat flux,	$W \cdot m^{-2}$
Q	Volumetric rate of channel flow,	$m^3 \cdot s^{-1}$
$q_{CHF,FB}$	CHF for flow boiling as defined in Eq. (3.31),	$W \cdot m^{-2}$
$q_{CHF,PB}$	CHF for pool boiling as defined in Eq. (4.1),	$W \cdot m^{-2}$
q_{co}	CHF in saturated boiling as defined in Eq. (3.8) and Eq. (3.12), $W \cdot m^{-2}$	
$q_{co,z}$	q_{co} predicted by Zuber as defined in Eq. (2.1),	$W \cdot m^{-2}$
q_{max}	When $\ddot{q}$ is at CHF,	$W \cdot m^{-2}$
$q_{max,axial}$	CHF occurs in axial flow,	$W \cdot m^{-2}$
$q_{max,cross}$	CHF occurs in cross flow,	$W \cdot m^{-2}$
r	Density ratio, or ρ_f/ρ_g	
r'	Instantaneous radius of bubble,	m
R	Radius of the cylinder,	m
R'	Dimensionless radius of cylinder as defined in Eq. (3.9)	
s	Instantaneous height of bubble center,	m

St	Strouhal number	
t	Time,	s
T_{sat}	Saturated temperature of liquid,	$^\circ C$
T_w	Temperature at the heated wall,	$^\circ C$
U	Liquid velocity corrected for profile and blockage,	$m \cdot s^{-1}$
U_g	Vapor velocity relative to liquid flow,	$m \cdot s^{-1}$
U_H	Helmholtz unstable value of U_g,	$m \cdot s^{-1}$
u_{TP}	Homogeneous flow velocity as defined in Eq. (3.33),	$m \cdot s^{-1}$
U_∞	Velocity of bulk liquid or liquid velocity at the inlet of control volume, $m \cdot s^{-1}$	
V	Instantaneous volume of bubble as defined in Eq. (3.6),	m^3
w	Channel width of flow,	m
W	Width of control volume,	m
We_f	Liquid Weber number	
We_g	Vapor Weber number	
x	Equilibrium quality of flow	
x'	The arc length from the front stagnation point of cylinder,	m
X_d	Diagonal pitch in tube bundles,	m
X_{dd}	Ratio of diagonal pitch to tube diameter, or X_d/D	
X_l	Longitudinal pitch in tube bundles,	m
X_{ll}	Ratio of longitudinal pitch to tube diameter, or X_l/D	
X_t	Transverse pitch in tube bundles,	m
X_{tt}	Ratio of transverse pitch to tube diameter, or X_t/D	

Greek Symbols

α	Vapor sheet thickness divided by $2R$
α'	Vapor sheet thickness as defined in Eq. (4.18)
α^*	Effective dimensionless vapor wake thickness as used in Eq. (4.19)
α_v	Void fraction

γ	$\mid \partial(\rho_f/\rho_g)/\partial P \mid_{saturation}$ used in Ahmad's second scaling factor	
δ	Thickness of vapor blanket used in Eq. (3.20) and Fig. 4-7,	m
δ_c	Critical thickness of liquid film as defined in Eq. (3.4),	m
Δh_{sub}	inlet subcooling,	$J \cdot kg^{-1}$
Δt_{sat}	Temperature of wall above liquid saturation temperature,	$^{\circ}C$
ϵ	Thermal diffusivity of liquid	
κ	Thermal conductivity of liquid,	$J \cdot s^{-1} \cdot m^{-1} \cdot ^{\circ} C^{-1}$
λ	Wavelength,	m
λ_c	Taylor critical wavelength,	m
λ'_D	most susceptible Taylor wavelength,	m
λ_H	Helmholtz wavelength,	m
μ_f	Liquid viscosity,	$kg \cdot m^{-1} \cdot s^{-1}$
μ_g	Vapor viscosity,	$kg \cdot m^{-1} \cdot s^{-1}$
ρ, ρ_{TP}	Homogeneous fluid density as defined in Eq. (3.32),	$k_g \cdot m^{-3}$
ρ_f	Saturated liquid density,	$k_g \cdot m^{-3}$
ρ_g	Saturated vapor density,	$k_g \cdot m^{-3}$
σ	Surface tension,	$N \cdot m^{-1}$
τ_d	Hovering period of bubble,	s
υ	Volumetric growth rate of bubble as defined in Eq. (3.2),	$m^3 \cdot s^{-1}$
ϕ	Dimensionless CHF as defined in Eq. (4.10)	
Ψ_k	Katto's scaling factor as in Table 6.3	
Ψ_σ	Ahmad's first scaling factor as shown in Table 6.3	
Ψ_γ	Ahmad's second scaling factor as shown in Table 6.3	

Chapter 1

Introduction

Boiling heat transfer is a very efficient means of energy transport. Numerous engineering applications have led to investigations of various aspects of boiling heat transfer, especially the mechanism of transition from nucleate to film boiling. Boiling heat transfer for flow across a cylinder or bank of cylinders has received little attention in thermal-hydraulics research. The departure from nucleate boiling (DNB), or the dryout threshold, is one of the main limits that characterizes the boiling curve of the whole flow field. Very little work has been done on the present problem in which the flow is normal to the axis of the cylinder. For pool boiling, the critical heat flux, or CHF, mechanism occurring on a horizontal single cylinder is reasonably well understood, and the geometry of a single cylinder in cross-flow boiling also provides a typical approach to the classical theory for the CHF. Besides, the single rod is the building block of a rod bundle, and more information might provide a base for attacking that far more complex problem.

For boiling inside a vertical tube, many correlations have been developed for the prediction of critical heat flux. Most of them are only applicable for a limited range of flow parameters. Groeneveld's (1986a, 1986b) CHF table look-up method is one of the methods providing wide ranges of system parameters. This method predicts not only water CHF but also the CHF for non-aqueous fluids, and can be used for a geometry other than a single vertical tube (e.g. bundle geometry). Assessment of various published correlations undertaken by ESDU (1986) shows that this tabular method is one of the most reliable methods of all published methods.

In the present study, the objective of this investigation is to develop a prediction method of CHF for cross-flow boiling. The CHF for cross flow predicted by relating it at the CHF for axial flow forms the initial idea of this study. It is obvious that the flow patterns of cross flow and axial flow are very different. The mechanisms of the CHF occurrences for both cases are not close to each other. Therefore, it is difficult to determine the relationship of CHF's between cross flow and axial flow from the theoretical point of view. However, most CHF prediction methods for cross flow and axial flow are empirical or semi-empirical. They are developed from the observation of parametric trends and some of these parameters are used in both cases. Thus the relationship of CHF's between cross flow and axial flow determined on the basis of using common parameters would be a possible and an appropriate approach. If it is possible, the investigation of the CHF relationship between cross flow and axial flow can lead to a correction factor to relate the CHF's in both cases. However, this approach may not be the best method. The semi-empirical and empirical methods are also investigated in this study.

The data base used to obtain the CHF for axial flow is based on Groeneveld's CHF look-up table, and the sources of experimental data for cross flow are obtained from Vliet (1962), Kezios and Lo (1958), Yilmaz and Westwater (1980), Diesselhorst et al. (1977), Pourdashti (1984), Hasan et al. (1981), Min (1975), Broussard and Westwater (1985), and Ungar and Eichhorn (1988).

The experimental observations of CHF trends from the literature about pool boiling, axial-flow boiling and cross-flow boiling are discussed in Chapter 2. In Chapter 3, the two best known analytical models for cross-flow CHF are introduced. The empirical correlations for cross-flow CHF are also reviewed in this chapter. The semi-empirical model to predict the CHF in cross-flow boiling by employing Lienhard and Eichhorn's (1976) assumption in their model and the hydrodynamic model to predict the vapor sheet thickness in Ungar and Eichhorn (1988) is presented in Chapter 4. The experimental CHF data for cross-flow boiling used in this semi-empirical analysis are illustrated in Appendix A.

Chapter 5 defines the characterization of velocity and diameter in cross-flow boiling for use by the following chapters. In Chapter 6, the prediction methods for CHF in axial flow are reviewed. Groeneveld's table look-up method is discussed together with the water and non-aqueous CHF tables shown in this chapter. The programs for predicting the water CHF and the CHF of non-aqueous fluids by Groeneveld's table look-up method are presented in Appendix B and Appendix C, respectively. A correction factor relating the cross-flow CHF with the CHF in axial-flow boiling is presented in Chapter 7. An empirical correlation for cross-flow CHF developed by correlating the experimental cross-flow CHF data is also presented in this chapter including the comparison of the accuracies of both prediction methods. The experimental cross-flow CHF data analyzed in Chapter 7 are illustrated in Appendix A. In Chapter 8, the discussion includes the parameter range and limitation of the semi-empirical model, correction factor method and the empirical correlation. and the conclusion contains the recommendation of the prediction method for cross-flow CHF.

Chapter 2

Literature Survey of Experimental Observations for CHF

2.1 Pool Boiling from A Flat Horizontal Plate

Pool boiling is defined as boiling from a heated surface submerged in a large volume of stagnant liquid which may be at or below its boiling point. The results of investigations into heat transfer rates in pool boiling are usually plotted on a graph of surface heat flux against heater wall temperature (T_w) or wall superheat ($T_w - T_{sat}$). For example, a curve for the boiling of water at atmospheric pressure is shown in Figure 2.1. The present study concentrates its interest on the CHF point, i.e., point D in Fig. 2.1, including the CHF occurring in flow boiling forced convection.

It is now generally accepted that the critical heat flux in pool boiling occurs as a result of a hydrodynamic flow pattern transition close to the heating surface. The mechanism is one in which insufficient liquid is able to reach the heating surface due to the rate at which vapor is leaving the surface. Zuber's (1958) model is most widely accepted, which predicts the CHF for pool boiling on an infinite, upward-facing, horizontal, and flat plate. Zuber idealized the flow pattern as a square array of vapor jets leaving the heated surface with a spacing corresponding to the most rapidly growing Taylor instability wavelength λ_c. The CHF therefore occurs when the vapor-liquid interface of the escape passage becomes unstable due to

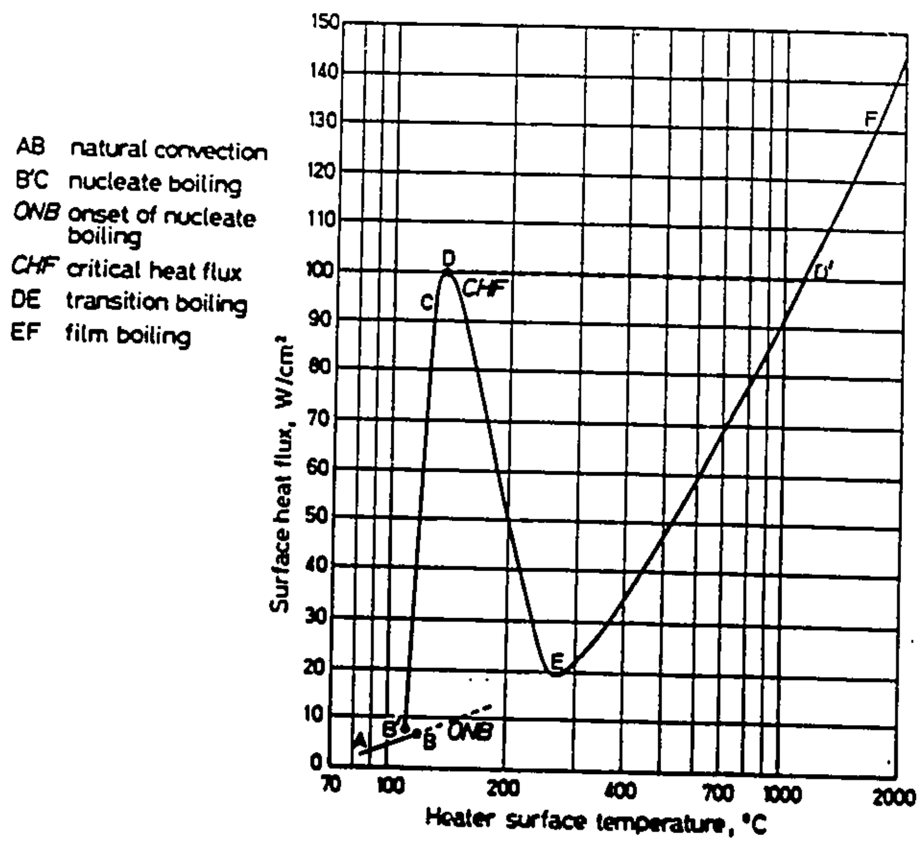

Figure 2.1: Pool boiling curve for water at atmospheric pressure

Helmholtz instability. However, the magnitude of the Helmholtz critical wavelength λ_H is unknown, so it is determined by assuming $\lambda_H = \pi\lambda_c/2$. In addition , a few approximations such as $3/\sqrt{2\pi} \cong 1$ are made to give the CHF as

$$q_{max} = \frac{\pi}{24} h_{fg} \sqrt{\rho_g} \sqrt[4]{\sigma g(\rho_f - \rho_g)} \tag{2.1}$$

Lienhard et al. (1973) continued Zuber's investigation with the same test conditions: pool boiling of an infinite, upward-facing, horizontal, and flat plate at atmospheric pressure. The CHF in this case was found 14 percent higher than Zuber's prediction. Lienhard and Hasan (1979a) extended the usefulness of the *mechanical energy stability criterion* adapted by Lienhard and Eichhorn (1976) to replace the need for a knowledge of Helmholtz wavelength, which is needed in the hydrodynamic descriptions of pool boiling. The geometries investigated include the infinite horizontal flat plate, the cylinder and the sphere. The result for an infinite horizontal flat plate agrees with Zuber's assumed value of the jet radius.

2.2 Pool Boiling from A Horizontal Cylinder

The geometry of a horizontal cylinder is of the most interest for present study. Yet most correlations and models of predicting CHF for a horizontal cylinder are adapted from the results which are used for flat plate pool boiling. Lienhard and Hasan (1979b) and Katto and Haramura (1983b) have derived very typical approaches for this geometry.

2.3 Axial-flow Boiling

CHF observations for axial flow have been conducted by numerous investigators. Many correlations have been used to predict the CHF for different limited ranges of applications. Groeneveld and Snoek (1982) concluded the commonly observed asymptotic trends, which can be attributed by :

1. CHF approaches the pool boiling CHF at low flows.
2. CHF approaches zero for quality and void fraction approaching unity.

3. CHF cannot be less than zero, not even for negative flow(down-flow).
4. CHF reaches a maximum within the approximate pressure range of 3-4 MPa.
5. CHF approaches zero when pressure approaches critical pressure.

Effects such as flux distribution, subcooling, or spacers which are correlated as parametric trends by different observations have been tabulated by Groeneveld and Snoek (1982) and illustrated in Table 2.1.

2.4 Cross-flow Boiling

Various investigations of the heat transfer rate for two-phase flow boiling across a tube or bundle have been undertaken with various specific conditions. Some of the experimentally observed trends will be discussed in the survey below.

Beecher (1948) investigated natural convection, saturated boiling of water at atmospheric pressure from a 0.61 *mm* platinum wire, and forced convection from a 1.2 *mm* OD. stainless-steel tube. The experiment showed that the CHF was inversely proportional to the 0.15 power of diameter over the entire velocity range from 0.36 to 3 m/s. Vliet and Leppert (1964a and b) also studied forced convection boiling from wires and tubes from 0.25 to 4.8 *mm* OD. placed normal to a stream of slightly subcooled water at velocities from 0.36 to 2.9 m/s, as well as the measurement for water at atmospheric pressure over a range of subcooling from 1.7 to 55.6 deg. C and velocity ranging from 0.15 to 3.4 m/s. They found that the CHF for nearly saturated water at atmospheric pressure was proportional to the 0.5 power of the fluid velocity and -0.15 power of the diameter.

Kezios and Lo (1958) investigated the effects of velocity and large values of subcooling on the CHF for water flowing horizontally and normal to 3.2 *mm* rods, and stated that the CHF was proportional to the 0.8 power of subcooling and 0.2 power of the mass flux. Mckee and Bell (1969) showed by experiment that when the diameter of the cylinder is increased beyond a certain value under the condition of fixed bulk liquid velocity, a rapid reduction of CHF takes place. The test conditions for their measurement were: 6.4-18 *mm* OD. heater diameter, 1.7 to 7.8 deg. C subcooled water for 124.2 kPa abs. and approach velocities of 1.0 and 1.66 m/s.

Table 2.1: Parametric trends for CHF in axial flow

Effect	Correction factor	References	Comments
Spacing device	$\frac{CHF_{with\ grids}}{CHF_{without\ grids}} = 1 + 0.1 \exp\left(-\frac{L_{sp}}{40 D_{hy}}\right)$	Smolin and Polyakov (1978)	Constants 0.1 and 40 must be dependent on spacer geometry.
	$\frac{CHF_{with\ grids}}{CHF_{without\ grids}} = 1 + \phi K \left(\frac{G}{1-\alpha}\right)^{0.6} D_{he}^{0.28} \exp\left(-\frac{\psi L_{sp}}{D_{hy}}\right)$	Tong (1975)	Based on experiments using PWR-type bundles and grids.
	ϕ, ψ are spacer and flow regime constants K = pressure loss coefficient of spacer L_{sp} = spacer pitch		N.B. Increases in CHF of over 200% have been observed for short spacer pitch. Spacers also improve post CHF heat transfer
Diameter	$\frac{CHF(D)}{CHF(D_o)} = \left(\frac{D_o}{D}\right)^{1/3}$	Doroshchuk et al. (1975)	Valid for $4 < D < 16$ mm, for $\Delta T_{sub} < 75^oC$ and burnout of the first kind (not for very high qualities). Valid for positive qualities only; $q_o = f(P)$.
	$\frac{CHF(D)}{CHF(D = 0.008)} = 1 + \frac{q_o}{CHF(D = 0.008)} \left(\frac{0.008}{D}\right)^{1/3} - 1$	Doroshchuk and Lantsman (1970)	
	$\frac{CHF(D)}{CHF(D_o)} = \left(\frac{D_o}{D}\right)^n$ $n = 0.4$, if $D > 10$ mm $n = 0.6$, if $D < 10$ mm	Blasi et al. (1967)	From Blasi's correlation. Ranges: $D = 0.003\text{-}0.0375$ m, $P = 270\text{-}14{,}000$ kPa, $G = 100\text{-}6000$ kg m^{-2} s^{-1}, $\frac{1}{1 + \rho_l/\rho_g} < \chi < 1.0$
	$\frac{CHF(D)}{CHF(D = 0.01)} = f(D)$	Becker (1967)	From Becker's correlation. Ranges: $D = 0.004\text{-}0.025$ m, $P = 270\text{-}10{,}000$ kPa, $G = 120\text{-}5400$ kg m^{-2} s^{-1}, $\chi = 0\text{-}0.5$

D (mm)	4	6	8	10	12	14	18	24	25
$f(D)$	1.18	1.176	1.085	1.00	0.973	0.982	0.94	0.917	0.90

Effect	Correction factor	References	Comments
Flow	$\frac{CHF(G)}{CHF(G = 1000(kg\ m^{-2}\ s^{-1}))} = \left(\frac{G}{1000}\right)^{0.68 \frac{P}{P_{cr}} - 1.2\chi - 0.3}$	Doroshchuk et al. (1975)	Derived from Doroschuk's correlation. Large-tube data base. Ranges: $D = 0.004\text{-}0.016$ m, $P = 290\text{-}15{,}600$ kPa, $G < 2000$ kg m^{-2} s^{-1}, $\Delta T_{sub} < 50^oC$
	$\frac{CHF(G)}{CHF(G_o)} = \left(\frac{G_o}{G}\right)^{1/2}$	Becker (1967)	From Becker's correlation. Large-tube data base. Ranges: $\chi = 0\text{-}0.6$, $G = 120\text{-}5400$ kg m^{-2} s^{-1}, $P = 270\text{-}10{,}000$ kPa
	$\frac{CHF(G)}{CHF(G_o)} = \frac{1 + 1.06\ 10^{-4}\ G}{1 + 1.06\ 10^{-4}\ G_o}$	Griffel and Bonilla (1965)	Tube data covered: $308 < G < 10{,}000$ kg m^{-2} s^{-1}, $3.5 < P < 10.5$ MPa, and negative χ($0 < \Delta T_{sub} < 65^oC$).

Table 2.1 (cont'd)

Effect	Correction factor	References	Comments
Pressure	$\frac{CHF(P)}{CHF(P_o)} = \left(\frac{1 - P/P_{cr}}{1 - P_o/P_{cr}}\right)^{0.1} \frac{CHF_{PB}(P)}{CHF_{PU}(P_o)}$	Tolubinsky et al. (1977)	From Levitan's correlation based on a large number of annuli data.
	where $CHF_{PU} = 0.14\, h_{fg}\, \rho_g^{1/2}\left[\sigma g(\rho_\ell - \rho_g)\right]^{1/4}$	Levitan and Lantsman (1977)	Ranges: P = 5000-20,000 kPa, $\chi < 0.3$ G = 250-5000 kg m^{-2} s^{-1}
	$\frac{CHF(P)}{CHF(P_o)} = \left(\frac{P_o}{P}\right)^{0.3234}$	Condie and Bengston (1978)	From RELAP 4-MOD 7 correlation. Based on large-bundle data base.
	$\frac{CHF(P)}{CHF(P_o)} = \frac{CHF_{PB}(P)}{CHF_{PU}(P_o)}$	Griffith et al. (1977)	Ranges: P = 690-15,200 kPa, χ = - 0.1-1.0 G = 100-4100 kg m^{-2} s^{-1} From Griffith-Zuber correlation for same void fraction. Valid for low flows only.
Adjacent Unheated Surface	$\frac{CHF_{adj\ unh\ surf}}{CHF_{ref}} = f(Dhe, Dhy, \chi, G, P)$	Tong (1972a)	Adjacent unheated surface robs liquid that would otherwise be available for cooling of the heated surface
Void and transients (low flow)	$\frac{CHF}{CHF_{PB}} = (1 - \alpha)$	Griffith et al. (1977)	At low flow (also during CCF) flow quality becomes meaningless: α becomes a much better parameter to describe the vapor presence.
Void and transients (blowdown)	$\frac{CHF}{CHF_{W-3}(\chi = 0)} = 1.33(0.96 - \alpha)^{1/2} + \frac{q_{steam}}{CHF_{W-3}(\chi = 0)}$	Hsu and Beckner (1977)	From Hsu-Beckner correlation. Increases CHF due to transient effect. Reference CHF (CHF at χ = 0, W-3 correlation) is fairly arbitrary. Recommended for high pressure, blowdown transients.
Axial flux distribution	$\frac{CHF_{non-UN}}{CHF_{UN}} = F = f(AFD, G, \chi)$	Tong (1972a)	Upstream AFD has a weak effect at highly subcooled conditions (local conditions dominate) but becomes important at higher enthalpies.
	CHF occurs when $q_{BLA} > CHF_{UN}$	Groeneveld (1981a)	In the annular flow regime, use boiling length average heat flux instead of local heat flux.
Flux spike	$\frac{CHF_{with\ spike}}{CHF_{ref}} = f(G, \chi, \frac{q_{sp}}{q_{avg}}, \frac{L_{sp}}{D})$	Groeneveld (1975)	Short flux spikes can significantly affect CHF in the subcooled region but usually have negligible effect in annular flow regime.

Table 2.1 (cont'd)

Local enthalpy ($\chi < 0$)	$\frac{CHF(\Delta T_{sub})}{CHF(\Delta T_{sub} = 0)} = 1 + B\,\Delta T_{sub}$ $B = 0.1\left(\frac{\rho_l}{\rho_g}\right)^{0.75}\left(\frac{Cp}{h_{fg}}\right)$	Ivey and Morris (1962)	Ivey's correction is based only on pool boiling results and agrees with water data at P < 1800 kPa.
	$\begin{array}{c\|c\|c\|c\|c} P(MPa) & 20 & 35\text{-}70 & 100 & 130 \\ \hline B\left(\frac{1}{^{o}C}\right) & 0.068 & 0.055 & 0.053 & 0.050 \end{array}$	Povarnin (see Tong, 1972a)	Povarnin's correction is based on small-diameter tubing (2-3 mm) and P = 2000 - 20,100 kPa.
Local enthalpy ($\chi > 0$)	$\frac{CHF(\chi)}{CHF(\chi_o)} = \frac{\chi_{max} - \chi}{\chi_{max} - \chi_o} \quad \chi_{max} = 1.0$ For very low G: $\chi_{max} = 1 - \frac{4\ MWR}{G\ Dhy}$ MWR = minimum wetting rate	Groeneveld (1981b)	Only for high-quality. χ_o is highest quality where CHF is known. MWR value reported by Norman and McIntyre (1960).
	$\frac{CHF(\chi)}{CHF(\chi = 0)} = e^{-1.5\chi}\left(\frac{G}{1000}\right)^{-1.2\chi}$	Doroshchuk et al. (1975)	From Doroshchuk's correlation. Ranges: P = 2900-15,600 kPa, ΔT_{sub} < 50°C, G < 2000 kg m^{-2} s^{-1}, D = 0.004-0.016 m. Burnout of the first kind only.
Cross section geometry	$\frac{CHF_{annulus}}{CHF_{tube\ (D = 8mm)}} = K_\chi K_P K_D$ $\begin{array}{c\|c\|c} P(MPa) & < 6.9 & > 6.9 \\ \hline K_P & 1 & 1.2\sqrt{P/9.8} \end{array} \quad \begin{array}{c\|c\|c} Dhy(mm) & < 8 & > 8 \\ \hline K_D & \left(\frac{Dhy}{D_i}\right)^{0.2} & \left(\frac{64}{D_i\ Dhy}\right)^{0.2} \end{array}$ $K_\chi = \min(1, e^{-2\chi})$	Levitan and Lantsman (1977)	Based on large number of annuli data and on tube CHF correlation from Doroshchuk et al. (1975) which was equally based on a large-tube data bank.
	CHF bundle = CHF annulus having equivalent D_i, D_o equiv. $D_i = d$ (= rod diameter) equiv. $D_o = \left[d(d + Dhe^{*})\right]^{1/2}, Dhe^{*} = \frac{4A}{n\ \pi d}\frac{q_{max}}{q_{avg}}$	Barnett (1968)	Barnett obtained excellent agreement using the equivalent annulus and his annulus CHF correlation.

[a]For definition and units of all symbols, see Nomenclature.

Broussard and Westwater (1985) studied the diameter and velocity effects of CHF for cross flow boiling by conducting the experiment with Freon-113 fluid and horizontal copper tubes of diameter 1.59-7.94 *mm* for pool boiling and 3.18-12.7 *mm* for flow boiling. The test fluid at atmospheric pressure flowed upward, normal to the heaters, at approach velocities of 2.4, 4.0 and 6.0 m/s. The experiment showed that, at a fixed velocity and wall temperature, smaller tubes resulted in higher heat flux values, except at low wall temperatures. The CHF was proportional to the 0.44 power of velocity and inversely proportional to the 0.28 power of diameter. Yilmaz and Westwater (1980) also made measurements of heat transfer to Freon-113 at near atmospheric pressure, boiling outside a 6.5 *mm* diameter horizontally steam-heated copper tube. Tests included pool boiling and also forced flow vertically upward at velocities of 2.4, 4.0 and 6.8 m/s. The CHF was proportional to the square root of velocity.

Hasan et al. (1982), Cumo et al. (1980) and Kezios et al. (1961) studied the CHF of cross flow by conducting the measurements of flow normal to the bundle. Hasan et al. (1982) observed the burn-out of horizontally heated cylinders in up-flow fluids, isopropanol and methanol, adjacent to one or two parallel unheated cylinders. The static pressure at the elevation of the rod bundle varied between 101 and 104 kPa and the diameter varied from 0.51 to 1.65 *mm*. They concluded that a parallel neutral cylinder, in the neighborhood of a cylindrical heater, has only a minor influence on CHF unless it is directly upstream with its centerline less than 4 diameters away from the heater. Cumo et al. (1980) investigated the influence of quality on CHF in flow boiling, employing a 9-tube bundle with cross flow of Freon-12. The diameter of each tube of the 9-tube bundle was 13.6 *mm* and the pressure was 7 times higher than the atmospheric pressure. This test condition was much different from those of other investigations mentioned above. Rather surprisingly, Cumo et al. observed that the CHF rises with quality. Kezios et al. (1961) reported the critical heat flux for a heated 3.2 *mm* diameter rod in a matrix of unheated rods. They concluded that critical heat flux in arrays is higher than in single rods, but there is a question of the proper characteristic velocity to use for comparison.

Chapter 3

Prediction Methods for CHF in Cross Flow

3.1 Analytical Models

3.1.1 Katto and Haramura's model (1983)

Katto and Haramura (1983a, 1983b) presented a hydrodynamic model of CHF applicable to both pool and forced convection boiling on submerged bodies in saturated liquid. The geometries of submerged bodies included a horizontal and infinitely flat plate, a horizontal and infinitely long cylinder, an upward-facing and horizontally small disk, a flat plate parallel to the flow, and a cylinder normal to the flow. In Katto and Haramura's hydrodynamic model (1983a, 1983b), for liquid flowing upward and normal to the cylinder at low velocities a flow pattern as illustrated in Figure 3.1 appears: a bubble-like flow, where the vapor generated at the cylinder wall forms a massive vapor bubble at approximately equal intervals. Each bubble departures from the cylinder when it has grown sufficiently. Thus, CHF can be determined from the energy balance at the interface of the bubble and liquid film around the cylinder.

In Fig. 3.1a, the λ_D' was given as

$$\lambda_D' = 2\sqrt{3}\pi\sqrt{\frac{\sigma}{g(\rho_f - \rho g)}\frac{1}{1 + \frac{2\sigma}{D^2 g(\rho_f - \rho_g)}}} \tag{3.1}$$

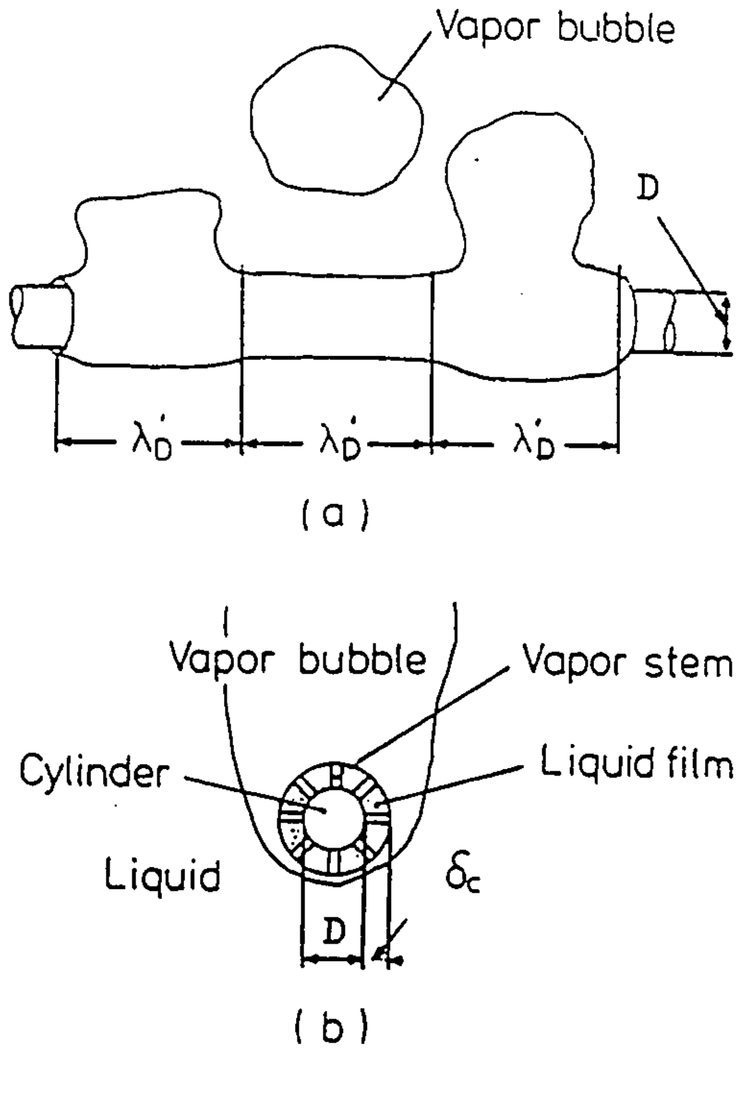

Figure 3.1: Pool boiling at high heat fluxes on a horizontal cylinder

which is the most susceptible (or dangerous) wavelength of Taylor instability and has been given by Lienhard and Wong (1964) for a horizontal, cylindrical vapor-liquid interface in a stationary bulk liquid. Fig. 3.1b shows a liquid film wetting the cylinder surface, and surrounded by a vapor bubble in which there are many columnar vapor stems in the liquid film when the film is sufficiently thick, so that the heat transferred from the cylindrical wall is absorbed by latent heat at the part of the vapor-liquid interface of the vapor stem near the heated surface. When the thickness of liquid film reduces considerably, evaporation takes place at the outer surface of the liquid film. Therefore, the volumetric growth rate υ of a vapor bubble surrounding the cylinder via the heat balance is

$$\upsilon = \frac{\pi D \lambda'_D \ddot{q}}{\rho_g h_{fg}} \tag{3.2}$$

The hovering period of the bubble attached to the solid wall is assumed as a mean value of τ_d. Haramura and Katto (1983a) postulated that the CHF appears at the end of a hovering period when the liquid film evaporates out and is not fed with liquid from the bulk region during the hovering period, for which the energy balance is given by

$$\tau_d \ddot{q} A_h = \rho_f \delta_c \left(A_h - A_v + A_h \frac{\delta_c}{D} \right) h_{fg} \tag{3.3}$$

where A_h is the area of the heated surface, A_v the cross-sectional area of the vapor stems, and δ_c the initial thickness of the liquid film. The δ_c is also the critical thickness of a liquid film capable of stabilizing itself on a solid wall based on the Helmholtz instability of the vapor-liquid interface of vapor stems and is given by

$$\delta_c = \frac{\pi}{2} \sigma \frac{\rho_f + \rho_g}{\rho_f \rho_g} \left(\frac{A_v}{A_h} \right)^2 \left(\frac{\rho_g h_{fg}}{\ddot{q}} \right)^2 \tag{3.4}$$

where A_v/A_h is a weak function of ρ_g/ρ_f and yields $A_v/A_h = 0.0584(\rho_g/\rho_f)^{0.2}$.

To solve for τ_d, Katto and Haramura (1983b) postulated a theoretical analysis of the bubble behavior such as illustrated in Fig. 3.2. In Fig. 3.2, a spherical bubble, being nourished with vapor from a fixed point P, is moving upward due to the buoyant force. For this bubble, the equation of motion is written as

$$\frac{d}{dt} \left[\left(\frac{11}{16} \rho_f + \rho_g \right) V \left(\frac{ds}{dt} - U_\infty \right) \right] = (\rho_f - \rho_g) V g \tag{3.5}$$

where 11/16 is the theoretical volumetric ratio of the accompanying liquid to a moving spherical bubble derived by Katto and Yokoya (1976), V the bubble volume

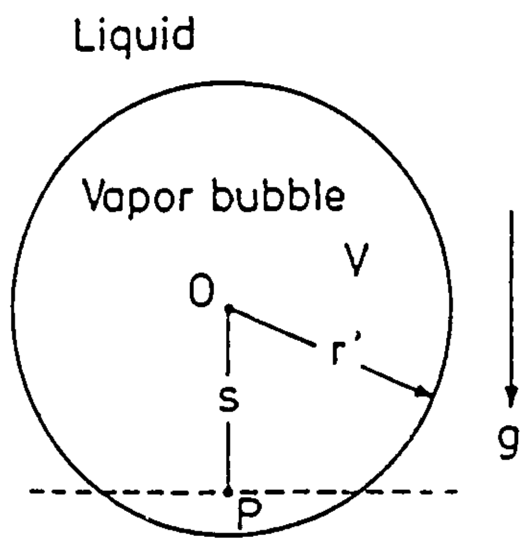

Figure 3.2: A model of a vapor bubble growing through the feed of vapor as well as rising due to buoyancy

at the time t after the onset of bubble growth, s the height of the bubble center measured from the fixed point P, and U_∞ the vertical upward velocity of bulk liquid. Note that $ds/dt - U_\infty$ is the relative velocity of the bubble center to the bulk liquid.

In equation (3.5), V is evaluated by

$$V = vt \tag{3.6}$$

Thus, solving equation (3.5) together with equation (3.6) for $s(t)$, and taking into account the initial condition $s = 0$ at $t = 0$ as well as the departure condition $s = r' = [3V/(4\pi)]^{1/3}$ at $t = \tau_d$, yields

$$\tau_d = \left(\frac{3}{4\pi}\right)^{1/5} \left[\frac{4(\xi\rho_f + \rho_g)}{g(\rho_f - \rho_g)}\right]^{3/5} v^{1/5} \left[1 + \frac{4(\xi\rho_f + \rho_g)U_\infty}{\tau_d g(\rho_f - \rho_g)}\right]^{3/5} \tag{3.7}$$

where

$$\xi = 11/16$$

Now, ignoring A_v/A_h as compared with unity in equation (3.3), since $A_v/A_h < 0.0584$, and solving equations (3.1)-(3.4) and (3.7) for the critical heat flux $\ddot{q}$, and finally writing the $\ddot{q}$ as q_{co} results in

$$\frac{q_{co}}{q_{co,z}} = \left(\frac{\sqrt{3}}{R'}\right)^{1/16} \left[1 - \frac{1}{2R'^2}\right]^{1/32} \left[1 + 0.156\left(\frac{\rho_g}{\rho_f}\right)^{0.4}\left(1 + \frac{\rho_g}{\rho_f}\right)\frac{1}{R'}\frac{1}{(q_{co}/q_{co,z})^2}\right]^{5/16}$$
$$\left[1 + 1.68\frac{\frac{11}{16} + \frac{\rho_g}{\rho_f}}{\left(\frac{\rho_g}{\rho_f}\right)^{0.4}\left(1 + \frac{\rho_g}{\rho_f}\right)} \frac{\left(\frac{q_{co}}{q_{co,z}}\right)^3}{1 + 0.156\left(\frac{\rho_g}{\rho_f}\right)^{0.4}\left(1 + \frac{\rho_g}{\rho_f}\right)\frac{1}{R'}\frac{1}{(q_{co}/q_{co,z})^2}} u'\right]^{1/16} \tag{3.8}$$

where

$$R' = \frac{D/2}{\sqrt{\frac{\sigma}{g(\rho_f - \rho_g)}}} \tag{3.9}$$

$$u' = \frac{U_\infty}{\left[\frac{\sigma g(\rho_f - \rho_g)}{\rho_g^2}\right]^{1/4}} \tag{3.10}$$

where U_∞ is the bulk mean velocity.

In the case of CHF with sheet-like vapor escape flow, if the bulk liquid velocity is sufficiently high, CHF is hardly affected by gravity, and the analysis of CHF in Katto and Haramura's model (1983b) is summarized as follow: *A liquid film flowing over a cylinder wall (see Fig. 3.3) receives saturated liquid constantly at the front stagnation point with δ_c in film thickness from the bulk flow of velocity U_∞, which*

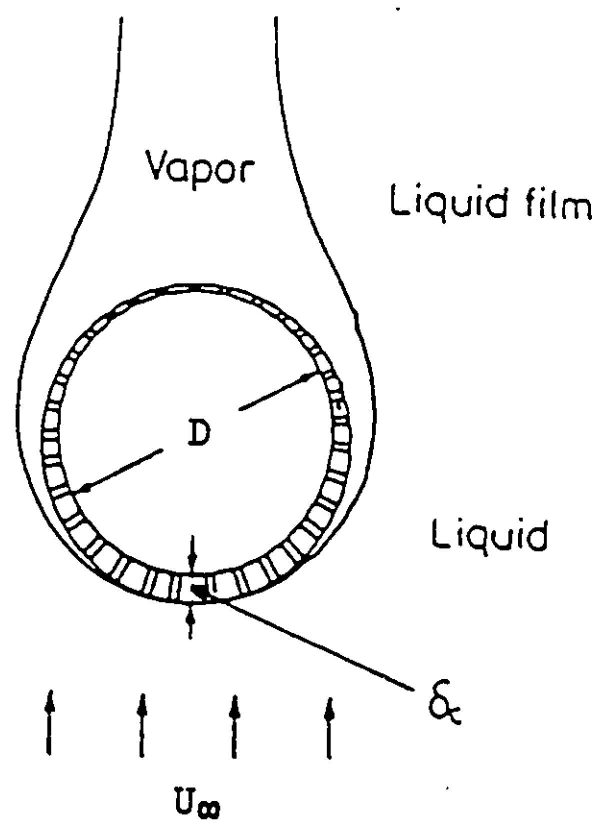

Figure 3.3: Nucleate boiling on a cylinder in a cross flow with a sheet-like escape flow of vapor at high heat fluxes

causes CHF when the liquid film flow dries up at the rear stagnation point, and the heat balance is written as

$$\frac{\ddot{q}\pi D}{2} = \rho_f \delta_c U_\infty h_{fg} \tag{3.11}$$

Solving equations (3.4), (3.11) and $A_v/A_h = 0.0584(\rho_g/\rho_f)^{0.2}$ for the critical heat flux $\ddot{q}$, and writing $\ddot{q}$ as q_{co} results in

$$\frac{q_{co}}{Gh_{fg}} = 0.151\left(\frac{\rho_g}{\rho_f}\right)^{0.467}\left(1+\frac{\rho_g}{\rho_f}\right)^{1/3}\left(\frac{\sigma\rho_f}{G^2 D}\right)^{1/3} \tag{3.12}$$

where

$G = U_\infty \rho_f$ the mass velocity of bulk liquid flow.

3.1.2 Lienhard and Eichhorn's model (1976)

Lienhard et al. (1970, 1973, 1973, 1964) extended Zuber's model to include finite bodies such as illustrated in Fig. 3.4. Furthermore, Lienhard et al. (1979a, 1979b, 1979, 1976) studied the CHF in forced convection boiling (see Fig. 3.5) as well as in pool boiling by replacing hydrodynamic instability analyses with a concept of *mechanical energy stability criterion*, which considers a balance between the kinetic energy of the vapor flow and the surface energy necessary to develop the liquid interface.

Lienhard and Eichhorn (1976) postulated that the heat generated from the heated cylinder can be accounted for by removal of vapor. Therefore, when the CHF occurs, the energy balance should be

$$q_{max} = \rho_g h_{fg} U_\infty \frac{A_j}{A_h}\left(1+\frac{U_g}{U_\infty}\right) \tag{3.13}$$

where U_g is vapor velocity relative to the velocity of incoming flow, A_j and A_h the cross-sectional area of the vapor jets leaving the cylinder and the area of heated surface. For the case of a heated cylinder, they assumed the width of the vapor sheet is equal to $2\alpha R$. Then

$$\frac{A_j}{A_h} = \frac{2\alpha RL}{2\pi RL} = \frac{\alpha}{\pi}$$

where L is the length of heated cylinder. Therefore the equation (3.13) becomes

$$\frac{\pi q_{max}}{\rho_g h_{fg} U_\infty} = \alpha + \alpha\left(\frac{U_g}{U_\infty}\right) \tag{3.14}$$

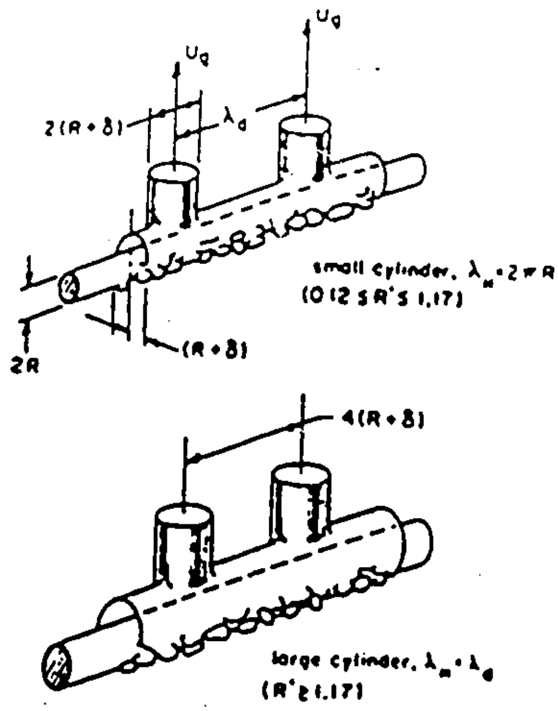

Figure 3.4: Liquid-vapor interface during pool boiling from cylinder

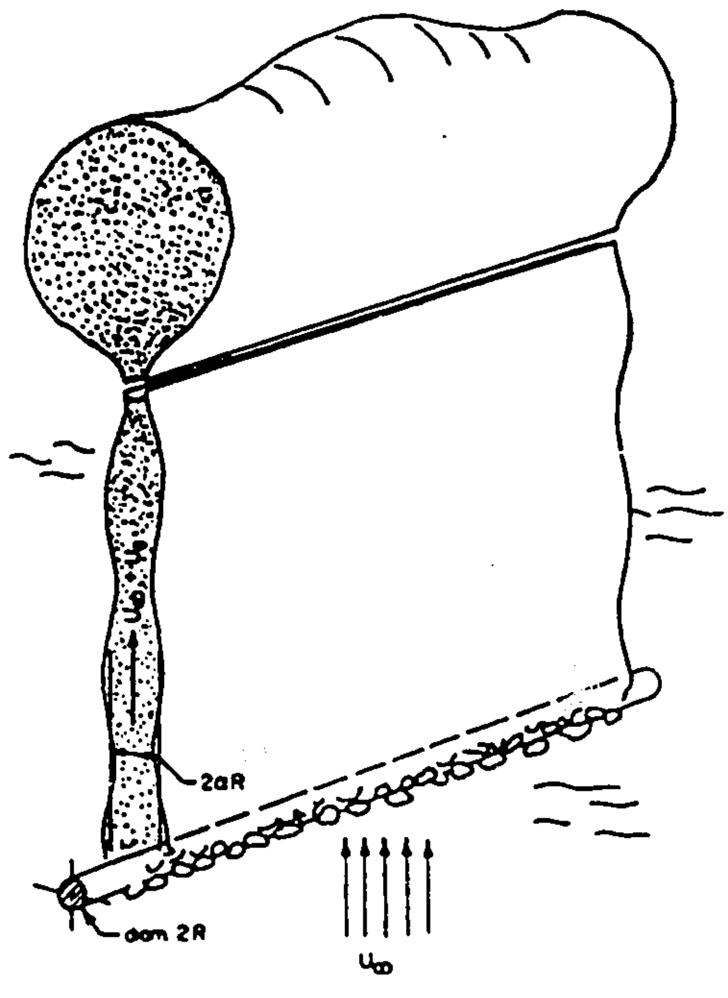

Figure 3.5: Vapor removal by the action of two-dimensional jets before burn-out occurs

When the U_g reaches the Helmholtz unstable velocity, U_H, the vapor sheet will collapse and cause the CHF. At this moment, the U_H is given by

$$\frac{U_H}{U_\infty} = \frac{2\pi}{U_\infty}\left(\frac{3\sigma R}{\rho_g \lambda_H^2}\right)^{1/2} = 2\pi\left(\frac{3}{2}\right)^{1/2}\left(\frac{1}{We_g}\right)^{1/2}\frac{2R}{\lambda_H} \tag{3.15}$$

Equation (3.15) cannot be solved because the term $2R/\lambda_H$ is unknown. Nevertheless Lienhard and Eichhorn used the model of *mechanical energy stability criterion* or *MESC* to resolve this problem, which should be satisfied at burn-out: *A little above the cylinder the liquid is again moving at U_∞. Hence Fig. 3.6 shows a control volume which moves upward with velocity, U_∞, relative to the cylinder. The top of the vapor sheet, which is observed to maintain a fixed average distance above the cylinder, will move downward in the control volume at an average speed U_∞. The detached bubbles have negligible surface area per unit volume in comparison with the sheet. Therefore the control volume loses surface energy at a rate equal to $\rho_g U_g (2\alpha R) U_g^2/2$.*

Then according to the mechanical energy balance along the control volume, which yields:

$$-2U_\infty \sigma + \frac{\rho_g 2\alpha R U_g^3}{2} = 0 \tag{3.16}$$

or

$$\frac{U_g}{U_\infty} = \frac{4^{1/3}}{(\alpha We_g)^{1/3}} \tag{3.17}$$

Thus, Lienhard and Eichhorn (1976) simplified this problem to correlate an appropriate value for α instead of calculating the U_H used in equation (3.15). Once the α is known, the CHF can be obtained. Substituting equation (3.17) into equation (3.14), gives

$$\phi = \alpha + \alpha\left(\frac{4}{\alpha We_g}\right)^{1/3} \tag{3.18}$$

where $\phi = \pi q_{max}/(\rho_g h_{fg} U_\infty)$. So, now the rest of the work is to find out the appropriate value of α.

For low velocity of flow, the liquid momentum, $\rho_f U_\infty^2$, does not significantly exceed the vapor momentum, $\rho_g U_g^2$. Hence the vapor can just flow straight up and the liquid cannot curve around to the back of the cylinder. In this case, α is probably close to unity and equation (3.18) yields

$$\phi = 1 + \left(\frac{4}{We_g}\right)^{1/3} \tag{3.19}$$

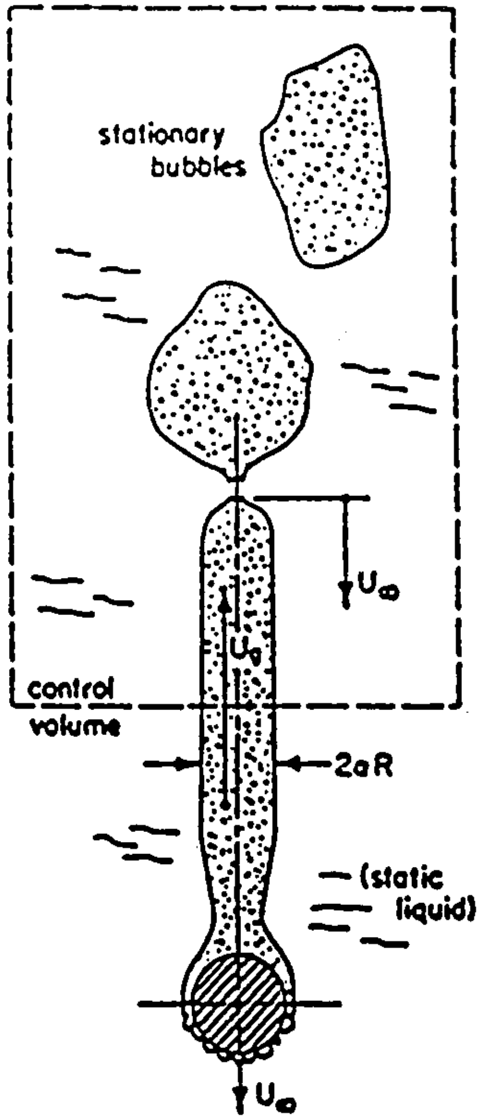

Figure 3.6: Control volume for kinetic/surface energy balance used in Lienhard and Eichhorn's MESC model

for low U_∞.

In the high flow condition, the liquid flow can be treated as a potential flow and the vapor moves without slip between the liquid and cylinder. Thus the interface will reach a velocity near $2U_\infty$ as illustrated in Fig. 3.7 for the horizontal diametral plane. Because the wake behavior has the advantage of suppressing vapor separation behind the cylinder, Bernoulli's equation can be used to describe both the liquid and vapor flow from station (1) to (2) as indicated in Fig. 3.7. Combining the two Bernoulli equations and the continuity equation shown in Fig. 3.7 to solve for α and using equation (3.17) to eliminate U_g/U_∞ at CHF, gives

$$1 + \left(\frac{4}{\alpha We_g}\right)^{1/3} = \frac{\left(\frac{3\rho_f}{\rho_g}\right)^{1/2}}{\left[\alpha^2\left(\frac{R}{\delta}\right)^2 - 1\right]^{1/2}} \tag{3.20}$$

where δ is the vapor blanket thickness shown in Fig. 3.7. Since the terms 1 and -1 in equation (3.20) are negligible compared to their accompanying terms, equation (3.20) gives

$$\alpha = constant\left(\frac{\rho_f}{\rho_g}\right)^{3/4} \tag{3.21}$$

where the constant should be determined on the basis of experimental results and yields

$$\alpha = \frac{\left(\frac{\rho_f}{\rho_g}\right)^{3/4}}{169} \tag{3.22}$$

Finally the equation (3.18) results in:

$$\frac{\pi q_{max}}{\rho_g h_{fg} U_\infty} = \frac{1}{169}\left(\frac{\rho_f}{\rho_g}\right)^{3/4} + \frac{1}{19.2}\left(\frac{\rho_f}{\rho_g}\right)^{1/2}\frac{1}{We_g^{1/3}} \tag{3.23}$$

for high U_∞.

3.1.3 Vliet and Leppert's correlation (1964a)

Vliet (1962) and Vliet and Leppert (1964a) measured the CHF for a slightly subcooled water stream flowing normal to wires and tubes of 0.25 to 4.8 mm OD. The velocity range of water varies from 0.36 to 2.9 m/s. They, therefore, presented a model for predicting the CHF in a cross flow of saturated liquid:

$$q_{co} = \frac{1.083\kappa\Delta t_{sat}}{\overline{f}\sqrt{\epsilon}}\sqrt{\frac{U}{D}} \tag{3.24}$$

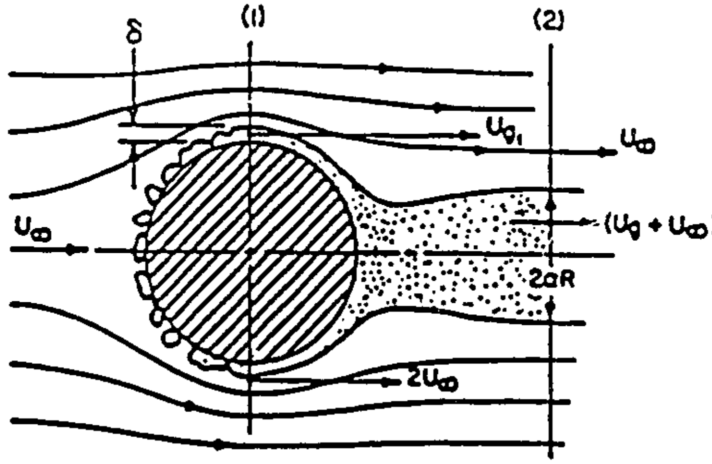

Bernouli equation:

liquid: $\frac{P_1}{\rho_l} + \frac{(2U_\infty)^2}{2} = \frac{U_\infty^2}{2}$

vapor: $\frac{P_1}{\rho_g} + \frac{(U_{g1}+U_\infty)^2}{2} = \frac{(U_g+U_\infty)^2}{2}$

Continuity: $2\delta(U_{g1} + U_\infty) = 2\alpha R(U_g + U_\infty)$

Figure 3.7: Potential flow model for the evaluation of α

where κ is the thermal conductivity of liquid, Δt_{sat} the superheat of heated wall, $\overline{f}$ the fraction of heat transferred directly to vapor while bubbles are on the heated surface, ϵ the thermal diffusivity of liquid, U the mean channel velocity corrected by blockage and velocity profile. Equation (3.24) is not practical for use because of the unknown parameter $\overline{f}$.

3.2 Empirical Approach

3.2.1 Yilmaz and Westwater's correlation (1980)

The CHF measurements were undertaken in Freon-113 flowing normal to a horizontally steam-heated copper tube of 6.5 mm diameter at near atmospheric pressure and at velocities of 2.4, 4.0, and 6.8 m/s. The CHF, therefore, was correlated using the dimensionless groups:

$$\frac{q_{max}}{\rho_g h_{fg} U_\infty} = 0.369 We_g^{-0.26} \tag{3.25}$$

where $We_g = \rho_g D U_\infty^2/\sigma$.

Note that the velocities used in Yilmaz and Westwater's experiments refer to the free stream velocity in the test section rather than that of Vliet and Leppert's (1964a) definition. Rearranging equation (3.25) gives the following expression

$$q_{max} \propto U_\infty^{0.48}$$

3.2.2 Hasan et al.'s correlation (1981)

Hasan et al. (1981) observed the CHF during the up-flow and down-flow of isopropanol and methanol over horizontal cylinders, beyond the influence of gravity. The experiments were conducted with 0.5-1.5 mm OD. wires placed in the up-flow stream at velocity varied from 0.261 to 2.435 m/s, as well as the 0.5-1.63 mm OD. wires placed in the down-flow stream at the velocity range of 0.197-2.57 m/s. They, therefore , presented a correlation to predict the CHF:

$$\frac{\pi q_{max}}{\rho_g h_{fg} \mid U_\infty \mid} = 0.000919 \frac{\rho_f}{\rho_g}\left(1 + \frac{16.3}{We_f^{1/3}}\right) \tag{3.26}$$

where We_f is the Weber number, $\rho_f U_\infty^2 D/\sigma$, and the liquid velocity is relative to cylinder instead of that corrected by the blockage factor.

The criterion for the gravity influence, then, was given:

$$G_c = 10$$

where

$$G_c = \frac{U_\infty}{\left(\frac{g\sigma}{\rho_f}\right)^{1/4}} \tag{3.27}$$

For $\mid G_c \mid > 10$, the influence of gravity on the CHF was assumed to be inconsequential.

3.2.3 Katto's correlation (1987)

Katto et al. (1987) presented an empirical correlation by employing the results of his CHF experiment and those of others investigators. Using water, Freon-113 and Freon-12, CHF experiments were conducted with a 1 mm OD. diameter uniformly heated cylindrical heater in a forced cross flow of $U_\infty = 0.59 - 7.1$ m/s and a wide range of $\rho_g/\rho_f = 0.000624 - 0.306$. The correlation for CHF, then, was presented:

$$\frac{q_{co}}{Gh_{fg}} = K\left(\frac{\sigma\rho_f}{G^2 D}\right)^m \tag{3.28}$$

where

$$K = 0.00588 + 0.5\left(\frac{\rho_g}{\rho_f}\right)^{1.11} \tag{3.29}$$

and

$$m = 0.42\left(\frac{\rho_g}{\rho_f}\right)^{0.0428} \tag{3.30}$$

Note that the velocity used in their experiments was referred to the bulk liquid flow, and the wide range of ρ_g/ρ_f implies that the test conditions might not be at atmospheric pressure.

3.2.4 Cumo et al.'s correlation (1979)

A measurement of CHF for fluid flowing normal to the tube bundles was investigated by Cumo et al. in 1979. A sketch of test section employed in a Freon-12 loop is described in Fig. 3.8. There are different aspects for which actual situations differ from those of other investigations:

1. multi-tube bundles through which boiling develops in a rather complex flow pattern instead of single tube.
2. tube diameters of the order of centimeters, instead of the order of millimeters.
3. two-phase inlet flow, instead of single phase flow.

The specific mass flow, G, is computed as a mean value through the bundle area and grouped around values of 41, 66, 91, and 116 kg/m^2s, while the quality x is referred to the inlet value up to 30%. The pressure through the test was constant at the value of 785 kPa, which corresponds to an equivalent pressure, for water, 4426 kPa. The central tube is the only tube heated among the 9-tube bundle. Cumo et al., then, presented a correlation to predict the CHF by employing their experimental results and based on Zuber's correlation:

$$\frac{q_{CHF,FB}}{q_{CHF,PB}} = \left(1 + \frac{C_2 h_{fg} \rho_g G^2}{q^2_{CHF,PB} \rho_{TP}}\right)^{1/2} \tag{3.31}$$

where

$$\rho_{TP} = \frac{1}{\left(\frac{x}{\rho_g} + \frac{1-x}{\rho_f}\right)} \tag{3.32}$$

$$u_{TP} = G\left(\frac{x}{\rho_g} + \frac{1-x}{\rho_g}\right) \tag{3.33}$$

and $q_{CHF,PB}$ is equal to the q_{max} illustrated in equation (2.1). A regression analysis through the data yields $C_2 = 0.002$.

3.2.5 Hwang and Yao's correlation (1984)

Hwang and Yao (1984) studied the effects of quality, flow velocity and channel blockage ratio on the boiling heat transfer and the CHF by placing a DC heated cylinder of 19.1 mm OD. horizontally in a rectangular channel with vertical upward Freon-113 flow at near atmospheric pressure. The flow velocity is varied in a range from 0.003 to 0.235 m/s, and the upstream flow quality is in a range from 0 to

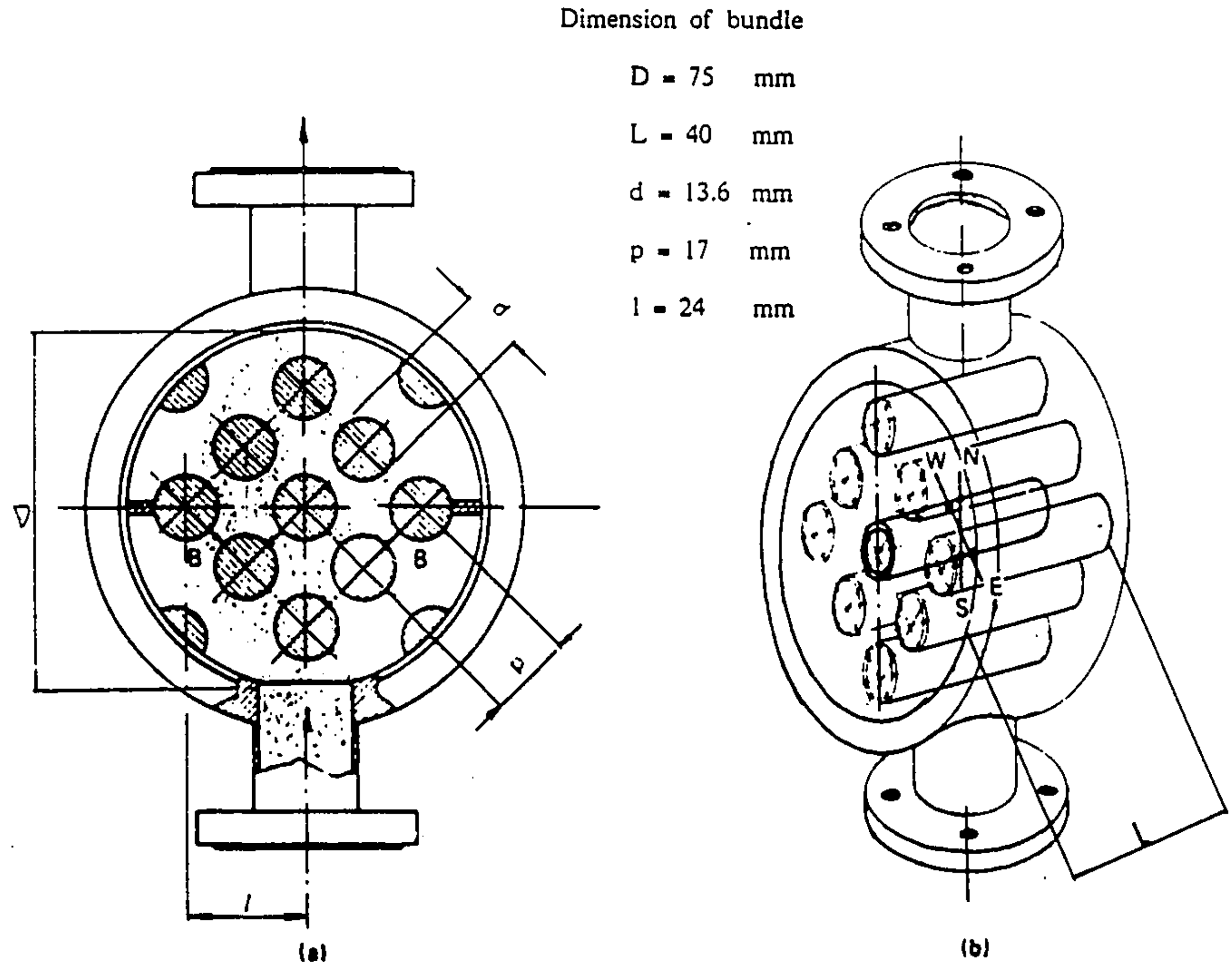

Figure 3.8: The visualized test section of Cumo's experiment

0.143. An empirical correlation for CHF, then, was presented:

$$\frac{q_{max}}{\rho_g h_{fg} U_\infty} = 0.594 We_g^{-0.476}(1-x)^{0.952}(R^*)^{0.36}\frac{1-\left(\frac{D}{w}\right)^{0.86}}{2.25+\left(\frac{\rho_g}{\rho_f}\right)^{0.15}} \tag{3.34}$$

where R^* is equivalent to R' expressed in equation (3.9). Hwang and Yao's empirical CHF correlation shows that the CHF decreases with increasing quality and increasing blockage ratio (D/w), whereas CHF increases weakly with increasing velocity. The main difference between Hwang and Yao's correlation and the other correlations mentioned above is that Hwang and Yao's correlation considered the quality effect as well as the blockage effect in the flow. However, the use of this empirical correlation is limited by the availability for the narrow range of velocity.

Chapter 4

Analysis of CHF for Cross Flow

4.1 Nature of Mass-energy Balance

4.1.1 General

In Chapter 3, Two analytical models of CHF for cross-flow boiling have been discussed. Their applications are restricted in region for the flow at saturated liquid condition. If the flow has quality effect, the energy equation across the heated surface should be reconsidered. In order to solve the energy equation for the flow has quality effect, the assumptions used in Lienhard and Eichhorn's $MESC$ model have been adapted rather than Katto and Haramura's hydrodynamic model. The reason to choose Lienhard and Eichhorn's model is that, unlike Katto and Haramura's model, Lienhard and Eichhorn avoided solving the hydrodynamic unstable problem (Taylor instability or Helmholtz instability) and replaced it by studying the mechanical energy balance between the core of vapor sheet and the interface of liquid and vapor phases. The phenomenon of the hydrodynamic instability is not well understood so far.

4.1.2 Flow in saturated liquid condition

Before setting up the control volume for present analysis, some assumptions of the flow conditions have been made:

(1) vapor removal is an action of a two-dimensional flow pattern

(2) thickness of vapor sheet is defined as $2\alpha R$, which is identical to Lienhard and Eichhorn's definition.

(3) saturated fluid flows across the heated cylinder

Then, a stationary control volume to describe these assumptions is illustrated in Fig. 4.1 and the equations of mass and energy balances for satisfying the flow condition are listed as follows:

For mass balance

$$\dot{m}_\infty = \dot{m}_l + \dot{m}_g \tag{4.1}$$

and for energy balance

$$\dot{m}_\infty h_f + \frac{1}{2}\dot{m}_\infty U_\infty^2 + \ddot{q}2\pi RL = \dot{m}_l h_f + \frac{1}{2}\dot{m}_l U_l^2 + \dot{m}_g h_g + \frac{1}{2}\dot{m}_g (U_\infty + U_g)^2 \tag{4.2}$$

where $\dot{m}_\infty$ mass flow rate of fluid at the inlet of the control volume, i.e, $\dot{m}_\infty = \rho_f U_\infty A_\infty$

$\dot{m}_l$ mass flow rate of liquid at the outlet of the control volume, i.e., $\dot{m}_l = \rho_f U_l A_\infty (1 - \alpha_v)$

$\dot{m}_g$ mass flow rate of vapor at the outlet of the control volume, i.e.,

$\dot{m}_g = \rho_g (U_\infty + U_g) A_\infty \alpha_v$, where A_∞ is the cross-sectional area of the control volume, or WL, α_v the void fraction in the control volume, i.e., $2\alpha R/W$, U_∞ and U_l liquid velocities at the inlet and outlet of the control volume, and U_g the vapor velocity relative to liquid flow.

h_f saturated enthalpy of liquid.

and

h_g saturated enthalpy of vapor, or $h_g = h_f + h_{fg}$.

Substituting the expressions of $\dot{m}_\infty$, $\dot{m}_l$ and $\dot{m}_g$ into equations (4.1) and (4.2), equation (4.1) yields

$$\rho_f U_\infty = \rho_f U_l (1 - \alpha_v) + \rho_g (U_\infty + U_g) \alpha_v \tag{4.3}$$

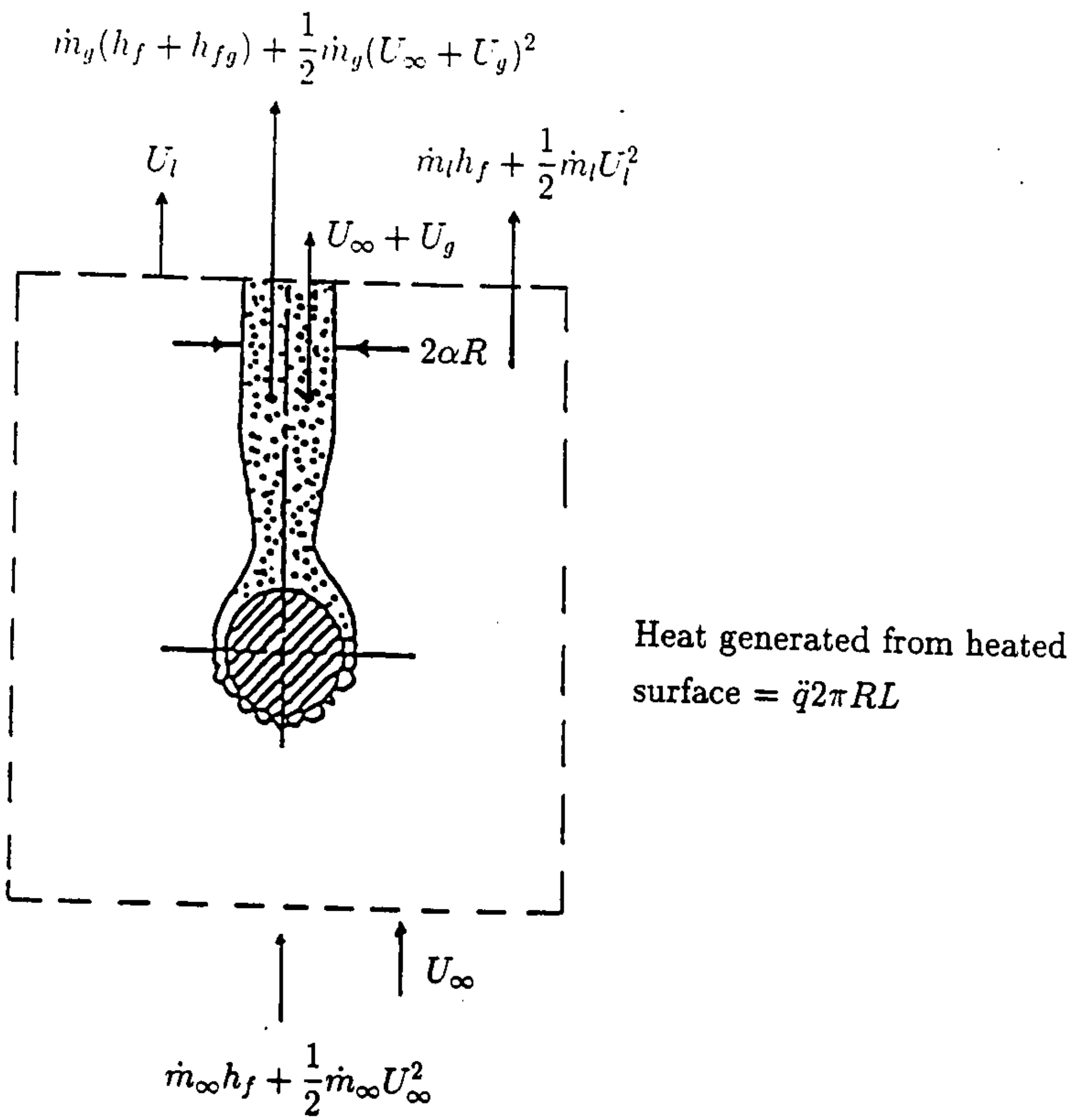

Figure 4.1: Control volume for mass-energy balance at saturated flow condition for present study

and equation (4.2) becomes

$$\begin{aligned}\frac{\ddot{q}2\pi RL}{A_\infty} &= \rho_f U_l(1-\alpha_v)h_f + \frac{1}{2}\rho_f U_l(1-\alpha_v)U_l^2 + \rho_g(U_\infty + U_g)\alpha_v h_f \\ &+\rho_g(U_\infty + U_g)\alpha_v h_{fg} + \frac{1}{2}\rho_g(U_\infty + U_g)\alpha_v(U_\infty + U_g)^2 - \rho_f U_\infty h_f \\ &-\frac{1}{2}\rho_f U_\infty U_\infty^2 \end{aligned} \tag{4.4}$$

In the last two terms of equation (4.4), components of $\rho_f U_\infty$ can be substituted by equation (4.3). If A_∞ is replaced by WL, equation (4.4) yields

$$\begin{aligned}\frac{\ddot{q}2\pi RL}{WL} &= \rho_f U_l(1-\alpha_v)h_f + \frac{1}{2}\rho_f U_l(1-\alpha_v)U_l^2 + \rho_g(U_\infty + U_g)\alpha_v h_f \\ &+\rho_g(U_\infty + U_g)\alpha_v h_{fg} + \frac{1}{2}\rho_g(U_\infty + U_g)\alpha_v(U_\infty + U_g)^2 - \rho_f U_l(1-\alpha_v)h_f \\ &-\rho_g(U_\infty + U_g)\alpha_v h_f - \frac{1}{2}[\rho_f U_l(1-\alpha_v) + \rho_g(U_\infty + U_g)\alpha_v]U_\infty^2 \end{aligned} \tag{4.5}$$

Equation (4.5) can be simplified because some pairs of the terms can be eliminated or combined with each other. It, then, results in

$$\begin{aligned}\frac{\ddot{q}2\pi R}{W} &= \frac{1}{2}\rho_f U_l(1-\alpha_v)(U_l^2 - U_\infty^2) + \rho_g(U_\infty + U_g)\alpha_v h_{fg} \\ &+\frac{1}{2}\rho_g(U_\infty + U_g)\alpha_v[(U_\infty + U_g)^2 - U_\infty^2] \end{aligned} \tag{4.6}$$

From Lienhard and Eichhorn's model, they assumed the downstream velocity of heated cylinder remains the same as that of the incoming flow. This implies that U_l is equal to U_∞. In the present case, it is convenient to adopt their assumption so that the first term at the right hand side of equation (4.6) can be cancelled out and yields

$$\frac{\ddot{q}2\pi R}{W\alpha_v} = \rho_g(U_\infty + U_g)h_{fg} + \frac{1}{2}\rho_g(U_\infty + U_g)[U_\infty^2 + 2U_\infty U_g + U_g^2 - U_\infty^2] \tag{4.7}$$

Because $\alpha_v = 2\alpha R/W$, equation (4.7) again can be simplified to

$$\frac{\pi\ddot{q}}{\alpha} = \rho_g h_{fg}(U_\infty + U_g)[1 + \frac{1}{2h_{fg}}(2U_\infty U_g + U_g^2)] \tag{4.8}$$

Again rearranging the equation (4.8), we finally obtain

$$\frac{\pi\ddot{q}}{\rho_g U_\infty h_{fg}} = \alpha\left(1 + \frac{U_g}{U_\infty}\right)\left[1 + \frac{U_\infty^2}{2h_{fg}}\left(\frac{U_g}{U_\infty}\right)\left(2 + \frac{U_g}{U_\infty}\right)\right]$$

or

$$\phi = \alpha\left(1 + \frac{U_g}{U_\infty}\right)\left[1 + \frac{1}{2}E_c\left(\frac{U_g}{U_\infty}\right)\left(2 + \frac{U_g}{U_\infty}\right)\right] \tag{4.9}$$

where

$$\phi = \frac{\pi \ddot{q}}{\rho_g U_\infty h_{fg}} \tag{4.10}$$

$$E_c = \frac{U_\infty^2}{h_{fg}}$$

E_c is the Eckert number during phase change.

Compared with equation (3.14), equation (4.9) is identical to equation (3.14) except the additional term, $E_c(U_g/U_\infty)(2 + U_g/U_\infty)/2$. From the present analysis with low-flow velocity this term is much smaller in comparison with unity because E_c is near the value at the order of -6. Even in the high-flow region, the influence by this term is still very small. In other words, we obtained a form close to equation (3.14).

4.1.3 Flow other than saturated liquid condition

The use of equations (3.14) and (4.9) are limited by the flow condition for which they can apply. In some cases, the flow at the inlet control volume may not be at saturated condition. Thus, in this section, an attempt to extend the analysis of mass-energy balance for boiling in cross-flow at which the flow is in other than a saturated liquid condition was also conducted. For this case, the third item of the previous assumptions should be modified to

(3) the equilibrium quality, x, of the flow may not be zero.

and an additional assumption is

(4) the variation of equilibrium quality in the bulk liquid across the heated cylinder is negligible.

According to the modified assumptions, some parameters denoted in the previous control volume should be corrected to satisfy the new flow condition as illustrated in Fig. 4.2. Thus the mass and energy balance equations can be rewritten as follows:

For mass balance

$$\dot{m}_\infty = \dot{m}_l + \dot{m}_g \tag{4.11}$$

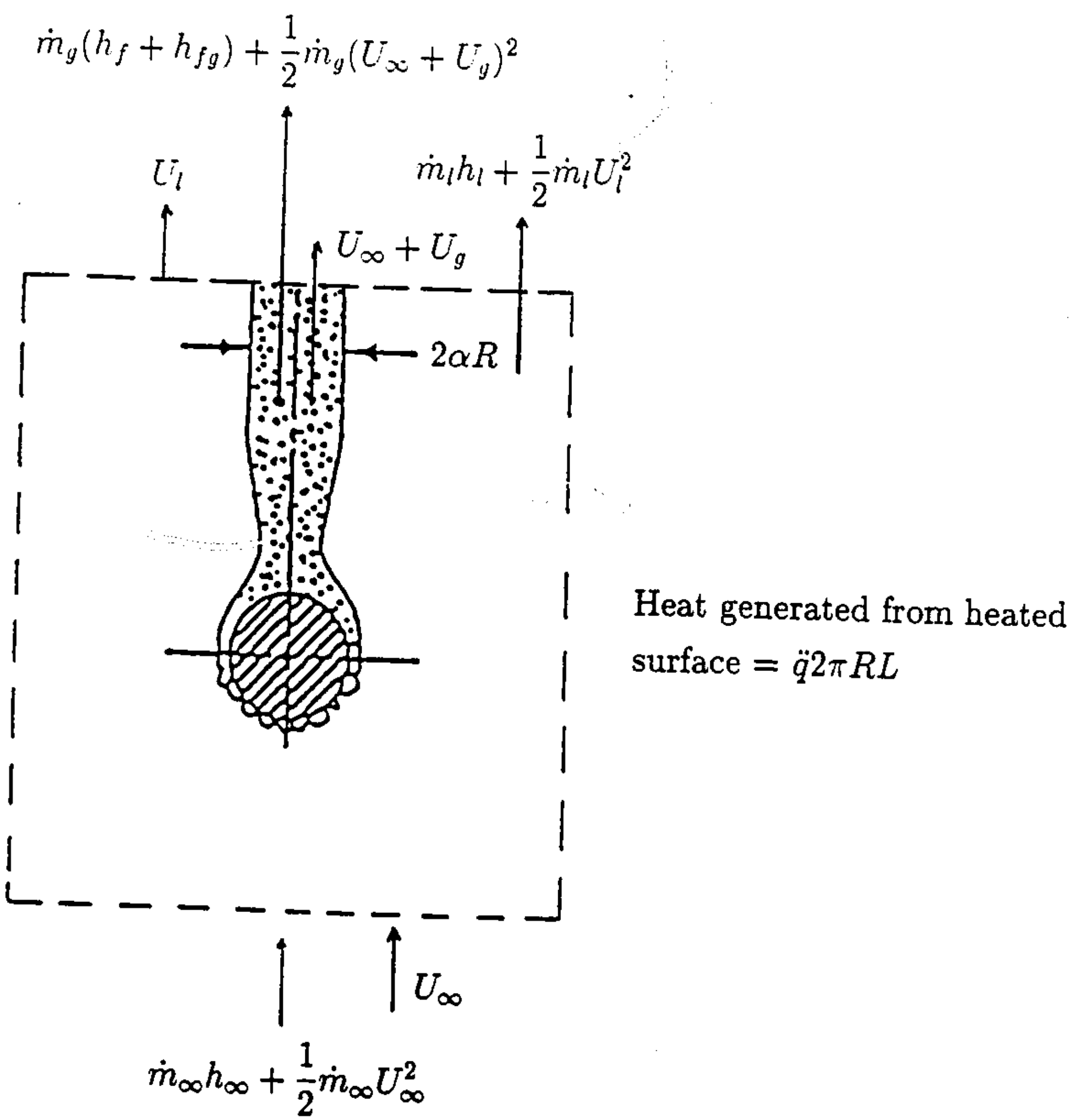

Figure 4.2: Control volume for mass-energy balance at $x \neq 0$ for present study

where

$$\dot{m}_\infty = \overline{\rho} U_\infty A_\infty$$
$$\dot{m}_l = \overline{\rho} U_l A_\infty (1-\alpha_v)$$
$$\dot{m}_g = \rho_g (U_\infty + U_g) A_\infty \alpha_v$$

$\overline{\rho}$ is the fluid density referring to the corresponding quality.

and

ρ_g is the vapor density.

and for the energy balance

$$\dot{m}_\infty h_\infty + \frac{1}{2}\dot{m}_\infty U_\infty^2 + \ddot{q}2\pi RL = \dot{m}_l h_l + \frac{1}{2}\dot{m}_l U_l^2 + \dot{m}_g h_g + \frac{1}{2}\dot{m}_g (U_\infty + U_g)^2$$

or

$$\ddot{q}2\pi RL = \dot{m}_l h_l + \frac{1}{2}\dot{m}_l U_l^2 + \dot{m}_g h_g + \frac{1}{2}\dot{m}_g (U_\infty + U_g)^2 - \dot{m}_\infty h_\infty - \frac{1}{2}\dot{m}_\infty U_\infty^2 \quad (4.12)$$

where

$$h_l = h_\infty = h_f + x h_f g$$
$$h_g = h_f + h_f g$$

Substituting $\dot{m}_\infty$, $\dot{m}_l$ and $\dot{m}_g$ into equations (4.11) and (4.12) with some manipulations for simplification, it yields

$$\overline{\rho} U_\infty = \overline{\rho} U_l (1-\alpha_v) + \rho_g (U_\infty + U_g)\alpha_v \quad (4.13)$$

and

$$\begin{aligned}\frac{\ddot{q}2\pi RL}{A_\infty} = {} & \overline{\rho} U_l (1-\alpha_v)(h_f + x h_{fg}) + \frac{1}{2}\overline{\rho} U_l (1-\alpha_v) U_l^2 + \rho_g (U_\infty + U_g)\alpha_v (h_f + h_{fg}) \\ & + \frac{1}{2}\rho_g (U_\infty + U_g)\alpha_v (U_\infty + U_g)^2 - \overline{\rho} U_\infty (h_f + x h_{fg}) - \frac{1}{2}\overline{\rho} U_\infty U_\infty^2 \quad (4.14)\end{aligned}$$

Combining equations (4.13) and (4.14) and following the similar manner of manipulation as in saturated liquid conditions, a new expression for CHF at flow conditions with a quality effect can be obtained

$$\phi = \alpha \left(1 + \frac{U_g}{U_\infty}\right)\left[1 + \frac{1}{2}\frac{U_\infty^2}{h_{fg}}\frac{U_g}{U_\infty}\left(2 + \frac{U_g}{U_\infty}\right) - x\right]$$

or

$$\phi = \alpha \left(1 + \frac{U_g}{U_\infty}\right)\left[1 + \frac{1}{2}E_c \frac{U_g}{U_\infty}\left(2 + \frac{U_g}{U_\infty}\right) - x\right] \quad (4.15)$$

Equation (4.15) is very similar to equation (4.9) except the difference of an additional term, x, in equation (4.15). If quality is zero, equation (4.15) is identical to equation (4.9). In other words, equation (4.9) is a special case of equation (4.15).

4.2 Evaluation of U_g/U_∞ and α

The objective of Lienhard and Eichhorn's *MESC* model is to solve the ratio of U_g over U_∞. Up to now, this model has been upgraded in several versions by later researchers. In present study, only the original version and the hydrodynamic prediction model presented by Ungar and Eichhorn (1988) are discussed.

4.2.1 Lienhard and Eichhorn's *MESC* model

In section 3.1.2, we have discussed the original *MESC* model postulated by Lienhard and Eichhorn (1976). The term U_g/U_∞ can be expressed by equation (3.17)

$$\frac{U_g}{U_\infty} = \left(\frac{4}{\alpha We_g}\right)^{1/3}$$

From the flow condition, We_g can be calculated according to $We_g = D\rho_g U_\infty^2/\sigma$, so the only unknown in equation (3.17) is α. Lienhard and Eichhorn, then, correlated the value of α for various fluids. The expression of empirical α is shown in equation (3.22) and a list of $\alpha's$ for different fluids is illustrated in Table 4.1. Note that the α is correlated on the basis of experimental results in saturated condition and is valid only for the region of high flow velocity, i.e., two-dimensional flow pattern of vapor. For the low flow velocity, they assumed that α is equal to unity.

4.2.2 Ungar and Eichhorn's hydrodynamic prediction model

Ungar and Eichhorn (1988) conducted experiments to observe the frequency of bubble break-off and the thickness of the vapor sheet for upward cross-flow boiling in order to evaluate the ratio of U_g over U_∞. They used various fluids heated by DC cylindrical heaters ranging from 0.38 to 2.12 *mm* in diameter. Their observation showed that the wake thickness may vary with the distance from the heater and bubble break-off from the wake in low speed up-flow is periodic. They, therefore, used α' in equation (3.14) instead of α to distinguish it from that used in Lienhard and Eichhorn's *MESC* model and modified the expression of U_g/U_∞ in equation (3.17).

Table 4.1: Empirical constant α for different test fluids obtained by Lienhard and Eichhorn (1976)

Liquid	ρ_f/ρ_g	α
water	1459.2	1.39
methanol	686.4	0.79
isopropanol	302.8	0.43
Freon-113	169	0.28

From their hydrodynamic study, CHF for upward cross flow is determined by the frequency of bubble break-off, the most rapidly growing wavelength in the wake, the wake thickness and the vapor velocity in the wake at CHF. The bubble break-off frequency is determined from the Strouhal number, which is defined as

$$St = \frac{fD}{U_\infty} = \frac{D}{\lambda} \tag{4.16}$$

where f is the frequency of vapor departure, D the heater diameter, λ the wavelength of the wave in the wake. The Strouhal number is also correlated on the basis of experimental results as

$$St = 0.947(Fr + 0.614)^{-1.5} \tag{4.17}$$

where Fr is the Froude number, $U_\infty/(gD)^{1/2}$. Since Hagerty and Shea (1955) have analyzed the stability of such a thin vapor sheet, their result was used by Kheyrandish and Lienhard (1985) to determine the most rapidly growing wavelength, or Helmholtz wavelength, λ_H,

$$\frac{\lambda_H}{D} = 2\pi \frac{U_\infty}{U_g} \sqrt{\frac{3\alpha'}{2We_g}} \tag{4.18}$$

Ungar and Eichhorn's experiments showed that waves move at the same velocity as the liquid. Therefore, at CHF, $f = U_\infty/\lambda_H$ where λ in equation (4.16) is replaced by λ_H. Thus, equation (4.18) yields

$$\frac{U_g}{U_\infty} = 2\pi St \sqrt{\frac{3\alpha^*}{2We_g}} \tag{4.19}$$

Ungar and Eichhorn used an effective wake thickness, α^*, in equation (4.19) because the actual wake thickness changes with the distance from the heater. The effective wake thickness is the thickness that determines the most rapidly growing wavelength in the wake. The α^*, then, is correlated and plotted against the Froude number for various fluids on the basis of their experimental results as well as the results obtained by Min (1975), Lienhard and Eichhorn (1976), Hasan et al. (1981), and Vliet and Leppert (1964). Only those data for $G_c \leq 8$ are included in their analysis, where G_c is expressed by equation (3.27). The final form of α^*, then, is correlated as

$$\alpha^* = 0.28 Fr^c \tag{4.20}$$

where

$$c = 0.137 r^{0.264} \tag{4.21}$$

$$r = \frac{\rho_f}{\rho_g}$$

4.2.3 Application of U_g/U_∞

Since U_g/U_∞ has been obtained by Lienhard and Eichhorn (1976) and Ungar and Eichhorn (1988) respectively, U_g/U_∞ is now ready to be substituted back into equation (3.14). The result obtained by Lienhard and Eichhorn has been shown in equation (3.18) and its alternative form is

$$\phi = \left[1 + \left(\frac{4}{\alpha We_g}\right)^{1/3}\right]\alpha \tag{4.22}$$

On the other hand, the result derived by Ungar and Eichhorn yields

$$\phi = \left(1 + 2\pi St\sqrt{\frac{3\alpha^*}{2We_g}}\right)\alpha^* \tag{4.23}$$

In addition, the term of U_g/U_∞ used in equation (4.9) and (4.15), which was obtained from present study, has the same meaning as that used in Lienhard and Eichhorn's $MESC$ model and Ungar and Eichhorn's hydrodynamic model. Therefore, equation (4.9) is able to predict CHF for cross flow by employing their derivations of U_g/U_∞. However, equation (4.15) cannot be used so far because the thickness of the vapor sheet at flow other than saturated condition hasn't been correlated. Thus, more work has to be done on this study. In fact, the measurement of thickness for vapor sheet is just a method to attack this problem for solving U_g/U_∞. However, the other approach can be attempted as long as the U_g/U_∞ can be derived easily and accurately.

4.3 Derivation of Effective Thickness of Vapor Sheet for The Flow with Quality Effect

Due to the lack of α^* which can be used in the flow at other than saturated liquid condition, efforts to find the α^* for flows with quality effect have been made in the present study. Compared with the α^* derived by Ungar and Eichhorn, the α^* obtained from the present study has an additional independent variable, that is, quality. Recall that, in equation (4.20), α^* is expressed as $\alpha^* = f(Fr)$, where the exponential variable of Fr is a function of density ratio only. However, in the present study α^* is postulated as $\alpha^* = f(Fr, 1-x)$ and both the exponential variables of Fr and $(1-x)$ are also a function of density ratio. Thus, the general expression of α^* is written as

$$\alpha^* = b\, Fr^c(1-x)^a \tag{4.24}$$

where a, b and c are empirical constants obtained by a least square method for the individual test fluid.

4.3.1 Calculations of α^* in present study

Instead of equation (3.14), equation (4.15) is used to calculate the values of α^* because of the consideration of the quality effect. However, the term of $\frac{1}{2}E_c(U_g/U_\infty)[2+(U_g/U_\infty)]$ in equation (4.15) is negligible because E_c results in a very small value in the low flow region. Thus, equation (4.15) can be reduced to

$$\phi = \alpha^* \left(1 + \frac{U_g}{U_\infty}\right)(1-x) \tag{4.25}$$

where U_g/U_∞ is employed from equation (4.19) and the Strouhal number (St) used in this equation is determined by equation (4.17) rather than equation (4.16). Ungar and Eichhorn obtained a very good result from correlating the Strouhal number based on experimental data of various fluids. It is shown in Figs. 4.3 – 4.5. One question could arise as to whether it is reasonable for the use of Strouhal number determined by equation (4.17) in the flow condition with quality effect. However, reviewing from equation (4.17) and the definition of Froude number, $Fr = U_\infty/(gD)^{1/2}$, the characteristic of the correlation for Strouhal number contains no fluid properties. As a result, Ungar and Eichhorn concluded that the frequency of bubble break-off in low speed up-flow is determined only by the cylinder diameter, the acceleration of gravity, and the speed of the flow. In addition, equation (4.17) was developed from experimental data for various fluids which have widely dissimilar physical properties. Thus, equation (4.17) is valid for any liquid in low speed up-flow and the flow condition with or without quality effect.

Now since the doubt for using equation (4.17) has been cleared, equations (4.19) and (4.25) can be combined and yield

$$\phi = \alpha^* \left(1 + 2\pi St\sqrt{\frac{3\alpha^*}{2We_g}}\right)(1-x) \tag{4.26}$$

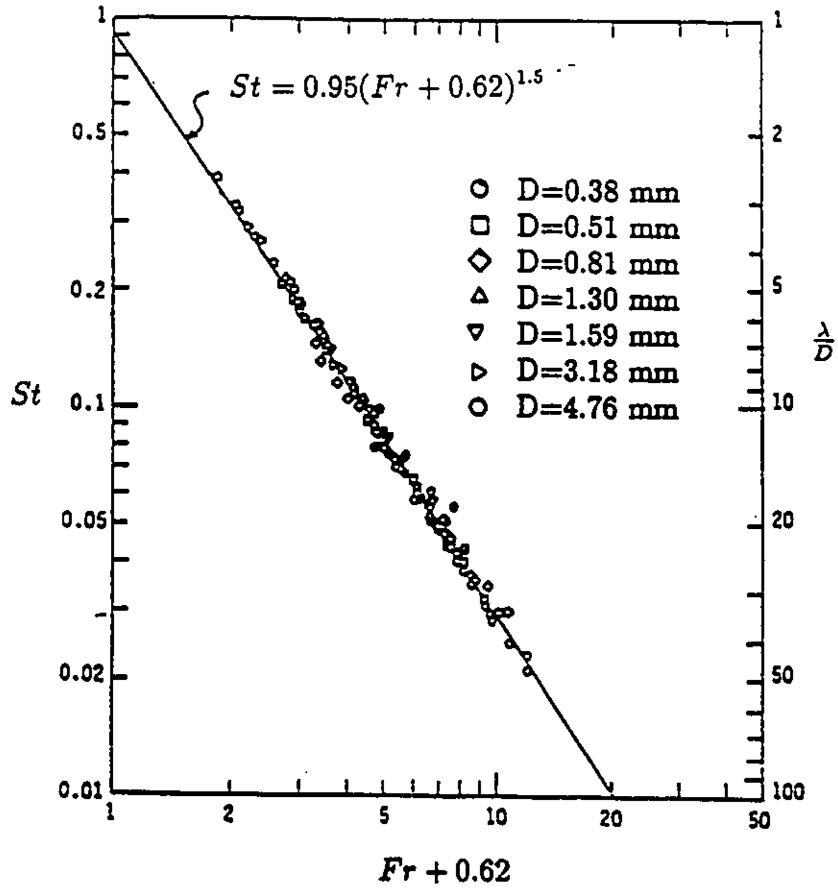

Figure 4.3: Strouhal number vs. Froude number obtained by Ungar and Eichhorn (1988) - acetone

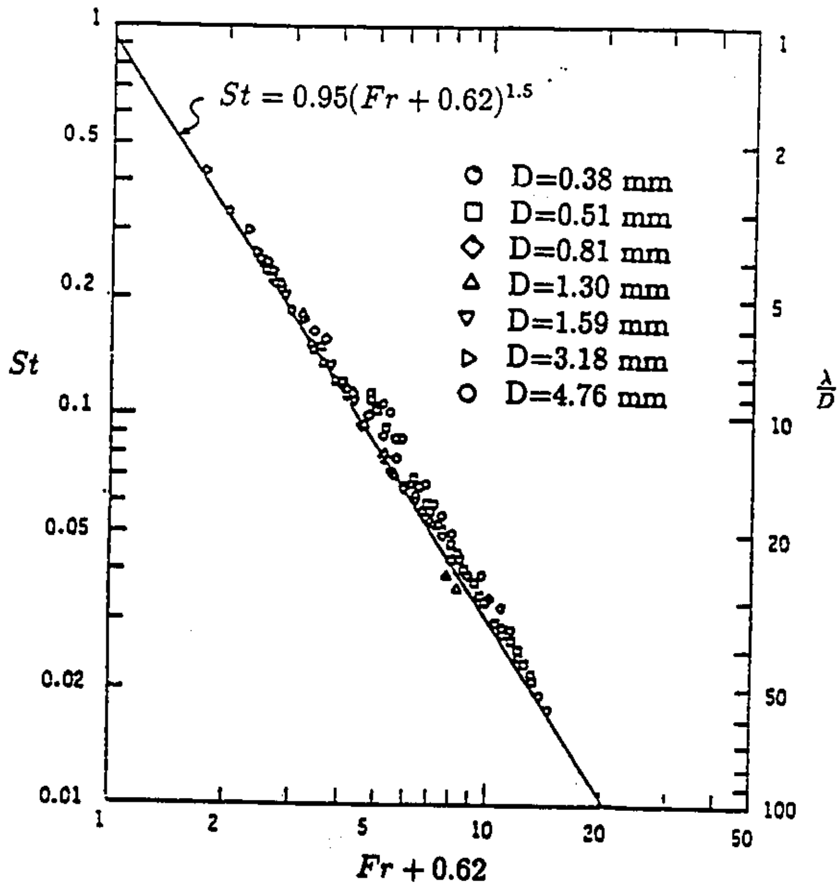

Figure 4.4: Strouhal number vs. Froude number obtained by Ungar and Eichhorn (1988) - isopropanol

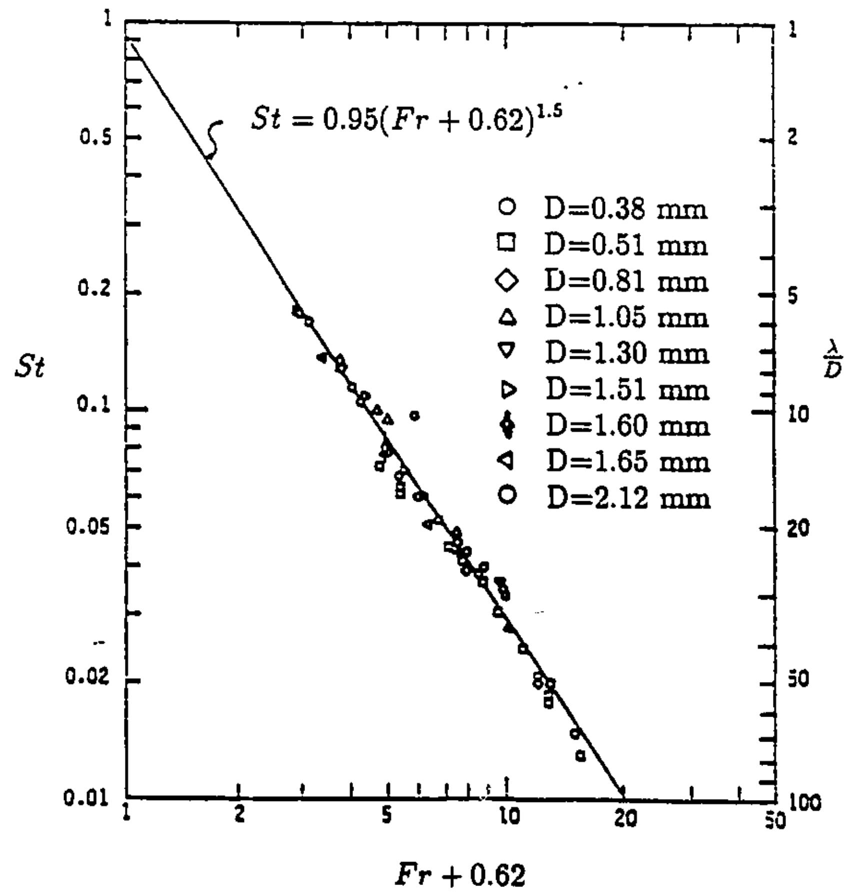

Figure 4.5: Strouhal number vs. Froude number obtained by Ungar and Eichhorn (1988) - water

The sources of experimental results used to evaluate α^* in the present study are listed in Table 4.2. Before correlating the calculated α^* to the form as illustrated in equation (4.24), whether the trends for α^* versus Fr and $(1-x)$ agree with the postulated equation have been observed first. Figures 4.6 – 4.13 show that the calculated values of α^* for all test fluids increase with increasing Fr. Also, Figures 4.14 – 4.16 show that the α^* increases when $(1-x)$ increases for the results obtained by Vliet (1962), Pourdashti (1984) and Min (1975). For correlating the α^* to the form of equation (4.24), each test fluid results in different values of a, b and c and they are listed in Table 4.3.

4.3.2 Correlations of Exponential Variables–a, b and c

As shown in Table 4.3, each value of the density ratio corresponds to a set of values a, b and c. Like Ungar and Eichhorn's correlation shown in equation (4.21), c can be expressed as a function of density ratio. However unlike Ungar and Eichhorn's result, in which b is constant along the range of density ratio and equivalent to 0.28 as shown in equation (4.20), the b obtained from present study is not constant with respect to different density ratios. Figs. 4.17 – 4.19 show the distributions of the values of c, a and b listed in Table 4.3 against the density ratio. Efforts have been made to correlate these three exponential values as a function of density ratio. They yield

$$a = 0.0186r^{0.825} \tag{4.27}$$

$$b = 0.341 - 5.7 \times 10^{-5}r \tag{4.28}$$

$$c = 0.086r^{0.329} \tag{4.29}$$

Substituting the above results into equation (4.24), results in

$$\alpha^* = (0.341 - 5.7 \times 10^{-5}r)Fr^{(0.086r^{0.329})}(1-x)^{0.0186r^{0.825}} \tag{4.30}$$

4.4 Assessment of Recommended Prediction Method and Discussion

Since equation (4.30) has illustrated the correlation for α^*, equation (4.26) is ready to predict the non-dimensional CHF, ϕ, while the dimensional prediction of

Table 4.2: Sources of CHF data for upward across single cylinder

Investigator	Number of data	cylinder diameter (mm)	density ratio	Froude number	quality	fluid
Pourdashti	40	6.35	50~100	0.24~1.14	-0.11~0.11	Freon-113
Hasan et al.	19	0.5~1.5	334.7	2.3~11.6	0	isopropanol
Ungar and Eichhorn	15	1.59~4.76	341.8	2.0~7.6	0	isopropanol
Ungar and Eichhorn	45	0.38~2.12	1553	2.2~12.3	0	water
Min	40	0.51~1.65	615	1.8~9.3	0	methanol
Min	62	0.51~1.02	1647	1.8~9.3	-0.02~0	water
Vliet	81	0.25~3.2	1460	1~7	-0.1~0	water
Diesselhorst et al.	31	3~7.5	1609	0.5~2.3	0	water

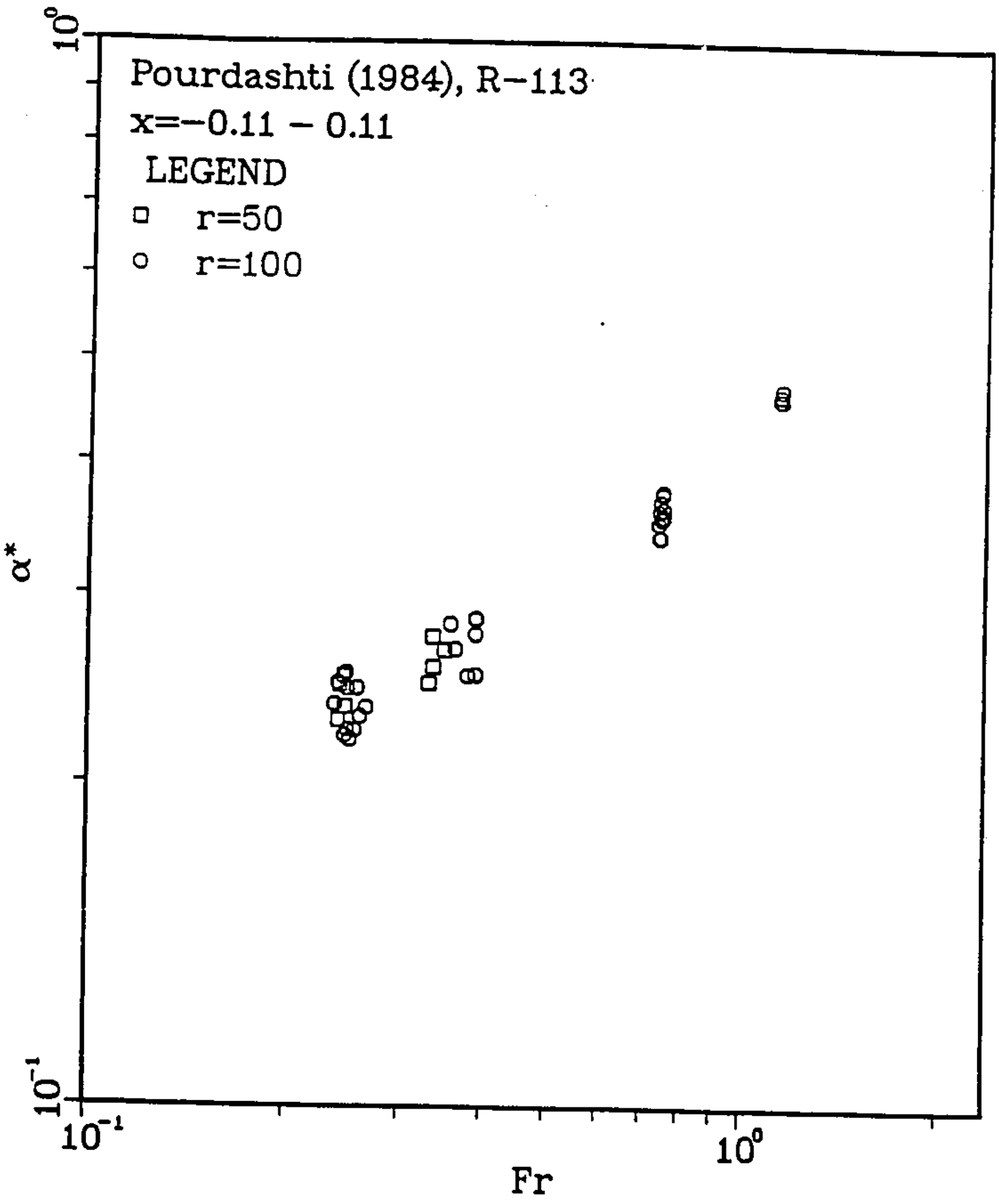

Figure 4.6: Effective vapor sheet thickness vs. Froude number

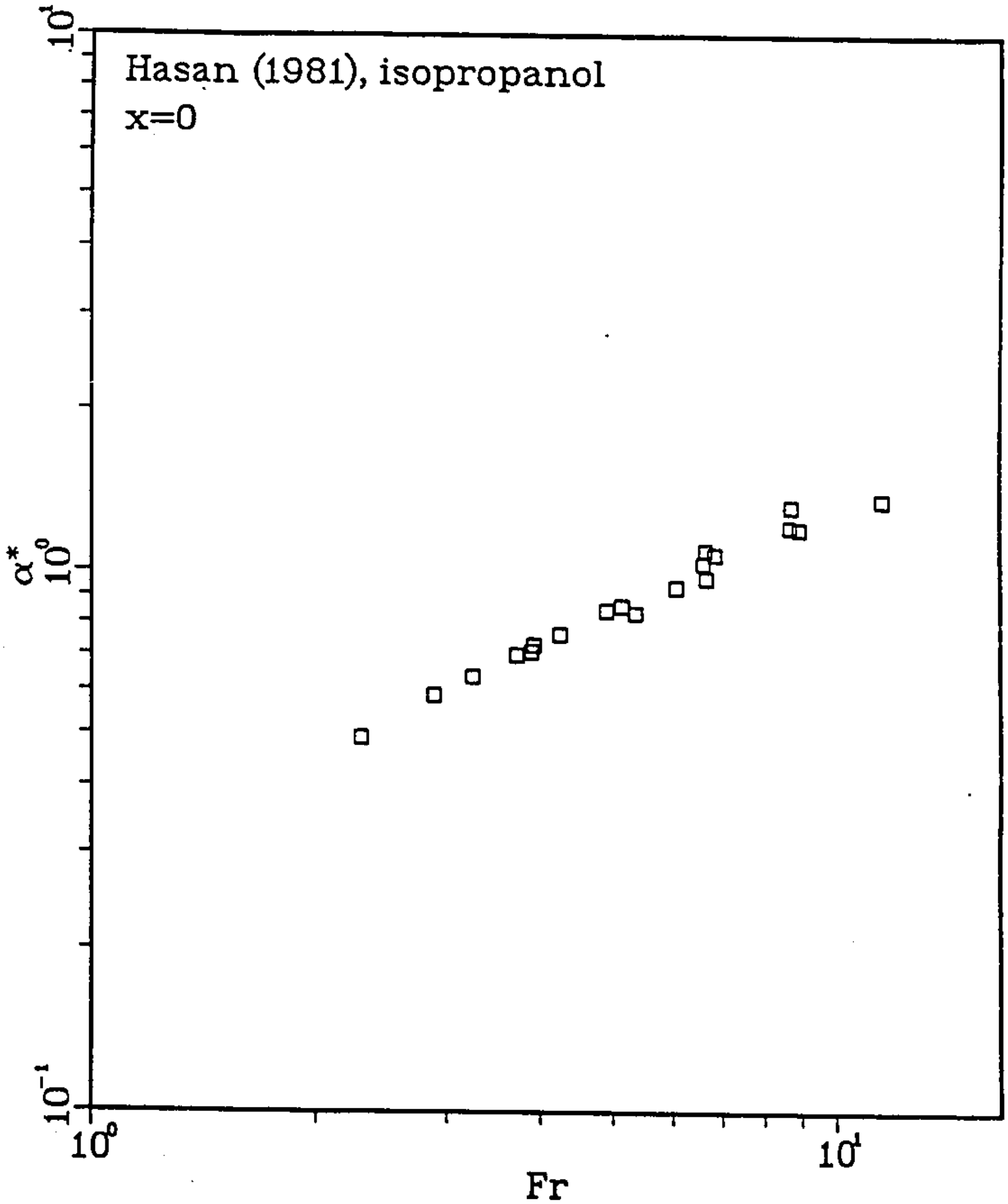

Figure 4.7: Effective vapor sheet thickness vs. Froude number

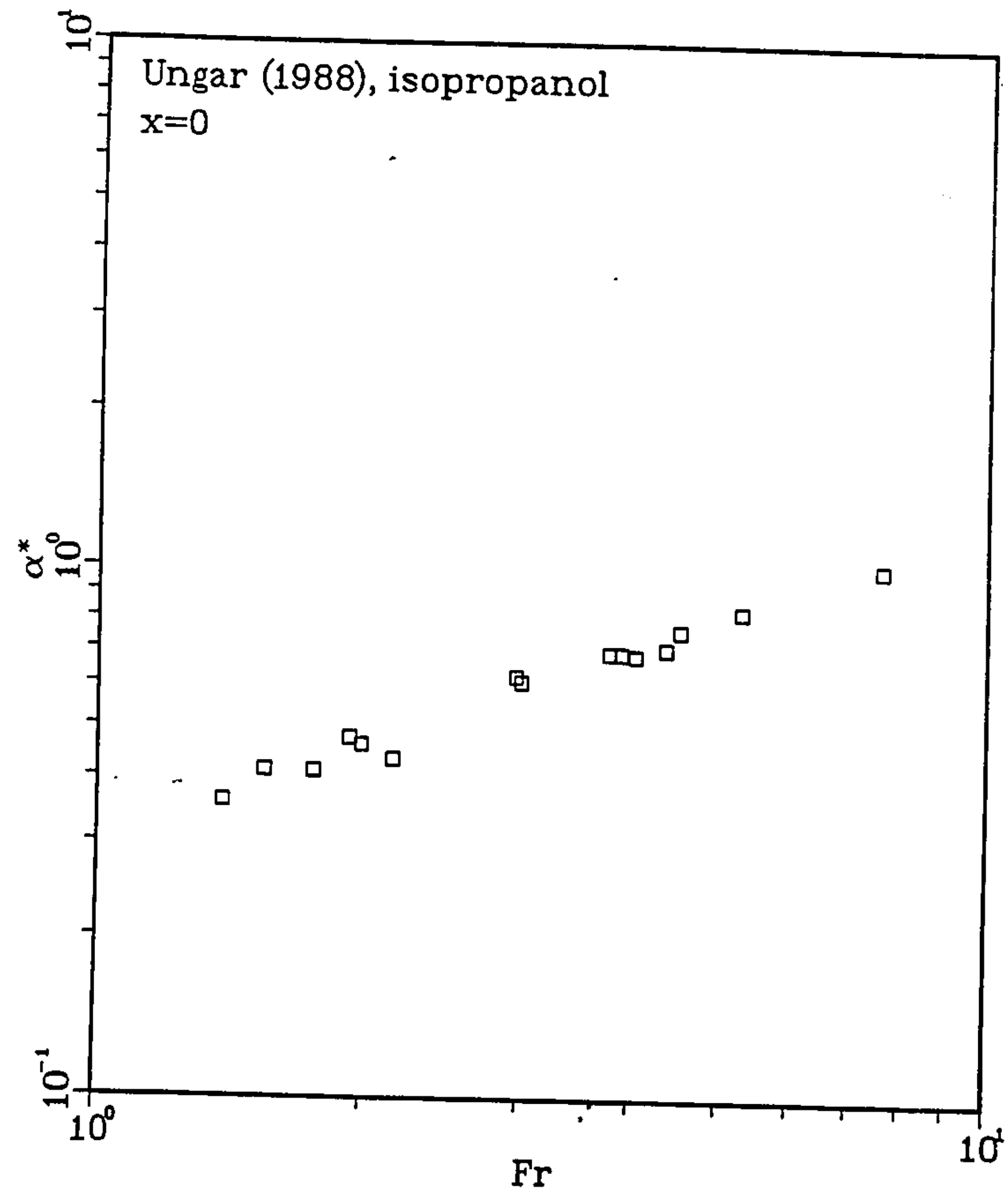

Figure 4.8: Effective vapor sheet thickness vs. Froude number

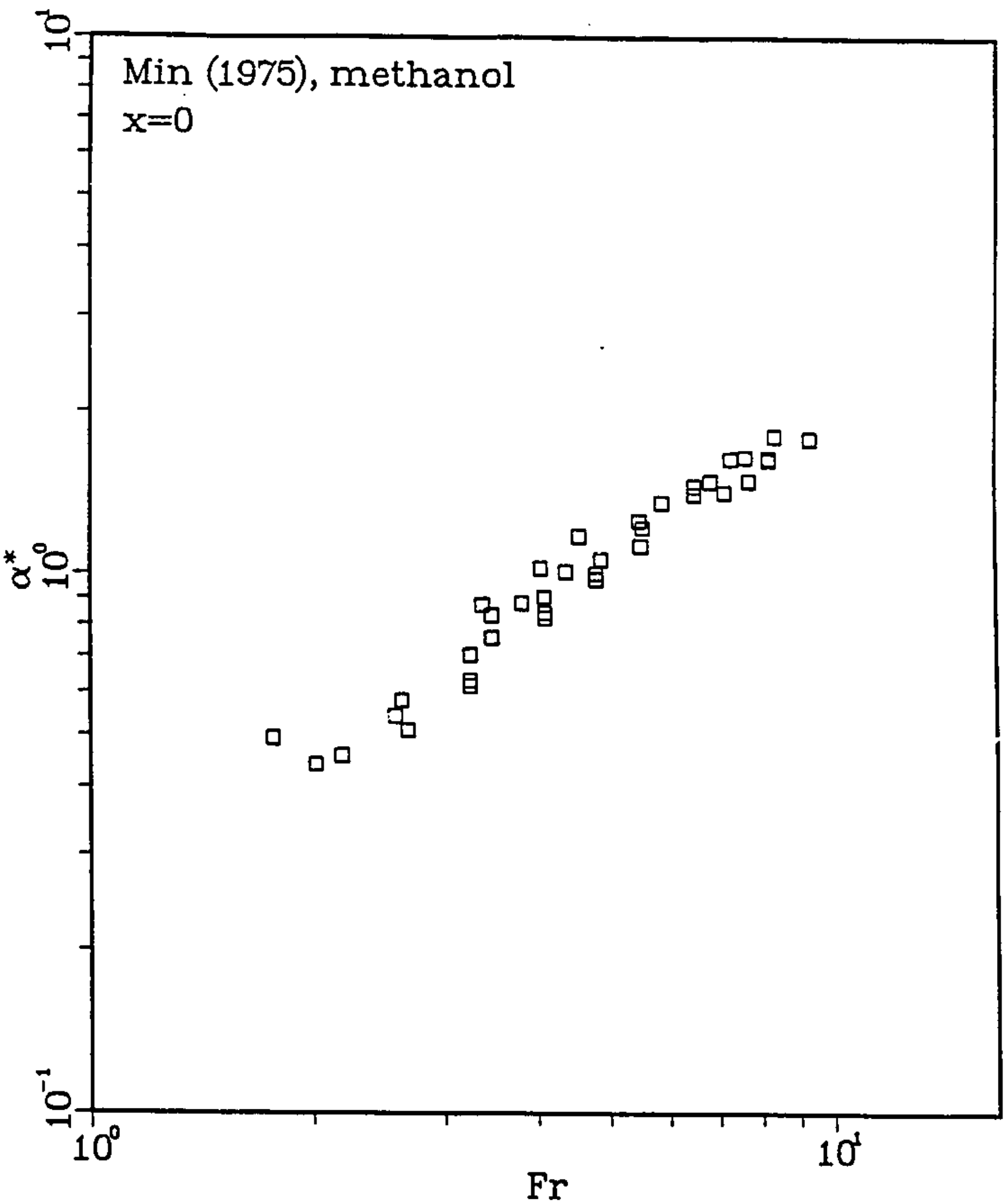

Figure 4.9: Effective vapor sheet thickness vs. Froude number

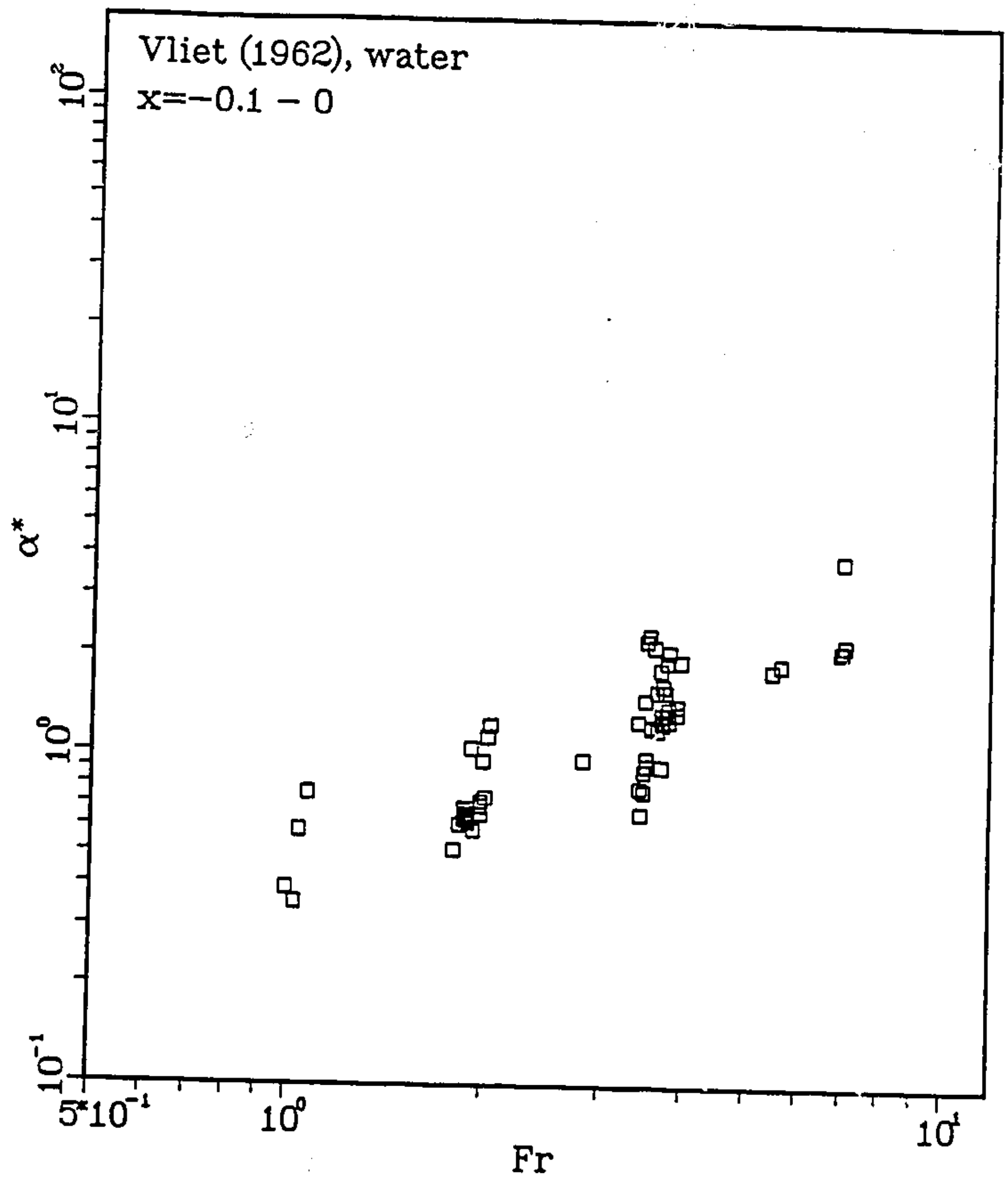

Figure 4.10: Effective vapor sheet thickness vs. Froude number

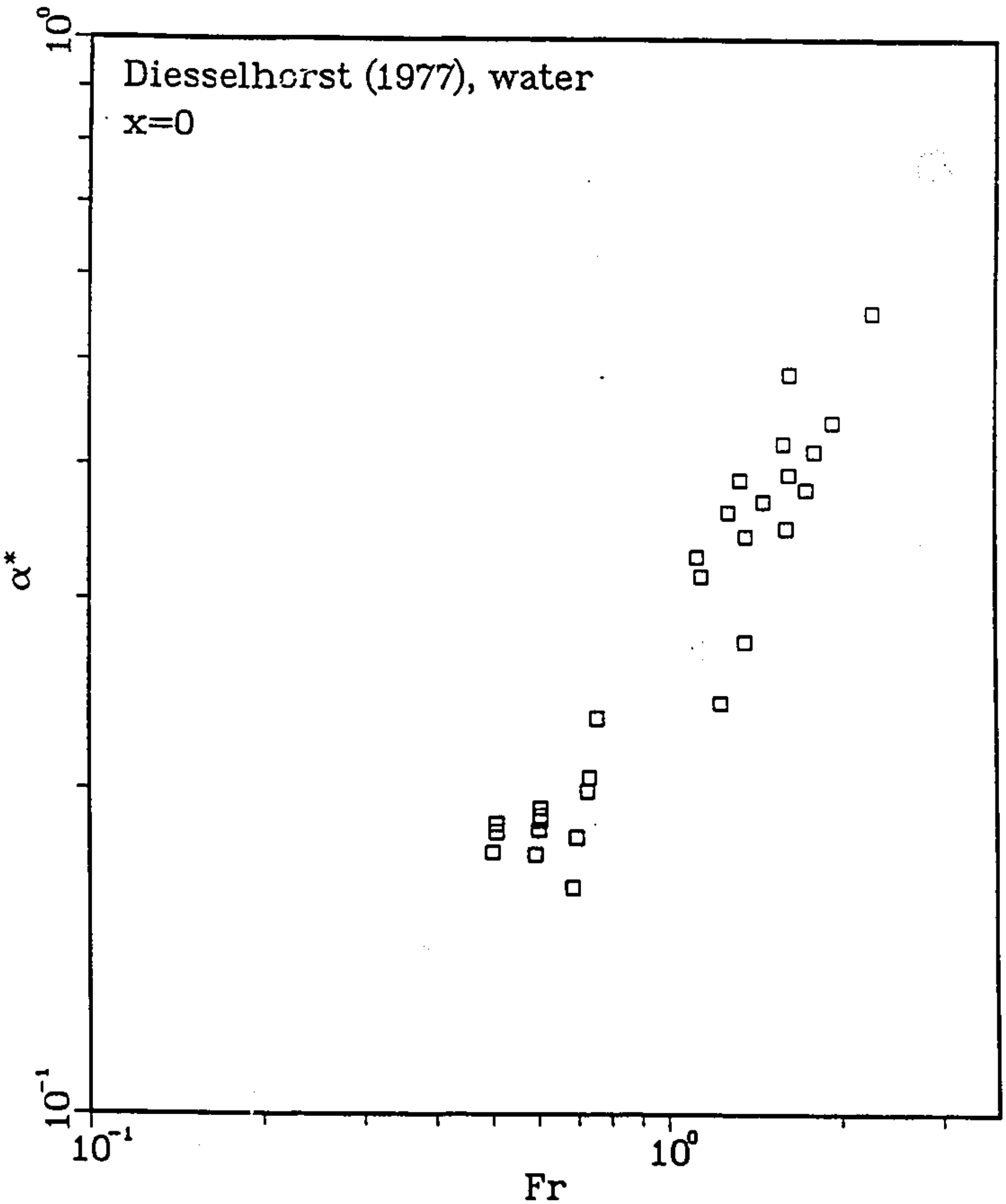

Figure 4.11: Effective vapor sheet thickness vs. Froude number

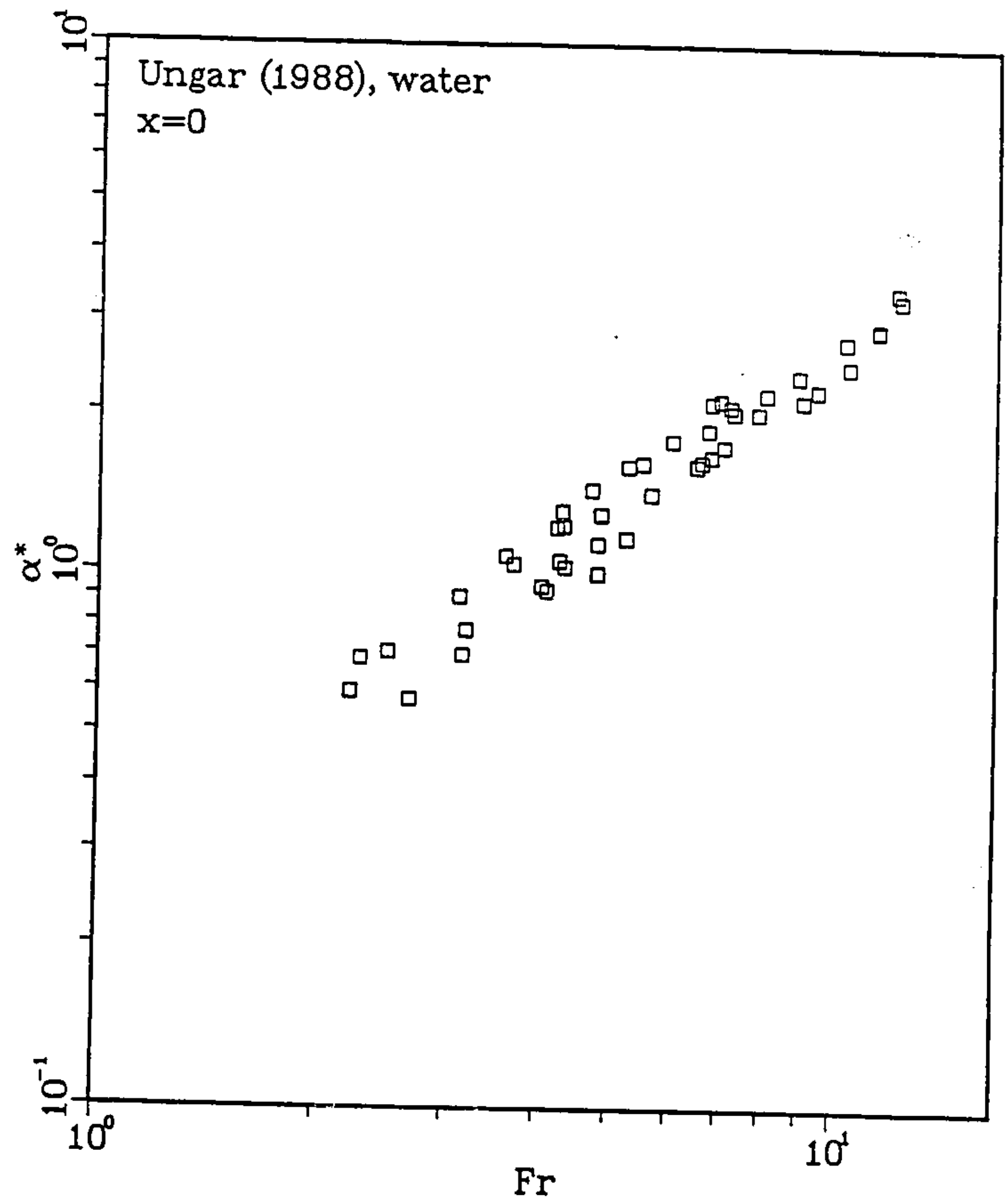

Figure 4.12: Effective vapor sheet thickness vs. Froude number

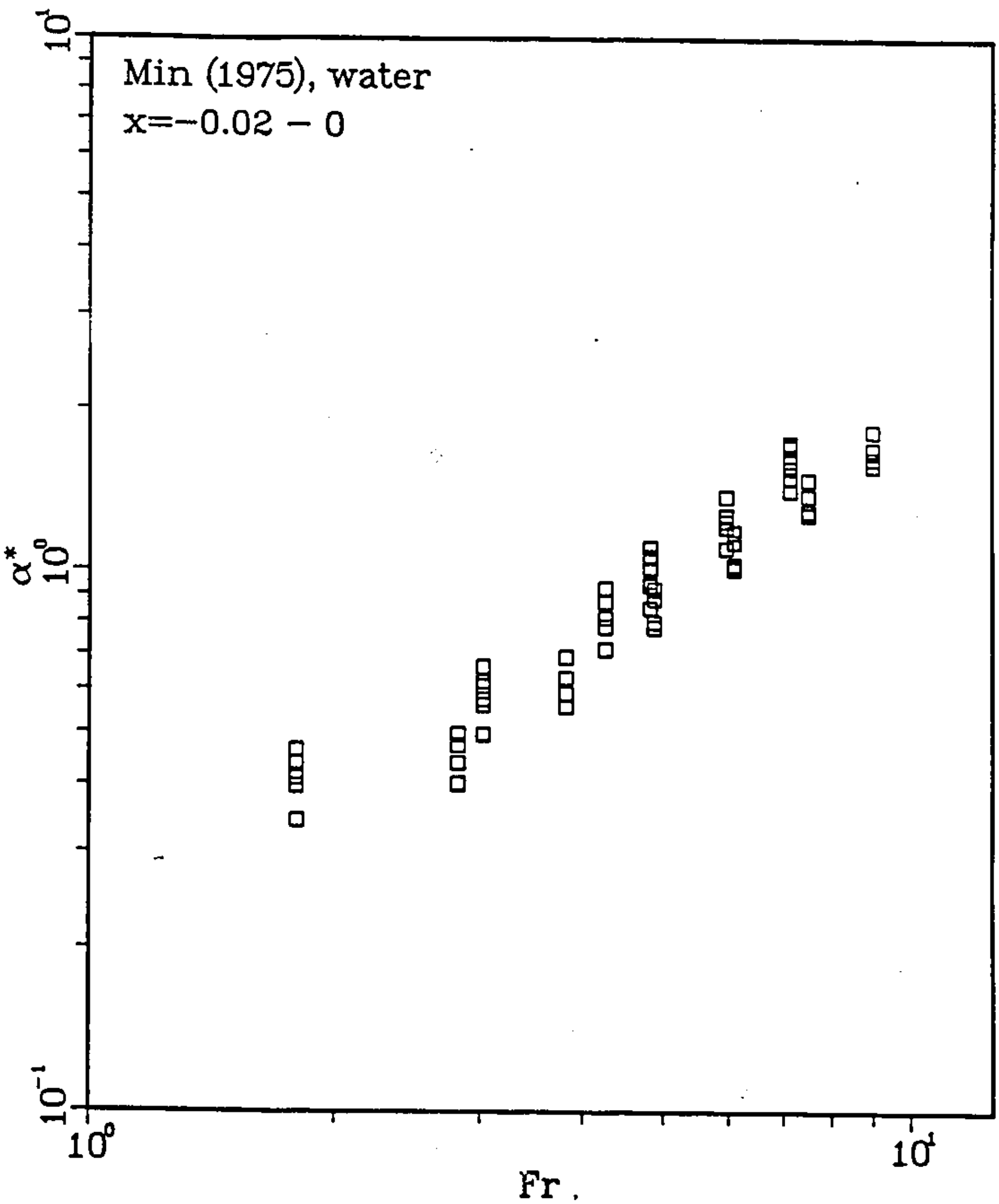

Figure 4.13: Effective vapor sheet thickness vs. Froude number

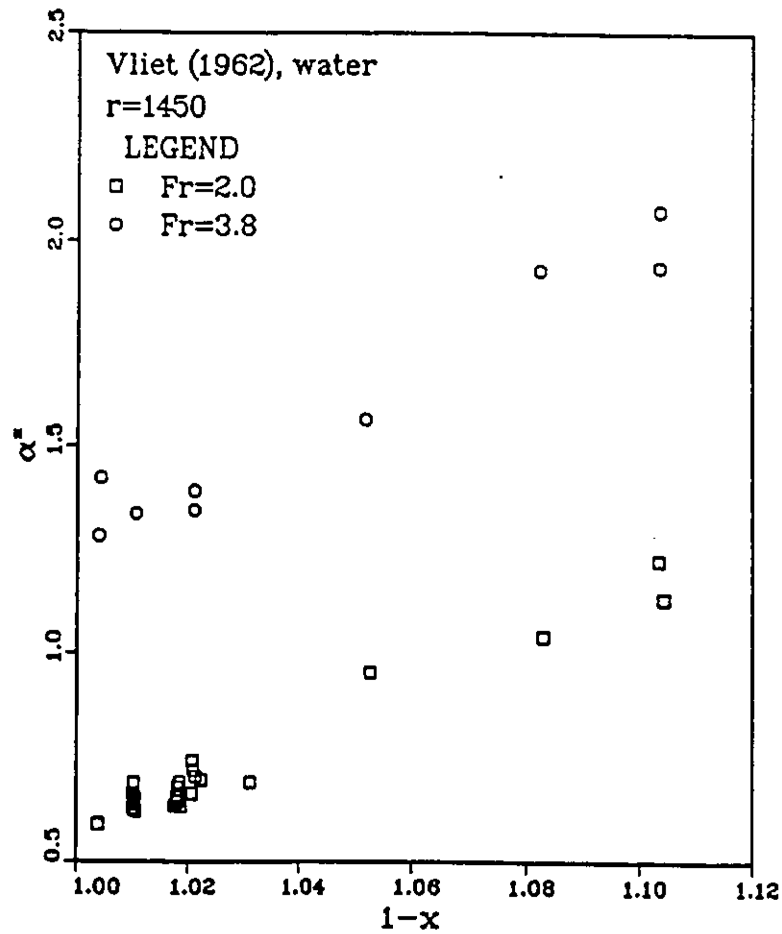

Figure 4.14: Effective vapor sheet thickness vs. $(1 - x)$

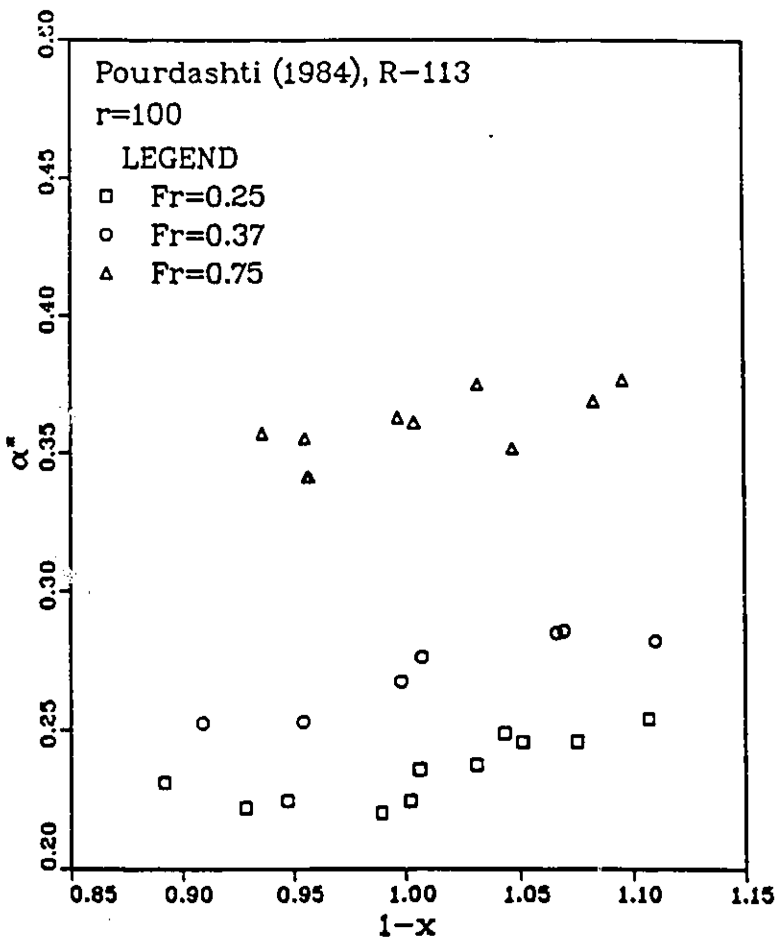

Figure 4.15: Effective vapor sheet thickness vs. $(1 - x)$

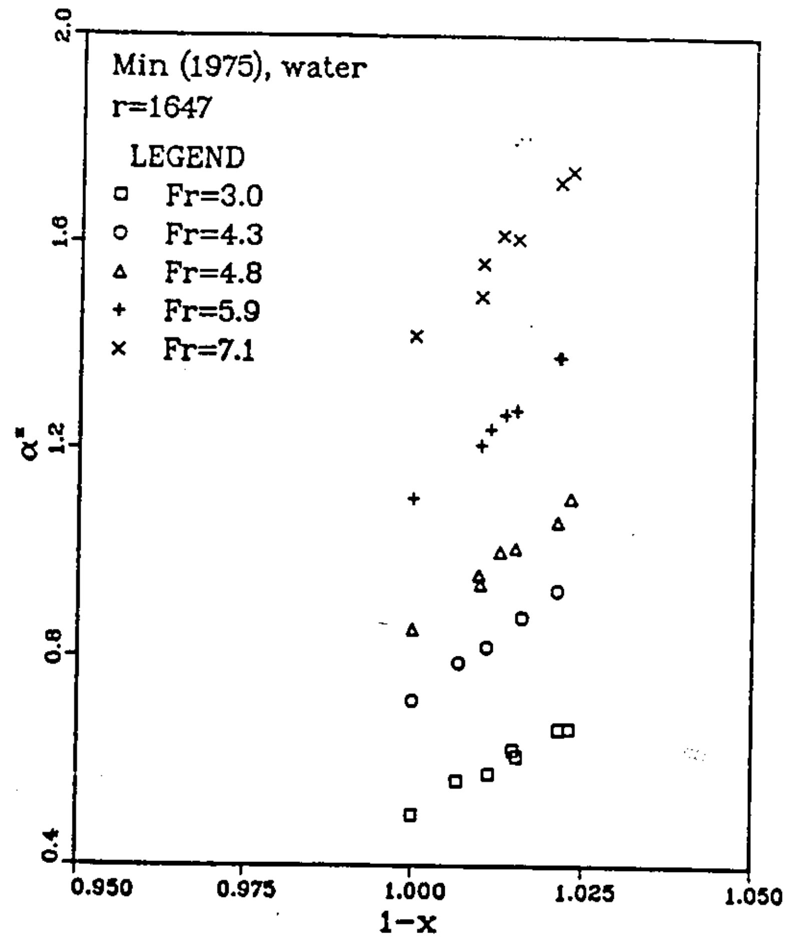

Figure 4.16: Effective vapor sheet thickness vs. $(1 - x)$

Table 4.3: Values of empirical variables obtained from different test sources

Investigator	ρ_f/ρ_g	a	b	c	fluid
Pourdashti (1984)	50	0.5501	0.3499	0.2574	Freon-113
Pourdashti (1984)	100	0.6812	0.4081	0.4105	Freon-113
Hasan et al. (1981)	334.7	0	0.2914	0.6590	isopropanol
Ungar and Eichhorn (1988)	341.8	0	0.3040	0.6020	isopropanol
Min (1975)	615	0	0.2340	0.9418	methanol
Vliet (1962)	1460	7.1713	0.3379	0.8443	water
Ungar and Eichhorn (1988)	1553	0	0.2640	0.9960	water
Diesselhorst et al. (1977)	1609	0	0.2692	0.7600	water
Min (1975)	1647	9.1792	0.1780	0.993	water

CHF is evaluated by $q_{max} = \phi \rho_g U_\infty h_{fg} / \pi$. The RMS error of the present prediction for each test fluid is listed in Table 4.4. In addition, Fig. 4.20 shows the comparison of measured CHF versus predicted CHF for all test data and represents 72% of the data with ±25% accuracy.

According to the results illustrated in Table 4.4, most test data give the RMS error lower than 25% or near 25% with only one exception of Min's (1975) water data. However, Min's methanol data gives around 20% of RMS error. It is acceptable even though the same data base has only 9.2% of RMS error with Ungar and Eichhorn's (1988) correlation. But one thing Ungar and Eichhorn did not point out in their study is that Min's water data gives more than 100% RMS error when using their correlation.

Hwang and Yao's (1984) CHF correlation has also been chosen to assess with the same test data used in the present analysis because only Hwang and Yao's correlation includes the quality effect for flow boiling across a single cylinder. However, Hwang and Yao's correlation has a narrower velocity range, which corresponds to $G_c \leq 2.8$ rather than $G_c \leq 8.0$ in present analysis. Therefore, both the RMS error for the flow condition of $G_c \leq 2.8$ and $G_c \leq 8.0$ have been calculated for the assessment of Hwang and Yao's correlation with all test fluids. These results are shown in Table 4.5. Though Hwang and Yao (1984) concluded that their correlation predicts the CHF well with their own experimental results, it seems not applicable to the other test results.

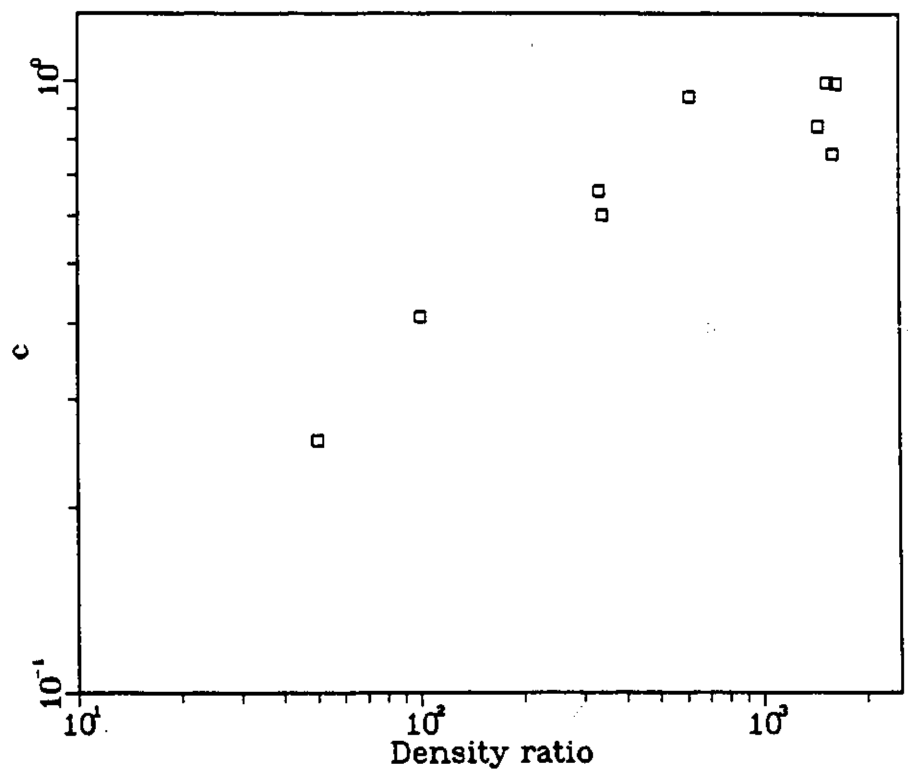

Figure 4.17: Exponential values of c vs. density ratio obtained from present study

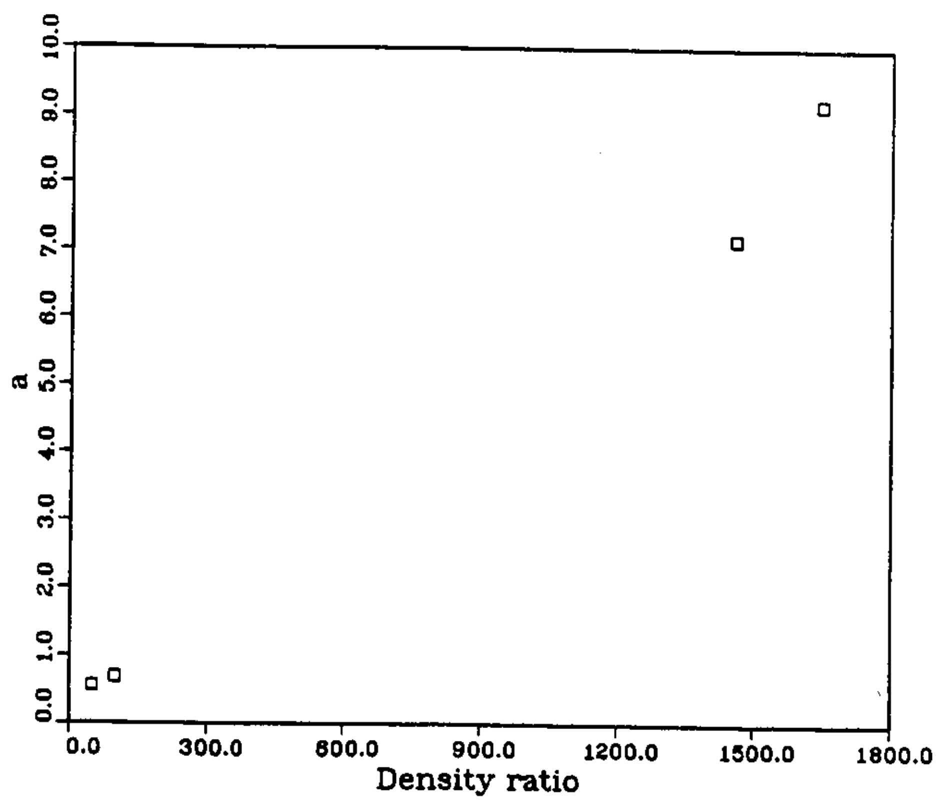

Figure 4.18: Exponential values of a vs. density ratio obtained from present study

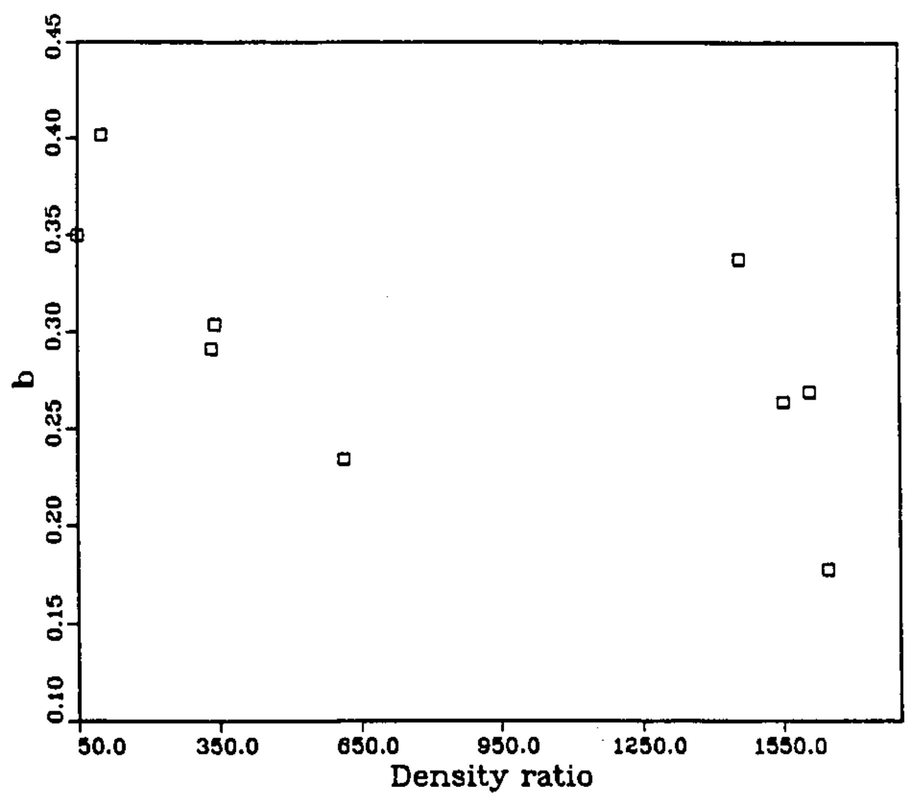

Figure 4.19: Constants b vs. density ratio obtained from present study

Table 4.4: Assessment of the present prediction of CHF to each test source

Data source	Number of data	Fluid	RMS error (%)
Pourdashti	40	Freon-113	21.75
Hasan et al.	19	isopropanol	7.36
Ungar and Eichhorn	15	isopropanol	8.64
Min	40	methanol	20.51
Vliet	81	water	27.74
Ungar and Eichhorn	45	water	18.64
Diesselhorst et al.	31	water	22.93
Min	62	water	65.63
	271*		22.08*

* Min's water data is not included.

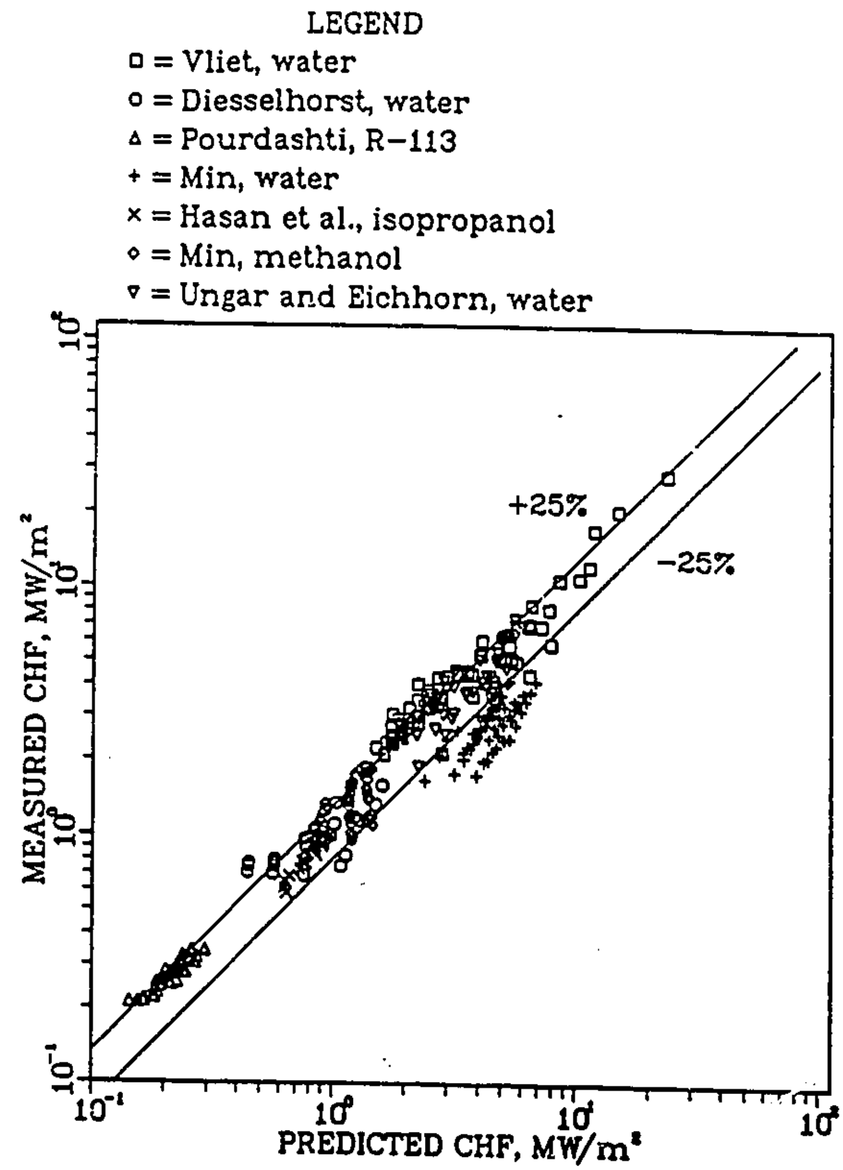

Figure 4.20: Comparison of CHF data predicted by Eq. (4.25) with measured CHF for different sources

Table 4.5: Assessment of the Hwang and Yao's prediction of CHF to each test source

Data source	Fluid	RMS error (%) $G_c \leq 8$	No. of data	RMS error (%) $G_c \leq 2.8$	No. of data
Pourdashti	Freon-113	46.75	40	45.78	36
Hasan et al.	isopropanol	32.94	19	31.37	4
Min	methanol	50.32	40	39.20	12
Vliet	water	66.46	81	58.16	42
Ungar and Eichhorn	water	61.84	45	51.59	10
Diesselhorst et al.	water	37.57	31	37.59	28
Min	water	48.47	62	39.44	24
		49.54*	197*	40.18*	78*

* The data for Pourdashti (1984) and Vliet (1962) are not included.

Chapter 5

Characterization of Velocity and Diameter for the Cross Flow

5.1 Blockage Effect for Flow Across Single Cylinder

In previous chapters, the use of velocity for cross-flow boiling is mainly the incoming flow velocity or the velocity in the bulk liquid because most analytical and experimental data on single-cylinder heat transfer refer to flow conditions at infinity, i.e., in the absence of channel walls. However, in engineering applications the flow experiences a significant blockage due to the presence of adjacent tubes and channel walls, which may exert an influence on heat transfer. Therefore, the following analysis of heat transfer for cross-flow boiling would include the factor of blockage effects for the fact of convenience.

5.1.1 Žukauskas and Žiugžda's correlation (1985)

The blockage factor used in Žukauskas and Žiugžda (1985) is defined as $K_q = D/w$, where D is the diameter of tube or cylinder and w the width of flow channel. Therefore the bulk velocity, U, varying across the cylinder due to the blockage effect can be expressed in terms of a modified form of the Hiemenz (1911) relationship:

$$\frac{U}{U_\infty} = A_1^* \left(\frac{x'}{D}\right) + A_2^* \left(\frac{x'}{D}\right)^3 + A_3^* \left(\frac{x'}{D}\right)^5 \qquad (5.1)$$

where

$$A_1^* = 3.6314 \left(1 + \frac{K_q}{2}\right)$$

$$A_2^* = -2.1709(1 - 12.1284K_q^{2.226} + 3.7376K_q)$$

and

$$A_3^* = -1.5144(1 + 18.542K_q^{2.277} - 6.878K_q)$$

and Hiemenz's original equation is written as:

$$\frac{U}{U_\infty} = 3.6314 \left(\frac{x'}{D}\right) - 2.1709 \left(\frac{x'}{D}\right)^3 - 1.5144 \left(\frac{x'}{D}\right)^5 \qquad (5.2)$$

where x' is the arc length from the front stagnation point of the cylinder. At $K_q = 0$, equation (5.1) reduces to the Hiemenz relation, or equation (5.2).

5.1.2 Narrowest cross section model

In the study for single-phase and two-phase convective heat transfer by Hwang and Yao (1984), the blockage effect has also been considered. However, rather than the velocity defined in section 5.1.1, the effective velocity is defined as the average velocity in the narrowest cross-sectional area. The velocity can be related to the free stream velocity, U_∞, as

$$\frac{U}{U_\infty} = \frac{w}{w - D} \qquad (5.3)$$

5.1.3 Mean flow area model

Flow velocities used in Perkins and Leppert's (1962), Vliet's (1962) and Vliet and Leppert's (1964a) measurements are the mean test channel velocity corrected for test element blockage and for velocity profile. The profile correction is used since the element is small compared to channel width and thus is in the environment of the centerline velocity, which is a function of the Reynolds number based on the channel width. Blockage effect is based on the concept that the average velocity flows through a mean flow area, i.e., the mean flow area is defined as the ratio of flow volume in the channel at the location of the test section to the test-section diameter. Figure 5.1 shows schematically the concept of derivations of mean flow area and average velocity. Thus, the mean flow area can be written as:

$$A_m = \frac{Channel\ volume - tube\ volume}{tube\ diameter}$$

or

$$A_m = \frac{\left(wD - \frac{\pi D^2}{4}\right) L}{D} = \left(w - \frac{\pi D}{4}\right) L \tag{5.4}$$

According to the conservation of volumetric rate of channel flow, $Q = UA_m = U_\infty A_\infty$, the average velocity can be obtained by:

$$U = U_\infty \left(\frac{A_\infty}{A_m}\right) \tag{5.5}$$

where $A_\infty / A_m = 4w/(4w - \pi D)$. Therefore, equation (5.5) can be rewritten as

$$U = \frac{U_\infty}{1 - \frac{\pi D}{4w}} \tag{5.6}$$

Vliet (1962) concluded that for forced convection non-boiling, the heat transfer coefficient is affected by blockage, and a similar effect may apply to the CHF — the CHF increases with blockage because the local velocity increases with the decreasing transverse pitch.

5.2 Blockage Effect for Flow Across Tube Bundles

A circular tube bundle is one of the most common heat transfer surfaces, particular in shell-and-tube exchangers. The most common tube arrays are staggered and in-line arrangements such as illustrated in Fig. 5.2.

5.2.1 Minimum intertube space model

A typical application of this model is used in Žukauskas's (1987) experiments. The blockage effect is described by the ratio of the transverse ($X_{tt} = X_t/D$), longitudinal ($X_{ll} = X_l/D$), or diagonal ($X_{dd} = X_d/D$) pitch, which are shown in Figure 5.2,

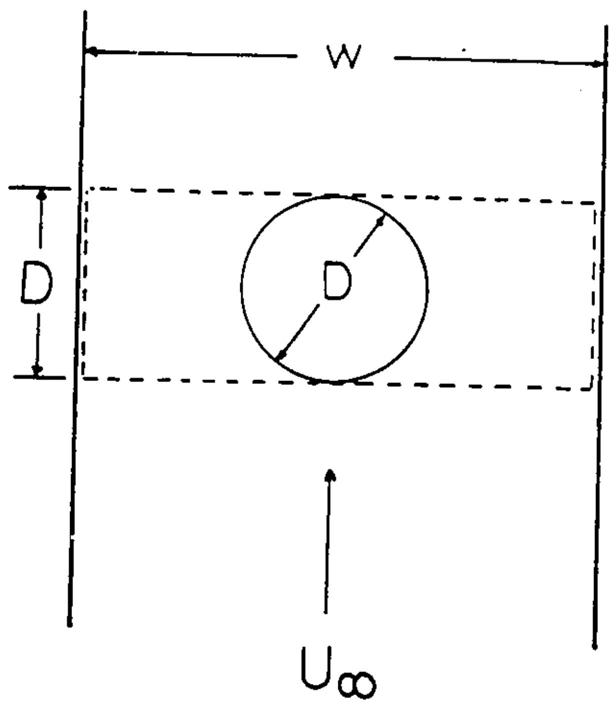

Figure 5.1: Control volume used to derive mean flow area across single cylinder

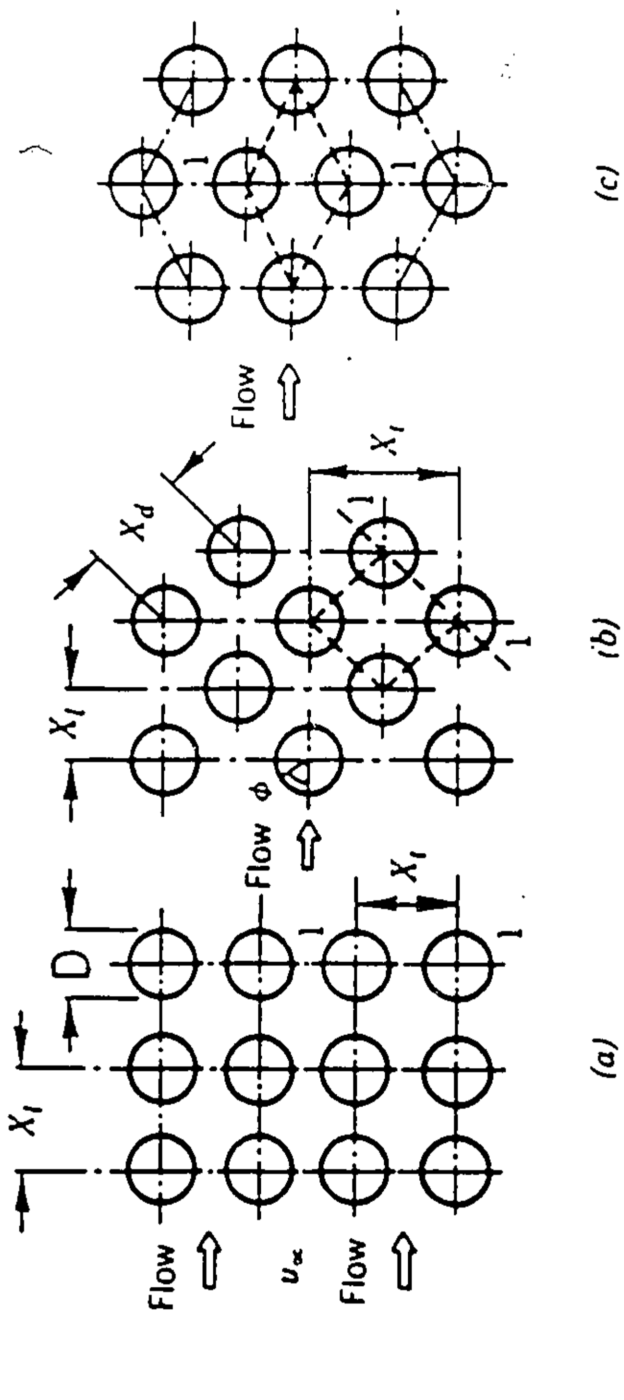

Figure 5.2: Most common types of tube bundles arrangements: (a) in-line. (b)–(c) staggered.

over the tube diameter. Žukauskas (1987) concluded that the transverse pitch has a significant effect on the velocity distribution in tube bundles. The average velocity in the minimum intertube space of a transverse tube row at a constant flow rate is given by:

$$U = U_\infty \frac{X_{tt}}{X_{tt} - 1} \tag{5.7}$$

and the blockage factor can be defined as the ratio of tube diameter of bundles over the transverse pitch and is equivalent to $1/X_{tt}$. The rate of velocity growth in the intertube space is mainly determined by the transverse pitch and it increases drastically at narrow pitches.

5.2.2 Mean flow area model

To extend the use of the mean flow area model for tube bundles, the control volume used to describe the derivation of a mean flow area is illustrated in Fig. 5.3. According to this control volume, the mean flow area is given by:

$$A_m = \frac{\left[wD' - n\left(\frac{\pi D^2}{4}\right)\right] L}{D'} \tag{5.8}$$

where n is the number of tubes in the control volume and D' the length of the control volume. Consequently, the average velocity can be obtained by substituting A_m into equation (5.5), yielding

$$U = U_\infty \frac{1}{1 - \frac{n}{wD'}\left(\frac{\pi D^2}{4}\right)} \tag{5.9}$$

In the following chapters, the use of the velocity for the analysis would refer to the mean flow area model because of the fact that most CHF's occur near the rear stagnation point and none of the models or correlations discussed above can characterize the flow velocity near the rear stagnation point successfully. However, the mean flow area model seems to be the most reasonable because the velocity is the average value across the cylinder or bundles.

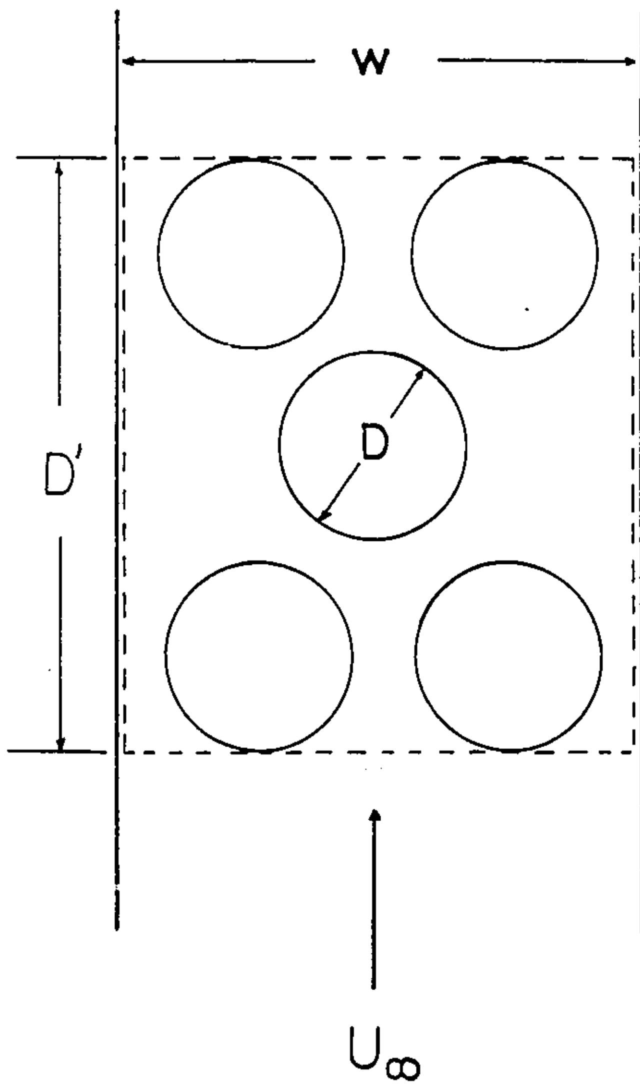

Figure 5.3: Control volume used to derive mean flow area across tube bundles

Chapter 6

Prediction Method for CHF in Axial Flow

The mechanism of boiling heat transfer including CHF has been introduced by Collier (1981). In present study the method for CHF prediction is only of interest for discussion.

6.1 CHF Prediction Methods for Water

6.1.1 Analytical model

CHF of annular flow in vertical tube is considered as the most practical system, where this type of CHF occurs as a result of liquid removal of the film (G_{LF}) leading to film dryout. The mechanisms of mass transfer from or to the liquid film are:

- Evaporation of liquid (q/h_{fg}) in the film;
- Entrainment of liquid droplets (G_E) from the film to the vapor core;
- Deposition of entrained liquid droplets (G_D) from the vapor core onto the liquid film.

The variation of liquid film flow rate with distance of the heated tube yields

$$\frac{dG_{LF}}{dL_h} = G_D - G_E - \frac{q}{h_{fg}} \tag{6.1}$$

As CHF is approached, the liquid film becomes very thin. Compared with other terms in equation (6.1), the dG_{LF}/dL_h term is assumed to be negligible. Then, if the evaporation rate (q/h_{fg}) exceeds the net deposition $(G_D - G_E)$, the liquid film breaks down which leads to dryout. Equation (6.1) is for a steady state and it ignores the effect of evaporation by other mechanisms such as liquid flashing resulting from the channel pressure gradient.

Some predictive methods have been proposed to calculate the CHF in annular flow. These methods are different mainly in their treatments of entrainment, deposition and evaporation processes and in the choice of boundary conditions. Perhaps the most widely accepted model was developed by Whalley et al. (1974, 1975, 1978) and Hewitt and Hutchinson (1976) at Harwell. This model is rather general and superior to most empirical models. However, more work needs to be done in advancing understanding of entrainment and evaporation processes.

6.1.2 Empirical correlations

As pointed out by Collier (1981), two types of empirical correlating procedure have been adopted. They are:

1. Correlations of an empirical nature which make no assumption whatever about the mechanisms involved in the critical heat flux condition, but solely attempt to find a functional relationship between the critical heat flux and the independent variables.

2. Correlations where attempts have been made to look at and write down equations for the hydrodynamic and heat transfer processes occurring in the heated channel and to relate these to the critical heat flux condition.

Probably the most general form of the empirical correlations is that by Macbeth (1963), which belongs to the first category mentioned above and assumes that the CHF is a linear function of inlet subcooling. Thus

$$q_{max} = A + B\Delta h_{sub}$$

or

$$q_{max} = \frac{A' + B'\Delta h_{sub}}{C' + L_h}$$

where Δh_{sub} is the inlet subcooling, L_h the tube length and A', B' and C' are related to the system parameters. Two of the most widely accepted correlations are the Bowring's correlation (1972) and Biasi's correlation (1967). The details of both correlations has been reviewed by Wong (1988).

6.2 CHF Prediction Methods for Non-aqueous Fluids

CHF prediction methods applicable to non-aqueous fluids can be categorized into three groups:

1. Fluid to fluid modelling of CHF: A technique that enables the CHF of a given system to be predicted using a modelling fluid rather than the working fluid (e.g. Barnett (1964), Stevens and Kirby (1964), and Ahmad (1973)).
2. Empirical dimensionless correlation: These are empirically derived dimensionless correlations that predict the CHF in a system regardless of the fluid type (e.g. Katto (1978), Katto and Ohno (1984), Shah (1979 and 1986) and Kutateladze(1963)).
3. Theoretical models: These theoretical models are based on the mechanism of CHF. They predict the CHF in a system within a dryout quality range regardless of fluid type used (e.g. Weisman and Pie (1983) and Whalley et al. (1973)).

All the above groups have been well reviewed by Kiameh (1986).

6.3 Table Look-up Method

The USSR Academy of Science (1977) has produced a series of standard tables of CHF. The CHF values are tabulated as a function of the local parameters G, x

and P for a tube of 8 mm inside diameter. The CHF for tube diameters other than 8 mm can be approximated by

$$q_{max} = q_{max,8mm} \left(\frac{D}{0.008}\right)^{-1/2} \tag{6.2}$$

for $4 \leq D \times 10^3 \leq 16 \;\; mm$.

Groeneveld et al. (1986a,1986b) developed an accurate and simple technique to predict CHF in water and non-aqueous fluids over a wide range of conditions. Groeneveld's look-up technique is also based on the local condition assumption, i.e.,

$$q_{max} = f(x, G, P, D) \tag{6.3}$$

The CHF table, or AECL-UO look-up table, is illustrated in Table 6.1. Although the standard CHF table is derived for very specific cases, i.e., upward flow in a uniformly heated 8 mm tube within table matrix conditions, it may also be used for other geometries and flow conditions: *CHF prediction for non-uniformly heat geometries, downward flow, flow in bundle geometries, etc. For these cases the table CHF value must be multiplied by correction factors* $K1$ *to* $K6$. The use of these correction factors is listed in Table 6.2. CHF values for a tube having a diameter other than 8 mm may be obtained by

$$q_{max} = q_{max,8mm} \left(\frac{D}{0.008}\right)^{-1/3} \tag{6.4}$$

for $4 \leq D \times 10^3 \leq 16 \;\; mm$.
The range of the table method is:

Pressure:	100 - 20,000 kPa
Mass flux:	0 - 7500 $kg/m^2/s$
Quality:	-50 to 100%

Groeneveld's look-up table is not dimensionless. However, the use of a CHF table for non-aqueous fluids can have two different approaches:

1. First method: The dimensional table is converted into dimensionless form by replacing P by ρ_f/ρ_g, q_{max} by $q_{max}/(Gh_{fg})$ and G by Ψ_K for Katto's scaling factor (Katto and Ohno (1984)), by Ψ_σ for Ahmad's first scaling factor (1973) and by Ψ_γ for Ahmad's second scaling factor (1973), where those expressions

Table 6.1: 1986 AECL-UO Critical Heat Flux look-up table (kW/m^2)

PRESS.	G								QUALITY													
(KPA)	(KG/M.M.S)	-0.50	-0.40	-0.30	-0.20	-0.15	-0.10	-0.05	0.00	0.05	0.10	0.15	0.20	0.25	0.30	0.40	0.50	0.60	0.70	0.80	0.90	1.00
100	0					3930	3430	2045	1200	1000	980	800	790	780	710	486	470	454	339	225	89	
100	50					4008	3500	2400	1700	1600	1500	1300	1250	1204	1126	899	850	800	501	355	350	
100	100					4800	4200	3100	2200	2100	2000	1450	1000	1000	955	950	950	900	660	430	335	
100	200					5600	4900	3800	2600	2550	2500	1500	1400	1300	1246	1200	1124	1100	854	474	460	
100	300					6400	5600	4500	3000	3000	3000	2500	2400	2300	2300	2168	1721	1448	818	481	450	
100	500					7200	6300	5200	3600	3550	3500	3200	3000	2500	2358	2350	2301	1220	700	651	440	
100	750					8000	7000	5900	5500	5000	4700	4249	4006	3104	3081	2933	2407	1317	911	700	400	
100	1000					8800	7600	6600	4800	4600	4406	3800	3600	3300	3300	3250	2503	1552	1100	600	300	
100	1500					9600	8200	7000	5500	4800	4600	4500	4451	4200	4000	3911	3105	2601	1100	600	300	
100	2000					10000	8800	7700	6000	5400	5300	5200	5100	5050	5000	4900	4549	2900	1100	600	300	
100	3000					10500	9400	8400	6500	6300	6000	5800	5700	5400	5300	5200	3900	2700	1100	600	300	
100	4000					11000	10000	9000	6900	6785	6650	6100	5300	5000	4600	4000	3000	2000	1000	500	300	
100	5000					11500	10600	9500	8000	7875	7600	7400	5200	4400	3800	3000	2500	1500	900	500	300	
100	7500					12000	11500	11000	10500	9233	9000	7500	5000	4000	3000	2200	2000	1200	800	400	300	
150	0				6273	4000	3500	2400	1350	1200	1100	1000	950	930	913	588	550	544	375	250	116	
150	50				6344	4100	3600	2700	1900	1800	1700	1500	1450	1416	1329	1002	900	873	539	419	400	
150	100				6397	4800	4200	3200	2400	2200	2000	1900	1800	1400	1093	1000	950	950	941	701	450	
150	200				6488	5400	4800	3500	2700	2600	2500	2100	1600	1400	1200	1200	1166	1150	1100	1000	500	
150	300				6571	6000	5400	4000	3000	2900	2800	2500	2400	1500	1400	1340	1300	1200	1200	800	500	
150	500				6721	6600	6000	4500	3700	3600	3500	3100	2700	1600	1500	1500	1400	1200	1100	670	450	
150	750				7400	7200	6600	5000	4300	4150	4000	3500	2800	1400	1399	1300	1200	1100	1000	650	400	
150	1000				8000	7800	7200	5500	5200	4500	3985	3400	3200	1200	1105	1100	1100	1000	1000	600	350	
150	1500				8600	8400	7600	6000	5500	4000	3800	3300	3100	2400	2000	1500	1300	1200	1100	550	300	
150	2000				9200	9000	8200	6200	5700	4700	4300	4100	4000	3500	3000	2500	2000	1700	1500	550	300	
150	3000				9800	9600	6240	5800	4800	4400	4300	4200	4100	3800	3300	3250	3200	2500	1000	500	300	
150	4000				10200	10000	6636	6000	5000	4600	4500	4300	4200	3600	2800	2800	2600	2000	1000	450	300	
150	5000				10700	10500	9900	9200	9145	7405	6500	5700	4000	3100	2600	2300	2000	1500	900	450	300	
150	7500				11200	11000	10400	9700	9500	8881	8000	6500	5000	3000	2200	1800	1600	1000	600	400	300	
200	0				5971	4820	3700	2774	1450	277	262	248	233	219	204	175	146	117	87	58	29	
200	50				6044	4955	4000	3094	2313	1794	1641	1562	1483	1405	1326	1244	1044	650	600	574	571	
200	100				6099	5000	4100	3200	2600	2300	2100	2000	1900	1300	1200	1109	800	767	750	750	516	
200	200				6193	5200	4300	3400	2800	2500	2300	2150	1400	1297	1200	1180	1100	1000	1000	1000	514	
200	300				6278	5400	4450	3500	3000	2700	2400	2200	2150	2100	2000	1829	1497	904	417	400	350	
200	500				6433	5600	4650	3700	3150	2900	2500	2400	2300	2250	2226	1759	1388	659	250	200	200	
200	750				6610	5800	4850	3900	3300	3000	2650	2500	2314	2159	1818	1590	1463	1000	600	450	300	
200	1000				6775	6000	5000	4000	3400	3000	2600	2500	2134	1939	1800	1700	1600	1000	600	450	300	
200	1500				7083	6200	4600	3800	3300	3000	2600	2500	2350	2169	1800	1700	1500	1000	600	450	300	
200	2000				7370	6400	4500	4000	3500	3000	2600	2500	2150	2050	1800	1700	1400	1000	600	450	300	
200	3000				7905	7000	5742	4287	3900	3000	2600	2500	2150	2050	1800	1700	1400	1000	600	450	300	
200	4000				8600	8500	6411	4800	4500	3000	2600	2500	2150	2050	1800	1700	1400	1000	600	450	300	
200	5000				8880	6607	6120	5267	4845	3000	2600	2500	2150	2050	1800	1700	1400	1000	600	450	300	
200	7500				9990	6990	6465	5581	5077	3000	2600	2500	2150	2050	1800	1700	1400	1000	600	450	300	
300	0				5631	4650	3667	2683	1700	325	308	291	274	257	240	205	171	137	103	68	34	
300	50				5712	5063	4292	3296	2975	2481	2327	2248	2168	2014	1860	1551	1067	535	500	500	450	
300	100				5772	5200	4500	3500	3400	3200	3000	2900	2800	2600	2400	1160	900	870	850	800	504	
300	200				5877	5600	4700	3600	3500	3200	2900	2800	1600	1463	1400	1400	1376	1300	1200	1181	569	
300	300				5971	4592	3324	3300	3250	3200	2800	2700	2600	2500	2400	2176	1785	1043	438	400	362	
300	500				6142	4634	3367	3300	3250	3200	2700	2600	2600	2600	2500	1946	1341	811	200	200	200	
300	750				6338	6000	5000	3900	3800	3200	2800	2700	2586	2475	2402	1526	868	490	418	250	200	
300	1000				6521	6200	5200	4000	3900	3200	2600	2500	2395	2208	2100	1800	1500	1200	700	400	200	
300	1500				6862	6400	4154	4100	4000	3200	2600	2600	2538	2360	2100	1800	1500	1200	700	400	200	
300	2000				7180	6600	4300	4200	4100	3200	2600	2500	2294	2200	2100	1800	1500	1200	700	400	200	
300	3000				8000	7778	5690	4800	4706	3200	2600	2500	2294	2200	2100	1800	1500	1200	700	400	200	
300	4000				8600	8443	6302	4518	4400	3200	2600	2500	2294	2200	2100	1800	1500	1200	700	400	200	
300	5000				8852	5419	4851	3967	3525	3200	2600	2500	2294	2200	2100	1800	1500	1200	700	400	200	
300	7500				10082	5816	5198	4236	3630	3200	2600	2500	2300	2200	2100	1800	1500	1200	700	400	200	
450	0				5363	4540	4222	2000	1968	380	360	340	320	300	280	240	200	160	150	120	110	
450	50				5454	5035	4627	2330	2250	2195	2115	2035	1993	1950	1870	1860	1625	600	550	543	500	
450	100				5522	5200	4100	3400	2900	2800	2700	2600	2550	2200	2000	1500	1123	1112	984	908	595	
450	200				5639	5600	4150	3400	3000	2800	2600	2550	2500	2200	1700	1600	1500	1400	1306	890	595	
450	300				5745	4145	2896	2850	2825	2800	2600	2500	2450	2400	2400	2300	2161	1583	755	447	408	
450	500				5939	4187	2939	2900	2850	2800	2600	2400	2400	2400	2300	2245	1784	1123	451	250	236	
450	750				6159	6000	4300	3400	3100	2800	2600	2300	2150	2000	1900	1355	879	707	467	350	316	
450	1000				6365	6200	4400	3400	3200	2800	2600	2100	1966	1786	1200	700	606	593	500	300	200	
450	1500				6749	6400	4145	3060	3000	2800	2600	2100	2086	1500	1000	700	665	600	500	300	200	
450	2000				7108	6600	3521	3400	3300	2800	2600	2100	1800	1500	1200	1100	1000	700	500	300	200	
450	3000				7775	7500	5752	4146	3716	2800	2600	2200	1800	1500	1200	1100	1000	700	500	300	200	
450	4000				8399	8000	6210	4292	4076	2800	2600	2200	1800	1500	1200	1100	1000	700	500	300	200	
450	5000				8991	6619	6002	5440	3500	2800	2600	2200	1900	1500	1200	1100	1000	700	500	300	200	
450	7500				10376	6878	6271	5707	3600	2800	2600	2200	2000	1500	1200	1100	1000	700	500	300	200	
700	0			6548	5153	4482	4264	2059	1488	448	424	401	377	354	330	283	236	189	97	72	70	
700	50			6652	5260	5021	4669	2488	2300	2212	2056	1825	1594	1363	1133	971	809	500	450	404	400	
700	100			6730	5339	5200	4200	3500	3000	2800	2600	2300	2000	1700	1400	1200	1000	830	820	816	578	
700	200			6865	5477	5300	4250	3600	3200	3000	2900	2700	2600	2500	2200	2000	1800	1700	1403	913	649	
700	300			6986	5601	5400	4300	3700	3400	3000	2900	2700	2600	2550	2500	2500	2500	1892	1093	628	533	
700	500			7208	5827	5700	4400	3800	3500	3000	2900	2800	2700	2650	2600	2600	2568	1360	644	385	353	
700	750			7460	6085	6000	4600	3900	3600	3000	2700	2600	2500	2400	2300	2284	1398	680	450	426	420	
700	1000			7696	6326	6200	5060	4094	3600	3000	2800	2700	2700	2695	1600	1595	914	467	260	250	200	
700	1500			8136	6775	6400	4991	4025	3600	3000	2500	2400	2300	2284	1200	1166	745	259	199	175	150	
700	2000			8547	7195	6600	5200	4400	3600	3000	2500	2200	1800	1500	1300	1300	900	250	200	200	150	
700	3000			9312	7976	6800	5400	4600	3600	3000	2500	2200	1800	1500	1300	1200	900	250	200	200	150	
700	4000			10026	8705	7000	5600	4800	3600	3000	2500	2200	1800	1500	1300	1200	900	250	200	200	150	
700	5000			10705	9397	7200	5800	4900	3600	3000	2500	2200	1900	1500	1300	1200	900	250	200	200	150	
700	7500			12294	11018	7400	6000	5000	3600	3000	2500	2200	2000	1600	1300	1200	900	250	200	200	150	
1000	0			8092	6551	4480	3866	3240	2620	509	483	456	429	402	375	322	268	214	161	107	54	
1000	50			8195	6657	5620	5092	4560	4105	3427	3271	3114	3032	2801	2569	2330	1942	1104	875	814	426	
1000	100			8271	6736	6000	5500	5000	4600	4400	4200	4000	3900	3600	3300	3000	2500	1600	1547	1070	659	
1000	200			8403	8100	8000	7500	7000	6000	5800	5600	5400	5100	4700	4400	4300	3352	2455	1704	1117	778	
1000	300			8522	8200	8000	7500	7000	6500	6300	5600	5400	5100	4700	4700	4671	3958	2571	1569	918	711	
1000	500			8738	8300	8000	7500	7000	6500	6200	5600	5400	5100	4700	4652	4600	3803	2087	1123	603	437	
1000	750			8985	8400	8000	7500	7000	6500	6100	5600	5400	5000	4900	4800	3940	2272	1106	696	527	466	
1000	1000			9217	8500	8000	7500	7000	6500	6000	5600	5400	5369	4923	4123	2905	1646	888	606	298	218	
1000	1500			9647	8500	8000	7500	7000	6500	5900	5300	5000	4925	4425	3325	2393	1328	613	256	188	100	
1000	2000			10049	8700	8000	7500	7000	6500	5700	5200	4800	4400	3600	3500	3474	2807	800	250	150	100	
1000	3000			10798	9362	8000	7500	7000	6500	5500	5100	4700	4200	4000	3962	3858	1300	750	250	150	100	
1000	4000			11497	10088	8000	7500	7000	6500	5300	5000	4500	4000	3400	2800	1850	1150	700	250	150	100	
1000	5000			12161	10778	8000	7500	7000	6500	5400	4900	4400	3800	3300	2600	1650	1000	650	250	150	100	
1000	7500			13716	12391	8000	7500	7000	6500	5500	4800	4300	3600	3200	2300	1500	900	600	250	150	100	

PRESS. (KPA)	G (KG/M.M.S)	-0.50	-0.40	-0.30	-0.20	-0.15	-0.10	-0.05	QUALITY 0.00	0.05	0.10	0.15	0.20	0.25	0.30	0.40	0.50	0.60	0.70	0.80	0.90	1.00
1500	0		8975	7713	6456	4525	4007	3488	2970	584	553	523	492	461	430	369	307	246	184	123	61	
1500	50		9088	7839	6576	5781	5100	4922	4200	4000	3513	3356	3273	3115	2883	2567	2327	1149	1021	879	426	
1500	100		9171	7928	6666	6200	5500	5400	5000	4300	4500	4300	4200	4000	3700	3300	3000	1600	1563	1081	637	
1500	200		9315	8083	7200	7100	6900	6600	6400	6200	6000	5700	5400	5000	4100	3600	3411	2788	2040	1265	816	
1500	300		9445	8222	7500	7400	7100	6700	6500	6300	6000	5700	5300	5200	5200	5110	4551	3539	2240	1271	855	
1500	500		9683	8477	7800	7700	7200	6700	6400	6100	5800	5500	5300	4800	4600	4500	4307	3103	1837	956	608	
1500	750		9954	8767	8100	8000	7200	6700	6300	5900	5600	5400	5200	5000	4800	4531	2944	1717	1082	707	451	
1500	1000		10207	9038	8200	8000	7200	6700	6250	5700	5600	5550	5500	5400	5220	3693	2081	1118	818	466	216	
1500	1500		10678	9543	8284	8000	7200	6700	6250	5500	5300	5275	5150	4849	4538	2893	1440	816	389	233	200	
1500	2000		11119	10015	8757	8000	7200	6700	6200	5500	5200	4900	4043	4000	3920	2578	1470	1000	800	400	200	
1500	3000		11939	10893	9637	7529	6720	6700	6100	5600	5100	4800	4700	4456	4307	4009	2100	1000	800	400	200	
1500	4000		12705	11714	10459	7645	6836	6700	6100	5600	5000	4700	3800	3800	3100	1900	1800	1000	800	400	200	
1500	5000		13433	12493	11239	8500	7500	6900	6300	5600	4800	4400	3600	3500	2600	1700	1500	1000	800	400	200	
1500	7500		15137	14317	13065	9000	8000	7100	6300	5500	4700	4100	3600	3300	2350	1600	1200	1000	800	400	200	
2000	0	9632	8569	7495	6421	4581	4130	3680	3230	643	609	575	541	507	474	406	338	271	203	135	68	
2000	50	9749	8692	7629	6550	5870	5420	4970	4700	3800	3752	3594	3510	3352	3118	2801	2710	1193	941	927	434	
2000	100	9836	8784	7729	6646	6300	5850	5400	5200	4900	4800	4600	4500	4300	4000	3600	3500	1700	1601	1206	762	
2000	200	9988	8944	7902	7100	7000	6900	6800	6700	6600	6300	6000	5600	5300	4800	4400	3402	2741	2169	1350	829	
2000	300	10124	9088	8058	7450	7400	7350	7200	6900	6600	6600	5900	5700	5500	5200	4500	4400	4329	2804	1516	879	
2000	500	10372	9349	8343	7800	7700	7600	7500	7200	6600	6600	5730	5348	5225	5200	5191	4480	3701	2446	1327	772	
2000	750	10656	9648	8668	8100	8100	7800	7600	7200	7000	6843	6405	5849	5666	5300	5222	3601	2349	1245	789	450	
2000	1000	10921	9928	8971	8300	8200	8100	7800	7714	7073	6745	6482	6202	5800	5792	4283	2752	1725	1012	584	382	
2000	1500	11414	10448	9536	8700	8500	8400	7800	7387	6771	6388	5892	4766	4687	4600	3197	1729	957	558	316	300	
2000	2000	11876	10934	10064	9000	8700	8500	7800	7000	6500	5800	5216	4471	4305	4133	2221	1019	481	415	400	300	
2000	3000	12735	11840	11047	9832	8944	8135	7800	7000	6200	5600	5240	4755	4662	4459	3393	1600	1200	1000	400	300	
2000	4000	13537	12685	11964	10713	9060	8251	7300	6500	6000	5500	5274	4779	4700	4415	3215	1400	1200	900	400	300	
2000	5000	14299	13489	12836	11550	10000	8500	6500	5000	4800	4600	4400	4267	4200	4081	2400	1400	1200	900	600	500	
2000	7500	16083	15369	14876	13507	10300	8500	5500	4800	4600	4400	4000	3483	3200	2800	1700	1500	1300	1100	800	600	
3000	0	8858	8031	7207	6380	4650	4290	3930	3570	919	690	651	613	575	536	460	383	306	240	235	231	
3000	50	8993	8181	7358	6518	6038	5573	5108	4868	4130	3997	3913	3753	3594	3359	3040	2721	2327	340	308	300	
3000	100	9093	8291	7470	6620	6500	6000	5500	5300	5200	5100	5000	4800	4600	4300	3900	3500	3000	1353	1058	758	
3000	200	9267	8484	7665	7300	7200	7100	6900	6700	6600	6500	6300	6000	5700	5400	4800	4000	3273	2203	1345	819	
3000	300	9424	8657	7841	7600	7500	7400	7352	7029	7000	7000	7000	6970	6600	6260	5463	4600	4538	2902	1673	978	
3000	500	9710	8973	8161	8000	8000	8000	7968	7645	7200	6500	6292	5886	5724	5699	5610	4283	3790	2723	1694	1039	
3000	750	10036	9334	8527	8400	8300	8100	8100	7800	7100	6695	6586	6197	6104	6100	5038	3594	2750	1851	1228	684	
3000	1000	10341	9671	8869	8500	8300	8200	8000	7711	6945	6700	6594	6432	5929	5299	4140	3312	2605	2201	1698	809	
3000	1500	10909	10299	9505	8800	8700	8248	7907	7265	6600	6587	5751	5105	4635	4505	3389	2523	2100	2000	1973	1208	
3000	2000	11440	10885	10099	9200	9100	9000	9000	8900	8818	7347	6167	5216	4592	4164	2817	2122	1209	1000	1000	600	
3000	3000	12429	11977	11206	10010	9500	9000	8500	8000	7858	6203	5450	4997	4486	3018	2100	2015	1100	1050	1000	600	
3000	4000	13351	12997	12239	10947	10500	9000	7027	6592	5973	5556	5047	4701	3959	2032	2000	1900	1750	1350	1000	600	
3000	5000	14228	13966	13221	11837	10800	8505	7094	5870	5383	5124	4591	4157	3611	1742	1500	1400	1350	1350	1000	600	
3000	7500	16281	16234	15518	13919	11200	8623	7035	5246	4389	4067	3900	3860	3188	1201	1200	1200	1100	1100	1000	700	
4500	0	8083	7488	6895	6294	4676	4400	4125	3850	1362	793	730	687	644	601	515	429	344	304	300	250	
4500	50	8250	7658	7055	6432	5669	5300	5006	4713	3941	3573	3482	3247	2711	2175	1629	1232	836	338	300	300	
4500	100	8374	7784	7174	6535	6000	5600	5300	5000	4800	4500	4400	4100	3400	2700	2000	1500	1000	980	866	744	
4500	200	8589	8004	7381	6900	6800	6700	6600	6000	5800	4900	4700	4600	4200	3700	3200	2900	2880	1645	1286	916	
4500	300	8783	8202	7567	7100	7000	6900	6490	6367	6300	5400	5300	5000	4700	4600	4374	3595	3365	2275	1633	1100	
4500	500	9136	8562	7906	7400	7300	7200	7106	6783	5900	5594	5229	4700	4652	4093	3509	3000	2920	2392	1801	1192	
4500	750	9539	8973	8294	7800	7700	7100	6777	6089	5816	5292	4841	4400	4307	4100	3835	2884	2611	2263	1705	1075	
4500	1000	9916	9357	8656	7816	7700	7009	6586	6110	5838	5173	4473	4295	4189	4100	3886	3370	2679	2150	2124	1531	
4500	1500	10617	10073	9330	8500	7768	5965	5534	5503	5462	5265	4728	4340	4147	4047	3333	2641	1744	1700	1668	1608	
4500	2000	11273	10741	9959	8600	6400	6382	5500	5405	5319	5132	4722	4409	4070	3564	2658	2050	1446	802	687	200	
4500	3000	12494	11986	11132	8700	6299	5955	5327	5000	4996	4798	4500	4216	3757	2817	1889	1382	1018	391	300	224	
4500	4000	13633	13148	12226	9215	8948	6831	6216	5446	4944	4525	4180	3779	3200	2481	1527	939	900	393	309	200	
4500	5000	14716	14252	13266	9890	8937	8000	6624	5241	4586	4101	3825	3541	2893	2122	1366	1200	1200	1100	1100	900	
4500	7500	17251	16835	15698	10510	9913	8833	7133	5109	4400	4000	3900	3653	2969	2355	2200	2200	1800	1500	1300	1000	
7000	0	7118	6752	6381	5997	4538	4348	4160	3970	1921	1221	868	761	713	666	570	475	380	350	300	250	
7000	50	7306	6927	6536	6127	5485	5137	4790	4443	3780	3380	3142	2965	2578	1966	1493	1169	920	535	500	500	
7000	100	7446	7057	6651	6223	5800	5400	5000	4600	4400	4100	3900	3700	3200	2400	1800	1400	1100	1100	1000	909	
7000	200	7688	7284	6852	6391	6200	6000	5500	5093	4800	4600	4500	4400	4000	3500	3000	2300	1600	1300	1289	1257	
7000	300	7907	7487	7032	6542	6400	6300	5600	5122	5000	4800	4700	4400	4100	4000	3500	3172	2201	1937	1531	1216	
7000	500	8305	7858	7361	6817	6500	6500	6000	5700	5600	5500	5300	4482	4456	3171	2539	2290	2222	2066	1532	952	
7000	750	8759	8282	7736	7131	7100	7000	6200	5500	5400	5300	4928	3727	3597	3296	2866	2524	2342	1992	1478	1167	
7000	1000	9184	8678	8087	7425	6800	6281	5758	5296	5100	4646	4057	3551	3356	3340	2998	2384	1771	1400	1300	1100	
7000	1500	9975	9416	8740	8000	7606	5366	4790	4766	4740	4378	3896	3545	3333	2956	2166	1525	992	900	714	700	
7000	2000	10713	-10104	9349	6980	6100	6044	4935	4728	4323	3685	3265	3179	2917	2423	1658	1023	776	327	189	115	
7000	3000	12089	11387	10485	7859	6192	5840	4995	4295	3832	3199	2932	2905	2521	1904	1049	521	349	213	171	124	
7000	4000	13373	12584	11544	8637	8317	6336	5694	4638	3742	2929	2614	2435	2085	1670	851	341	255	234	175	110	
7000	5000	14593	13721	12550	9487	8696	7889	6408	4682	3470	2600	2400	2325	2000	1466	846	600	400	300	250	150	
7000	7500	17447	16381	14903	10262	9817	8841	7042	4783	3636	2941	2570	2512	2200	2143	1853	700	500	400	300	400	
10000	0	4731	4566	4396	4218	4144	4019	3894	3770	2280	1584	1101	918	748	698	598	498	399	250	250	200	
10000	50	4930	4745	4551	4347	4300	4230	4050	4018	3495	2946	2545	2180	1837	1524	1200	950	700	365	300	300	
10000	100	5078	4877	4666	4500	4400	4300	4200	4100	3500	2887	2850	2835	2800	2167	2081	1700	1662	1123	710	700	
10000	200	5336	5108	4866	4610	4600	4500	4450	4400	2721	2500	2500	2462	2422	2032	1672	1600	1543	1450	1432	1275	
10000	300	5568	5315	5046	4760	4700	4262	4075	4007	3725	3400	3353	3200	3164	2741	2398	1826	1617	1377	1125	855	
10000	500	5600	5500	5400	5344	5200	5184	4454	3600	3500	3485	3300	2859	2744	2390	2161	1443	1082	925	723	528	
10000	750	5800	5600	5500	4776	4650	4600	4463	3768	3500	3428	3177	2870	2640	2135	1683	1363	1107	776	491	284	
10000	1000	6924	6200	5908	4873	4400	4300	4254	4052	3713	3376	3121	2827	2393	1844	1061	865	595	395	350	310	
10000	1500	7763	6900	6476	5772	4747	4678	4413	3903	3581	3166	2699	2204	1873	1273	871	572	379	350	300	283	
10000	2000	8547	7982	6686	6400	5776	5066	4385	3955	3458	2768	2178	1772	1367	1027	666	386	300	250	230	166	
10000	3000	11650	9289	8298	6700	6700	5473	4476	3952	3232	2374	1793	1494	1259	944	542	267	223	220	209	168	
10000	4000	12289	10508	9489	7170	7134	5995	4637	3874	3110	2213	1624	1378	1190	846	454	227	200	200	177	160	
10000	5000	13179	11414	10337	8300	8223	7226	5831	4235	2929	2047	1579	1461	1245	1128	703	600	500	400	177	160	
10000	7500	14766	13009	11908	8703	8615	7704	6241	4778	3561	2773	2277	2187	2100	2000	1872	1000	500	400	170	160	
15000	0	3308	3249	3187	3117	3103	3046	2987	2930	2206	1731	1395	1145	952	798	577	481	385	121	113	110	
15000	50	3434	3363	3287	3204	3176	3087	2997	2908	2501	2158	1999	1786	1663	1549	1419	795	696	286	262	250	
15000	100	3528	3446	3361	3269	3200	3100	3000	2900	2400	2097	2054	1905	1881	1740	1664	1468	1249	816	544	500	
15000	200	3690	3592	3490	3381	3200	3200	3000	2500	1636	1400	1400	1389	1376	1300	1275	1150	1132	870	643	600	
15000	300	3837	3724	3606	3482	3300	2900	2800	2772	2770	2560	2478	2201	2095	1692	1488	1112	816	576	336	300	
15000	500	3800	3750	3700	3549	3528	3313	3007	2200	2100	2100	2050	1640	1584	1300	1097	634	335	284	236	178	
15000	750	3587	3400	3350	2910	2700	2600	2600	2510	2196	2088	1969	1541	1401	1168	769	517	400	400	400	173	
15000	1000	3200	3150	3100	2980	2600	2599	2300	2300	2183	1806	1466	1229	1108	930	425	263	242	225	200	173	
15000	1500	4300	4100	3947	3770	3331	3246	2838	2270	1928	1549	1264	1032	850	644	335	220	196	190	180	173	
15000	2000	5530	5091	4433	4180	3670	3244	2715	2391	2104	1673	1272	913	718	529	299	222	192	190	180	173	
15000	3000	6904	5218	5163	4629	4236	3578	2967	2726	2288	1722	1239	1017	869	634	431	286	250	225	200	173	
15000	4000	7402	5300	5100	4734	4581	3906	3200	2953	2525	1906	1476	1234	1111	732	514	324	300	225	200	173	
15000	5000	8573	7329	6303	5703	5700	3158	4356	3567	2841	2244	1802	1577	1340	1103	790	760	750	710	400	200	
15000	7500	10140	9040	7881	6401	6089	5567	4749	4406	3800	2983	2441	2309	2113	1971	1562	1000	950	910	400	200	
20000	0	1211	1204	1202	1150	1107	1087	1066	1045	907	791	692	607	533	467	357	269	200	150	100	50	
20000	50	1300	1300	1294	1205	1133	1101	1069	1037	922	813	762	687	642	598	544	308	264	199	170	146	
20000	100	1400	1400	1362	1351	1142	1106	1070	1034	927	820	765	713	678	642	606	321	285	250	185	150	
20000	200	1558	1500	1500	1465	1142	1142	1070	1034	927	820	800	[illegible]	800	750	679	676	675	574	323	300	
20000	300	1600	1600	1587	1500	1400	1300	1231	1200	1100	1050	1000	1000	900	850	789	657	456	282	183	150	
20000	500	1665	1649	1450	1400	1300	1235	1100	1063	950	915	900	674	657	508	393	325	179	172	150	150	
20000	750	1838	1819	1500	1400	1300	1300	1250	1250	1219	1164	1085	656	541	516	431	328	218	200	200	150	
20000	1000	1580	1414	1232	1200	1108	1100	1000	977	961	801	714	629	620	611	387	254	178	110	100	98	
20000	1500	2500	2249	1997	1800	1750	1712	1399	1174	1054	943	864	730	679	621	375	250	131	110	100	98	
20000	2000	3261	2878	2458	2098	1648	1565	1500	1498	1420	1354	1274	1087	960	793	568	388	195	110	100	98	
20000	3000	3939	3176	3017	2671	2233	2008	1958	1900	1716	1598	1461	1308	1197	1001	801	550	189	110	100	98	
20000	4000	4365	4000	3891	2939	2576	2300	2250	2235	1960	1854	1679	1525	1430	1159	948	654	189	182	178	143	
20000	5000	4843	4000	3881	3732	3215	2875	2588	2357	2150	2015	1745	1717	1687	1381	965	568	268	253	250	214	
20000	7500	5101	5017	4900	3849	3300	3228	3250	3200	3185	2594	2500	2469	2398	1902	1486	1034	339	325	321	250	

Table 6.2: CHF correction factors

Factor	Form	Comments
K_1, subchannel or tube cross section factor	For $0.002\ m < D_{hy} < 0.016\ m$: $K_1 = \left(\frac{0.008}{D_{hy}}\right)^{1/3}$ For $D_{hy} > 0.016\ m$: $K_1 = \left(\frac{0.008}{0.016}\right)^{1/3} = 0.79$	Includes the observed diameter effect on CHF. This effect is quality-dependent and could be included by replacing the exponent 1/3 by $(2 - X)/4$ (requires verification)
K_2, bundle factor	$K_2 = \min[0.8, 0.8 \exp(-0.5X^{1/3})]$	Predicts the correct trend of quality on the bundle correction factor
K_3, grid spacer factor	$K_3 = 1 + A \exp(-B\ L_{sp}/D_{hy})$ $A = 1.5K^{0.5}\left(\frac{G}{1000}\right)^{0.2}, \quad B = 0.10$	Ideally A and B should be obtained for each grid spacer as the pressure loss coefficient K is insufficient to completely express the grid spacer effect
K_4, heated length factor	$L/D_{hy} \geq 5$: $K_4 = \exp\left(\frac{D_{hy}}{L} e^{2\alpha}\right)$ α evaluated from homogeneous model $\alpha = X/[X + \rho_g/\rho_l(1 - X)]$	Inclusion of α correctly predicts the diminishing length effect at subcooled conditions. The length effect is particularly noticeable if $L/D_{hy} < 10$ for subcooled burnout and $L/D_{hy} < 100$ for two-phase dryout
K_5, axial flux distribution factor	$X > 0$: $K_5 = q_{BLA}/q_{LOCAL}$ $X < 0$: $K_5 = 1.0$	Tong's [17] F factor may also be used but only within narrow ranges of conditions
K_6, flow factor, horizontal flow	Stratified flow ($G < G_1$) $K_6 = 0.0$ Nonstratified flow ($G > G_2$) $K_6 = 1.0$ Intermediate ($G_1 < G < G_2$) $K_6 = \frac{G - G_1}{G_2 - G_1}$	G_1 mass flux boundary between fully stratified and intermittent flow (kg/m² s) G_2 mass flux boundary between intermittent and annular flow (kg/m² s) To find G_1 and G_2 use Taitel and Dukler's [18] flow regime map
K_6, flow factor, vertical flow	$G < -400$ kg/m² s or $X = 0.0$ $K_6 = 1.0$ $-50 < G < 10$ kg/m² s $CHF = CHF_{G=0,X=0}(1 - \alpha)C_1$ $10 < G < 100$ kg/m² s, $-400 < G < -50$ kg/m² s: linear interpolation	$\alpha < 0.8$ $C_1 = 1.0$ $\alpha > 0.8$ $C_1 = \frac{0.8 + 0.2\rho_l/\rho_g}{\alpha + (1 - \alpha)\rho_l/\rho_g}$

of Ψ_K, Ψ_σ and Ψ_γ are illustrated in Table 6.3. Those scaling factors are commonly used in fluid modelling technique that enables the thermal and hydraulic behaviors of a given system to be predicted using a modelling fluid rather than the working fluid. The analysis shows that the prediction errors of the three dimensionless groups (Ψ_K, Ψ_σ and Ψ_γ) are approximately equal. The use of Ψ_K is recommended because of its simplest form. Thus, a dimensionless CHF table can be created and it is demonstrated in Table 6.4. (For detail, see Groeneveld et al. (1986b)).

2. Second method: The parameters of non-aqueous fluids are converted into the water-equivalent parameters so that a value of CHF can be obtained from the dimensional CHF table. Then, the real CHF for a non-aqueous fluid is calculated by:

$$CHF_{non-aqueous} = \left(\frac{CHF}{Gh_{fg}}\right)(Gh_{fg})_{non-aqueous}$$

The detail procedure can be seen in Leung (1986).

The deviations of the CHF values predicted by both methods are very little. In present work, the CHF values for non-aqueous fluids are predicted by the second method. In summary, Groeneveld's look-up CHF table predicts CHF adequately for a non-aqueous fluid as well as water. The accuracy for this table has been tested by Groeneveld et al. (1986a, 1986b).

Table 6.3: Dimensionless groups for flow parameter

Investigator	Form
Katto's scaling factor (Katto and Ohno (1984))	$\Psi_K = \frac{GD^{0.5}}{\sigma^{0.5}\rho_f^{0.5}}$
Ahmad's first scaling factor (1973)	$\Psi_\sigma = \left(\frac{G^2D}{\rho_f\sigma}\right)^{2/3} \times \left(\frac{GD}{\mu_f}\right)^{-0.133} \times \left(\frac{GD}{\mu_g}\right)^{-0.2}$
Ahmad's second scaling factor (1973)	$\Psi_\gamma = \left(\frac{GD}{\mu_f}\right) \times \left(\frac{\gamma^{1/2}\mu_f^{2/3}}{D\rho_f^{1/2}}\right) \times \left(\frac{\mu_f}{\mu_g}\right)^{1/8}$

Table 6.4: Non-dimensional CHF table

ρ_l/ρ_g	ϕ_k	-.50	-.40	-.30	-.20	-.15	-.10	-.05	0.00	.05	.10	.15	.20	.25	.30	.40	.50	.60	.70	.80	.90	1.00
1623.3	.60	0	0	0	0	355092	310086	212630	150613	141753	132894	115174	110745	106669	99759	79647	75306	70876	44386	31451	31008	0
1623.3	1.19	0	0	0	0	212630	186051	137323	97455	93025	88596	64232	44298	44298	42304	42083	42083	39868	29236	19048	14839	0
1623.3	2.38	0	0	0	0	124034	108530	84166	57587	56479	55372	33223	31008	28793	27597	26578	24895	24363	18915	10499	10188	0
1623.3	3.57	0	0	0	0	94502	82689	66447	44298	44298	44298	36915	35438	33961	33961	32012	25412	21381	12078	7102	4644	0
1623.3	5.95	0	0	0	0	63789	55815	46069	31894	31451	31008	28350	26578	22149	20890	20820	20385	10808	6201	5767	3898	0
1623.3	8.93	0	0	0	0	47251	41344	34847	32485	29532	27760	25096	23661	18333	18197	17323	14216	7778	5380	4136	2362	0
1623.3	11.91	0	0	0	0	38982	33666	29236	21263	20377	19517	16833	15947	14618	14618	14396	11087	6875	4872	2657	1328	0
1623.3	17.86	0	0	0	0	28350	26216	20672	16242	14175	13584	13289	13144	12403	11812	11549	9169	7681	3248	1771	885	0
1623.3	23.81	0	0	0	0	22149	19491	17054	13289	11960	11738	11517	11295	11185	11074	10853	10075	6423	2436	1328	664	0
1623.3	35.72	0	0	0	0	15504	13880	12403	9597	9302	8859	8564	8416	7973	7825	7678	5758	3986	1624	885	442	0
1623.3	47.63	0	0	0	0	12181	11074	9967	7641	7514	7364	6755	5869	5537	5094	4429	3322	2214	1107	553	332	0
1623.3	59.53	0	0	0	0	10188	9391	8416	7087	6976	6733	6556	4606	3898	3366	2657	2214	1328	797	442	265	0
1623.3	89.30	0	0	0	0	7087	6792	6497	6201	5453	5315	4429	2953	2362	1771	1299	1181	708	472	236	177	0
1100.7	.61	0	0	0	570054	368414	323486	242614	170728	161743	152757	134785	130293	127237	119420	90036	80871	78445	48433	37650	35942	0
1100.7	1.22	0	0	0	287408	215657	188700	143771	107828	98843	89857	85364	80871	62900	49107	44928	42682	42682	42277	31494	20217	0
1100.7	2.44	0	0	0	145748	121307	107828	78625	60653	58407	56160	47175	35942	31450	26957	26957	26193	25833	24710	22464	11232	0
1100.7	3.66	0	0	0	98408	89857	80871	59904	44928	43431	41933	37440	35942	22464	20966	20068	19469	17971	17971	11980	7488	0
1100.7	6.10	0	0	0	60393	59305	53914	40435	33247	32348	31450	27855	24261	14377	13478	13478	12580	10782	9884	6020	4043	0
1100.7	9.15	0	0	0	44329	43131	39537	29952	25759	24860	23961	20966	16773	8386	8380	7787	7188	4589	5990	3893	2396	0
1100.7	12.20	0	0	0	35942	35044	32348	24710	23362	20217	17904	15275	14377	5391	4964	4942	4942	4432	4492	2695	1572	0
1100.7	18.30	0	0	0	25759	25160	22763	17971	16473	11980	11381	9884	9235	7188	5990	4492	3193	3596	3294	1647	898	0
1100.7	24.40	0	0	0	20667	20217	18420	13927	12804	10558	9659	9210	8945	7862	6739	5616	4492	3818	3369	1235	673	0
1100.7	36.60	0	0	0	14676	14377	9345	8686	7188	6589	6439	6290	6140	5690	4942	4867	4792	3744	1497	748	449	0
1100.7	48.80	0	0	0	11456	11232	7453	6739	5616	5166	5094	4829	4717	4043	3145	3145	2920	2246	1123	505	336	0
1100.7	61.00	0	0	0	9614	9435	8895	8266	8217	4693	5860	5121	3594	2785	2336	2066	1797	1347	808	404	269	0
1100.7	91.[illegible]1	0	0	0	6709	6589	6230	5810	5695	5320	4792	3893	2995	1797	1317	1078	958	599	359	239	179	0
834.7	.62	0	0	0	549175	450226	363451	281130	210166	163008	149186	141927	134749	127662	120484	113033	94860	59060	54517	52155	51882	0
834.7	1.24	0	0	0	277086	227157	206269	145380	118121	104492	95406	90862	86319	59060	54517	50383	36345	34845	36073	34073	23442	0
834.7	2.49	0	0	0	140678	118121	97677	77233	63604	56789	52446	48838	31802	29462	27258	26804	24987	22715	22715	22715	11675	0
834.7	3.73	0	0	0	95072	81776	67390	53003	45431	40888	36345	33316	32559	31802	30287	27698	22670	13690	6314	6057	5300	0
834.7	6.22	0	0	0	58452	50883	42251	31619	28621	26350	22715	21807	20898	20444	20226	15982	12611	5987	2271	1817	1817	0
834.7	9.33	0	0	0	40040	35133	29379	23624	19989	18172	16052	15143	14017	13078	11012	9631	8862	6057	3634	2725	1817	0
834.7	12.44	0	0	0	30779	27258	22715	18172	15446	13629	11812	11357	9695	8809	8177	7723	7269	4543	2725	2044	1362	0
834.7	18.66	0	0	0	21452	18778	11932	11509	9994	9086	7874	7571	7117	6569	5451	5148	4543	3028	1817	1362	908	0
834.7	24.88	0	0	0	16741	14538	10222	9086	7950	6814	5906	5678	4883	4656	4088	3861	3180	2271	1362	1022	681	0
834.7	37.32	0	0	0	11971	10600	8695	6492	5906	4543	3937	3785	3255	3104	2725	2574	2120	1514	908	681	454	0
834.7	49.76	0	0	0	9767	9654	7281	5451	5111	3407	2953	2839	2441	2328	2044	1930	1590	1135	681	511	340	0
834.7	62.20	0	0	0	8068	6003	5560	4785	4402	2725	2362	2271	1953	1862	1635	1544	1272	908	545	408	272	0
834.7	93.31	0	0	0	6051	4234	3916	3380	3075	1817	1574	1514	1302	1241	1090	1029	848	605	363	272	181	0
564.1	.64	0	0	0	528213	468197	396899	304795	275111	229428	215187	207882	200484	186243	172002	143427	98670	49473	46237	46237	41613	0
564.1	1.28	0	0	0	266880	240433	208067	161830	157206	147958	138711	134087	129464	120216	110969	53635	41613	40226	39301	36989	23303	0
564.1	2.57	0	0	0	135867	129464	108657	83226	80915	73979	67043	64732	36989	33822	32366	32366	31911	30054	27742	27303	13154	0
564.1	3.85	0	0	0	92027	70773	51230	50860	50090	49319	43154	41613	40072	38530	36939	33537	27511	16075	6750	6164	5579	0
564.1	6.42	0	0	0	56797	42852	31136	30516	30054	29591	24968	1043	24043	24043	23118	17995	12400	7499	1849	1849	1849	0
564.1	9.63	0	0	0	39073	36989	30824	24043	23426	19727	17261	15645	15942	15258	14808	9407	5351	3020	2576	1541	1232	0
564.1	12.83	0	0	0	30151	20667	24043	18494	18032	14795	12021	11559	11073	10209	9709	5322	6935	5548	3236	1849	924	0
564.1	19.25	0	0	0	21151	19727	12804	12638	12329	9863	8014	8014	7823	7274	6473	5548	4623	3698	2157	1232	616	0
564.1	25.67	0	0	0	16599	15258	9940	9709	9478	7397	6010	5779	5303	5086	4854	4161	3467	2774	1618	924	462	0
564.1	38.50	0	0	0	12329	11987	8769	7397	7253	4931	4007	3853	3535	3390	3236	2774	2311	1849	1078	616	308	0
564.1	51.33	0	0	0	9940	9759	7284	5222	5086	3698	3005	2889	2653	2543	2427	2080	1733	1387	809	462	231	0
564.1	64.17	0	0	0	8185	5011	4485	3668	3259	2959	2404	2311	2121	2034	1941	1664	1387	1109	647	369	184	0
564.1	96.25	0	0	0	6215	3585	3204	2611	2237	1972	1602	1541	1417	1356	1294	1109	924	739	431	246	123	0
380.1	.67	0	0	0	514707	475165	436661	219887	212338	207147	199597	192047	188084	184026	176476	175532	153355	56623	51904	51244	47186	0
380.1	1.33	0	0	0	260562	245168	193463	160433	136840	132121	127402	122684	120324	103809	94372	70779	52990	52471	46431	42845	28075	0
380.1	2.66	0	0	0	133041	132121	97911	80216	70779	66060	61342	60162	58982	51904	40100	37748	35389	33030	30812	20997	14037	0
380.1	3.99	0	0	0	90361	65195	45550	44826	44433	44040	40894	39321	38535	37748	37748	36176	33989	24898	11875	7030	4417	0
380.1	6.65	0	0	0	56047	39513	27736	27368	26896	26424	24536	22649	22649	22649	21705	21186	16836	10598	4256	2359	2227	0
380.1	9.98	0	0	0	38749	37748	27053	21391	19503	17616	16357	14470	13526	12582	11953	8524	5530	4448	2938	2202	1988	0
380.1	13.31	0	0	0	30034	29255	20761	16043	15099	13212	12260	9909	9276	8427	5662	3303	2859	3798	2359	1415	943	0
380.1	19.5[illegible]	0	0	0	21230	20132	13039	9625	9437	8808	8178	6606	6562	4718	3145	2202	2091	1887	1572	943	629	0
380.1	26.6[illegible]	0	0	0	16769	15571	8307	8021	7785	6606	6134	4954	4246	3538	2831	2595	2359	1651	1179	707	471	0
380.1	39.[illegible]2	0	0	0	12229	11796	9047	6521	5844	4404	4089	3460	2831	2359	1887	1730	1572	1101	786	471	314	0
380.1	53.23	0	0	0	9907	9437	7325	5063	4808	3303	3067	2595	2123	1769	1415	1297	1179	825	589	353	235	0
380.1	66.54	0	0	0	8485	6246	5664	5133	3303	2642	2453	2076	1793	1415	1132	1038	943	660	471	283	188	0
380.1	99.81	0	0	0	6528	4327	3945	3590	2264	1761	1635	1384	1258	943	754	692	629	440	314	188	125	0

Table 6.4 cont'd

p_t/p_s	ϕ_s	-.50	-.40	-.30	-.20	-.15	-.10	-.05	0.00	.05	.10	.15	.20	.25	.30	.40	.50	.60	.70	.80	.90	1.00
246.1	.70	0	0	644425	509572	486419	452318	241029	222816	214291	199178	176000	154421	132043	109761	94067	78373	48438	43594	39138	38750	0
246.1	1.39	0	0	325990	258612	251880	203441	169534	145315	135627	125940	111408	96876	82345	67813	58126	48438	40203	39719	39525	27597	0
246.1	2.79	0	0	166265	132648	128361	102931	87189	77501	72657	70235	65191	62970	60548	53282	48438	43594	41172	33979	22112	15716	0
246.1	4.18	0	0	112797	90436	87189	69428	59740	54896	48438	46821	43594	41980	41172	40365	40365	40365	30548	17647	10139	8605	0
246.1	6.97	0	0	69828	56450	55219	42625	36813	33906	29063	28094	27125	26156	25672	25188	25188	24077	13175	6238	3729	3419	0
246.1	10.46	0	0	48180	39299	38750	29708	25188	23250	19375	17437	16792	16146	15500	14854	14751	9028	4391	2906	2751	2712	0
246.1	13.95	0	0	37278	30642	30031	24509	19830	17437	14531	13562	13078	13078	13054	7750	7725	4427	2262	1259	1210	968	0
246.1	20.92	0	0	26273	21878	20667	16117	12997	11625	9687	8073	7750	7427	7375	3875	3765	2605	836	642	565	484	0
246.1	27.90	0	0	20700	17425	15984	12594	10656	8718	7265	6054	5328	4359	3632	3148	3148	2179	605	484	484	363	0
246.1	41.85	0	0	15035	12878	10979	8718	7427	5812	4843	4036	3552	2906	2421	2099	1937	1453	403	322	322	242	0
246.1	55.80	0	0	12141	10541	8476	6781	5812	4359	3632	3027	2664	2179	1816	1574	1453	1089	302	242	242	181	0
246.1	69.75	0	0	10370	9103	6975	5618	4746	3487	2906	2421	2131	1840	1453	1259	1162	871	242	193	193	145	0
246.1	104.62	0	0	7940	7115	4779	3975	3229	2325	1937	1614	1420	1291	1033	839	775	581	161	129	129	96	0
172.3	.73	0	0	814155	661358	558334	505079	453026	407822	340465	324966	309369	301222	278273	255224	231480	192933	109680	86929	80869	42322	0
172.3	1.46	0	0	410853	334603	298043	273206	248369	228500	218565	208630	198695	193728	178826	163923	149021	124184	79478	76845	53151	32735	0
172.3	2.92	0	0	200705	201179	198695	186277	173858	149021	144054	139086	134119	126668	116733	109282	106798	83253	60974	42322	27742	19323	0
172.3	4.38	0	0	141107	135775	132463	124184	115905	107626	104315	92724	89413	84445	77822	77822	77342	65536	42570	25979	15200	11772	0
172.3	7.30	0	0	86810	82458	79478	74510	69543	64576	61595	55634	53647	50667	46693	46216	45700	37781	20733	11156	5990	4341	0
172.3	10.95	0	0	59509	55634	52985	49673	46362	43050	40401	37089	35765	33115	32453	31791	26095	15047	7325	4609	3490	3086	0
172.3	14.60	0	0	45784	42222	39739	37255	34771	32288	29838	27817	26823	26669	24454	20480	14430	8176	4411	3010	1480	1082	0
172.3	21.90	0	0	31946	28148	26492	24836	23181	21525	19518	17551	16557	16309	14653	11011	7924	4397	2030	847	622	331	0
172.3	29.20	0	0	24918	21608	19869	18627	17385	16144	14157	12915	11921	10928	8941	8692	8628	6971	1986	620	372	248	0
172.3	43.80	0	0	17879	15501	13246	12418	11590	10762	9104	8444	7782	6954	6621	4560	6388	2152	1241	413	248	165	0
172.3	58.39	0	0	14277	12527	9934	9313	8692	8072	6581	6209	5588	4967	4222	3477	2297	1428	869	310	186	124	0
172.3	72.99	0	0	12081	10707	7947	7451	6954	6457	5364	4868	4371	3775	3278	2583	1639	993	645	248	149	99	0
172.3	109.49	0	0	9004	8206	5298	4967	4636	4305	3642	3179	2847	2384	2119	1521	993	596	197	165	99	66	0
114.1	.78	0	934588	806144	676260	594504	524471	506166	431918	411350	361268	345123	336587	320339	296480	263984	239303	118160	104957	90394	43808	0
114.1	1.55	0	471561	407648	342757	318796	282803	277661	257094	221100	231184	221100	215959	205675	190249	169682	154256	82270	80367	55583	32753	0
114.1	3.11	0	239403	207869	185107	182536	177194	169682	164540	159398	154256	146543	138830	128547	105408	92553	87694	71677	52447	32522	20978	0
114.1	4.66	0	161083	140921	128547	126033	121191	114835	111407	107979	102837	97695	90839	89125	89125	87583	78002	60657	38392	21764	14654	0
114.1	7.77	0	99577	87175	80213	79184	74043	68901	65816	62730	59645	56560	54503	49362	47305	46276	44292	31910	16891	9831	6252	0
114.1	11.65	0	68243	60105	55532	54846	49162	45934	43191	40449	38392	37021	35650	34279	32908	31063	20183	11771	7418	4847	3091	0
114.1	15.54	0	52483	46472	42163	41135	37021	34450	32136	29308	28794	28537	20280	27766	26840	18988	10700	5748	4206	2396	1110	0
114.1	23.31	0	36603	32712	28396	27423	24681	22967	21424	18853	18167	18082	17653	16621	15555	9916	4936	2797	1333	798	685	0
114.1	31.08	0	28586	25747	22513	20567	18510	17225	15939	14140	13368	12597	10394	10283	10078	6627	3779	2570	2056	1028	514	0
114.1	46.62	0	20462	18670	16517	12904	11517	11483	10455	9598	8741	8227	8055	7637	7182	6871	3539	1713	1371	685	342	0
114.1	62.16	0	16331	15058	13444	9827	8787	8612	7841	7198	6427	6041	4684	4884	3984	2442	2313	1285	1028	514	257	0
114.1	77.70	0	13814	12847	11557	8741	7712	7095	6478	5758	4936	4524	3702	3599	2673	1748	1542	1028	822	411	205	0
114.1	116.55	0	10377	9815	8957	6170	5484	4867	4319	3770	3222	2810	2468	2262	1611	1096	822	685	548	274	137	0
84.6	.82	1032607	920650	808058	693771	621746	574082	526418	497820	402493	397409	380673	371776	355041	330256	296679	287041	126361	99870	98187	45968	0
84.6	1.64	520911	465197	409325	351969	333645	309813	285982	275390	259502	254206	243614	238319	227726	211838	190654	185358	90031	84788	63869	40355	0
84.6	3.28	264480	236935	209243	188006	185358	182710	180062	177414	174766	166822	158878	148282	140343	127103	116511	100074	72587	57454	35747	21951	0
84.6	4.92	178721	160432	142249	131516	130633	129751	127103	121807	116511	116511	104153	100623	97092	91796	79439	77674	76420	49499	26762	15517	0
84.6	8.20	109859	99023	88368	82617	81557	80498	79439	76261	69906	69906	60691	56645	55342	55078	54982	47451	39200	25907	14055	8176	0
84.6	12.30	75245	68127	61207	57196	57196	55078	53665	50841	49429	48320	45227	41301	40009	37424	36874	25427	16586	8791	5571	3177	0
84.6	16.39	57837	52578	47510	43956	43426	42897	41308	40853	37458	35721	34328	32845	30716	30674	22682	14574	9135	5359	3092	2023	0
84.6	24.59	40298	36888	33668	30716	30010	29657	27539	26080	23905	22553	20802	16827	16548	16240	11287	6104	3378	1970	1115	1059	0
84.6	32.79	31447	28951	26649	23831	23037	22507	20654	18535	17211	15358	13864	11839	11399	10944	9881	2698	1273	1098	1059	794	0
84.6	49.18	22481	20901	19501	17356	15789	14360	13769	12357	10944	9885	9250	8394	8229	7871	5989	2824	2118	1765	706	529	0
84.6	65.58	17922	16794	15840	14183	11995	10924	9267	8605	7943	7281	6982	6327	6222	5845	4256	1853	1588	1191	529	397	0
84.6	81.97	15145	14287	13595	12233	10591	9003	6884	5295	5084	4872	4560	4519	4448	4322	2542	1482	1271	953	635	529	0
84.6	122.96	11356	10852	10504	9537	7273	6002	3883	3389	3248	3106	2824	2459	2259	1977	1200	1059	917	776	564	423	0
54.8	.90	1002815	912269	820495	726826	673301	621449	569596	542834	460539	445708	436341	418499	400769	374564	338992	303420	259485	37913	34345	33453	0
54.8	1.80	506983	462267	416492	369100	362409	314532	306654	295503	289927	284352	278776	267625	256474	239748	217445	195143	167266	75437	58989	42262	0
54.8	3.60	258342	236514	213682	203507	200719	197931	192355	186780	183992	181204	175629	167266	158902	150539	133812	111510	91243	61414	37695	22831	0
54.8	5.40	175146	160891	145725	141246	139388	137529	136637	130634	130095	130095	130095	129538	122661	116342	101530	85491	84339	53934	31092	18176	0
54.8	9.00	108276	100058	91003	89208	89208	89208	88851	65249	80287	72481	70162	65635	63828	63549	62557	47760	42262	30364	18889	11585	0
54.8	13.50	74608	69389	63390	62446	61702	60215	60215	57985	52781	49770	48960	45068	45377	45347	37452	26717	20443	13760	9129	5084	0
54.8	18.00	57656	53921	49449	47392	46276	45719	44604	42592	38722	37356	36765	35861	33057	29544	23082	18466	14524	12271	9467	4510	0
54.8	27.00	40549	30291	35330	32709	32338	30658	29390	27004	24532	24484	21376	18975	17228	16745	12596	9378	7805	7434	7333	4690	0
54.8	36.00	31892	30344	28151	25647	25360	25089	25089	24811	24582	20481	17178	14540	12801	11608	7853	5915	3370	2787	2787	1672	0
54.8	54.00	23099	22259	20826	18603	17655	16726	15797	14868	14604	11528	10128	9286	8337	5608	3902	3744	2044	1951	1858	1115	0
54.8	71.99	18609	18116	17059	15258	14535	12544	9794	9188	8325	7744	7034	6552	5518	2832	2787	2643	2439	1881	1393	836	0
54.8	89.99	15865	15571	14742	13199	12043	9481	7910	6545	6002	5713	5119	4635	4026	1942	1672	1561	1505	1505	1115	669	0
54.8	134.99	12101	12068	11536	10347	8326	6410	5229	3899	3262	3023	2899	2869	2369	892	892	892	817	817	743	520	0

Table 6.4 cont'd

ϕ_t/ϕ_g	ϕ_m	-.50	-.40	-.30	-.20	-.15	-.10	-.05	0.00	.05	.10	.15	.20	.25	.30	.40	.50	.60	.70	.80	.90	1.00
34.7	1.02	984948	914271	842280	767901	676808	632754	597654	562674	470506	426572	415708	387691	323660	259668	194482	147085	99808	40353	35816	35816	0
34.7	2.04	499876	464656	428243	390099	358163	334285	316377	298469	286530	268622	263652	244744	202959	161173	119387	89540	59693	58499	51694	44412	0
34.7	4.07	256355	238894	220300	205943	202959	199974	196989	179081	173112	146249	140280	137295	125357	110433	95510	86556	85959	49098	38383	27339	0
34.7	6.11	174763	163203	150567	141275	139285	137295	129137	126690	125357	107468	105459	99489	93520	91530	87033	71533	66956	45267	32493	21887	0
34.7	10.19	109072	102219	94387	88346	87153	15959	84836	80980	79438	66785	62427	56112	55539	46865	41893	35816	34861	28557	21501	14231	0
34.7	15.28	75922	71417	66013	62081	61285	36510	53939	48463	46290	42119	38530	35020	34280	32632	30523	22954	20781	18011	13570	8556	0
34.7	20.37	59192	55855	51671	46656	45964	41839	39314	36472	34849	30879	26701	25638	25005	24474	23197	20116	15991	12834	12678	9139	0
34.7	30.56	42251	40086	37129	33826	30913	23738	22023	21899	21736	20952	18815	17271	16503	16105	13263	10510	6540	6765	6637	6399	0
34.7	40.74	33646	32059	29724	25668	19102	19048	16415	16132	15875	15317	14093	13159	12147	10637	7933	6118	4315	2393	2050	596	0
34.7	61.11	24860	23849	22150	17311	12533	11849	10599	9948	9941	9547	8954	8388	7475	5605	3758	2749	2025	778	596	445	0
34.7	81.48	20345	19621	18245	13751	13353	10194	9276	8127	7378	6752	6238	5639	4775	3702	2278	1401	1343	586	461	298	0
34.7	101.85	17569	17015	15837	11807	10669	9551	7908	6257	5475	4896	4566	4227	3453	2533	1630	1432	1432	1313	1313	1076	0
34.7	152.78	13730	13399	12494	8365	7889	7030	5677	4066	3502	3183	3104	2907	2363	1874	1751	1751	1432	1193	1034	795	0
20.3	1.23	970436	920091	860159	813632	728557	682333	636242	590151	502087	448956	417343	393832	342428	261138	198311	155275	122201	71062	66413	66413	0
20.3	2.47	494516	468681	441717	413292	385199	358633	332068	305502	292220	272295	259013	245730	212523	159392	119544	92979	73055	73055	66413	60370	0
20.3	4.94	255294	241878	227533	212224	205882	199240	182637	169122	159392	152791	149430	146110	132827	116223	99620	76375	53130	43168	42803	41740	0
20.3	7.41	175044	165746	155673	144826	141682	139468	123972	113390	110689	106261	104048	97406	90765	88551	77482	70221	48725	42881	33893	26919	0
20.3	12.34	110313	104375	97774	90548	86337	86337	79696	75711	74383	73055	70398	59533	59187	42119	33724	30417	29514	27442	20349	12645	0
20.3	18.52	77562	73338	68503	63146	62871	61986	54901	48703	47817	46932	43638	33003	31851	29186	25378	22350	20738	17639	13087	10333	0
20.3	24.69	60994	57633	53708	49312	45161	41714	38240	35172	33870	30855	26944	23583	22288	22182	19910	15833	11761	9297	8633	7305	0
20.3	37.03	44165	41693	38697	35420	33676	23758	21208	21101	20986	19383	17249	15695	14757	13087	9590	6752	4392	3984	3161	3099	0
20.3	49.38	35574	33552	31045	23178	20256	20070	16387	15700	14355	12236	10842	10556	9686	8046	5505	3397	2576	1085	627	381	0
20.3	74.06	26762	25203	23211	17398	13707	12928	11057	9508	8483	7081	6490	6431	5580	4215	2322	1153	772	471	378	274	0
20.3	98.75	22203	20891	19166	14340	13809	10516	9453	7700	6212	4863	4340	4042	3461	2772	1412	566	423	388	290	182	0
20.3	123.44	19383	18225	16669	12601	11550	10478	8511	6218	4609	3453	3187	3088	2656	1947	1123	796	531	398	332	199	0
20.3	185.16	15449	14503	13196	9087	8693	7828	6235	4235	3219	2604	2275	2224	1948	1897	1640	619	442	354	265	177	0
12.4	1.56	747306	719263	689856	658933	651808	641198	611913	609062	529784	446564	385779	330451	278458	231013	181900	144004	106108	55327	45475	45475	0
12.4	3.12	384870	369635	353644	341062	333483	325904	318325	310746	265271	218810	216006	214869	212216	164240	157722	128805	125965	85114	53812	53054	0
12.4	6.24	202212	193572	184401	174699	174120	170531	168636	166741	103114	94739	94739	93299	91783	77004	63361	60633	58473	54949	54266	48317	0
12.4	9.36	140669	134277	127481	120256	118740	107674	102950	101232	94108	85897	84709	80844	79935	69248	60582	46131	40651	34788	28421	21600	0
12.4	15.61	84886	83370	81855	81006	78823	78580	67515	54570	53054	57826	50022	43337	41594	36228	32757	21873	16401	14021	10959	8003	0
12.4	23.41	58612	56591	55580	48264	46990	46485	45101	38077	35369	34641	32105	29002	26678	21575	17007	13773	11186	7841	4961	2869	0
12.4	31.22	52478	46999	44777	36913	33348	32590	32241	30710	28141	25587	[illegible]	21426	18136	13975	8041	6555	4509	2993	2652	2149	0
12.4	46.82	39224	34864	32721	29164	23985	23836	22297	19721	10094	15997	13637	11136	9463	6432	4400	2890	1915	1768	1515	1429	0
12.4	62.43	31389	30248	25337	24253	21888	19198	16617	14987	13104	10489	8253	6715	5256	3891	2523	1462	1136	947	871	629	0
12.4	93.65	29132	23467	20963	16926	16926	13836	11308	9984	8165	5997	4529	3774	3180	2384	1369	674	563	555	528	424	0
12.4	124.86	23285	9910	17979	13585	13517	11359	8786	7340	5892	4193	3077	2611	2254	1602	860	430	378	378	335	303	0
12.4	156.08	19977	7301	15669	12581	12464	10953	8838	6419	4439	3102	2393	2214	1887	1709	1065	909	757	606	268	242	0
12.4	234.11	14421	[illegible]	12033	8794	8705	7785	6306	4828	3598	2802	2301	2210	2122	2021	1891	1010	505	404	171	161	0
6.2	2.50	684198	670053	654910	638373	632794	615061	597129	579397	498305	429965	398285	355847	331340	308626	282725	150397	138672	56983	52201	49810	0
6.2	4.99	351463	343294	334827	325661	318788	308825	298863	288901	239091	208905	204622	189778	187387	173341	165769	146244	124426	81290	54193	49810	0
6.2	9.99	183801	178919	173839	168409	159394	159394	149431	124526	81496	69734	69734	69186	68539	64753	63508	57282	56385	43335	32028	29886	0
6.2	14.98	127415	123661	119744	115627	109583	96300	92979	92050	91983	85010	82287	73088	69568	56186	49412	36926	27096	19127	11157	9962	0
6.2	24.97	75712	74715	73719	71109	70252	66009	59912	43833	41840	41840	40844	32675	31560	25901	21856	12631	6674	5658	4702	3546	0
6.2	37.45	47645	45161	44497	38653	35863	34535	34535	33339	29169	27734	26153	20468	18609	15514	10214	6867	5313	5313	5313	2297	0
6.2	49.93	31878	31380	30882	29687	25901	25891	22912	22912	21747	17991	14604	12243	11038	9264	4233	2620	2410	2241	1992	1723	0
6.2	74.90	28558	27229	26213	25038	22122	21558	18848	15076	12806	10287	8394	6853	5645	4277	2224	1461	1301	1261	1195	1148	0
6.2	99.87	27545	25358	22081	20820	18280	16158	13523	11909	10480	8333	6335	4547	3576	2634	1489	1105	956	946	896	861	0
6.2	149.80	22926	17327	17144	15371	14066	11881	9852	9052	7597	5738	4313	3377	2885	2105	1431	949	830	747	664	574	0
6.2	199.74	18438	13199	12701	11790	11409	9728	7969	7354	6288	4746	3676	3073	2766	1823	1280	806	747	560	498	430	0
6.2	249.67	17081	14602	12558	11362	11356	10276	8679	7106	5660	4471	3590	3142	2669	2197	1574	1514	1494	1414	796	398	0
6.2	374.51	13468	12007	10468	8502	8087	7394	6308	5852	5047	3962	3242	3067	2806	2618	2074	1328	1261	1208	531	265	0
2.9	5.99	439373	439373	437145	434642	382931	372115	361300	350485	311617	274777	257540	232193	216983	202111	183861	104097	89226	67257	57456	49345	0
2.9	11.99	236585	236585	230164	228305	192986	186902	180819	174735	156653	138571	132657	120489	114575	108491	102407	54245	48162	42247	31263	25348	0
2.9	23.97	130967	126742	126742	123785	96493	96493	90409	87367	78326	69285	67595	67595	67595	63371	57372	57118	57034	48500	27291	25348	0
2.9	35.96	90127	90127	89395	84494	78861	73228	69342	67595	61962	59148	56329	56329	50696	47880	44444	37008	25686	15885	10308	8449	0
2.9	59.94	56773	55732	49007	47317	43937	41740	37177	35927	32108	30925	30414	22775	22205	17169	13282	10984	6049	5813	5069	5069	0
2.9	89.90	41413	40985	33797	31544	29291	29291	28164	28164	27466	26227	24447	14780	12189	11626	9711	7390	4911	4506	4506	3379	0
2.9	119.87	26700	23895	20819	20278	18588	18588	16898	16510	16239	13536	12065	10629	10477	10325	6539	4292	3008	1858	1689	1656	0
2.9	179.81	28164	25337	22498	20278	19715	19287	15761	13226	11874	10633	9733	8224	7548	6996	4224	2816	1475	1239	1126	1104	0
2.9	239.74	27553	24317	20768	17727	13924	13223	12674	12657	11998	11440	10764	[illegible]	8111	6700	4799	3278	[illegible]	929	844	828	0
2.9	359.61	22188	17896	16794	15045	12578	11265	11029	10702	9666	9001	8229	[illegible]	6742	5638	4512	[illegible]	1658	519	563	552	0
2.9	479.48	18441	16898	16438	12416	10882	9716	9505	9442	8280	7832	7093	6442	6041	4896	4005	2762	798	768	752	624	0
2.9	599.35	13657	13519	13116	12613	10866	9716	8719	7966	7266	6810	5897	5603	5431	4397	3261	1919	905	855	844	773	0
2.9	839.03	11493	11304	11040	8672	7435	7273	7210	7210	7176	5844	5632	5563	5403	4285	3348	2329	763	732	723	563	0

Chapter 7

Derivation of Correction Factor Method and Empirical Correlation for Cross-Flow CHF

As mentioned in Chapter 1, the objective of the present work is to predict the CHF in cross-flow boiling where a semi-empirical correlation has been presented in Chapter 4. In this chapter, a correction factor method is derived by relating the CHF's between cross flow and axial flow. To obtain the CHF for axial-flow boiling, Groeneveld's table look-up method is used as a standard in the present work. An empirical correlation for cross-flow CHF is also presented in this chapter.

7.1 CHF Relationship Between Cross and Axial Flows

The relationship of CHF's between cross flow and axial flow is defined as

$$KCHF = \frac{q_{max,cross}}{q_{max,axial}} \tag{7.1}$$

where

$q_{max,cross}$ CHF for cross flow

$q_{max,axial}$ CHF for axial flow

The $KCHF$ thus defined can be called the correction factor for correcting the CHF in axial flow to that of cross flow. It was mentioned in Chapter 1 that there are difficulties of the CHF in relating the cross and axial flows due to different flow patterns. In such circumstances, the observation of parametric trends on $KCHF$ may be an appropriate approach to attack this problem. Since the fluids involved in present study are not only water but also non-aqueous fluids such as Freon-113, dimensionless parameters are more appropriate to be used in the investigation. For axial flow, the dimensional parameters used in Groeneveld's look-up table as indicated in equation (6.3) are P, G and D, and the CHF is expressed by q_{max}. The dimensionless form of these parameters can be expressed by replacing q_{max} by Bo (Boiling number), P by r (density ratio), G by Fr (Froude number) and D by $D/0.008$, where Bo is $q_{max}/(Gh_{fg})$ and $D/0.008$ is the ratio of cylinder or tube diameter over 0.008 m. For cross flow, reviewing the existing correlations which are tabulated in Table 7.1, the dimensionless parameters used by these correlations are density ratio (r), vapor Weber number (We_g), liquid Weber number (We_f), or Katto's scaling factor (Ψ_k or $G^2D/\sigma/\rho_f$).

One of the important parameters, quality, is not used in these correlations because these correlations are developed on the basis of experimental data at saturated condition ($x = 0$). The empirical correlation presented by Hwang and Yao (1984) as illustrated in equation (3.34) has included the quality effect. However, their quality range can only apply to the saturated condition at $x \geq 0$. Consequently, the use of these correlations is limited to a narrower quality range. In present study, an attempt has been made to include the quality effect across the subcooled and saturated regions as well as the effects of pressure, mass flux and diameter. Table 7.2 lists the parameter ranges for various experimental sources used in this analysis.

7.2 Parametric Trends of $KCHF$

In present work the dimensionless parameters used to observe the trends of $KCHF$ are the density ratio (r), Froude number (Fr), quality (x) and $D/0.008$. The choice of $D/0.008$ is to be consistent with the use of Groeneveld's table look-up method. The question is why the Froude number is chosen rather than Katto's scaling factor (liquid Weber number) or Ahmad's first and second scaling factors. The analysis shows that Katto's and Ahmad's scaling factors have very similar

Table 7.1: CHF correlation for cross flow

Investigator	Form
Lienhard and Eichhorn (1976)	
For low U_∞	$\frac{\pi q_{max}}{\rho_g h_{fg} U_\infty} = 1 + \left(\frac{4}{We_g}\right)^{1/3}$
for high U_∞	$\frac{\pi q_{max}}{\rho_g h_{fg} U_\infty} = \frac{1}{169}\left(\frac{\rho_f}{\rho_g}\right)^{3/4} + \frac{1}{19.2}\left(\frac{\rho_f}{\rho_g}\right)^{1/2} \frac{1}{We_g^{1/3}}$
Katto and Haramura (1983b)	
For high U_∞	$\frac{q_{co}}{G h_{fg}} = 0.151\left(\frac{\rho_g}{\rho_f}\right)^{0.467}\left(1 + \frac{\rho_g}{\rho_f}\right)^{1/3}\left(\frac{\sigma \rho_f}{G^2 D}\right)^{1/3}$
Yilmaz and Westwater (1980)	$\frac{q_{max}}{\rho_g h_{fg} U_\infty} = 0.369 We_g^{-0.26}$
Hasan et al. (1981)	$\frac{\pi q_{max}}{\rho_g h_{fg} \lvert U_\infty \rvert} = 0.000919 \frac{\rho_f}{\rho_g}\left(1 + \frac{16.3}{We_f^{1/3}}\right)$
Katto (1987)	$\frac{q_{co}}{G h_{fg}} = K\left(\frac{\sigma \rho_f}{G^2 D}\right)^m$ where $K = 0.00588 + 0.5\left(\frac{\rho_g}{\rho_f}\right)^{1.11}$ $m = 0.42\left(\frac{\rho_g}{\rho_f}\right)^{0.0428}$

Table 7.2: Sources of CHF data for cross-flow boiling used in present analysis

	Data sources				
Parameter	Broussard and Westwater (1985)	Yilmaz (1980)	Pourdashti (1984)	Kezios and Lo (1958)	Vliet (1962)
Density Ratio	205	205	50~100	800~1360	1460
Froude number	9~36	11~31	0.3~1.6	1.75~12	1.1~19
D/0.008	0.4~1.6	0.8	0.8	0.4	0.4~0.6
Quality	0	0	-0.11~0.11	-0.21~-0.04	-0.1~0
Fluid	Freon-113	Freon-113	Freon-113	water	water

effects on the $KCHF$ trend. This implies that the viscosity is not a major effect on the CHF occurrence. In addition, the Froude number shows a more smooth trend on $KCHF$ than Katto's scaling factor does. This means that the surface tension is not a major effect either. However, the Froude number doesn't involve any property of the fluid such as liquid density and vapor density. Thus, the Froude number leads to a result which is not as complicated as those using the other parameters.

The effects of these parameters on $KCHF$ trend are shown from Fig. 7.1 to Fig. 7.4. These figures show scattering distribution of $KCHF$ vs. all parameters and it seems not possible to observe clear parametric trends from these figures. Recall that in equation (7.1) the $q_{max,cross}$ and $q_{max,axial}$ should relate with these parameters directly, not the $KCHF$. Therefore, the observation of parametric trends on $q_{max,cross}$ and $q_{max,axial}$ is more useful than that on $KCHF$. Because $q_{max,cross}$ and $q_{max,axial}$ are dimensional while the parameters of Fr, r, x and $D/0.008$ are non-dimensional, equation (7.1) should be modified. Since the Boiling number (Bo) is used to represent the dimensionless form of CHF, equation (7.1) can be rewritten to

$$KCHF = \frac{\frac{q_{max,cross}}{Gh_{fg}}}{\frac{q_{max,axial}}{Gh_{fg}}} = \frac{Bo_{cross}}{Bo_{axial}} \tag{7.2}$$

The terms of Gh_{fg} shown in the numerator and denominator are equivalent to each other so that they can be eliminated. According to equation (7.2), the following analysis leads to the observation of parametric trends on Bo_{cross} and Bo_{axial}.

7.3 Parametric Trends of CHF

7.3.1 Mass flux effect

The Froude number Fr is usually used to represent the velocity or mass flux effect in the non-dimensional correlating technique. As discussed in Chapter 4, the Froude number has been used successfully in Ungar and Eichhorn's (1988) model. It is obvious that the flow patterns for axial and cross flows are completely different because the former is internal flow and the latter is external flow to the heated element. However, the external flow is still confined by the channel walls. Therefore, the Froude number hereby represents only the extent of velocity or mass flux effect in the flow channel. For cross-flow boiling, the Froude number is calculated based

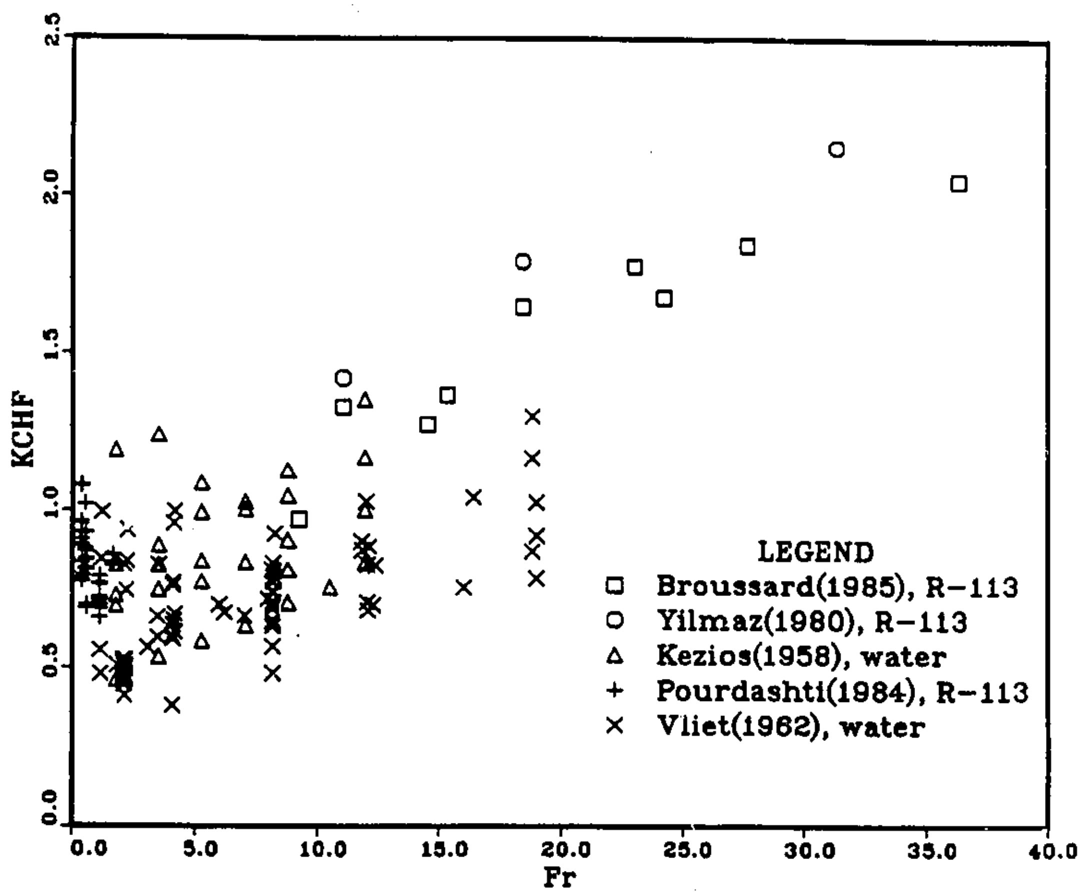

Figure 7.1: Distribution of $KCHF$ vs. Fr in present analysis

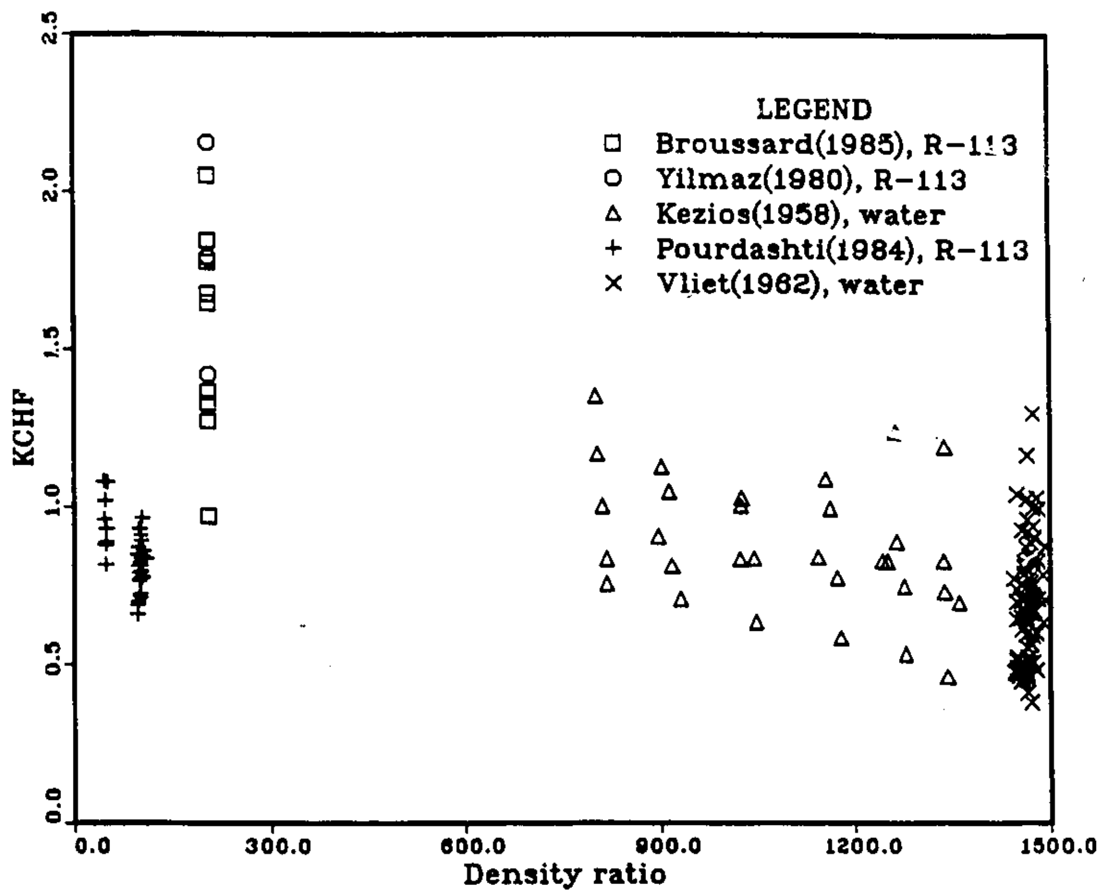

Figure 7.2: Distribution of $KCHF$ vs. r in present analysis

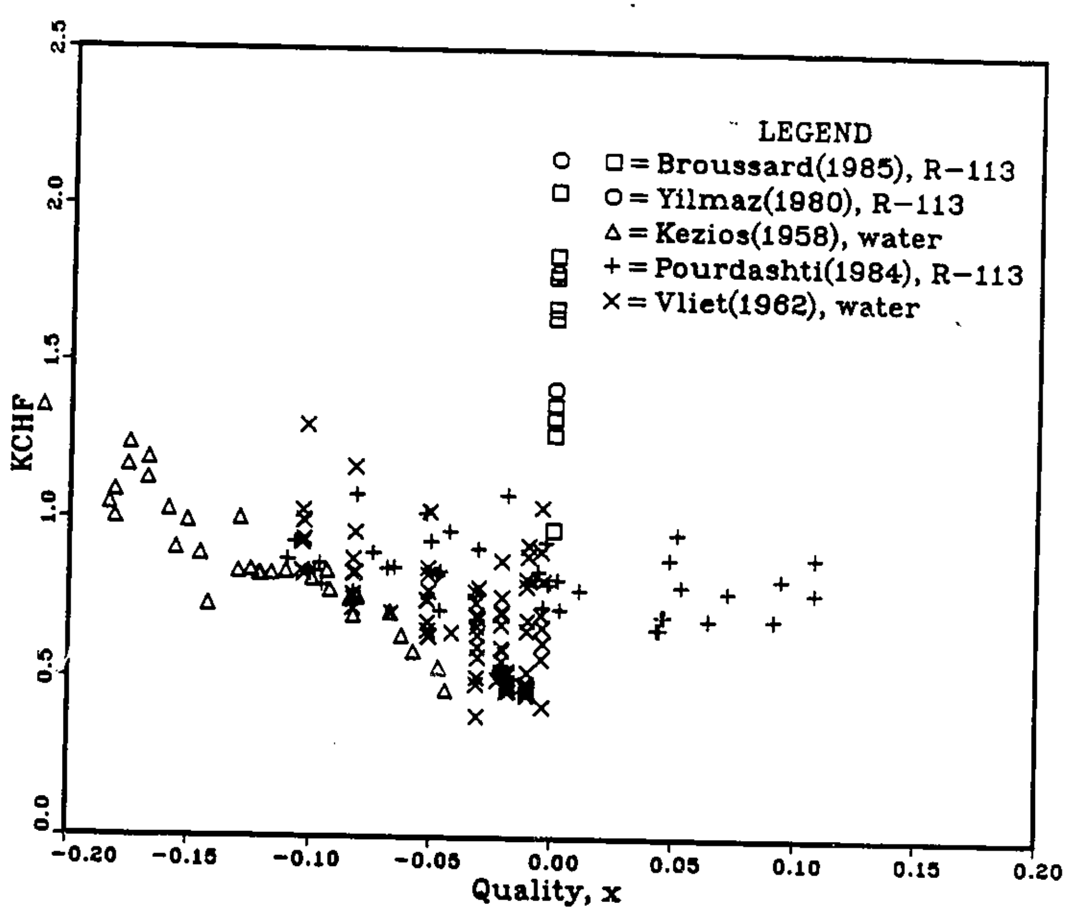

Figure 7.3: Distribution of $KCHF$ vs. x in present analysis

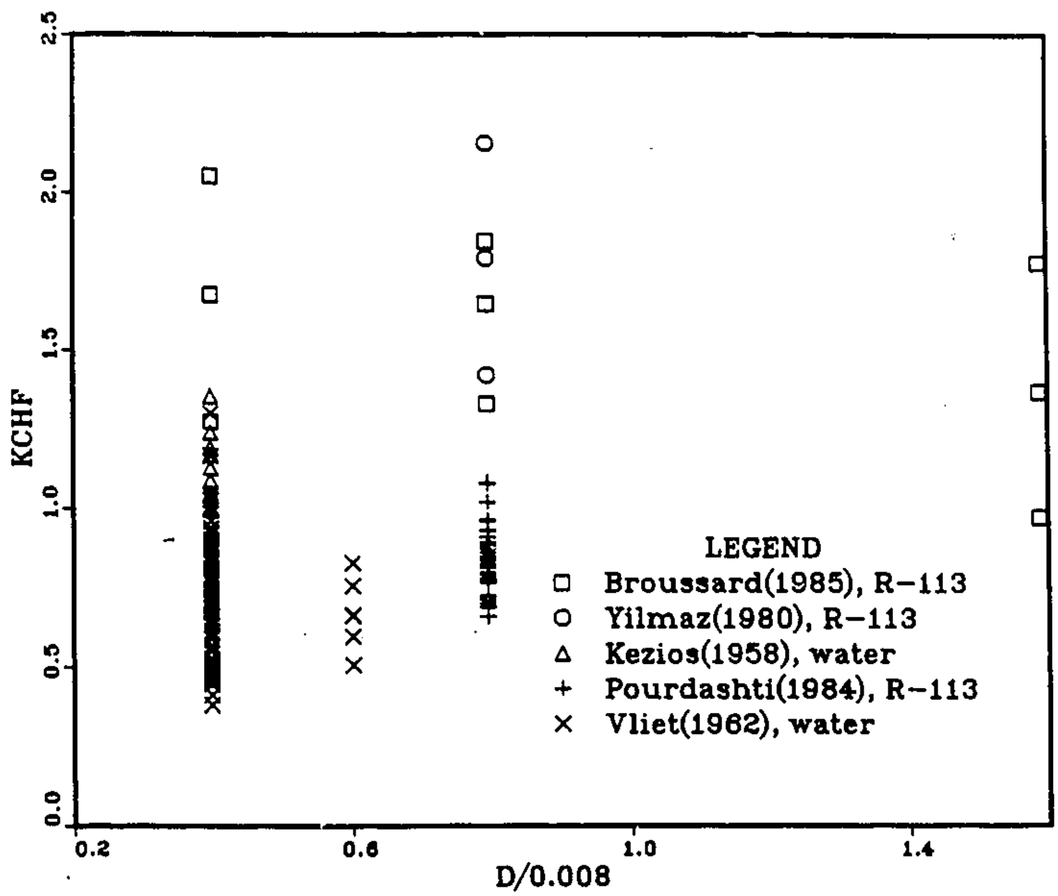

Figure 7.4: Distribution of $KCHF$ vs. $D/0.008$ in present analysis

on the velocity (U) which is obtained from the mean flow area model as discussed in Chapter 5. Fig. 7.5 shows the mass flux effect on the dimensionless CHF (Bo) for cross flow in different investigations, while Fig. 7.6 shows the same effect on boiling number for axial flow predicted by Groeneveld's table look-up method corresponding to the same test conditions of the previous figure. These two figures show that there are similar trends of Bo vs. Fr for both the cross and axial flows.

7.3.2 Quality effect

For quality less than zero, generally the Boiling number increases with decreasing quality for both axial and cross flows, and the absolute value of the slope for this trend becomes smaller when Fr becomes larger (see Figure 7.7 to 7.10), while in the region of quality greater than zero, the Boiling number decreases when quality increases. In Fig. 7.11 and Fig. 7.12, the trends for quality effect on Boiling number are continuous across the subcooled and saturated regions for both axial and cross flows, and the trends of quality effect on Boiling number for both cases are very similar to each other. Thus, the Boiling number can be correlated as a function of quality, or $Bo = f(.., x, ..)$, for axial and cross flows, respectively. However, in practical application it is more useful to express the quality effect by $Bo = f(.., 1-x, ..)$. In such case, the parameter $1 - x$ has a positively proportional effect on Bo.

7.3.3 Diameter effect

In Chapter 6, the diameter effect on CHF in axial flow has been introduced by equations (6.2) and (6.4). They show that the CHF increases when the diameter decreases. For cross flow, the diameter effect has been introduced by Broussard and Westwater (1985), Beecher (1948), and Vliet and Leppert (1964a and 1964b) as discussed in Section 2.4. All of these investigations indicated that the CHF is inversely proportional to the diameter. Fig. 7.13 shows the effect of dimensionless diameter ($D/0.008$) on the trend of Bo for Broussard and Westwater's (1985) investigation.

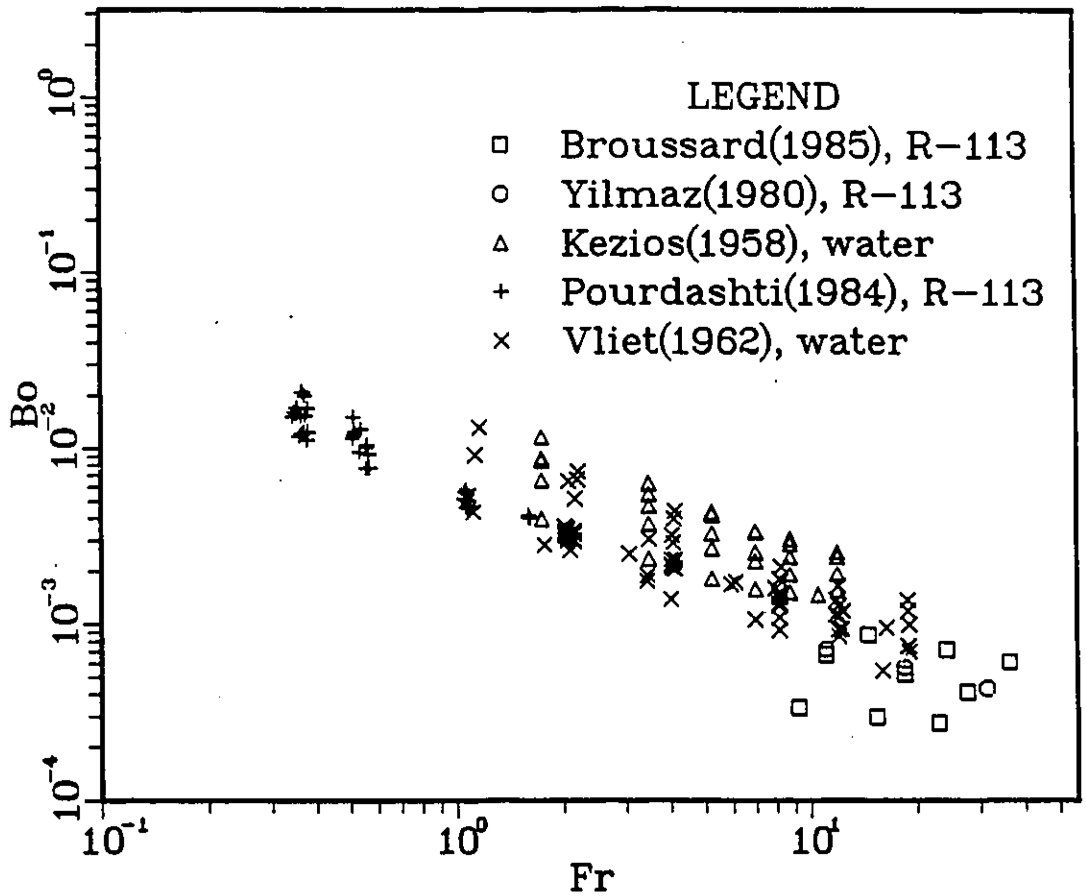

Figure 7.5: Dimensionless CHF vs. Fr for all cross flow experimental data used in present analysis

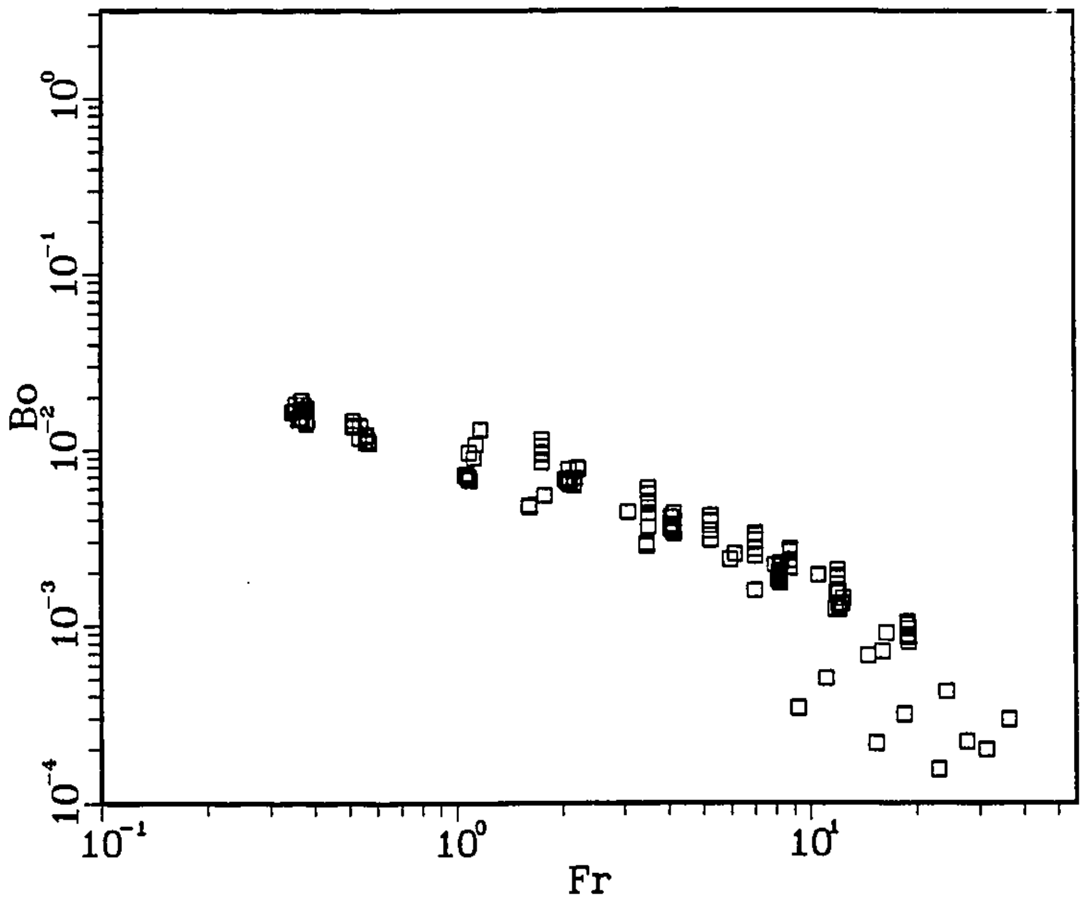

Figure 7.6: Dimensionless CHF for axial flow predicted by Groeneveld's look-up method vs. Fr with the same parameter ranges of previous figure

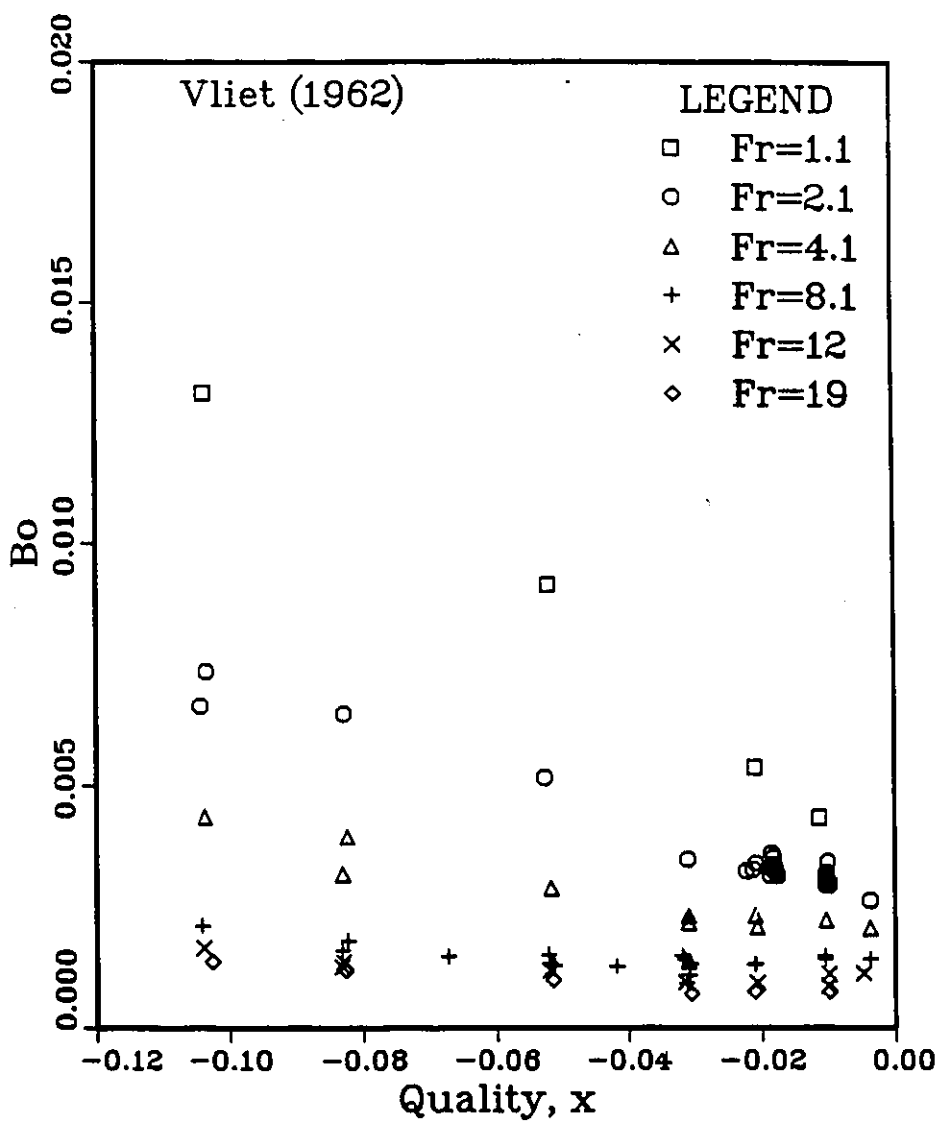

Figure 7.7: Quality effect on the dimensionless CHF for Vliet's (1962) cross flow data.

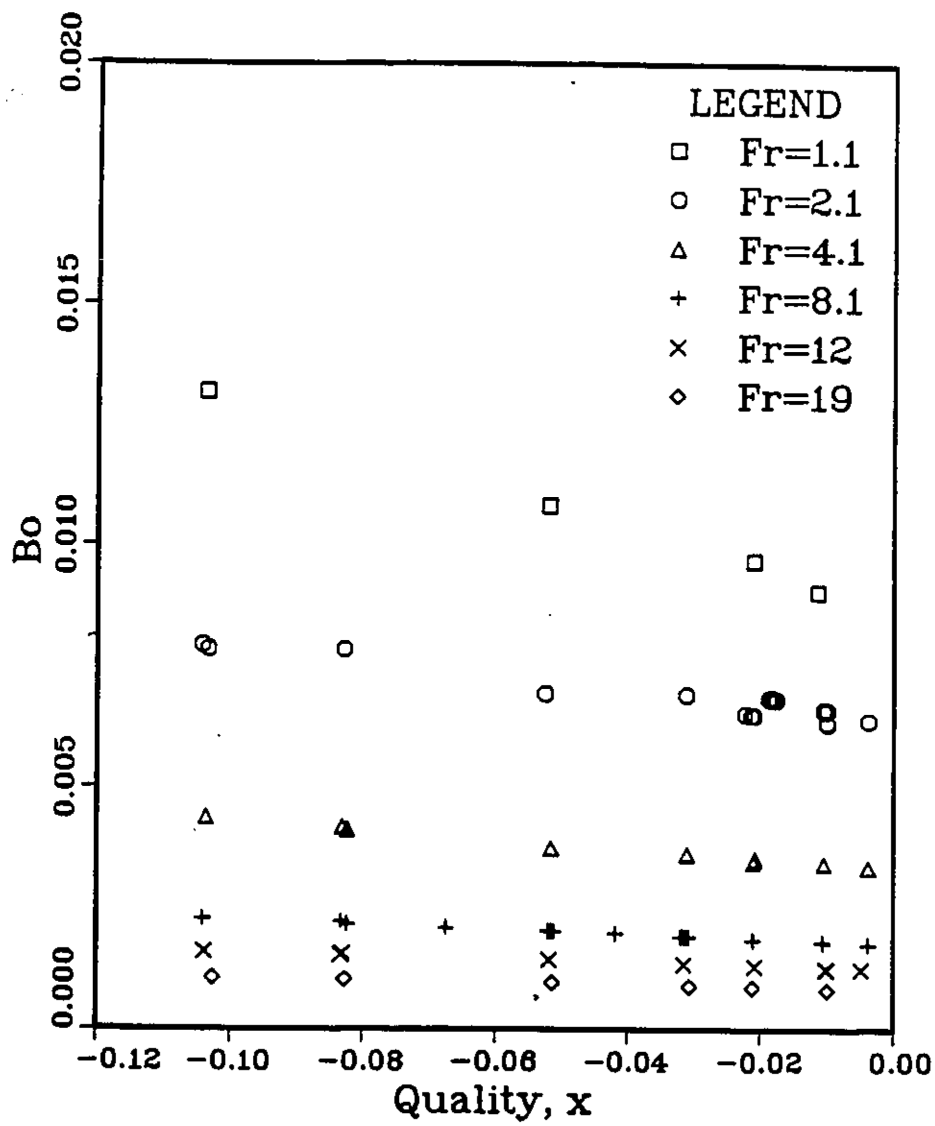

Figure 7.8: Quality effect on the dimensionless CHF for axial flow predicted by Groeneveld's table look-up method according to Vliet's test condition

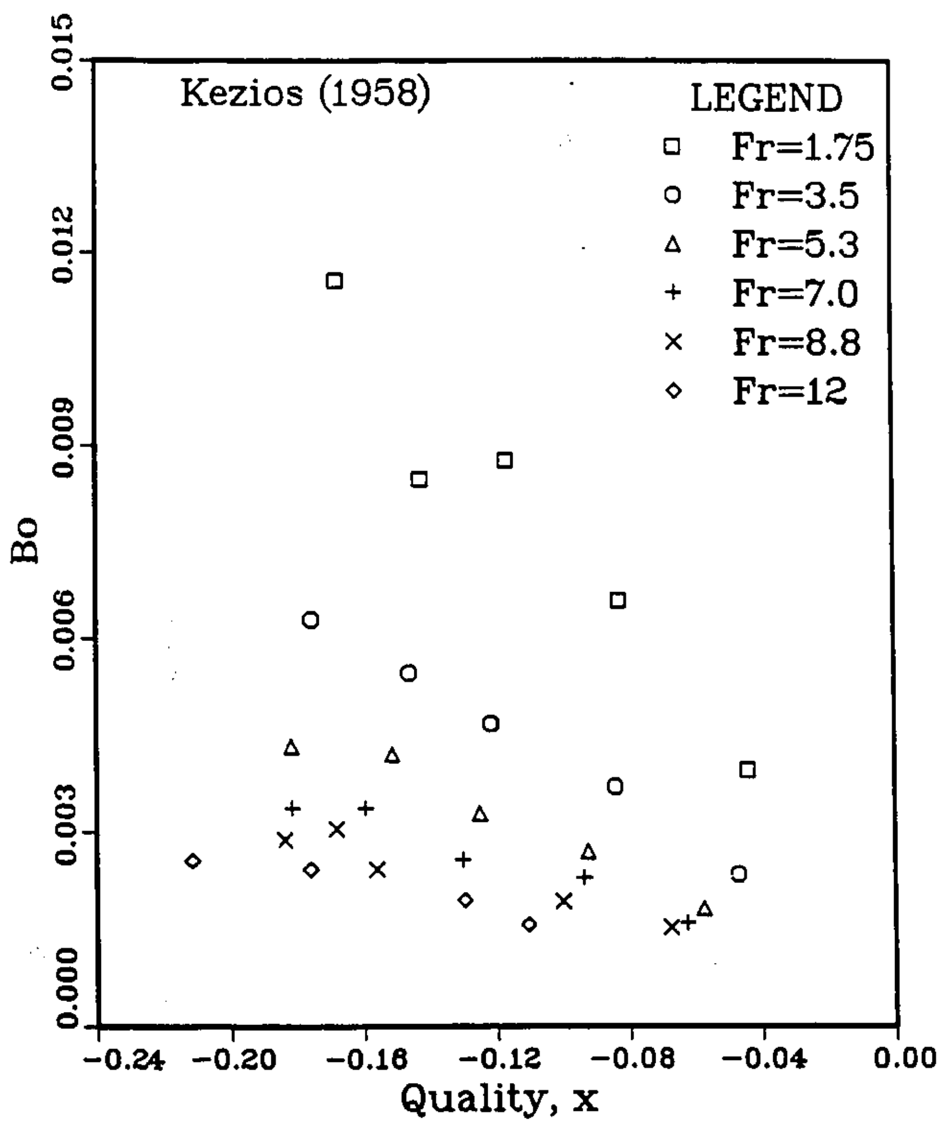

Figure 7.9: Quality effect on the dimensionless CHF for Kezios's (1958) cross flow data

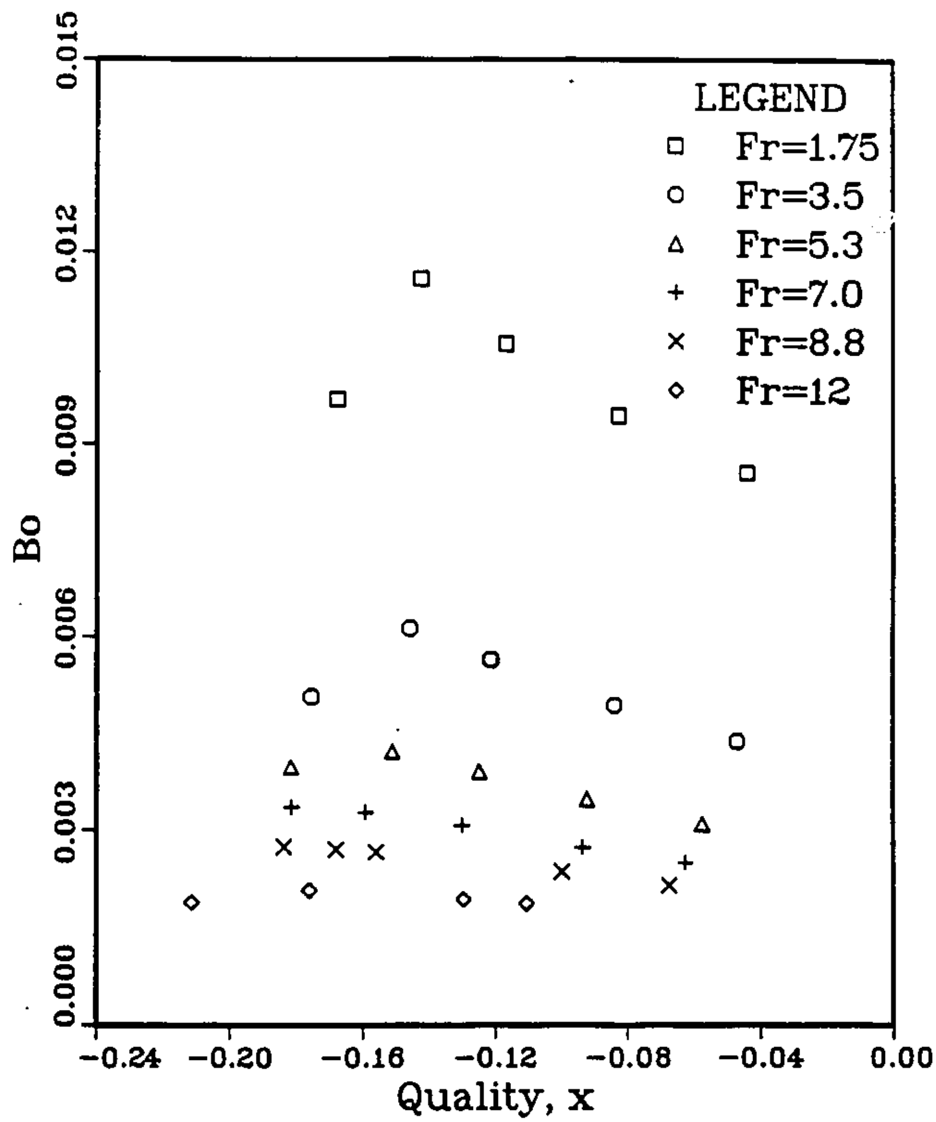

Figure 7.10: Quality effect on the dimensionless CHF for axial flow predicted by Groeneveld's table look-up method according to Kezios's test condition

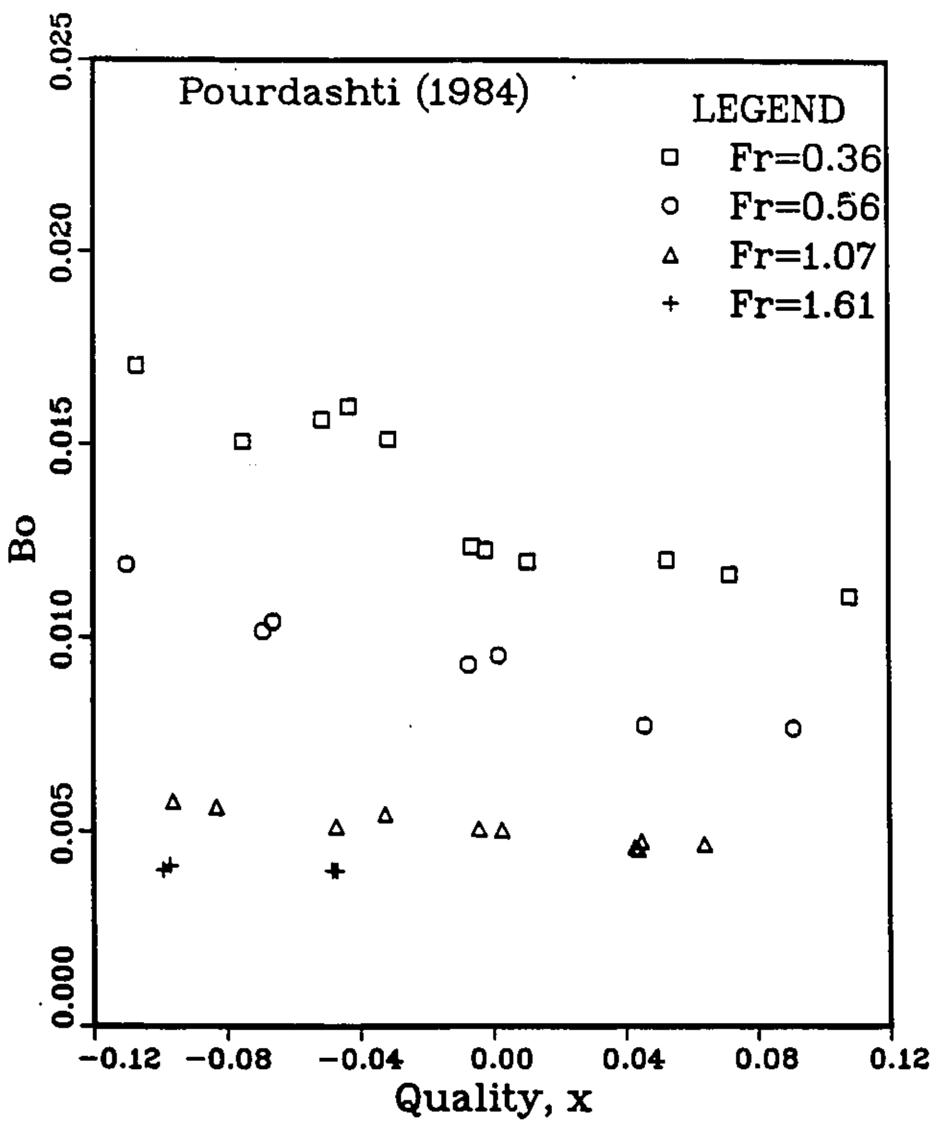

Figure 7.11: Quality effect on the dimensionless CHF for Pourdashti's (1984) cross flow data

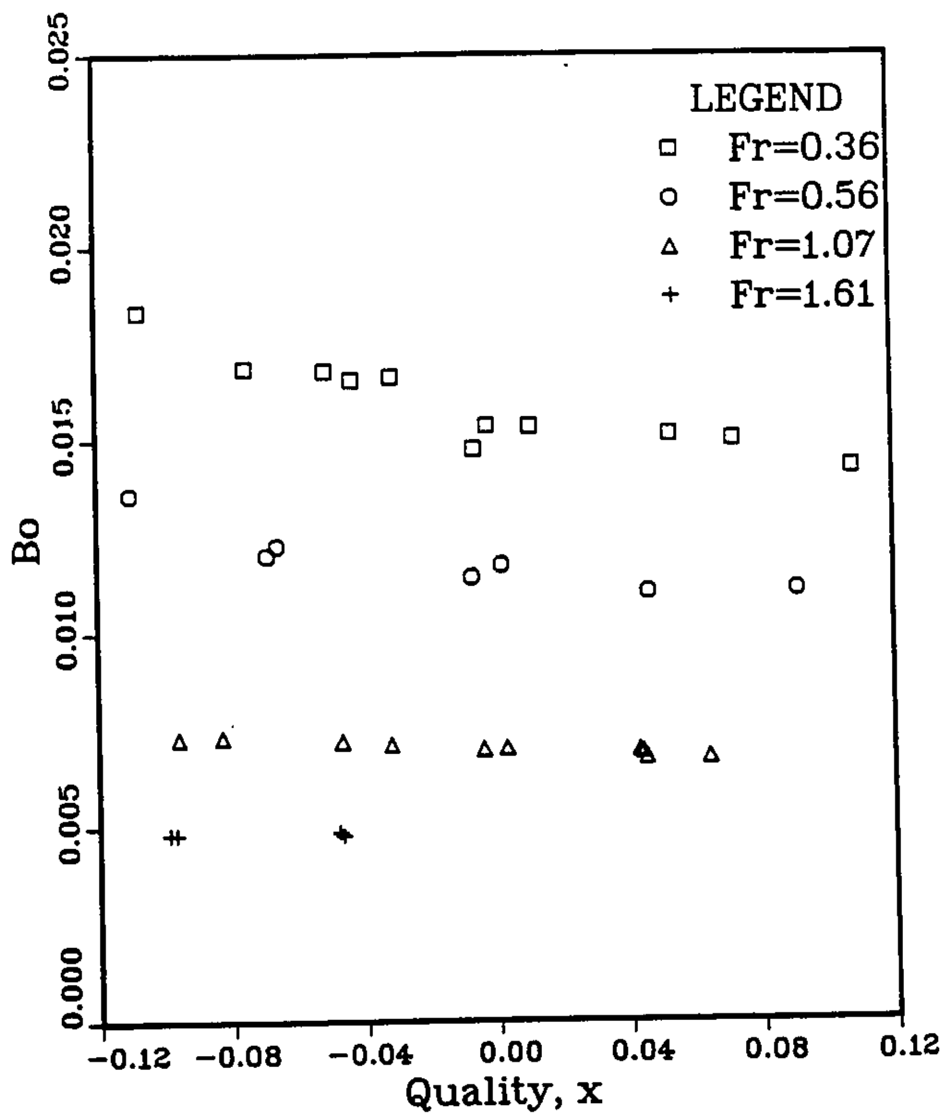

Figure 7.12: Quality effect on the dimensionless CHF for axial flow predicted by Groeneveld's table look-up method according to Pourdashti's test condition

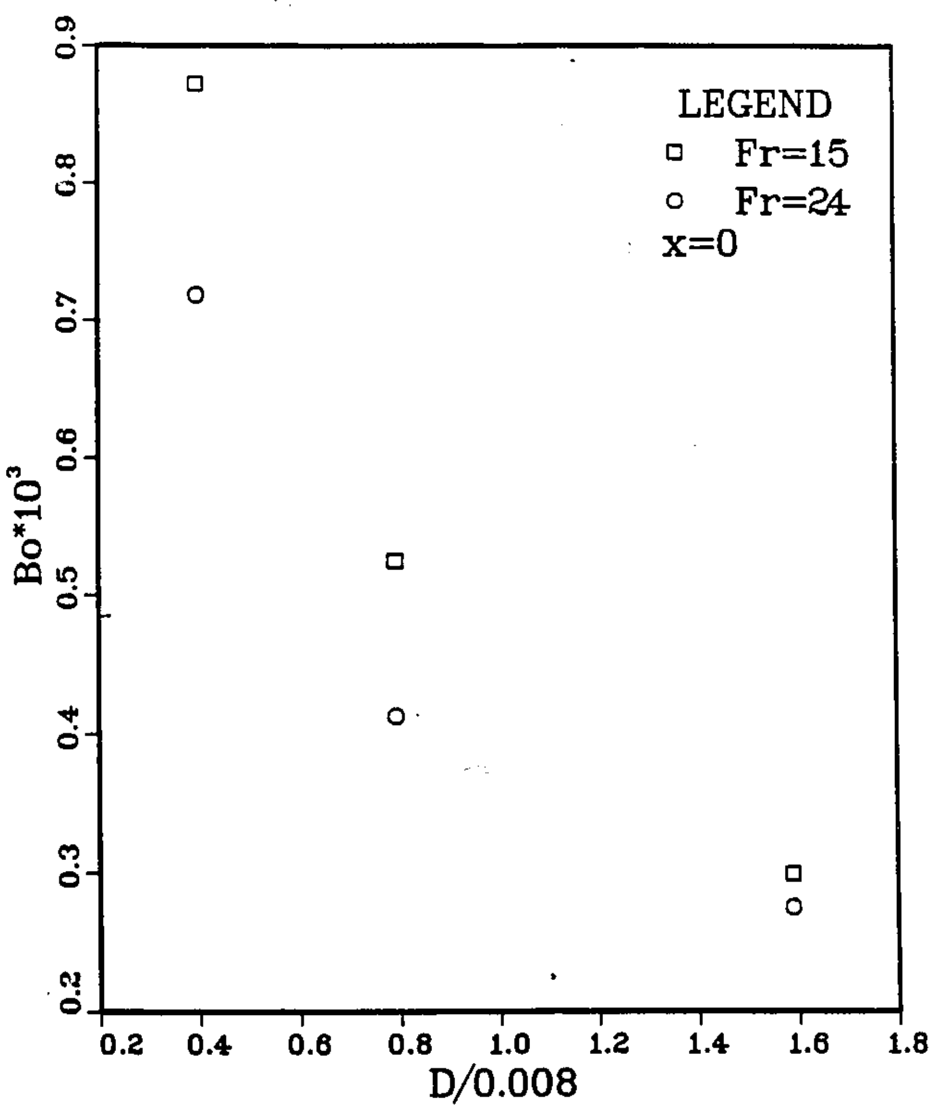

Figure 7.13: Dimensionless diameter effect on the trend of Bo for the investigation by Broussard and Westwater (1985)

7.3.4 Density ratio effect

Because of the scatter in the distribution of the cross-flow CHF data for different investigation sources, the density ratio effect on Bo is not clear. For axial-flow boiling, the CHF data predicted from Groeneveld's look-up table also shows a fluctuation at the same range of the test parameters of cross flow. However, the density ratio effect is still an important parameter to predict the CHF for both the cross and axial flows as shown in the latter analysis.

7.4 Derivation of $KCHF$

Since parametric trends of Bo_{cross} and Bo_{axial} have been observed in Section 7.3, which show that most parameters result in smooth trends on Bo_{cross} and Bo_{axial}, it implies that Bo_{cross} and Bo_{axial} relate directly with these parameters. According to equation (7.2), $KCHF$ should also relate with these parameters in spite of the scattering distributions of $KCHF$ vs. Fr, r, x and $D/0.008$ as shown from Fig. 7.1 to Fig. 7.4. Thus, an empirical correlation for $KCHF$ can be obtained by using the regression method:

$$KCHF = 3.25Fr^{0.207}r^{-0.274}(1-x)^{0.04+0.003r}\left(\frac{D}{0.008}\right)^{0.094} \tag{7.3}$$

also equation (7.3) can be expressed by

$$\frac{q_{max,cross}}{q_{max,axial}} = 3.25Fr^{0.207}r^{-0.274}(1-x)^{0.04+0.003r}\left(\frac{D}{0.008}\right)^{0.094} \tag{7.4}$$

From the result shown in equation (7.4), the CHF for cross-flow boiling can be predicted by multiplying the CHF obtained from Groeneveld's look-up table to the correction factor $KCHF$. The procedure is that:

1. Select the local parameters of test condition (e.g. P, G, D and x).
2. Calculate the CHF for axial flow from Groeneveld's look-up table with the inputs of P, G, D and x.
3. Calculate the dimensionless parameters Fr, r and $D/0.008$ from the inputs of P, G and D.

4. Calculate the CHF for cross-flow boiling by using equation (7.4).

The RMS error for the cross-flow CHF obtained from the above procedure and compared to the experimental data is 16.2%. For each test source, the RMS error is illustrated in Table 7.3.

7.5 Empirical CHF Correlation for Cross-flow Boiling

As emphasized before, the objective of this study is to predict the CHF in cross-flow boiling. After the observation of the parametric trends on Bo as discussed in Section 7.3, one question would come up, i.e. whether the CHF in cross flow can be predicted by correlating Bo_{cross} as a function of Fr, r, x and $D/0.008$ directly. If the result is more accurate than that predicted by using the correction factor, why bother to use the correction factor method. Therefore, an empirical correlation of Bo_{cross} vs. Fr, r, x and $D/0.008$ is also obtained by using the regression method:

$$Bo_{cross} = 0.018Fr^{-0.758}r^{-0.29}(1-x)^{1.068+0.0048r}\left(\frac{D}{0.008}\right)^{-0.92} \quad (7.5)$$

For CHF in cross-flow boiling, it can be calculated by:

$$q_{max,cross} = Bo_{cross} \times Gh_{fg} \quad (7.6)$$

Recall that in Section 7.3.4 the density ratio effect on Bo can not be observed because of the scatter in the distribution of CHF data. But, from equation (7.5) this parameter shows a simply and inversely proportional effect on Bo_{cross}. This effect also can be seen schematically in Fig. 7.14. The RMS error for this correlation with the total 177 data is 13.4%. A summary of the assessment for this correlation to the individual data source is illustrated in Table 7.4. Note that Kezios and Lo's CHF data were taken for the fluid flowing horizontally and across the heated cylinder.

7.6 Discussion

Surprisingly we result in two prediction methods for CHF in cross-flow boiling in this chapter. The results show that the CHF for cross-flow boiling predicted by

Table 7.3: Assessment of the CHF predicted by correction factor method to individual test source

Data source	Number of data	RMS error (%)
Broussard and Westwater (1985)	9	18.6
Yilmaz (1980)	3	23.9
Pourdashti (1984)	40	14.6
Kezios and Lo (1958)	31	18.6
Vliet (1962)	94	15.1
All data	177	16.2

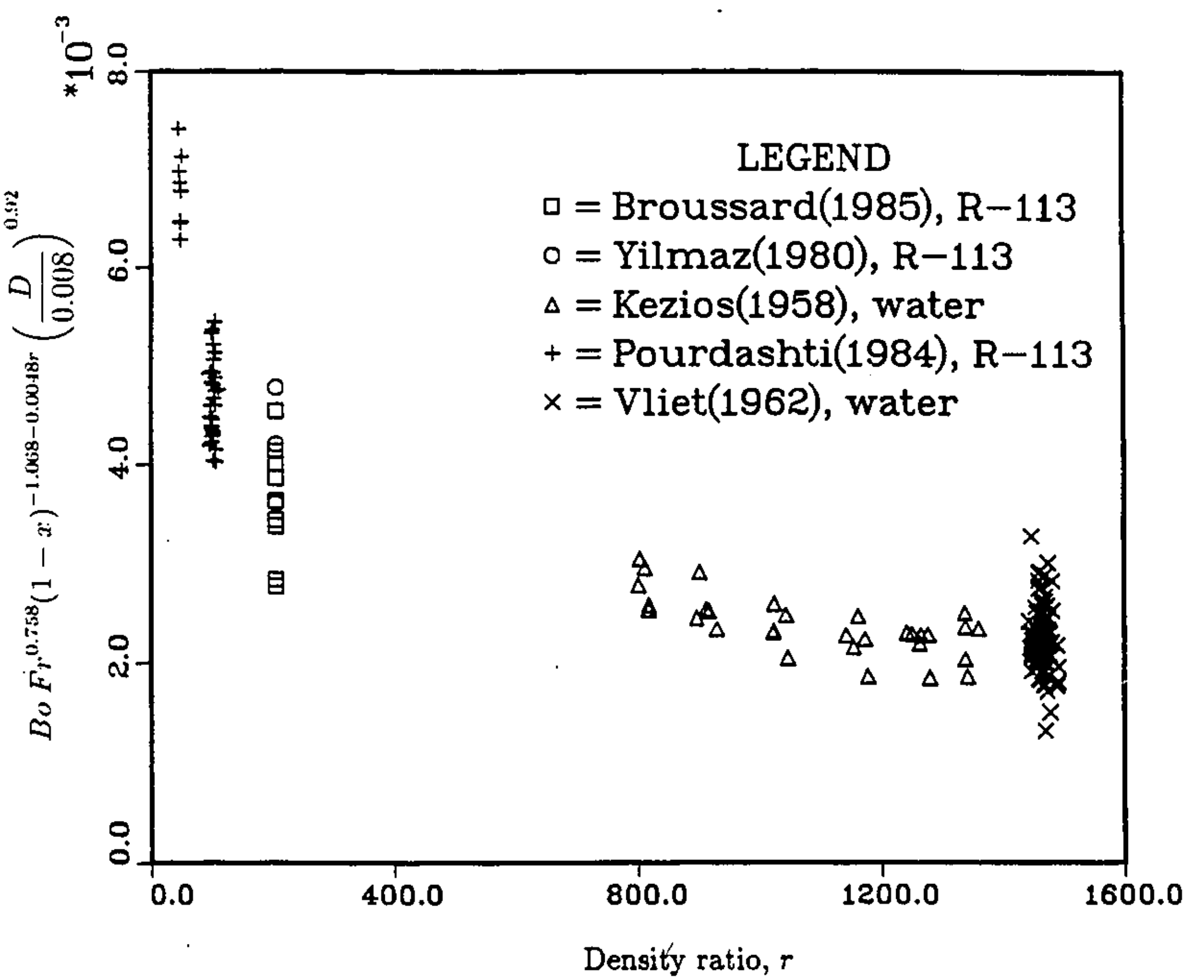

Figure 7.14: Density ratio effect on the trend of dimensionless CHF for all cross flow data

Table 7.4: Assessment of empirical CHF correlation for cross flow to each test source

Data source	Number of data	fluid	RMS error (%)
Broussard and Westwater (1985)	9	freon-113	19.4
Yilmaz (1980)	3	freon-113	13
Pourdashti (1984)	40	freon-113	10.4
Kezios and Lo (1958)	31	water	9.6
Vliet (1962)	94	water	14.9
All data	177		13.4

the empirical correlation illustrated in equation (7.5) is more accurate than that calculated by multiplying the correction factor to the axial-flow CHF predicted by Groeneveld's look-up table. However, the difference of the RMS error between both methods is less than 3%, which is due to the prediction error for Groeneveld's table look-up method with the actual value of axial-flow CHF.

The comparisons of cross-flow CHF predicted by both methods with the experimental data are illustrated from Fig. 7.15 to Fig. 7.21. From these figures, in most cases the equation (7.5) does predict the CHF more accurately than the correction factor method. The comparison of experimental CHF vs. the CHF predicted by the empirical correlation, equation (7.5), is shown in Fig. 7.22, which represents about 80% of the data with ±15% accuracy.

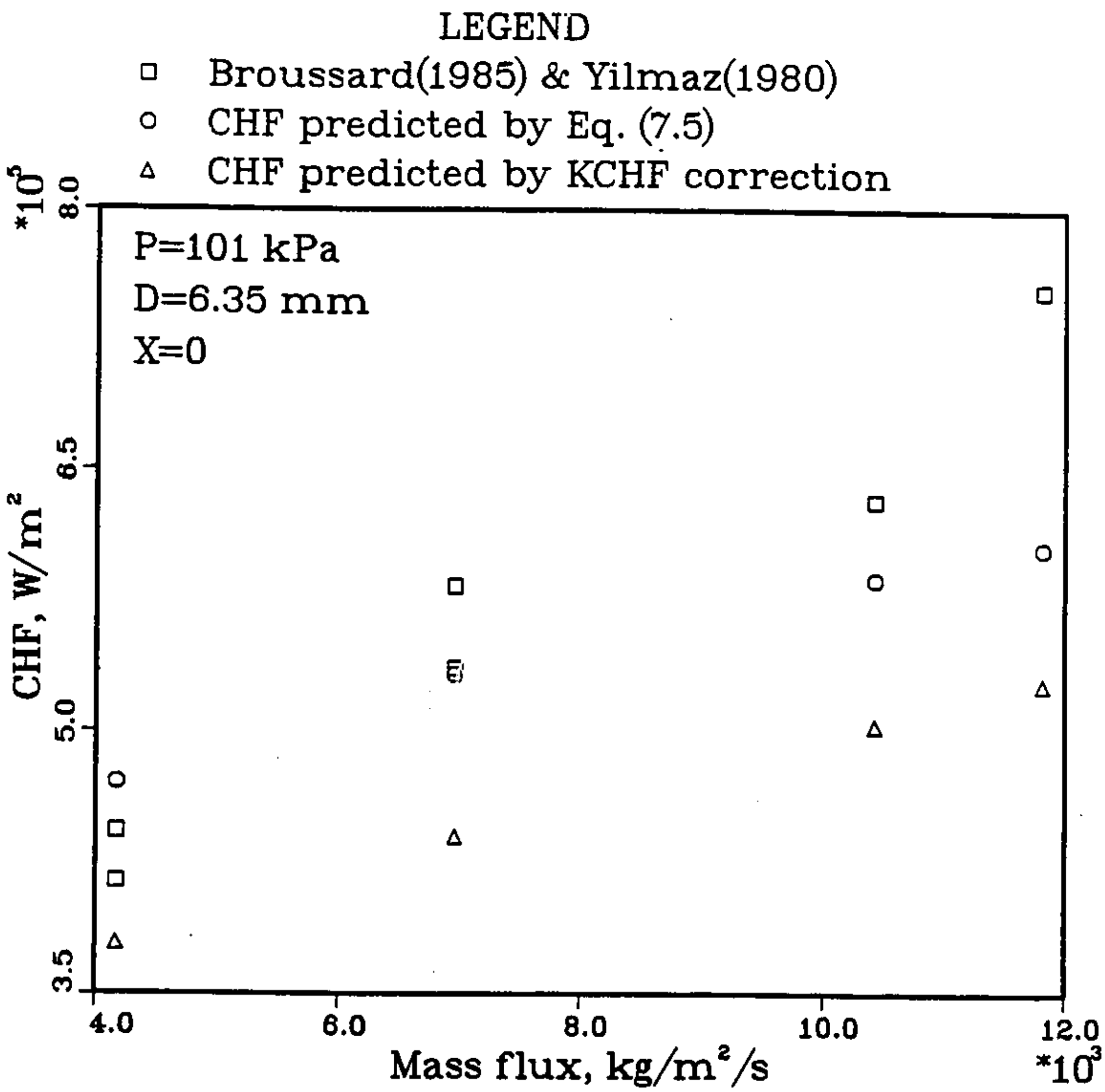

Figure 7.15: Comparison of measured CHF with the CHF's calculated by both prediction methods on the effect of mass flux

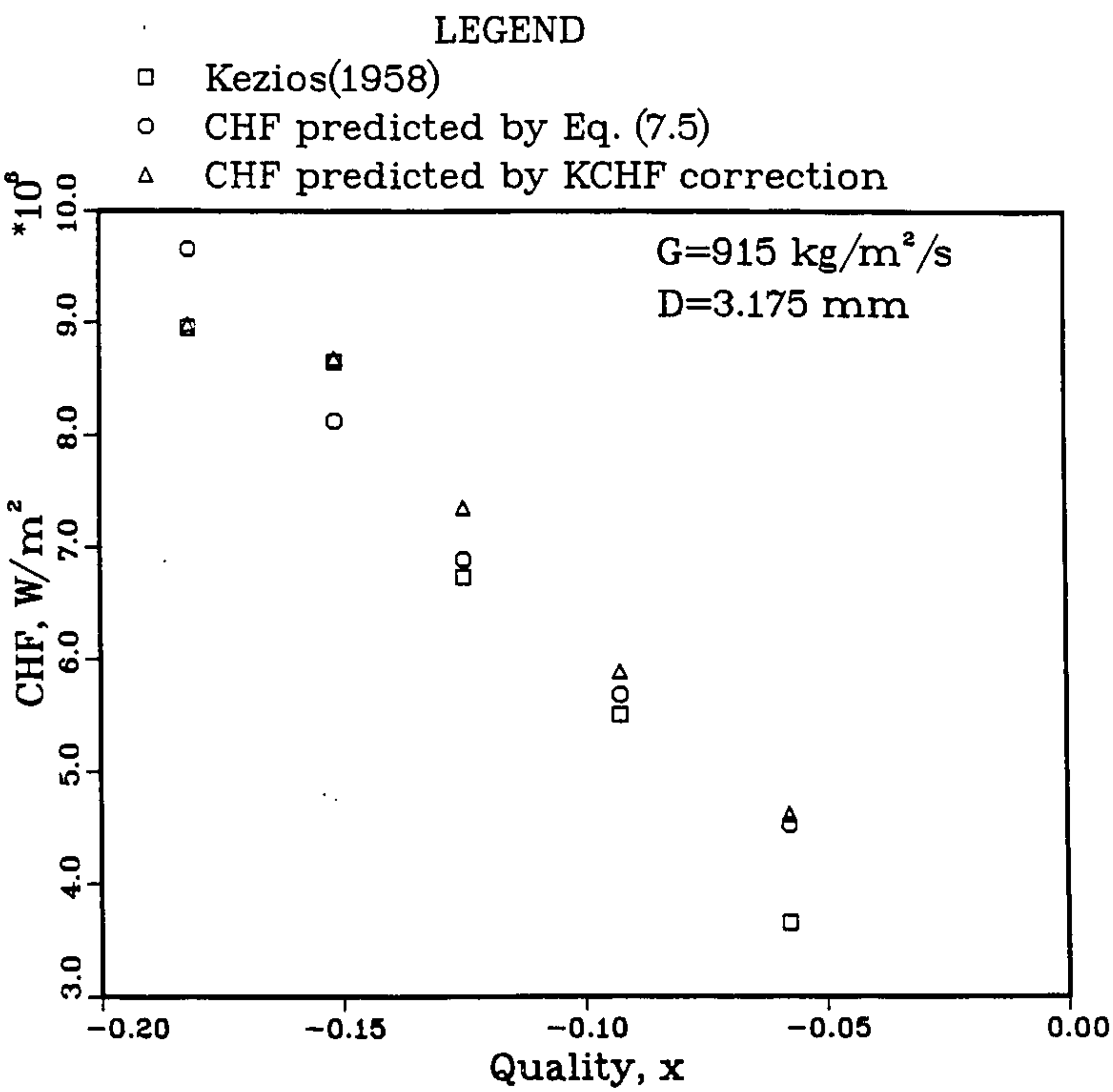

Figure 7.16: Comparison of measured CHF with the CHF's calculated by both prediction methods on the effect of quality

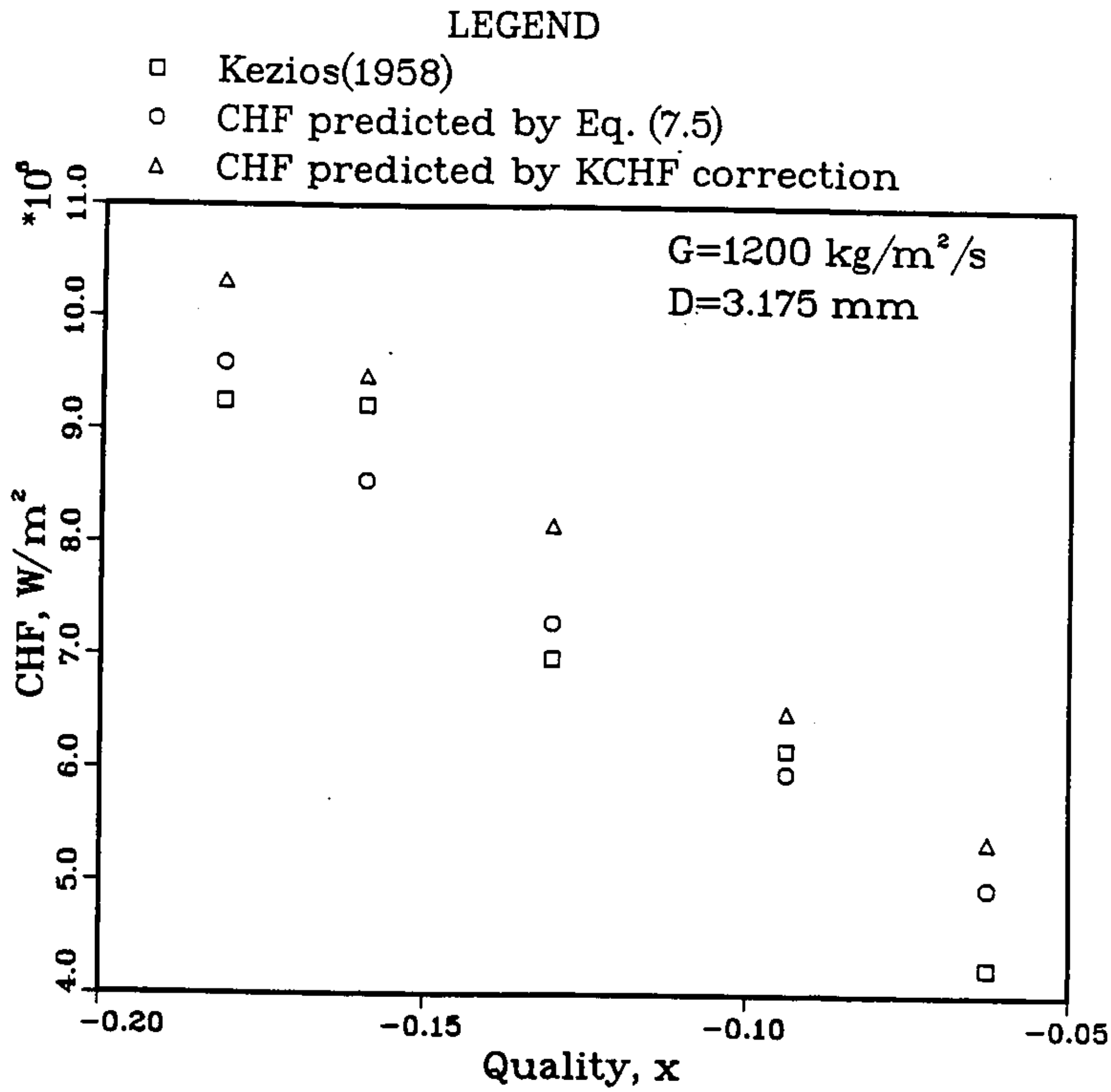

Figure 7.17: Comparison of measured CHF with the CHF's calculated by both prediction methods on the effect of quality

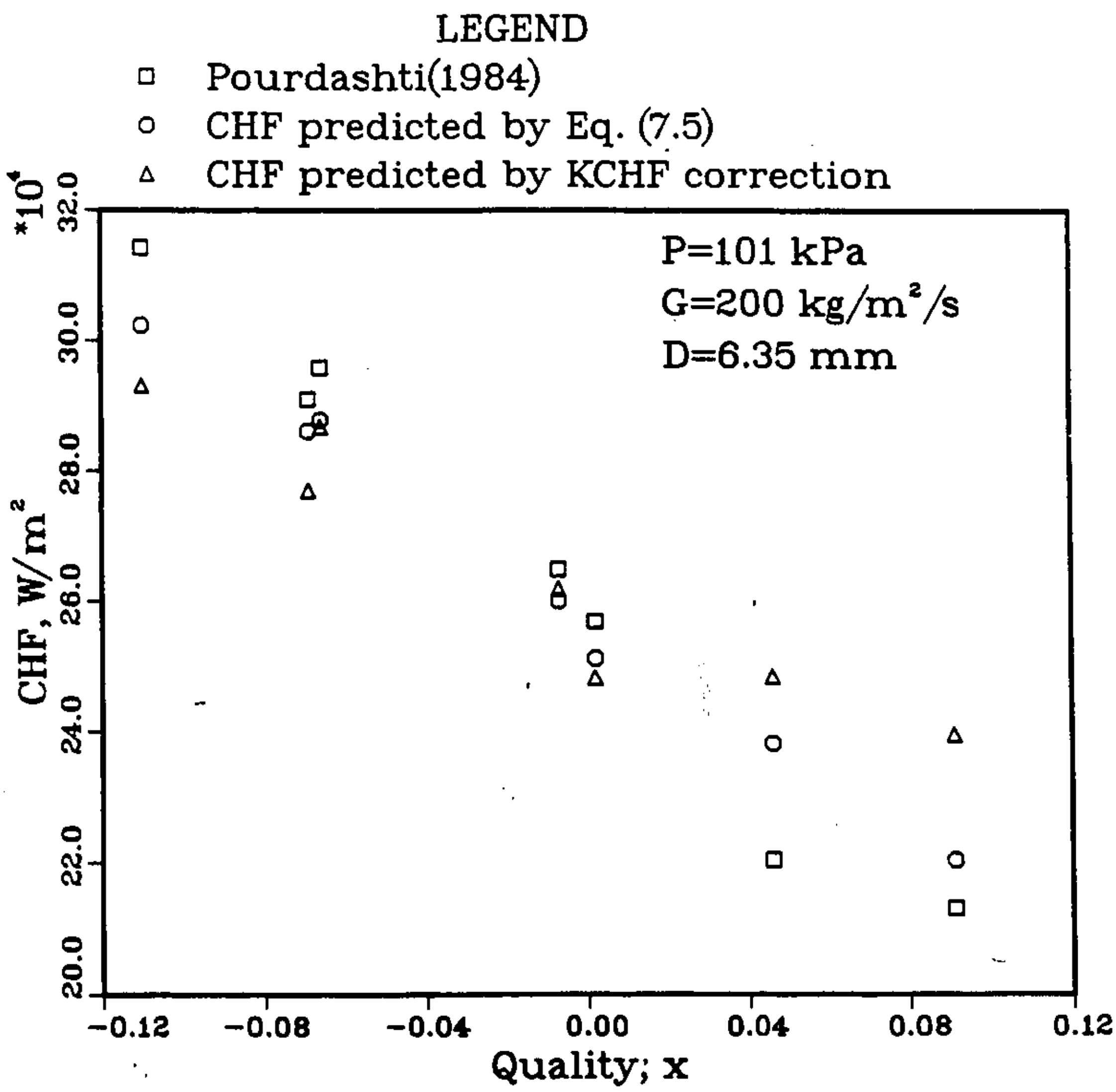

Figure 7.18: Comparison of measured CHF with the CHF's calculated by both prediction methods on the effect of quality

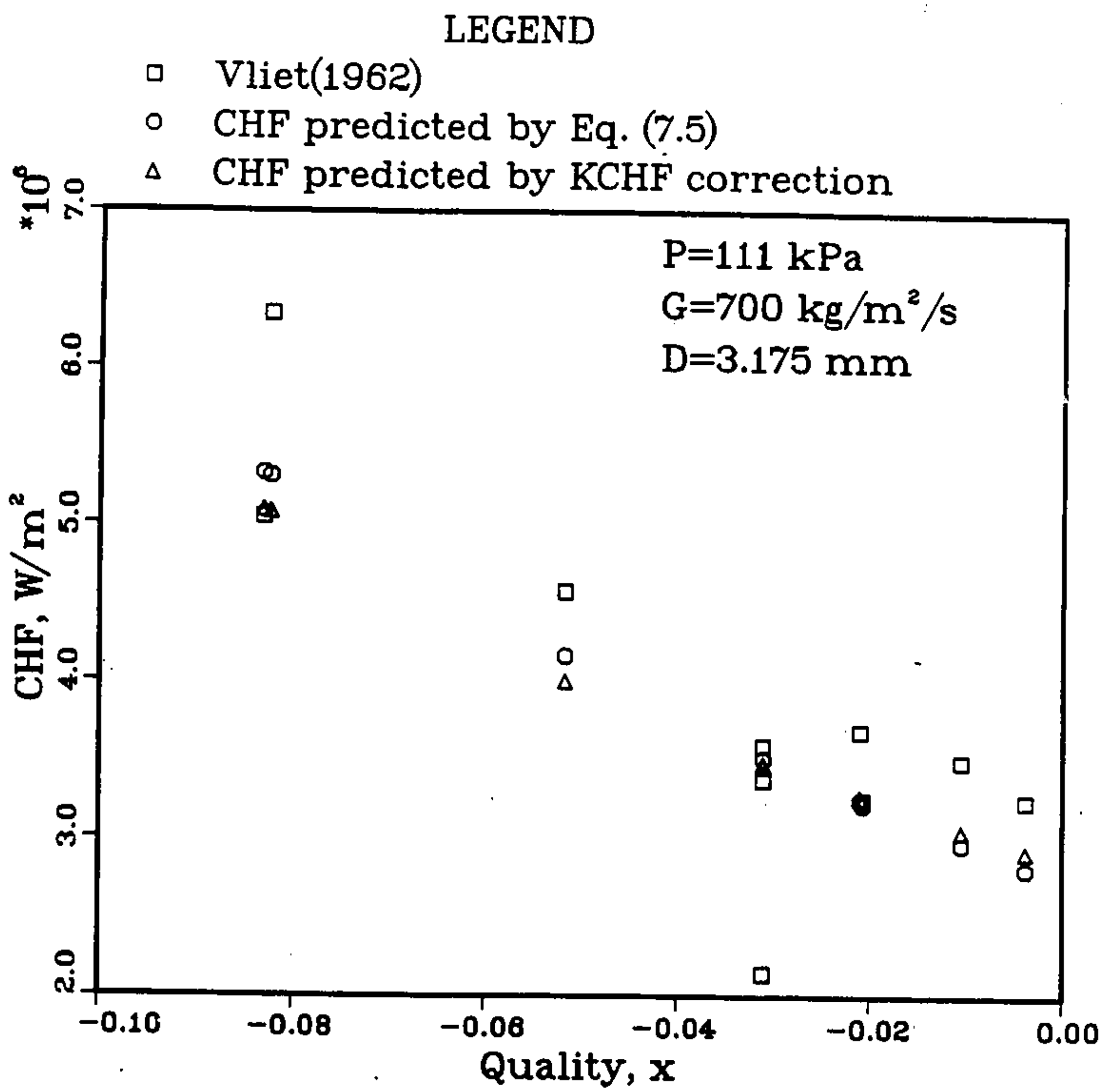

Figure 7.19: Comparison of measured CHF with the CHF's calculated by both prediction methods on the effect of quality

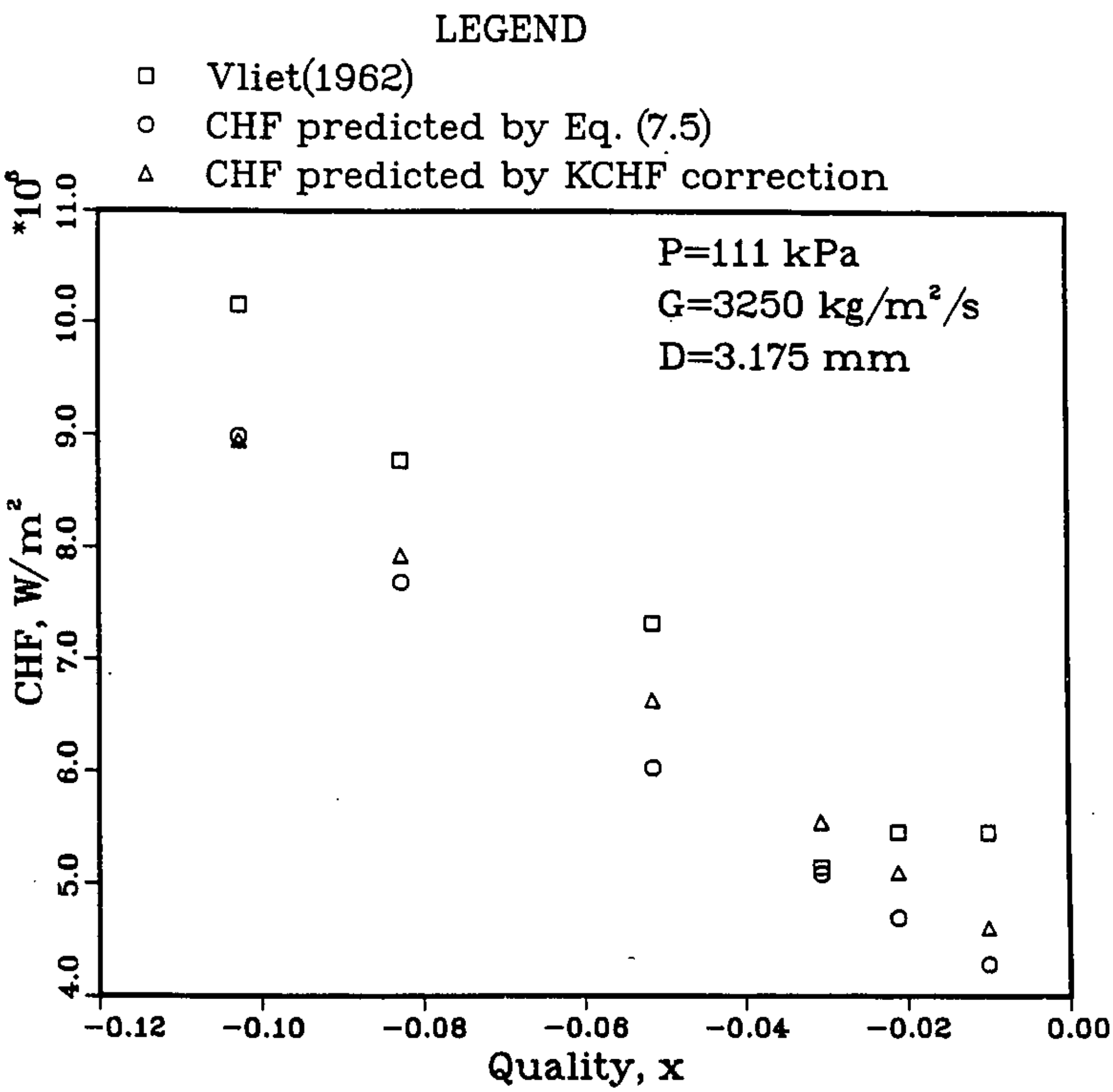

Figure 7.20: Comparison of measured CHF with the CHF's calculated by both prediction methods on the effect of quality

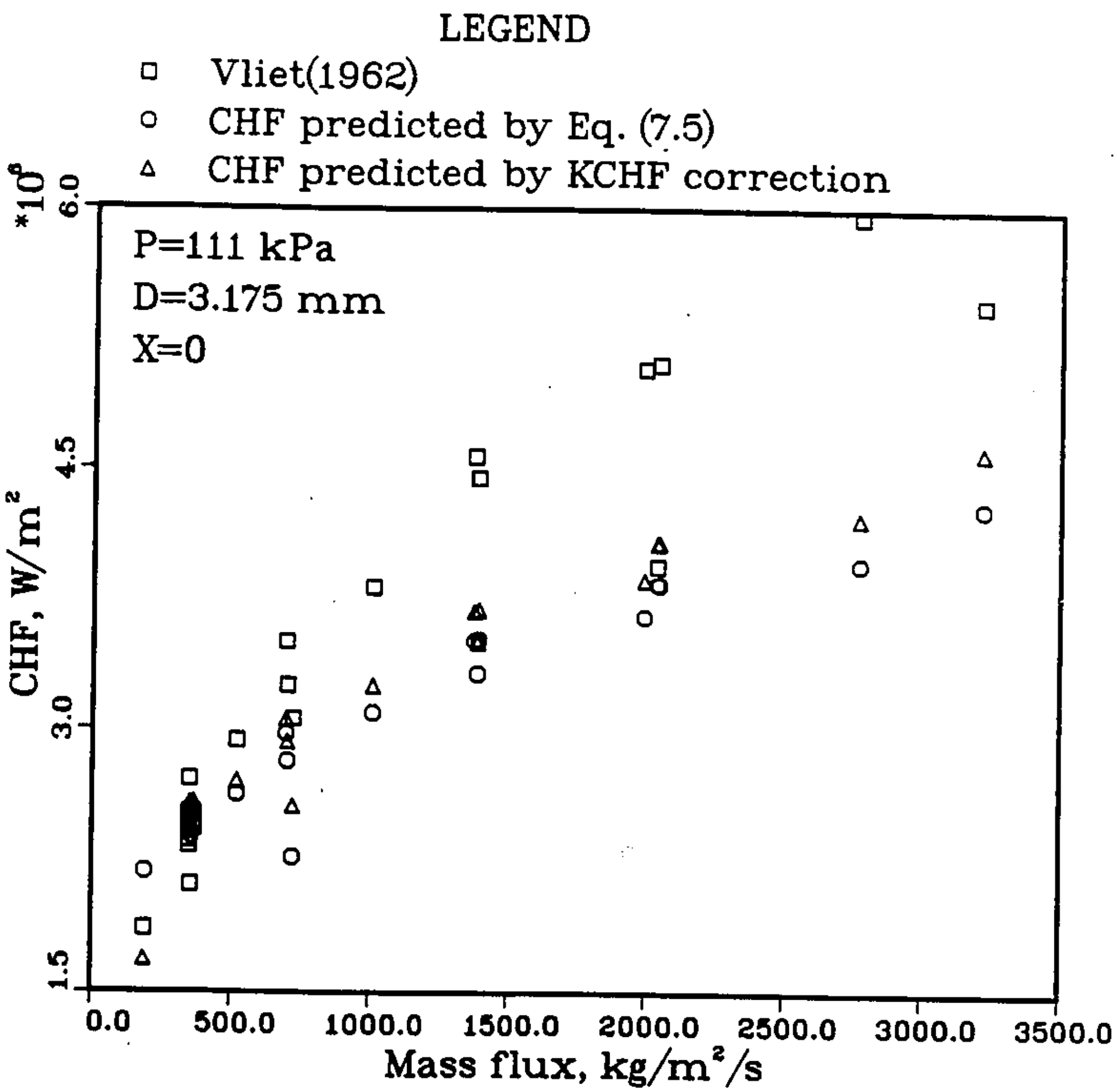

Figure 7.21: Comparison of measured CHF with the CHF's calculated by both prediction methods on the effect of mass flux

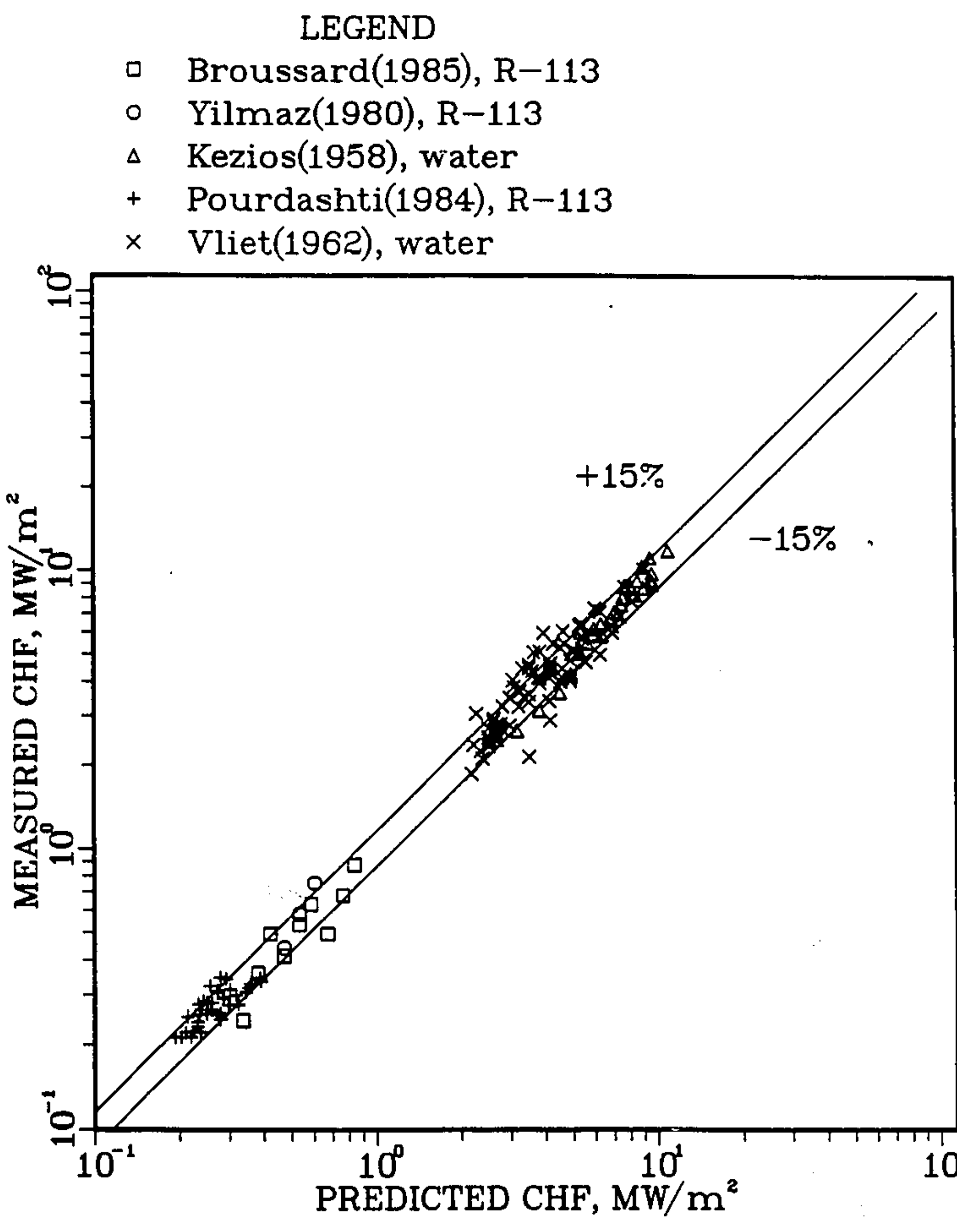

Figure 7.22: Comparison of measured CHF vs. the CHF predicted by equation (7.5)

Chapter 8

Discussion and Conclusion

A semi-empirical model for predicting the cross-flow CHF including the quality effect is presented in this work. The result (equation (4.15)) is analogous to that of Lienhard and Eichhorn (equation (3.14)) except the last bracket in equation (4.15). Because of the small value of E_c in the second term of the last bracket, equation (4.15) can be simplified to equation (4.25). Thus, equation (4.25) is applicable to a wider ranger of quality region and is identical to Lienhard and Eichhorn's (1976) result (see equation (3.14)) at the special case for $x = 0$. However, this model needs some empirical constants to obtain the key term of U_g/U_∞. Ungar and Eichhorn's (1988) hydrodynamic prediction method is used to express U_g/U_∞ and to obtain these empirical constants on the basis of various experimental data. Compared with Ungar and Eichhorn's correlation for effective vapor sheet thickness, which is shown in equation (4.20), the correlation presented by this work has an additional empirical constant for the quality parameter (see equation (4.24)). Unlike Ungar and Eichhorn's correlation for α^*, which shows the coefficient b is constant, the coefficient b obtained from present work is expressed in equation (4.28) because the distribution of coefficient b varies with the density ratio and has no smooth trend. Therefore, the accuracy for this model would be affected in certain ranges of density ratio. The applicable range for this model is restricted for G_c up to the value of 8, where G_c is illustrated in equation (3.27). Thus, the applicable range is attributed to the low flow region according to Ungar and Eichhorn's (1988) observation.
The other parameter ranges for this model are:

Density ratio: 50 - 1650

Quality:	-11.0 to 11.0%

The diameter effect is not included in this analysis. However, according to the definition of Froude number, the diameter effect should have an implicit influence on the derivation of effective vapor sheet thickness. The experimental data used in this analysis are chosen according to the parameter range which meets the limitation that $G_c \leq 8$. Four types of fluid are used in this analysis: water, Freon-113, isopropanol and methanol. Because the model derived in present study is based on the assumption that the fluid flows across single cylinder, this model can not be applied to the bundle case. Efforts for applying this model to bundles should be made in the future.

An empirical correlation for cross-flow CHF is also developed in present work. In addition, the relationship of CHF's between cross flow and axial flow is investigated in the study, resulting in a correction factor to relate the CHF's in both cases. Unlike the semi-empirical CHF correlation for cross-flow boiling developed in Chapter 4, which can only apply to $G_c \leq 8$, the empirical CHF correlation for cross-flow boiling and the correction factor ($KCHF$) developed in Chapter 7 are applicable to a wider range of flow velocity (e.g. $G_c > 8$). The first consideration of choosing the experimental data for analysis is that the outside diameter in cross flow should be close to the range of $4 \leq D \times 10^3 \leq 16$ mm in order to correspond with the range used in Groeneveld's look-up table. However, because of the lack of experimental CHF data for cross flow, diameter which is in the range of $3 \leq D \times 10^3 \leq 4$ mm is also acceptable in the analysis.
The other parameter ranges are:

Froude number:	0.35 - 36
Density ratio:	50 - 1490
Quality:	-21 to 11%

Since the parameter range is different than that used in Chapter 4 for semi-empirical correlation, the experimental data sources used in both analyses may not be the same. Thus, only two types of fluid can be used in this analysis to satisfy the diameter range. They are water and Freon-113. However, the accuracy of the empirical correlation for cross flow is acceptable (13.4% of RMS error), which is indicated in Table 7.4. Compared with the result that the CHF calculated by multiplying a correction factor to the CHF predicted from Groeneveld's look-up table

(16.2% of RMS error), the CHF predicted by the empirical correlation is slightly more accurate. However, the analysis only involves limiting experimental data which have a narrower range than that used in Groeneveld's look-up table. If more data with wider parameter range are available, the deviation of both approaches with experimental data probably can be reduced to a satisfactory level.

In summary, the CHF of cross-flow boiling predicted by the empirical correlation, equation (7.5), is recommended. Though the CHF of cross flow predicted by the correction factor method is not as accurate as that predicted by equation (7.5), the idea to investigate the relationship of CHF's between these two different flow patterns is found with a reasonable result. Besides, the availability of axial-flow CHF data for wider parameter range (see Section 6.3) is very attractive to be used to predict the cross-flow CHF in which the experimental data is not available in certain range. The semi-empirical model presented in Chapter 4 is an improvement of Ungar and Eichhorn's (1988) hydrodynamic model and Lienhard and Eichhorn's (1976) $MESC$ model to be applied for a wider quality range. However, more work has to be done, either the theoretical derivation or experimental investigation, to reduce the level of RMS error.

1. Ahmad, S.Y., (1973), *Fluid to fluid modelling of critical heat flux: A compensated distortion model*, Int. J. Heat Mass Transfer, Vol. 16, pp. 641-662.

2. Barnett, P.G., (1964), *An experimental investigation to determine the scaling laws of forced convective boiling heat transfer, Part 1. The preliminary examination using burn-out data for water and arcton 12*, AEEW-R363

3. Beecher, N., (1948), MS thesis, Chemical Engineering Department, Massachusetts Institute of Technology.

4. Biasi, L., Clerici, G.C., Garribba, S., Sala, R. and Tozzi, A., (1967), *Studies on burn-out: Part 3*, Energia Nucleare, 14(9), pp. 530-536.

5. Bowring, R.W., (1972), *A simple but accurate round tube uniform heat flux, dryout correlation over the pressure range 0.17-17 MN/m^2 (100-2500 psia)*, AEEW-R789, UKAEA, Winfrith.

6. Broussard, R. A. and Westwater, J. W., (1985), *Diameter and velocity effects for cross-flow Boiling*, AIAA Journal, Vol. 23, No.10, Oct. 1985

7. Collier, J.G., (1981), *Convective boiling and condensation*, 2nd Ed., McGraw-Hill, New York.

8. Cumo, M., Farello, G. E., Gasiorowski, J., Iovino, G. and Naviglio A., (1980), *Quality influence on the departure from nucleate boiling in cross flows through bundles*, Nuclear Technology, Vol. 49, Aug., pp. 337-346

9. Diesselhorst, T., Grigull, U. and Hahne, E., (1977), *Hydrodynamic and surface effects on the peak heat flux in pool boiling*, Heat Transfer in Boiling, Chapter 6, pp. 99-135.

10. ESDU, (1986), *Boiling inside tubes: Critical heat flux for upward flow in uniformly heated vertical tubes*, Engineering Sciences Data Unit Item Number 86032, 251-259 Regent Street, London, England W1R 8E5.

11. Groeneveld, D. C. and Snoek, C. W., (1982), *A comprehensive examination of heat transfer correlations suitable for reactor safety analysis*, Multiphase Science and technology, Chapter 3, Hemisphere Pub. Corp., Washington.

12. Groeneveld, D. C., Cheng, S. C. and Doan, T., (1986a), *1986 AECL-UO critical heat flux lookup table*, Heat Transfer Engineering, Vol. 7, No. 1-2, pp. 46-62.

13. Groeneveld, D. C., Kiameh, B. P. and Cheng, S., C., (1986b), *Prediction of critical heat flux (CHF) for non-aqueous fluid in forced convective boiling*, Proceedings of 8th Int. Heat Transfer Conf., San Francisco, California, Vol. 5, pp. 2209-2214.

14. Hagerty, W. W. and Shea, I. F., (1955), *A study of the stability of plane fluid sheets*, ASME Journal of Applied Mechanics, Vol. 22, pp. 509-514

15. Hasan, M. Z., Hasan, M. M., Eichhorn, R. and Lienhard, J. H., (1981), *Boiling burn-out during cross-flow over cylinders, beyond the influence of gravity*, ASME Journal of Heat Transfer, Vol. 103, pp. 478-484.

16. Hasan, M. M., Eichhorn, R. and Lienhard, J. H., (1982), *Burn-out during flow across a small cylinder influence by parallel cylinders*, Heat Transfer 1982, Proceedings of the 7th International Heat Transfer Conference.

17. Hewitt, G.F. and Hutchinson, P., (1976), *A mathematical model of two-phase annular flow heat and mass transfer*, 5th All Union Conf., Minsk, May 17-20, paper 3.79.

18. Hiemenz, K., (1911), *Die grenzschicht an einem in den gleichformigen flüssigkeitsstrom eingetauschten geraden kreiszylinder*, Drs. Göttingen.

19. Hwang, T.H. and Yao, S.C., (1984), *Boiling heat transfer of a horizontal cylinder at low quality cross-flow*, ASME HTD, Vol. 38, pp. 9-17.

20. Katto, Y., (1978) *A generalized correlation of critical heat flux for the forced convection boiling in vertical uniformly heated round tubes*. Int. J. Heat Mass Transfer, Vol. 21, pp. 1527-1542.

21. Katto, Y. and Ohno, H., (1984), *An improved version of the generalized correlation of critical heat flux for the forced convective boiling in uniformly heated vertical tubes*, Int. J. Heat Mass Transfer, Vol. 27, No. 9, pp. 1641-1648

22. Katto, Y., Yokoya, S., Miake, S. and Taniguchi, M., (1987), *Critical heat flux on a uniformly heated cylinder in a cross flow of saturated liquid over a very wide range of vapor-to-liquid density ratio*, Int. J. Heat Mass Transfer, Vol. 30, No. 9, pp. 1971-1977.

23. Katto, Y. and Haramura, Y., (1983a), *A new hydrodynamic model of critical heat flux applicable widely to both pool and forced convection boiling on submerged bodies in saturated liquid*, Int. J. Heat Mass Transfer, Vol. 26, No. 3, pp. 389-399.

24. Katto, Y. and Haramura, Y., (1983b), *Critical heat flux on a uniformly heated horizontal cylinder in an upward cross flow of saturated liquid*, Int. J. Heat Mass Transfer, Vol. 26, No. 8, pp. 1199-1205.

25. Katto, Y. and Yokoya, S., (1976), *Behavior of a vapor mass in saturated nucleate and transition pool Boiling*, Heat Transfer - Japan. Res. 5(2), pp. 45-65.

26. Kezios, S. P. and Lo, R. K., (1958), *Heat transfer from rods normal to subcooled water flow for non-boiling and surface boiling conditions up to and including*

burn-out, Argon National Laboratory Report ANL-5822.

27. Kezios S. P., Kim, T. S. and Rafchielc, F. M., (1961), *Burn-out in crossed rod matrices under forced convection flow of water*, Paper No. 31, International Developments in Heat Transfer, Vol. 2, pp. 262.

28. Kheyrandish, K. and Lienhard, J. H., (1985). *Mechanisms of burn-out in saturated ans subcooled flow boiling over a cylinder.* AIChE/ASME Nat'l. Heat Transfer Conf., Denver. Co., Aug. 4-7, pp. 25-31.

29. Kiameh, B.P., (1986), *Prediction of critical heat flux (CHF) for non-aqueous fluids in forced convective boiling*, M.A.Sc. Thesis of the Dept. of Mechanical Engineering, University of Ottawa.

30. Kutateladze, S.S., (1963), *Fundamentals of heat transfer*, Academic Press Inc., New York.

31. Leung, L.K.H., (1986), *Critical heat flux prediction for non-aqueous fluids*, The 1987 Compendium of Thermalhydraulic Correlations and Fluid Properties (First revision), AECL, 1988.

32. Lienhard, J. H. and Hasan, M. Z., (1979a), *Correlation of burn-out data for disk heaters cooled by liquid jets*, ASME Journal of Heat Transfer, Vol. 101, pp. 383-384.

33. Lienhard, J. H. and Hasan, M. Z., (1979b), *On predicting boiling burn-out with the mechanical energy stability criterion*, ASME Journal of Heat Transfer, Vol. 101, pp. 276-279.

34. Lienhard, J. H. and Eichhorn, R., (1979), *On predicting boiling burn-out for heater cooled by liquid jets*, Int. J. Heat Mass Transfer, Vol. 22, pp. 774-776.

35. Lienhard, J. H. and Eichhorn, R., (1976), *Peak boiling heat flux on cylinder in a cross flow*, Int. J. Heat Mass Transfer, Vol. 19, pp. 1135-1142.

36. Lienhard, J. H. and Dhir, V. K., (1973), *Hydrodynamic prediction of peak pool-boiling heat fluxes from finite bodies*, ASME Journal of Heat Transfer, Vol. 95, pp. 152-158.

37. Lienhard, J. H., Dhir, V. K. and Riherd, D. M., (1973), *Peak pool boiling heat-flux measurements on finite horizontal flat plates*, ASME Journal of Heat Transfer, Vol. 95, pp. 477-482.

38. Lienhard, J. H. and Wong, P. T. Y., (1964), *The dominant unstable wavelength and minimum heat flux during film boiling on a horizontal cylinder*, ASME Journal of Heat Transfer, Vol. 86, pp. 220-226.

39. Macbeth, R.V., (1963), *Burn-out analysis: Part 4, Application of a local conditions hypothesis to wall data for uniformly heated round tubes and rectangular channels*, AEEW-R267, UKAEA, Winfrith.

40. Mckee, H. R. and Bell, K. J., (1969) *Forced convection boiling from a cylinder normal to the flow*, Chemical Engineering Progress, Symposium Series, Vol. 65, No. 92, pp. 222-230.

41. Min, T.K., (1975), *Boiling on cylinder in cross flow - Low velocity peak heat flux measurements for water and methanol*, M.S. thesis, Mechanical Engineering Department, University of Kentucky.

42. Perkins, H. and Leppert, G., (1962), *Forced convection heat transfer from a uniformly heated cylinder*, ASME, Journal of Heat Transfer, Vol. 84, pp. 257-263.

43. Pourdashti, M., (1984), *Critical heat flux on a horizontal tube in an upward two- phase cross-flow*, MS thesis, Mechanical Engineering Department, University of Wisconsin-Milwaukee.

44. Shah, M.M., (1979), *A generalized graphical method for predicting CHF in uniformly heated vertical tubes*, Int. J. Heat Mass Transfer, Vol. 22, pp. 557-568.

45. Shah, M.M., (1986), *Further development and verification of the Shah correlation for CHF in uniformly heated vertical tubes*, Project Report B-65. Copies available from the author.

46. Stevens, G.F. and kirby, G.J., (1964), *A quantitative comparison between burn-out data for water at 1000 lb/in^2 and freon-12 at 155 lb/in^2 (Abs.) uniformly heated round tubes, vertical up-flow*, United Kingdom Atomic Energy Authority, Report No. AEEW-R327.

47. Sun, K. H. and Lienhard, J. H., (1970), *The peak pool boiling heat flux on horizontal cylinders*, Int. J. Heat Mass Transfer, Vol. 13, pp. 1425-1439.

48. Ungar, E. K. and Eichhorn, R., (1988), *A new hydrodynamic prediction of the peak heat flux from horizontal cylinder in low speed up-flow*, ASME/AIChE Heat Transfer Conference, Houston, TX, July.

49. USSR Academy of Science, (1977), *Tabular data for calculating burn-out when boiling water in uniformly heated round tubes*, Thermal Engineering, pp. 77-79, Sept., or Teploenergitika, 23(9), pp. 90-92, (1976).

50. Vliet, G. C. (1962), *Local boiling peak heat flux for water flowing normal to cylinder*, PhD thesis, Mechanical Engineering Department, Stanford University.

51. Vliet, G. C. and Leppert, G., (1964a), *Critical heat flux for nearly saturated water flowing normal to a cylinder*, ASME Journal of Heat Transfer, Vol. 86, pp. 59-67.

52. Vliet, G. C. and Leppert, G., (1964b), *Critical heat flux for subcooled water flowing normal to a cylinder*, ASME Journal of Heat Transfer, Vol. 86, pp. 68-74.

53. Weisman, J. and Pei, B.S., (1983), *Prediction of critical heat flux in flow boiling at low qualities*, Int. J. Heat Mass Transfer, Vol. 26, pp. 1463-1477.

54. Whalley, P.B., Hutchinson, P. and Hewitt, G.F., (1973), *The calculation of critical heat flux in forced convective boiling*, Atomic Energy Research Establishment - R7520 Harwell, Berkshire.

55. Whalley, P.B., Hutchinson, P. and Hewitt, G.F., (1974), *The calculation of critical heat flux in forced convective boiling*, Heat Transfer, 4, pp. 290-294.

56. Whalley, P.B., Hutchinson, P. and Hewitt, G.F., (1975), *Prediction of annular flow parameters for transient conditions and for complex geometries*, European Two-phase Flow Group meet., Haifa, paper 2.1.

57. Whalley, P.B., Hutchinson, P. and James, P.W., (1978), *the calculation of critical heat flux in complex situations using an annular flow model*, Proc. 6th Int. Heat Transfer conf., Toronto, 5, pp. 65-70.

58. Wong, Y.L., (1988), *Generalized CHF prediction for horizontal tubes with uniform heat flux*, M.A.Sc. Thesis of the Dept. of Mechanical Engineering, University of Ottawa.

59. Yilmaz, S. and Westwater, J. W., (1980), *Effect of velocity on heat transfer to boiling Freon-113*, ASME Journal of Heat Transfer, Vol. 102, pp. 26-31.

60. Zuber, N. (1958), *On the stability of boiling heat transfer*, ASME Journal of Heat Transfer, Vol. 80, pp. 711.

61. Žukauskas, A. A. and Žiugžda J., (1985), *Heat transfer of a cylinder in cross flow*, Hemisphere, Washington, pp. 208.

62. Žukauskas, A., (1987), *Convective heat transfer in cross flow*, Handbook of single-phase convective heat transfer, Chapter 6, Wiley-Interscience, New York.

Appendix A

Tabulation of Experimental CHF Data in Cross-flow Boiling

Because of the parameter ranges used in the semi-empirical model and the correction factor method as well as in the empirical CHF correlation are different, the experimental CHF data used in these analyses come from various sources. Table A.1 illustrates the cross-flow CHF data used in the semi-empirical model, while Table A.2 shows the cross-flow CHF data analyzed in the correction factor method and the empirical prediction method.

Table A.1: CHF data for cross-flow used in semi-empirical model

Fluid: Freon-113

Source: Pourdashti (1984)

Pressure	Mass flux	Diameter	Quality	CHF	St	Fr	α^*
kPa	$kg/m^2/s$	m		W/m^2			
187.7	103	0.00635	-0.006	241000	1.1465	0.26632	0.2357
200.9	99.51	0.00635	-0.075	282200	1.1633	0.25787	0.2457
208.2	96.08	0.00635	-0.051	281900	1.1802	0.24949	0.2456
197.7	98.33	0.00635	0.011	221800	1.1762	0.25148	0.2201
201.1	100	0.00635	-0.002	230900	1.1676	0.25568	0.2244
197.7	96.6	0.00635	0.072	212000	1.1846	0.24737	0.2219
197.7	101.6	0.00635	0.108	212000	1.1574	0.2608	0.231
197.1	152	0.00635	-0.069	291000	0.9417	0.38975	0.2856
214.5	151.9	0.00635	-0.066	295800	0.9412	0.3901	0.2849
208.7	152	0.00635	-0.007	264900	0.94178	0.38969	0.2761
208	151.9	0.00635	0.046	220400	0.9414	0.38996	0.2529
211.4	148.3	0.00635	0.091	213100	0.95634	0.37948	0.2524
202.8	287.1	0.00635	-0.047	277400	0.60148	0.73938	0.3517
206.7	291	0.00635	0.003	275300	0.59296	0.75232	0.3629
213.4	288	0.00635	0.044	245800	0.59758	0.74526	0.3414
213.4	286.4	0.00635	0.043	246600	0.59962	0.74217	0.3414
396.1	95.79	0.00635	-0.082	347400	1.187	0.24621	0.2524
430.9	94.97	0.00635	-0.019	323300	1.1939	0.24286	0.2474
424.4	96.58	0.00635	0.051	278600	1.1844	0.24745	0.2361
404.5	95.21	0.00635	0.108	251000	1.196	0.2419	0.2293
418.2	131.8	0.00635	-0.053	342600	1.0225	0.33613	0.2745
405.1	137.3	0.00635	-0.003	305800	1.0001	0.35028	0.2666
411.8	131.7	0.00635	0.048	280600	1.0217	0.33663	0.2571
411.8	129.8	0.00635	0.094	255400	1.029	0.33213	0.2484
194.9	442.7	0.00635	-0.097	346000	0.40741	1.1407	0.4721
194.9	442.9	0.00635	-0.099	336600	0.40768	1.1399	0.462
202	438.7	0.00635	-0.047	329800	0.40901	1.1362	0.4662
205.8	437.3	0.00635	-0.048	329500	0.41061	1.1316	0.4624

(Table A.1 cont'd)

Pressure kPa	Mass flux $kg/m^2/s$	Diameter m	Quality	CHF W/m^2	St	Fr	α^*
209	141.1	0.00635	-0.11	314200	0.99005	0.3568	0.282
202.1	97.75	0.00635	0.053	220800	1.1805	0.24938	0.2246
205.6	97.47	0.00635	-0.107	311900	1.1827	0.24829	0.2541
198.5	94.73	0.00635	-0.043	285000	1.1965	0.24162	0.2487
202.2	93.36	0.00635	-0.031	265600	1.2034	0.23838	0.2374
213	291.2	0.00635	0.064	255200	0.59333	0.75175	0.3571
206	293.9	0.00635	-0.096	319200	0.59422	0.75037	0.3766
206.1	290.8	0.00635	-0.083	307700	0.59887	0.74331	0.3688
206.2	291.7	0.00635	-0.032	298900	0.59485	0.74941	0.3749
202.4	288.8	0.00635	-0.004	275400	0.59979	0.74192	0.361
209.6	289.9	0.00635	0.045	258200	0.59632	0.74717	0.3554
202.3	143.2	0.00635	0.002	256900	0.98042	0.36315	0.2674

(Table A.1 cont'd)

Fluid: isopropanol

Source: Hasan et al. (1981)

Pressure	Mass flux	Diameter	Quality	CHF	St	Fr	α^*
kPa	$kg/m^2/s$	m		W/m^2			
101	204.8	0.0015	0	585000	0.19026	2.3012	0.4909
101	256.9	0.0015	0	615000	0.14458	2.8868	0.588
101	378	0.0015	0	650000	0.088344	4.2476	0.7617
101	457.3	0.0015	0	685000	0.06864	5.1384	0.8601
101	593.1	0.0015	0	730000	0.048229	6.6643	0.9691
101	212.9	0.00081	0	770000	0.12444	3.2549	0.636
101	256.9	0.00081	0	775000	0.09782	3.9284	0.7266
101	320.8	0.00081	0	785000	0.073043	4.9049	0.8437
101	447.7	0.00081	0	865000	0.046472	6.8466	1.074
101	584.3	0.00081	0	900000	0.032097	8.9342	1.1992
101	191.6	0.0005	0	925000	0.10465	3.7286	0.697
101	200.4	0.0005	0	900000	0.098743	3.9	0.7071
101	275.3	0.0005	0	830000	0.064903	5.3571	0.8358
101	311.9	0.0005	0	865000	0.054784	6.0714	0.9326
101	339.1	0.0005	0	928000	0.048875	6.6	1.0316
101	341.3	0.0005	0	1000000	0.048443	6.6429	1.093
101	445.5	0.0005	0	955000	0.033469	8.6714	1.2093
101	447.7	0.0005	0	1070000	0.033239	8.7143	1.3205
101	596	0.0005	0	1000000	0.022185	11.6	1.3621

(Table A.1 cont'd)

Fluid: isopropanol

Source: Ungar and Eichhorn (1988)

Pressure	Mass flux	Diameter	Quality	CHF	St	Fr	α^*
kPa	$kg/m^2/s$	m		W/m^2			
101	198.2	0.00159	0	539000	0.20497	2.16	0.4346
101	345	0.00159	0	644000	0.10317	3.77	0.695
101	484.4	0.00159	0	670000	0.066013	5.29	0.8358
101	697.3	0.00159	0	781000	0.040154	7.61	1.0137
101	227.5	0.00318	0	460000	0.2589	1.76	0.4122
101	249.6	0.00318	0	525000	0.23339	1.93	0.4771
101	389	0.00318	0	534000	0.13784	3	0.6111
101	565.2	0.00318	0	550000	0.085367	4.36	0.7088
101	587.2	0.00318	0	604000	0.081408	4.52	0.7684
101	719.3	0.00318	0	648000	0.29748	1.55	0.4137
101	220.2	0.00476	0	396000	0.33381	1.39	0.3607
101	315.6	0.00476	0	432000	0.22537	1.99	0.4636
101	469.8	0.00476	0	515000	0.14016	2.96	0.6256
101	616.6	0.00476	0	540000	0.099072	3.89	0.6932
101	638.6	0.00476	0	531000	0.094626	4.03	0.687

(Table A.1 cont'd)

Fluid: methanol

Source: Min (1975)

Pressure kPa	Mass flux $kg/m^2/s$	Diameter m	Quality	CHF W/m^2	St	Fr	α^*
101	142.5	0.00051	0	1100000	0.15786	2.6875	0.5099
101	172.5	0.00051	0	1210000	0.12452	3.2533	0.6304
101	217.5	0.00051	0	1420000	0.092466	4.102	0.8415
101	255	0.00051	0	1520000	0.074982	4.8093	0.9964
101	292.5	0.00051	0	1560000	0.062388	5.5165	1.1244
101	408.8	0.00051	0	1670000	0.039439	7.709	1.4876
101	435.1	0.00051	0	1810000	0.036165	8.2041	1.6386
101	495.1	0.00051	0	1840000	0.030174	9.3357	1.7869
101	142.5	0.00051	0	1100000	0.15786	2.6875	0.5099
101	172.5	0.00051	0	1170000	0.12452	3.2533	0.6162
101	217.5	0.00051	0	1380000	0.092466	4.102	0.8252
101	255	0.00051	0	1470000	0.074982	4.8093	0.9737
101	292.5	0.00051	0	1560000	0.062388	5.5165	1.1244
101	378.8	0.00051	0	1670000	0.043832	7.1432	1.4156
101	435.1	0.00051	0	1790000	0.036165	8.2041	1.6256
101	495.1	0.00051	0	1830000	0.030174	9.3357	1.7798
101	232.5	0.00081	0	1380000	0.11435	3.4794	0.8322
101	393.8	0.00081	0	1620000	0.057059	5.8926	1.3526
101	457.6	0.00081	0	1620000	0.046472	6.8466	1.4833
101	510.1	0.00081	0	1720000	0.039991	7.6323	1.6456
101	558.8	0.00081	0	1830000	0.035216	8.3618	1.8031
101	135	0.00081	0	980000	0.22149	2.0203	0.4405
101	176.3	0.00081	0	1100000	0.16151	2.6376	0.5796
101	232.5	0.00081	0	1200000	0.11435	3.4794	0.7561
101	273.8	0.00081	0	1300000	0.092623	4.0967	0.901
101	326.3	0.00081	0	1370000	0.073491	4.8824	1.0589
101	371.3	0.00081	0	1470000	0.061793	5.5558	1.2147
101	435.1	0.00081	0	1560000	0.049805	6.5099	1.401

(Table A.1 cont'd)

Pressure	Mass flux	Diameter	Quality	CHF	St	Fr	α^*
kPa	$kg/m^2/s$	m		W/m^2			
101	146.3	0.00081	0	950000	0.20183	2.1887	0.4572
101	172.5	0.00081	0	1020000	0.16578	2.5815	0.5419
101	217.5	0.00081	0	1160000	0.12444	3.2549	0.703
101	255	0.00081	0	1350000	0.10156	3.8161	0.8779
101	292.5	0.00081	0	1420000	0.084923	4.3773	1.0049
101	367.5	0.00081	0	1550000	0.062646	5.4997	1.2527
101	435.1	0.00081	0	1640000	0.049805	6.5099	1.4525
101	487.6	0.00081	0	1760000	0.042572	7.2955	1.6333
101	168.8	0.00165	0	960000	0.25737	1.7694	0.4931
101	322.5	0.00165	0	1150000	0.11857	3.3815	0.8714
101	386.3	0.00165	0	1220000	0.094019	4.05	1.0202
101	435.1	0.00165	0	1340000	0.080439	4.5611	1.1719

(Table A.1 cont'd)

Fluid: water

Source: Vliet (1962)

Pressure kPa	Mass flux $kg/m^2/s$	Diameter m	Quality	CHF W/m^2	St	Fr	α^*
111.9	174.7	0.003175	-0.01141	1861000	0.44874	1.0313	0.3546
111.4	170	0.003175	-0.02104	2240000	0.46204	0.99954	0.3918
111.2	180.1	0.003175	-0.05201	4038000	0.44232	1.0471	0.5865
110.1	188.3	0.003175	-0.1036	6057000	0.42995	1.0789	0.7609
111.4	327	0.003175	-0.00383	2114000	0.23261	1.9356	0.59
111.9	335.8	0.003175	-0.01006	2429000	0.22625	1.9832	0.656
111.4	335.9	0.003175	-0.00995	2461000	0.22625	1.9832	0.6625
111.4	318	0.003175	-0.01762	2461000	0.24158	1.8722	0.6328
111.6	318	0.003175	-0.01794	2524000	0.24158	1.8722	0.6432
111.6	318	0.003175	-0.01794	2524000	0.24158	1.8722	0.6432
111.6	318.1	0.003175	-0.01877	2461000	0.24158	1.8722	0.632
111.6	318.1	0.003175	-0.01845	2618000	0.24158	1.8722	0.6592
111.6	318	0.003175	-0.01804	2587000	0.24158	1.8722	0.654
111.6	318	0.003175	-0.01804	2587000	0.24158	1.8722	0.654
111.6	318.1	0.003175	-0.01845	2618000	0.24158	1.8722	0.6592
112.7	318	0.003175	-0.01825	2524000	0.24158	1.8722	0.6414
112.7	318	0.003175	-0.01825	2618000	0.24158	1.8722	0.6575
112.7	318	0.003175	-0.01825	2555000	0.24158	1.8722	0.6468
112.7	318	0.003175	-0.01825	2745000	0.24158	1.8722	0.6788
112.7	318	0.003175	-0.01857	2808000	0.24158	1.8722	0.6891
111.6	337.5	0.003175	-0.02239	2681000	0.22625	1.9832	0.696
111.2	337.4	0.003175	-0.02135	2713000	0.22625	1.9832	0.7028
111.2	337.3	0.003175	-0.02094	2808000	0.22625	1.9832	0.7194
111	325.1	0.003175	-0.03119	2776000	0.23702	1.9039	0.6893
111	343.9	0.003175	-0.05263	4353000	0.22419	1.9991	0.9538
110.1	333.3	0.003175	-0.08282	5300000	0.2348	1.9198	1.0401
110.3	354.5	0.003175	-0.1043	5773000	0.22017	2.0308	1.1318
110.8	357.1	0.003175	-0.1034	6435000	0.2182	2.0467	1.2241

(Table A.1 cont'd)

Pressure kPa	Mass flux $kg/m^2/s$	Diameter m	Quality	CHF W/m^2	St	Fr	α^*
111.4	322.5	0.003175	-0.01016	2713000	0.23702	1.9039	0.6874
111.4	322.5	0.003175	-0.01047	2366000	0.23702	1.9039	0.6266
111.6	322.5	0.003175	-0.01048	2524000	0.23702	1.9039	0.6541
111.6	322.5	0.003175	-0.01027	2524000	0.23702	1.9039	0.6542
112.9	322.4	0.003175	-0.01048	2492000	0.23702	1.9039	0.6465
112.5	322.4	0.003175	-0.01037	2492000	0.23702	1.9039	0.6473
112.3	322.4	0.003175	-0.01048	2334000	0.23702	1.9039	0.6196
112.3	322.4	0.003175	-0.01048	2492000	0.23702	1.9039	0.6476
112.5	322.4	0.003175	-0.01037	2429000	0.23702	1.9039	0.6361
112.3	322.4	0.003175	-0.01048	2461000	0.23702	1.9039	0.642
112.1	322.4	0.003175	-0.00995	2366000	0.23702	1.9039	0.6258
111	477.2	0.003175	-0.00435	2934000	0.14855	2.8241	0.9681
112.1	643.2	0.003175	-0.00384	3249000	0.10185	3.8078	1.2831
112.3	639.5	0.003175	-0.01048	3502000	0.10295	3.7761	1.3368
110.6	647.7	0.003175	-0.02104	3691000	0.10185	3.8078	1.3914
110.8	634.1	0.003175	-0.02073	3249000	0.10465	3.7285	1.2543
110.3	633.9	0.003175	-0.03108	3375000	0.10523	3.7126	1.2767
111	633.9	0.003175	-0.03108	2145000	0.10523	3.7126	0.9295
111.6	633.8	0.003175	-0.03109	3596000	0.10523	3.7126	1.3292
111.2	646.6	0.003175	-0.0517	4574000	0.10352	3.7602	1.5649
111.4	655.4	0.003175	-0.08233	6341000	0.10295	3.7761	1.9274
111	647.3	0.003175	-0.08305	5047000	0.10465	3.7285	1.6325
110.8	664.5	0.003175	-0.1037	7098000	0.10185	3.8078	2.0718
111	925.1	0.003175	-0.00477	3817000	0.063048	5.4737	1.8303
112.1	971.2	0.003175	-0.05203	4133000	0.060431	5.6482	1.9036
110.8	307.6	0.000812	-0.02073	3628000	0.25113	1.8087	0.5136
110.8	313	0.001626	-0.02073	3312000	0.24628	1.8404	0.614
110.8	321.1	0.002393	-0.02073	2997000	0.23928	1.888	0.6631
110.8	342.7	0.004806	-0.02083	2366000	0.22216	2.015	0.7415
111.9	584.3	0.000256	-0.00415	4416000	0.11522	3.4587	0.6657

(Table A.1 cont'd)

Pressure kPa	Mass flux $kg/m^2/s$	Diameter m	Quality	CHF W/m^2	St	Fr	α^*
111.9	589.7	0.000502	-0.00415	4006000	0.11388	3.4905	0.7796
112.3	595	0.000812	-0.00404	4448000	0.11258	3.5222	0.9818
110.8	605.8	0.001623	-0.00373	4290000	0.11003	3.5857	1.2135
111.6	662.1	0.004803	-0.00415	3060000	0.098128	3.9188	1.4229
111.9	585.5	0.000256	-0.02105	5899000	0.11589	3.4429	0.7976
111.6	593.6	0.000502	-0.02084	4984000	0.11388	3.4905	0.8947
111.6	599	0.000810	-0.02073	4196000	0.11258	3.5222	0.9335
111.6	609.7	0.001626	-0.02063	4448000	0.11003	3.5857	1.2275
111.6	623.2	0.002393	-0.02053	3533000	0.10699	3.665	1.2011
111.6	666.5	0.004803	-0.02104	2871000	0.098128	3.9188	1.3447
111.2	589.3	0.000256	-0.05191	12150000	0.11658	3.427	1.2696
111.2	603	0.000812	-0.0518	8454000	0.11323	3.5063	1.4709
111.2	627.5	0.002393	-0.0517	5331000	0.10759	3.6491	1.559
110.8	614.7	0.000502	-0.1038	20500000	0.11258	3.5222	2.2296
111.2	620.2	0.000812	-0.1039	17100000	0.11129	3.5539	2.3186
112.7	631.1	0.001626	-0.1036	10760000	0.1088	3.6174	2.1364
110.6	631.2	0.001626	-0.1035	10730000	0.1088	3.6174	2.1443
112.7	645	0.002398	-0.1039	6940000	0.10581	3.6967	1.8189
110.8	692.2	0.004806	-0.1036	5142000	0.096603	3.9664	1.9364
111.9	1186	0.000256	-0.03109	10850000	0.045529	6.9492	2.0999
112.3	1194	0.000502	-0.03141	8139000	0.045103	6.9968	2.1128
110.6	1206	0.000812	-0.03108	6940000	0.044545	7.0603	2.198
110.3	1221	0.000256	-0.1039	28710000	0.045103	6.9968	3.9562

(Table A.1 cont'd)

Fluid: water

Source: Diesselhorst et al. (1977)

Pressure	Mass flux	Diameter	Quality	CHF	St	Fr	α^*
kPa	$kg/m^2/s$	m		W/m^2			
101	132.2	0.0075	0	770000	0.79573	0.50902	0.1855
101	130.3	0.0075	0	710000	0.80364	0.50164	0.1746
101	132.2	0.0075	0	750000	0.79573	0.50902	0.1823
101	297.1	0.0075	0	900000	0.40647	1.1435	0.3149
101	292.3	0.0075	0	970000	0.41295	1.125	0.3281
101	331.5	0.0075	0	1000000	0.3644	1.2762	0.3615
101	347.8	0.0075	0	1060000	0.34699	1.3389	0.3874
101	140.9	0.006	0	800000	0.70258	0.60622	0.1918
101	139.9	0.006	0	750000	0.70615	0.60209	0.1831
101	138	0.006	0	700000	0.7134	0.59385	0.1737
101	139.9	0.006	0	750000	0.70615	0.60209	0.1831
101	140.9	0.006	0	780000	0.70258	0.60622	0.1886
101	140.9	0.006	0	770000	0.70258	0.60622	0.187
101	318.1	0.006	0	960000	0.33909	1.3691	0.3433
101	342.1	0.006	0	1000000	0.31427	1.4722	0.3697
101	371.8	0.006	0	1110000	0.28745	1.6001	0.4187
101	381.4	0.006	0	1350000	0.2796	1.6413	0.4864
101	132.2	0.004	0	800000	0.63088	0.69701	0.1803
101	130.3	0.004	0	690000	0.63824	0.6869	0.162
101	132.2	0.004	0	800000	0.63088	0.69701	0.1803
101	234.8	0.004	0	750000	0.37591	1.2374	0.2404
101	258.7	0.004	0	830000	0.34049	1.3637	0.2739
101	310.5	0.004	0	1180000	0.28051	1.6364	0.3918
101	343	0.004	0	1150000	0.25121	1.8082	0.412
101	119.8	0.003	0	1030000	0.60846	0.72901	0.1989
101	120.7	0.003	0	1070000	0.60451	0.73485	0.2049
101	124.6	0.003	0	1260000	0.58916	0.75818	0.2325
101	265.4	0.003	0	1150000	0.28447	1.6155	0.3491

(Table A.1 cont'd)

Pressure	Mass flux	Diameter	Quality	CHF	St	Fr	α^*
kPa	$kg/m^2/s$	m		W/m^2			
101	287.5	0.003	0	1200000	0.2606	1.7496	0.3796
101	320	0.003	0	1330000	0.23094	1.9479	0.4386
101	375.6	0.003	0	1590000	0.19174	2.2862	0.5547

(Table A.1 cont'd)

Fluid: water

Source: Min (1975)

Pressure kPa	Mass flux $kg/m^2/s$	Diameter m	Quality	CHF W/m^2	St	Fr	α^*
98.54	192.4	0.00051	-0.00825	2016000	0.14823	2.829	0.4399
98.54	192.8	0.00051	-0.01445	2262000	0.14823	2.829	0.4732
98.54	193.5	0.00051	-0.02374	2453000	0.14823	2.829	0.4966
98.54	259.5	0.00051	-0.00618	2180000	0.10146	3.8191	0.5924
98.54	260.3	0.00051	-0.01445	2423000	0.10146	3.8191	0.6326
98.54	261.1	0.00051	-0.0227	2790000	0.10146	3.8191	0.6918
98.54	331.6	0.00051	-0.00618	2534000	0.073539	4.88	0.8031
98.54	332.8	0.00051	-0.01547	2957000	0.073539	4.88	0.886
98.54	333.7	0.00051	-0.0227	3172000	0.073539	4.88	0.9246
98.54	413.3	0.00051	-0.00618	2791000	0.054651	6.0823	1.0287
98.54	414.6	0.00051	-0.01445	3246000	0.054651	6.0823	1.1339
98.54	415.9	0.00051	-0.0227	3480000	0.054651	6.0823	1.1824
98.54	509.6	0.00051	-0.00722	3062000	0.040997	7.4968	1.2979
98.54	510.8	0.00051	-0.01341	3396000	0.040997	7.4968	1.3878
98.54	512.6	0.00051	-0.0227	3784000	0.040997	7.4968	1.4856
98.54	610.6	0.00051	-0.00722	3469000	0.031857	8.9821	1.6302
98.54	612	0.00051	-0.01341	3698000	0.031857	8.9821	1.6971
98.54	614.2	0.00051	-0.0227	4180000	0.031857	8.9821	1.8362
98.54	173.3	0.001024	-0.01063	2087000	0.25299	1.7968	0.3981
98.54	173.4	0.001024	-0.01269	2200000	0.25299	1.7968	0.4118
98.54	173.6	0.001024	-0.01579	2435000	0.25299	1.7968	0.4399
98.54	174.1	0.001024	-0.02301	2657000	0.25299	1.7968	0.4641
98.54	259.5	0.00081	-0.00650	2146000	0.13611	3.0305	0.5626
98.54	260.4	0.00081	-0.01475	2511000	0.13611	3.0305	0.6219
98.54	261.2	0.00081	-0.02301	2783000	0.13611	3.0305	0.6628
98.54	260	0.00081	-0.0112	2233000	0.13611	3.0305	0.576
98.54	260.4	0.00081	-0.01534	2441000	0.13611	3.0305	0.6099
98.54	261	0.00081	-0.02153	2776000	0.13611	3.0305	0.6623

(Table A.1 cont'd)

Pressure kPa	Mass flux $kg/m^2/s$	Diameter m	Quality	CHF W/m^2	St	Fr	α^*
98.54	365.3	0.00081	-0.00670	2358000	0.08787	4.2651	0.7887
98.54	365.9	0.00081	-0.01083	2504000	0.08787	4.2651	0.8192
98.54	366.6	0.00081	-0.01599	2780000	0.08787	4.2651	0.8764
98.54	367.3	0.00081	-0.02116	3044000	0.08787	4.2651	0.9288
98.54	413.9	0.00081	-0.00981	2649000	0.074631	4.8263	0.941
98.54	414.7	0.00081	-0.01497	2955000	0.074631	4.8263	1.0102
98.54	415.7	0.00081	-0.02116	3201000	0.074631	4.8263	1.0623
98.54	413.8	0.00081	-0.00960	2721000	0.074631	4.8263	0.9584
98.54	414.3	0.00081	-0.01269	2919000	0.074631	4.8263	1.0033
98.54	416	0.00081	-0.02307	3408000	0.074631	4.8263	1.1071
98.54	510.1	0.00081	-0.00981	2994000	0.056329	5.9487	1.2087
98.54	511.1	0.00081	-0.01497	3256000	0.056329	5.9487	1.276
98.54	512.3	0.00081	-0.02116	3671000	0.056329	5.9487	1.3797
98.54	611.2	0.00081	-0.00981	3536000	0.043968	7.1272	1.5602
98.54	612.4	0.00081	-0.01497	3712000	0.043968	7.1272	1.6079
98.54	613.8	0.00081	-0.02116	4109000	0.043968	7.1272	1.718
98.54	510.4	0.00081	-0.01115	3110000	0.056329	5.9487	1.2396
98.54	510.8	0.00081	-0.01332	3220000	0.056329	5.9487	1.2677
98.54	512.4	0.00081	-0.02155	3670000	0.056329	5.9487	1.3791
98.54	611.1	0.00081	-0.00960	3327000	0.043968	7.1272	1.4958
98.54	611.9	0.00081	-0.01269	3727000	0.043968	7.1272	1.615
98.54	614.2	0.00081	-0.02299	4192000	0.043968	7.1272	1.7398
98.54	261.2	0.00081	0	1770000	0.13611	3.0305	0.4963
98.54	367.6	0.00081	0	2030000	0.08787	4.2651	0.7156
98.54	415.9	0.00081	0	2270000	0.074631	4.8263	0.8526
98.54	512.7	0.00081	0	2600000	0.056329	5.9487	1.1043
98.54	614.2	0.00081	0	3052000	0.043968	7.1272	1.4181
98.54	174.1	0.00102	0	1660000	0.25243	1.8004	0.344
98.54	193.5	0.00051	0	1750000	0.14823	2.829	0.4023
98.54	261.2	0.00051	0	1990000	0.10146	3.8191	0.5594

(Table A.1 cont'd)

Pressure	Mass flux	Diameter	Quality	CHF	St	Fr	α^*
kPa	$kg/m^2/s$	m		W/m^2			
98.54	333.7	0.00051	0	2440000	0.073539	4.88	0.786
98.54	415.9	0.00051	0	2710000	0.054651	6.0823	1.0125
98.54	512.7	0.00051	0	2980000	0.040997	7.4968	1.2802
98.54	614.2	0.00051	0	3300000	0.031857	8.9821	1.5824

(Table A.1 cont'd)

Fluid: water

Source: Ungar and Eichhorn (1988)

Pressure kPa	Mass flux $kg/m^2/s$	Diameter m	Quality	CHF W/m^2	St	Fr	α^*
104.8	363.8	0.00081	0	3686000	0.08787	4.2651	1.0541
104.8	622.4	0.00081	0	5085000	0.042572	7.2955	2.0183
104.8	976.6	0.00081	0	5434000	0.022605	11.448	2.9019
104.8	306.4	0.00105	0	2544000	0.12944	3.1546	0.6979
104.8	392.6	0.00105	0	2968000	0.094266	4.0418	0.9429
104.8	421.3	0.00105	0	3097000	0.085948	4.3376	1.0266
104.8	641.5	0.00105	0	3768000	0.048825	6.6049	1.6275
104.8	660.7	0.00105	0	3780000	0.046891	6.8021	1.667
104.8	919.2	0.00105	0	4153000	0.029601	9.4638	2.234
104.8	1015	0.00105	0	4411000	0.025734	10.45	2.4758
104.8	344.7	0.0013	0	2674000	0.12767	3.1895	0.7777
104.8	976.6	0.0013	0	3815000	0.031587	9.0368	2.1272
104.8	258.5	0.00151	0	2531000	0.19854	2.2195	0.5947
104.8	363.8	0.00151	0	3168000	0.13105	3.1238	0.8987
104.8	430.9	0.00151	0	3219000	0.10572	3.6992	1.036
104.8	564.9	0.00151	0	3281000	0.074143	4.8501	1.2923
104.8	641.5	0.00151	0	3951000	0.062523	5.5077	1.6162
104.8	785.1	0.00151	0	3964000	0.047478	6.7408	1.8713
104.8	813.9	0.00151	0	4596000	0.045186	6.9874	2.1294
104.8	507.5	0.0016	0	3422000	0.088756	4.2326	1.219
104.8	325.5	0.00165	0	1886000	0.15885	2.6738	0.5769
104.8	526.6	0.00165	0	3328000	0.086271	4.3252	1.2265
104.8	689.4	0.00165	0	3070000	0.06023	5.6621	1.4144
104.8	316	0.00212	0	2589000	0.19142	2.2895	0.6876
104.8	344.7	0.00212	0	2454000	0.17253	2.4976	0.7075
104.8	497.9	0.00212	0	3019000	0.10918	3.6076	1.0741
104.8	593.6	0.00212	0	3328000	0.086898	4.3014	1.3091
104.8	651.1	0.00212	0	3459000	0.076923	4.7177	1.4382

(Table A.1 cont'd)

Pressure kPa	Mass flux $kg/m^2/s$	Diameter m	Quality	CHF W/m^2	St	Fr	α^*
104.8	727.7	0.00212	0	3574000	0.066304	5.2727	1.5922
104.8	833	0.00212	0	3686000	0.055225	6.0358	1.7831
104.8	938.3	0.00212	0	4173000	0.04692	6.799	2.1018
104.8	995.8	0.00212	0	3896000	0.043228	7.2153	2.0724
104.8	306.4	0.00038	0	4699000	0.066796	5.2438	1.1666
104.8	459.6	0.00038	0	6333000	0.038351	7.8657	2.0139
104.8	670.2	0.00038	0	6969000	0.022542	11.471	2.9212
104.8	277.7	0.00051	0	3940000	0.092466	4.102	0.9244
104.8	325.5	0.00051	0	3626000	0.074982	4.8093	0.998
104.8	325.5	0.00051	0	4388000	0.074982	4.8093	1.1352
104.8	440.4	0.00051	0	5010000	0.049839	6.5067	1.5986
104.8	478.7	0.00051	0	5141000	0.044438	7.0725	1.743
104.8	545.8	0.00051	0	6125000	0.037053	8.0626	2.187
104.8	603.2	0.00051	0	6125000	0.032213	8.9113	2.3695
104.8	699	0.00051	0	6464000	0.026172	10.326	2.7574
104.8	823.4	0.00051	0	7406000	0.020731	12.165	3.422
104.8	833	0.00051	0	6989000	0.020392	12.306	3.3111

Table A.2: CHF data for cross-flow used in correction factor and empirical prediction methods

Fluid: Freon-113

Source: Broussard and Westwater (1985)

Pressure kPa	Mass flux $kg/m^2/s$	Diameter m	Quality	Fr	CHF_{cross} W/m^2	CHF_{axial} W/m^2	$KCHF$
101.4	3879	0.00318	0	14.53941	497200	390300	1.274
101.4	6466	0.00318	0	24.23802	681600	406600	1.676
101.4	9699	0.00318	0	36.35420	876000	427000	2.052
101.4	4171	0.00635	0	11.06229	413900	311400	1.329
101.4	6952	0.00635	0	18.43848	535900	325300	1.647
101.4	10430	0.00635	0	27.66173	632800	342700	1.846
101.4	4911	0.0127	0	9.210444	243200	250100	0.9726
101.4	8185	0.0127	0	15.35263	360000	263100	1.368
101.4	12280	0.0127	0	23.02752	496800	279400	1.778

(Table A.2 cont'd)

Fluid: Freon-113

Source: Yilmaz (1980)

Pressure kPa	Mass flux $kg/m^2/s$	Diameter m	Quality	Fr	CHF_{cross} W/m^2	CHF_{axial} W/m^2	$KCHF$
101.4	4171	0.00635	0	11.06229	442500	311400	1.421
101.4	6952	0.00635	0	18.43848	583100	325300	1.792
101.4	11820	0.00635	0	31.34782	754100	349700	2.156

(Table A.2 cont'd)

Fluid: Freon-113

Source: Pourdashti (1984)

Pressure kPa	Mass flux $kg/m^2/s$	Diameter m	Quality	Fr	CHF_{cross} W/m^2	CHF_{axial} W/m^2	$KCHF$
202	126.3	0.00635	-0.031	0.346012	265600	292200	0.9092
197.9	128.2	0.00635	-0.043	0.349658	285000	295400	0.9649
207.5	130	0.00635	-0.051	0.354185	281900	302600	0.9316
197.2	130.7	0.00635	0.072	0.360556	212000	273200	0.7761
204.8	131.9	0.00635	-0.107	0.354826	311900	335800	0.9288
202	132.3	0.00635	0.053	0.365804	220800	278100	0.794
197.2	133.1	0.00635	0.011	0.366285	221800	284200	0.7805
200.6	134.7	0.00635	-0.075	0.364202	282200	315800	0.8937
200.6	135.4	0.00635	-0.002	0.371894	230900	289100	0.7985
197.2	137.4	0.00635	0.108	0.379267	212000	273100	0.7763
187.5	139.4	0.00635	-0.006	0.381390	241000	287700	0.8377
208.2	191	0.00635	-0.11	0.513649	314200	359800	0.8735
202	193.8	0.00635	0.002	0.534083	256900	316200	0.8125
211	200.8	0.00635	0.091	0.556119	213100	308400	0.6911
214.4	205.6	0.00635	-0.066	0.559725	295800	348300	0.8491
207.5	205.6	0.00635	0.046	0.568940	220400	314700	0.7004
196.5	205.7	0.00635	-0.069	0.556520	291000	344100	0.8458
208.2	205.7	0.00635	-0.007	0.566536	264900	325800	0.8133
213	387.6	0.00635	0.043	1.074977	246600	373300	0.6606
202.7	388.5	0.00635	-0.047	1.058950	277400	388800	0.7134
213	389.8	0.00635	0.044	1.081788	245800	373000	0.6591
202	390.9	0.00635	-0.004	1.075778	275400	379700	0.7253
208.9	392.3	0.00635	0.045	1.085795	258200	368600	0.7004
205.5	393.6	0.00635	-0.083	1.064960	307700	400000	0.7694
206.2	393.9	0.00635	0.003	1.087397	275300	383000	0.7189
212.4	394	0.00635	0.064	1.092205	255200	369700	0.6904
205.5	394.8	0.00635	-0.032	1.081788	298900	390100	0.7664
205.5	397.7	0.00635	-0.096	1.072573	319200	402700	0.7926

(Table A.2 cont'd)

Pressure kPa	Mass flux $kg/m^2/s$	Diameter m	Quality	Fr	CHF_{cross} W/m^2	CHF_{axial} W/m^2	$KCHF$
204.8	591.8	0.00635	-0.048	1.613467	329500	399100	0.8255
202	593.8	0.00635	-0.047	1.617073	329800	394300	0.8365
194.4	599.2	0.00635	-0.097	1.609060	346000	402000	0.8607
194.4	599.4	0.00635	-0.099	1.608659	336600	402600	0.836
396.4	129.6	0.00635	-0.082	0.367808	347400	322100	1.078
403.3	128.9	0.00635	0.108	0.374218	251000	282900	0.8874
404	185.8	0.00635	-0.003	0.537688	305800	328600	0.9308
410.9	175.7	0.00635	0.094	0.510844	255400	312300	0.8176
410.9	178.2	0.00635	0.048	0.518056	280600	318600	0.8809
417.8	178.4	0.00635	-0.053	0.512447	342600	335400	1.021
424	130.7	0.00635	0.051	0.380949	278600	289900	0.961
430.9	128.5	0.00635	-0.019	0.373056	323300	298900	1.082

(Table A.2 cont'd)

Fluid: water

Source: Kezios and Lo (1958)

Pressure kPa	Mass flux $kg/m^2/s$	Diameter m	Quality	Fr	CHF_{cross} W/m^2	CHF_{axial} W/m^2	$KCHF$
122	300.3	0.003175	-0.04418	1.753129	2665000	5754000	0.4632
120.3	304.1	0.003175	-0.08285	1.753129	4488000	6438000	0.6971
122.6	306.6	0.003175	-0.1167	1.753129	6020000	7258000	0.8295
122.4	308	0.003175	-0.1425	1.753129	5847000	7994000	0.7314
122.4	309	0.003175	-0.1678	1.753129	8009000	6717000	1.192
128.3	600.6	0.003175	-0.04718	3.506258	3147000	5885000	0.5347
128.5	607.7	0.003175	-0.08419	3.506258	5033000	6713000	0.7497
132.2	613.1	0.003175	-0.1213	3.506258	6407000	7728000	0.829
131.4	613.2	0.003175	-0.1216	3.506258	6406000	7735000	0.8282
129.8	616.1	0.003175	-0.146	3.506258	7524000	8446000	0.8909
130	618.2	0.003175	-0.1755	3.506258	8699000	7008000	1.241
139.7	902.7	0.003175	-0.05767	5.259387	3655000	6247000	0.585
140.3	912.4	0.003175	-0.09251	5.259387	5498000	7087000	0.7758
144.2	919.4	0.003175	-0.1249	5.259387	6732000	8005000	0.8409
141.7	924.1	0.003175	-0.1513	5.259387	8656000	8699000	0.9951
142.6	927.3	0.003175	-0.1816	5.259387	8955000	8225000	1.089
158	1202.7	0.003175	-0.06268	7.014783	4246000	6674000	0.6362
158.4	1214.5	0.003175	-0.09378	7.014783	6174000	7375000	0.8372
161.7	1225.4	0.003175	-0.1302	7.014783	6974000	8349000	0.8353
161.4	1232.1	0.003175	-0.1593	7.014783	9218000	8962000	1.029
161.7	1235.5	0.003175	-0.1814	7.014783	9249000	9203000	1.005
178.5	1502.1	0.003175	-0.06765	8.765646	5056000	7138000	0.7084
181.1	1517.2	0.003175	-0.09999	8.765646	6446000	7924000	0.8135
185.4	1537	0.003175	-0.1561	8.765646	8205000	9050000	0.9066
184.4	1540.1	0.003175	-0.1681	8.765646	10370000	9192000	1.128
182	1543.5	0.003175	-0.1838	8.765646	9830000	9372000	1.049
204.1	1805.8	0.003175	-0.08142	10.51650	5871000	7750000	0.7576
204.1	2065.1	0.003175	-0.1106	11.92173	7095000	8489000	0.8358

(Table A.2 cont'd)

Pressure kPa	Mass flux $kg/m^2/s$	Diameter m	Quality	Fr	CHF_{cross} W/m^2	CHF_{axial} W/m^2	$KCHF$
205.8	2075.3	0.003175	-0.1297	11.92173	8855000	8825000	1.003
207.9	2094.6	0.003175	-0.1761	11.92173	11170000	9548000	1.17
208.6	2102.5	0.003175	-0.2116	11.92173	11830000	8735000	1.354

(Table A.2 cont'd)

Fluid: water

Source: Vliet (1962)

Pressure kPa	Mass flux $kg/m^2/s$	Diameter m	Quality	Fr	CHF_{cross} W/m^2	CHF_{axial} W/m^2	$KCHF$
111.4	356.1	0.003175	-0.00383	2.107268	2114000	5112000	0.4134
111.9	1386.4	0.003175	-0.00383	8.204690	4448000	5500000	0.8087
112.1	700.5	0.003175	-0.00384	4.144841	3249000	5294000	0.6137
111.6	721.1	0.004803	-0.00415	3.468538	3060000	4621000	0.6622
111	519.8	0.003175	-0.00435	3.073925	2934000	5205000	0.5637
112.7	2773.2	0.003175	-0.00456	16.40938	5962000	5720000	1.042
111	1007.6	0.003175	-0.00477	5.960866	3817000	5444000	0.7012
110.6	1992	0.003175	-0.00487	11.78007	5079000	5621000	0.9035
111.4	3218.9	0.003175	-0.00995	18.99884	5457000	5930000	0.9203
111.4	365.8	0.003175	-0.00995	2.158830	2461000	5205000	0.4727
112.1	351.1	0.003175	-0.00995	2.072704	2366000	5204000	0.4546
111	2045.7	0.003175	-0.01006	12.07472	5110000	5768000	0.8861
111.9	365.8	0.003175	-0.01006	2.158830	2429000	5211000	0.4661
111.4	351.2	0.003175	-0.01016	2.072704	2713000	5201000	0.5216
111	2040	0.003175	-0.01016	12.03505	3943000	5769000	0.6835
111.6	351.2	0.003175	-0.01027	2.072704	2524000	5205000	0.4849
112.5	351.1	0.003175	-0.01038	2.072704	2492000	5215000	0.4779
112.5	351.1	0.003175	-0.01038	2.072704	2429000	5215000	0.4658
111.4	351.2	0.003175	-0.01047	2.072704	2366000	5206000	0.4545
112.9	351.1	0.003175	-0.01048	2.072704	2492000	5220000	0.4774
111.6	351.2	0.003175	-0.01048	2.072704	2524000	5208000	0.4846
112.3	696.5	0.003175	-0.01048	4.110277	3502000	5378000	0.6511
112.3	351.2	0.003175	-0.01048	2.072704	2334000	5214000	0.4477
112.3	351.2	0.003175	-0.01048	2.072704	2492000	5214000	0.478
112.3	351.2	0.003175	-0.01048	2.072704	2461000	5214000	0.4719
111.9	1390.2	0.003175	-0.01058	8.204690	4448000	5625000	0.7908
111.9	1375.6	0.003175	-0.01068	8.119696	4574000	5623000	0.8135
111.9	190.3	0.003175	-0.01141	1.122478	1861000	3869000	0.4811

(Table A.2 cont'd)

Pressure	Mass flux	Diameter	Quality	Fr	CHF_{cross}	CHF_{axial}	$KCHF$
kPa	$kg/m^2/s$	m			W/m^2	W/m^2	
111.4	346.3	0.003175	-0.01762	2.038140	2461000	5308000	0.4636
111.6	346.4	0.003175	-0.01794	2.038140	2524000	5314000	0.4749
111.6	346.4	0.003175	-0.01794	2.038140	2524000	5314000	0.4749
111.6	346.4	0.003175	-0.01804	2.038140	2587000	5315000	0.4866
111.6	346.4	0.003175	-0.01804	2.038140	2587000	5315000	0.4866
112.7	346.3	0.003175	-0.01825	2.038140	2524000	5328000	0.4737
112.7	346.3	0.003175	-0.01825	2.038140	2618000	5328000	0.4914
112.7	346.3	0.003175	-0.01825	2.038140	2555000	5328000	0.4796
112.7	346.3	0.003175	-0.01825	2.038140	2745000	5328000	0.5151
111.6	346.4	0.003175	-0.01845	2.038140	2618000	5322000	0.492
111.6	346.4	0.003175	-0.01845	2.038140	2618000	5322000	0.492
112.7	346.4	0.003175	-0.01857	2.038140	2808000	5333000	0.5265
111.6	346.5	0.003175	-0.01877	2.038140	2461000	5326000	0.462
110.8	690.7	0.003175	-0.02073	4.058715	3249000	5494000	0.5914
110.1	2045.8	0.003175	-0.02083	12.01805	4290000	6049000	0.7092
110.8	373.3	0.004806	-0.02083	1.782776	2366000	4667000	0.5069
112.3	3349.6	0.004806	-0.02084	16.00399	4133000	5460000	0.7568
111.2	367.4	0.003175	-0.02094	2.158830	2808000	5362000	0.5237
110.6	1393.3	0.003175	-0.02104	8.187691	4133000	5812000	0.7111
110.6	705.5	0.003175	-0.02104	4.144841	3691000	5504000	0.6706
111.6	725.9	0.004803	-0.02104	3.468538	2871000	4809000	0.5969
111.4	185.2	0.003175	-0.02104	1.087914	2240000	4030000	0.5558
112.1	1392.9	0.003175	-0.02115	8.187691	4101000	5821000	0.7045
111.6	3203.5	0.003175	-0.02115	18.82319	5457000	6259000	0.8719
111.2	367.4	0.003175	-0.02135	2.158830	2713000	5368000	0.5054
111.6	367.5	0.003175	-0.02239	2.158830	2681000	5386000	0.4978
109.5	3245.6	0.003175	-0.03065	18.99884	5142000	6542000	0.786
111.2	1392.3	0.003175	-0.03078	8.153694	4133000	5994000	0.6895

(Table A.2 cont'd)

Pressure kPa	Mass flux $kg/m^2/s$	Diameter m	Quality	Fr	CHF_{cross} W/m^2	CHF_{axial} W/m^2	$KCHF$
111	1392.4	0.003175	-0.03098	8.153694	3407000	5997000	0.5682
111	690.3	0.003175	-0.03108	4.041149	2145000	5628000	0.3812
110.3	690.4	0.003175	-0.03108	4.041149	3375000	5624000	0.6002
111.6	690.3	0.003175	-0.03109	4.041149	3596000	5632000	0.6386
111	354	0.003175	-0.03119	2.072704	2776000	5504000	0.5044
111	1466.4	0.004806	-0.03129	6.977281	3502000	5264000	0.6652
110.3	1392.8	0.003175	-0.03139	8.153694	2902000	6001000	0.4836
112.7	2094.3	0.003175	-0.03152	12.26170	4448000	6348000	0.7007
112.7	1395.3	0.003175	-0.03172	8.170692	4448000	6020000	0.7389
113.2	1395.4	0.003175	-0.03204	8.170692	4669000	6027000	0.7746
112.7	1397.4	0.003175	-0.04188	8.153694	4006000	6208000	0.6454
111.2	1402.3	0.003175	-0.05129	8.153694	4038000	6379000	0.633
111.4	3268.1	0.003175	-0.0515	18.99884	7319000	7137000	1.026
109.5	1399.9	0.003175	-0.05167	8.136695	4038000	6377000	0.6332
111.2	704.2	0.003175	-0.0517	4.093279	4574000	5914000	0.7734
111.9	2127.4	0.003175	-0.05192	12.36369	5678000	6867000	0.8269
111.2	196.1	0.003175	-0.05201	1.140043	4038000	4770000	0.8465
111.6	1402.5	0.003175	-0.05202	8.153694	4164000	6393000	0.6513
112.1	1057.8	0.003175	-0.05203	6.147851	4133000	6113000	0.676
111.6	1402.6	0.003175	-0.05212	8.153694	4763000	6395000	0.7449
111	374.5	0.003175	-0.05263	2.175829	4353000	5828000	0.747
109.3	1415.8	0.003175	-0.06732	8.187691	4700000	6661000	0.7056
111	1421.6	0.003175	-0.08232	8.187691	5773000	6931000	0.8329
111.4	713.8	0.003175	-0.08233	4.110277	6341000	6605000	0.96
111.4	3269.1	0.003175	-0.08264	18.82319	8770000	7512000	1.167
110.1	363	0.003175	-0.08282	2.089702	5300000	6394000	0.8289
109.3	2052.3	0.003175	-0.08301	11.81407	6309000	7204000	0.8758
111	704.9	0.003175	-0.08305	4.058715	5047000	6614000	0.7631

(Table A.2 cont'd)

Pressure kPa	Mass flux $kg/m^2/s$	Diameter m	Quality	Fr	CHF_{cross} W/m^2	CHF_{axial} W/m^2	$KCHF$
110.8	1382.9	0.003175	-0.08315	7.961042	4984000	6927000	0.7195
110.8	2088	0.003175	-0.08325	12.01805	5994000	7220000	0.8301
110.8	3286	0.003175	-0.1026	18.82319	10160000	7811000	1.3
110.8	389	0.003175	-0.1034	2.227958	6435000	6861000	0.938
110.1	205.1	0.003175	-0.1036	1.174607	6057000	6083000	0.9956
110.8	753.8	0.004806	-0.1036	3.509365	5142000	6207000	0.8284
110.8	723.7	0.003175	-0.1037	4.144841	7098000	7116000	0.9975
110.3	2089.9	0.003175	-0.1039	11.96706	7760000	7539000	1.029
112.1	1441.3	0.003175	-0.1041	8.255686	6845000	7378000	0.9278
110.3	386	0.003175	-0.1043	2.210393	5773000	6882000	0.8388

Appendix B

Program for Predicting The Water CHF Data by Groeneveld's Table Look-up Method

This chapter includes two programs. The first one is a program which predicts the water CHF data by interpolation or extrapolation from the given conditions, while the second one is a data file which contains the CHF table as illustrated in Table 6.1. This data file is read by the first program.

```
      SUBROUTINE CALCHF(P,G,D,X,CHF)

C*******************************************************************
C                                                                  *
C     Subroutine CALCHF                                            *
C                                                                  *
C     This subroutine is used to obtain the CHF from table of discrete *
C     values.  The table was presented by Groeneveld et al..       *
C                                                                  *
C*******************************************************************

C*******************************************************************
C                                                                  *
C     Variable declaration:                                        *
C                                                                  *
C     Character:                                                   *
C     GEOM    : a single character variable for channel geometry.  *
C     UNIT    : a single character variable for unit.              *
C     FLUID   : a single character variable for fluid type.        *
C     ORIENT  : a single character variable for channel orientation. *
C     STATE   : a single character variable for state of the system. *
C                                                                  *
C     Real:                                                        *
C     X       : provided quality.                                  *
C     D       : provided diameter.                                 
C     G       : provided mass flux.                                *
C     P       : provided pressure.                                 *
C     INTRP3  : the interpolated value.                            *
C     PX      : discrete value of quality.                         *
C     PG      : discrete value of mass flux.                       *
C     PP      : discrete value of pressure.                        *
C     CHFTAB  : a set of 4410 discrete values of CHF arranged in three-*
C               dimensional arrays.                                *
C                                                                  *
C     Logical:                                                     *
C     NFLG    : Program termination flag.                          *
C     Flag    : Step termination flag.                             *
C                                                                  *
C*******************************************************************

      REAL CHFTAB(21,14,15),PX(21),PG(14),PP(15),INTRP3
      LOGICAL FLAG

C*******************************************************************
C                                                                  *
C     Call up two  common blocks to pass some variables in and out the *
C     subroutine.                                                  *
C                                                                  *
C*******************************************************************

      COMMON/TABLE/CHFTAB
      COMMON/ROWS/PX,PG,PP,IX,IG,IP
         PH2O = P
         GH2O = G
C*******************************************************************
```

Figure B.1: Program for the water CHF prediction by Groeneveld's table look-up method

```
C                                                                    *
C     Initialize the flag and range pointer.                         *
C                                                                    *
C*********************************************************************

      FLAG = .TRUE.
      IX = 20
      IG = 13
      IP = 14

C*********************************************************************
C                                                                    *
C     Locate the discrete value of quality bounding the input value. *
C                                                                    *
C*********************************************************************

      DO 100 I=1,20
         IF((X .LE. PX(I+1)) .AND. FLAG)THEN
            IX = I
            FLAG = .FALSE.
         END IF
 100  CONTINUE

C*********************************************************************
C                                                                    *
C     Re-initialize the flag.                                        *
C     Locate the discrete value of mass flux bounding the input value. *
C                                                                    *
C*********************************************************************

      FLAG = .TRUE.
      DO 200 I=1,13
         IF((GH2O .LE. PG(I+1)) .AND. FLAG)THEN
            IG = I
            FLAG = .FALSE.
         END IF
 200  CONTINUE

C*********************************************************************
C                                                                    *
C     Re-initialize the flag.                                        *
C     Locate the discrete value of pressure bounding the input value. *
C                                                                    *
C*********************************************************************

      FLAG = .TRUE.
      DO 300 I=1,14
         IF((PH2O .LE. PP(I+1)) .AND. FLAG)THEN
            IP = I
            FLAG = .FALSE.
         END IF
 300  CONTINUE

C*********************************************************************
C                                                                    *
```

```
C      Calculate modification factor for tube diameter other than 0.008.*
C                                                                        *
C*************************************************************************

       IF(D .GT. 0.016)THEN
          CK1 = 0.7937
       ELSE IF(D .LT. 0.002)THEN
          CK1 = 1.5874
       ELSE
          CK1 = (0.008/D)**(1./3)
       END IF
          CHF = INTRP3(X,GH2O,PH2O)*CK1
       RETURN
       END
       REAL FUNCTION INTRP3(X,G,P)
C*************************************************************************
C                                                                        *
C      Function INTRP3                                                   *
C                                                                        *
C      This function is used to set up the parameters for linear         *
C      interpolation in CHF evaluation.  The parameters are the slope,   *
C      and two boundary points.                                          *
C                                                                        *
C*************************************************************************

C*************************************************************************
C                                                                        *
C      Variable declaration:                                             *
C                                                                        *
C      Real:                                                             *
C      X        : provided quality.                                      *
C      G        : provided mass flux.                                    *
C      P        : provided pressure.                                     *
C      INTERP   : the interpolated value.                                *
C      PX       : discrete value of quality.                             *
C      PG       : discrete value of mass flux.                           *
C      PP       : discrete value of pressure.                            *
C      CHFTAB   : a set of 4410 discrete value of CHF arranged in three- *
C                 dimensional arrays.                                    *
C                                                                        *
C*************************************************************************

       REAL INTERP,CHFTAB(21,14,15),PX(21),PG(14),PP(15)

C*************************************************************************
C                                                                        *
C      Call up two common blocks to pass some variables in and out the  *
C      subroutine.                                                       *
C                                                                        *
C*************************************************************************

       COMMON/TABLE/CHFTAB
       COMMON/ROWS/PX,PG,PP,IX,IG,IP
```

```
C**********************************************************************
C                                                                     *
C     Linear interpolate the pressure value.                          *
C                                                                     *
C**********************************************************************

      PARAM = (P-PP(IP))/(PP(IP+1)-PP(IP))
      C1    = INTERP(CHFTAB(IX,IG,IP),CHFTAB(IX,IG,IP+1),PARAM)
      C2    = INTERP(CHFTAB(IX,IG+1,IP),CHFTAB(IX,IG+1,IP+1),PARAM)
      C3    = INTERP(CHFTAB(IX+1,IG,IP),CHFTAB(IX+1,IG,IP+1),PARAM)
      C4    = INTERP(CHFTAB(IX+1,IG+1,IP),CHFTAB(IX+1,IG+1,IP+1),PARAM)

C**********************************************************************
C                                                                     *
C     Linear interpolate the mass flux value.                         *
C                                                                     *
C**********************************************************************

      PARAM = (G-PG(IG))/(PG(IG+1)-PG(IG))
      C5    = INTERP(C1,C2,PARAM)
      C6    = INTERP(C3,C4,PARAM)

C**********************************************************************
C                                                                     *
C     Linear interpolate the quality value.                           *
C                                                                     *
C**********************************************************************

      PARAM = (X-PX(IX))/(PX(IX+1)-PX(IX))
      INTRP3 = INTERP(C5,C6,PARAM)
      RETURN
      END
      REAL FUNCTION INTERP(A1,A2,P)

C**********************************************************************
C                                                                     *
C     Function INTERP                                                 *
C                                                                     *
C     This function is used to interpolate value linearly.            *
C     It requires the slope of the function and two boundary points.  *
C                                                                     *
C**********************************************************************

C**********************************************************************
C                                                                     *
C     Variable declaration:                                           *
C                                                                     *
C     Real:                                                           *
C     INTERP  : the interpolated value.                               *
C     P       : slope of the function.                                *
C     A1,A2   : the two bounds.                                       *
C                                                                     *
C**********************************************************************

      INTERP = A1 + (A2-A1)*P
```

```
      RETURN
      END

                  SUBROUTINE READCHF

C***********************************************************************
C                                                                      *
C     READ CHF DATA FROM CHFDA2.DATA                                   *
C                                                                      *
C***********************************************************************

      IMPLICIT REAL (A-H,O-Z)
      DIMENSION CHF(15,14,21),CHFTAB(21,14,15)
      COMMON/TABLE/CHFTAB

      OPEN(UNIT=1,FILE='CHFDA2 DATA')
      DO 1 I=1,15
         READ(1,4) K
4        FORMAT(/,I1)
         DO 2 J=1,14
            READ(1,3) (CHF(I,J,K),K=1,21)
3           FORMAT(3(T10,7F9.1,/))
2        CONTINUE
1     CONTINUE
      DO 100 I=1,15
         DO 200 J=1,14
            DO 300 K=1,21
               CHFTAB(K,J,I)=CHF(I,J,K)
300         CONTINUE
200      CONTINUE
100   CONTINUE
      CLOSE(1)
      RETURN
      END
      BLOCK DATA TBCHF1
      REAL PX(21),PG(14),PP(15)
      COMMON/ROWS/PX,PG,PP,IX,IG,IP
      DATA PX/-.5,-.4,-.3,-.2,-.15,-.1,-.05,0.,.05,.1,.15,.2,.25,
     +        .3,.4,.5,.6,.7,.8,.9,1./
      DATA PG/0.,50.,100.,200.,300.,500.,750.,1000.,1500.,2000.,
     +        3000.,4000.,5000.,7500./
      DATA PP/100.,150.,200.,300.,450.,700.,1000.,1500.,2000.,
     +        3000.,4500.,7000.,10000.,15000.,20000./
      END
```

```
PRESSURE ROW      1

G    1        0.0       0.0       0.0       0.0    3930.0    3000.0    2100.0
           1300.0     950.0     875.0     800.0     750.0     700.0     675.0
            600.0     520.0     454.0     340.0     240.0     230.0       0.0

G    2        0.0       0.0       0.0       0.0    4008.0    3500.0    2400.0
           1700.0    1500.0    1300.0    1140.0    1000.0     950.0     875.0
            750.0     600.0     500.0     475.0     400.0     375.0       0.0

G    3        0.0       0.0       0.0       0.0    4600.0    3700.0    2900.0
           2100.0    1700.0    1400.0    1200.0    1100.0    1000.0     900.0
            800.0     700.0     600.0     520.0     450.0     430.0       0.0

G    4        0.0       0.0       0.0       0.0    5200.0    4300.0    3400.0
           2600.0    2200.0    2100.0    1900.0    1600.0    1300.0    1100.0
            900.0     800.0     700.0     600.0     520.0     460.0       0.0

G    5        0.0       0.0       0.0       0.0    6000.0    4800.0    4200.0
           3600.0    3200.0    2900.0    2700.0    2500.0    2200.0    1900.0
           1100.0     900.0     820.0     750.0     650.0     500.0       0.0

G    6        0.0       0.0       0.0       0.0    6200.0    5000.0    4200.0
           3700.0    3300.0    3000.0    2900.0    2700.0    2400.0    2100.0
           1500.0    1100.0    1000.0     950.0     750.0     600.0       0.0

G    7        0.0       0.0       0.0       0.0    6300.0    5100.0    4300.0
           3800.0    3400.9    3100.0    3000.0    2800.0    2500.0    2200.0
           1800.0    1350.0    1100.0     980.0     775.0     620.0       0.0

G    8        0.0       0.0       0.0       0.0    6400.0    5200.0    4400.0
           3900.0    3500.0    3200.0    3100.0    2850.0    2550.0    2350.0
           1900.0    1460.0    1200.0     875.0     620.0     450.0       0.0

G    9        0.0       0.0       0.0       0.0    6500.0    5300.0    4700.0
           3950.0    3550.0    3300.0    3150.0    2875.0    2600.0    2375.0
           2000.0    1600.0    1300.0     800.0     560.0     375.0       0.0

G   10        0.0       0.0       0.0       0.0    6600.0    5400.0    5000.0
           4000.0    3700.0    3400.0    3175.0    2900.0    2700.0    2400.0
           1830.0    1500.0    1100.0     725.0     450.0     300.0       0.0

G   11        0.0       0.0       0.0       0.0    6800.0    5600.0    5200.0
           4100.0    4000.0    3500.0    3300.0    3000.0    2800.0    2500.0
           1700.0    1400.0     900.0     650.0     380.4     225.0       0.0

G   12        0.0       0.0       0.0       0.0    7000.0    5800.0    5300.0
           4200.0    4100.0    3800.0    3500.0    3100.0    2900.0    2600.0
           1600.0    1200.0     700.0     575.0     320.0     160.0       0.0

G   13        0.0       0.0       0.0       0.0    7130.0    6000.0    5400.0
           4300.3    4200.0    4000.0    3700.0    3200.0    3000.0    2700.0
           1400.0    1100.0     600.0     500.0     270.0     140.0       0.0

G   14        0.0       0.0       0.0       0.0    7250.0    6200.0    5700.0
```

Figure B.2: Data file of Groeneveld's CHF look-up table

		4400.6	4300.0	4200.0	3900.0	3400.0	3200.0	2800.0
		1200.0	900.0	550.0	425.0	230.0	130.0	0.0

PRESSURE ROW 2

G	1	0.0	0.0	0.0	6273.0	4700.0	3400.0	2500.0
		1800.0	1200.0	1000.0	900.0	800.0	750.0	700.0
		650.0	600.0	5[illegible]5.0	450.0	375.0	300.0	0.0
G	2	0.0	0.0	0.[illegible]	6344.0	4800.0	3800.0	3000.0
		2200.0	1700.0	1500[illegible]	1300.0	1100.0	1000.0	900.0
		800.0	700.0	600.[illegible]	539.0	450.0	420.0	0.0
G	3	0.0	0.0	0.0	6397.0	5000.0	4017.4	3200.0
		2400.0	1800.0	1600.0	1400.0	1150.0	1050.0	950.0
		850.0	750.0	675.0	580.0	510.0	450.0	0.0
G	4	0.0	0.0	0.0	6488.0	5444.0	4700.0	3800.0
		3100.0	2600.0	2400.0	2300.0	2100.0	1500.0	1400.0
		1000.0	850.0	775.0	700.0	600.0	500.0	0.0
G	5	0.0	0.0	0.0	6571.0	6050.0	5200.0	4400.0
		4000.0	3600.0	3000.0	2900.0	2800.0	2500.0	2200.0
		1200.0	1000.0	950.0	920.0	720.0	650.0	0.0
G	6	0.0	0.0	0.0	6700.0	6300.0	5300.0	4420.0
		4050.0	3650.0	3200.0	3100.0	2900.0	2600.0	2250.0
		1600.0	1300.0	1200.0	1000.0	850.0	700.0	0.0
G	7	0.0	0.0	0.0	6800.0	6350.0	5350.0	4450.0
		4100.0	3700.0	3300.0	3200.0	3000.0	2700.0	2500.0
		1900.0	1500.0	1250.0	1050.0	900.0	720.0	0.0
G	8	0.0	0.0	0.0	6850.0	6450.0	5400.0	4500.0
		4150.0	3725.0	3400.0	3250.0	3100.0	2800.0	2515.0
		2000.0	1630.0	1310.0	920.0	625.0	455.0	0.0
G	9	0.0	0.0	0.0	6900.0	6560.0	5445.0	4840.0
		4160.0	3745.0	3500.0	3300.0	3150.0	2850.0	2530.0
		2075.0	1650.0	1320.0	825.0	565.0	380.0	0.0
G	10	0.0	0.0	0.0	7000.0	6700.0	5550.0	5020.0
		4180.0	3800.0	3600.0	3400.0	3200.0	2900.0	2600.0
		1860.0	1520.0	1200.0	750.0	455.0	305.0	0.0
G	11	0.0	0.0	0.0	7500.0	7000.0	5700.4	5220.0
		4200.0	4100.0	3800.0	3600.0	3250.0	3000.0	2700.0
		1730.0	1420.0	910.0	675.0	385.0	230.0	0.0
G	12	0.0	0.0	0.0	8200.0	7200.0	5850.0	5320.0
		4250.0	4200.0	4000.0	3900.0	3350.0	3100.0	2800.0
		1630.0	1220.0	710.0	600.0	325.0	165.0	0.0
G	13	0.0	0.0	0.0	8900.0	7350.0	6050.0	5420.0
		4350.0	4300.0	4150.0	4100.0	3450.0	3200.0	2900.0

	1430.0	1110.0	610.0	525.0	275.0	146.0	0.0
G 14	0.0	0.0	0.0	9500.0	7450.0	6250.0	5720.0
	4450.0	4400.0	4300.0	4250.0	4650.0	3350.0	3100.0
	1230.0	910.0	560.0	450.0	240.0	136.0	0.0

PRESSURE ROW 3

G 1	0.0	0.0	0.0	6300.0	4800.0	3800.0	2900.0
	2200.0	1500.0	1100.0	950.0	850.0	775.0	725.0
	675.0	625.0	550.0	460.0	380.0	300.0	0.0
G 2	0.0	0.0	0.0	6350.0	4955.0	4000.0	3200.0
	2500.0	1900.0	1600.0	1400.0	1300.0	1150.0	1126.0
	1000.0	750.0	650.0	550.0	460.0	430.0	0.0
G 3	0.0	0.0	0.0	6400.0	5050.0	4100.0	3250.0
	2600.0	2300.0	2100.0	1900.0	1700.0	1400.0	1300.0
	1100.0	800.0	750.0	600.0	540.0	500.0	0.0
G 4	0.0	0.0	0.0	6500.0	5800.4	4900.0	4000.0
	3550.0	3300.0	2800.0	2800.0	2400.0	1800.0	1500.0
	1200.0	900.0	850.0	800.0	700.0	600.0	0.0
G 5	0.0	0.0	0.0	6580.0	6040.0	5250.0	4450.0
	4050.0	3650.0	3200.0	3100.0	2850.0	2550.0	2250.0
	1500.0	1200.0	1100.0	925.0	810.0	651.0	0.0
G 6	0.0	0.0	0.0	6800.0	6400.0	5500.0	4700.0
	4100.0	3700.0	3300.0	3200.0	2950.0	2650.0	2300.0
	1900.0	1500.0	1300.0	1050.0	875.0	725.0	0.0
G 7	0.0	0.0	0.0	6900.0	6450.0	5900.0	4900.0
	4150.0	3725.0	3400.0	3250.0	3050.0	2750.0	2550.0
	2050.0	1600.0	1310.0	1060.0	910.0	728.0	0.0
G 8	0.0	0.0	0.0	7000.0	6500.0	6000.0	5000.0
	4200.0	3800.0	3500.0	3300.0	3150.0	2850.0	2580.0
	2070.0	1630.0	1320.0	920.0	630.0	460.0	0.0
G 9	0.0	0.0	0.0	7083.0	6600.0	6050.0	5030.0
	4235.0	3835.0	3550.0	3350.0	3200.0	2900.0	2580.0
	2100.0	1650.0	1330.0	845.0	570.0	385.0	0.0
G 10	0.0	0.0	0.0	7200.0	6700.0	6100.0	5050.0
	4300.0	3900.0	3800.0	3500.0	3300.0	2950.0	2700.0
	1885.0	1520.0	1210.0	770.0	460.0	310.0	0.0
G 11	0.0	0.0	0.0	7600.0	7150.0	6150.0	5240.0
	4400.0	4150.0	3900.0	3700.0	3400.0	3050.0	2800.0
	1755.0	1420.0	920.0	695.0	390.0	235.0	0.0
G 12	0.0	0.0	0.0	8400.0	7350.0	6200.0	5340.0
	4500.0	4350.0	4100.0	3900.0	3500.0	3150.0	2900.0
	1655.0	1220.0	720.0	620.0	330.0	170.0	0.0

G	13	0.0	0.0	0.0	9400.0	7500.0	6250.0	5440.0
		4650.0	4425.0	4200.0	4000.0	3600.0	3230.0	3000.0
		1455.0	1120.0	620.0	545.0	280.0	152.0	0.0
G	14	0.0	0.0	0.0	10100.0	7600.0	6350.0	5740.0
		4800.0	4500.0	4350.0	4200.0	3800.0	3370.0	3200.0
		1255.0	920.0	570.0	470.0	240.0	142.0	0.0

PRESSURE ROW 4

G	1	0.0	0.0	0.0	6320.0	4900.0	3900.7	3000.0
		2250.0	1550.0	1200.0	960.0	860.0	785.0	740.0
		685.0	635.0	560.0	470.0	385.0	300.0	0.0
G	2	0.0	0.0	0.0	6375.0	5063.0	4100.0	3296.0
		2600.0	2300.0	2027.0	1700.0	1500.0	1614.0	1465.0
		1250.0	900.0	700.0	570.0	480.0	450.0	0.0
G	3	0.0	0.0	0.0	6470.0	5200.0	4200.0	3300.0
		2700.0	2500.0	2400.0	2000.0	1800.0	1700.0	1500.0
		1300.0	1000.0	850.0	650.0	575.0	550.0	0.0
G	4	0.0	0.0	0.0	6550.0	5850.0	5000.0	4150.0
		3650.0	3400.0	3200.0	2900.0	2500.0	2100.0	1800.0
		1600.0	1250.0	950.0	820.0	710.0	569.0	0.0
G	5	0.0	0.0	0.0	6600.0	6060.0	5275.0	4475.0
		4075.0	3675.0	3375.0	3175.0	2875.0	2675.0	2375.0
		1800.0	1400.0	1250.0	1000.0	830.0	575.0	0.0
G	6	0.0	0.0	0.0	6850.0	6450.0	5600.0	4800.0
		4150.0	3720.0	3420.0	3220.0	3000.0	2700.0	2400.0
		1950.0	1540.0	1310.0	1060.0	880.0	730.0	0.0
G	7	0.0	0.0	0.0	6950.0	6860.0	5925.0	4925.0
		4160.0	3740.0	3500.0	3250.0	3100.0	2800.0	2560.0
		2070.0	1670.0	1320.0	1070.0	920.0	731.0	0.0
G	8	0.0	0.0	0.0	7025.0	6700.0	6005.0	5005.0
		4205.0	3820.0	3650.0	3350.0	3150.0	2900.0	2600.0
		2090.0	1675.0	1325.0	960.0	635.0	470.0	0.0
G	9	0.0	0.0	0.0	7100.0	6800.0	6060.0	5050.0
		4245.0	3850.0	3720.0	3380.0	3250.0	2950.0	2650.0
		2115.0	1680.0	1350.0	870.0	575.0	395.0	0.0
G	10	0.0	0.0	0.0	7400.0	6900.0	6120.2	5080.0
		4330.0	4000.0	3800.0	3410.0	3350.0	3000.0	2750.0
		1900.0	1525.0	1230.0	795.0	470.0	320.0	0.0
G	11	0.0	0.0	0.0	7800.0	7300.0	6200.0	5280.0
		4500.0	4300.0	4000.0	3950.0	3500.0	3100.0	2900.0
		1770.0	1420.0	930.0	715.0	400.0	245.0	0.0

G 12	0.0	0.0	0.0	8700.0	7500.0	6400.0	5380.0
	4600.0	4475.0	4200.0	4100.0	3600.0	3200.0	3000.0
	1670.0	1230.0	730.0	640.0	340.0	180.0	0.0
G 13	0.0	0.0	0.0	9400.0	7650.0	6500.0	5480.0
	4800.0	4550.0	4300.0	4200.0	3700.0	3260.0	3100.0
	1470.0	1130.0	630.0	565.0	290.0	164.0	0.0
G 14	0.0	0.0	0.0	10100.0	7750.0	6600.0	5780.0
	4900.0	4625.0	4400.0	4300.0	3850.0	3390.0	3200.0
	1270.0	940.0	590.0	500.0	270.0	156.0	0.0

PRESSURE ROW 5

G 1	0.0	0.0	0.0	6370.0	5000.0	3950.0	3050.0
	2300.0	1700.0	1300.0	1050.0	900.0	850.0	800.0
	730.0	645.0	570.0	500.0	410.0	390.0	0.0
G 2	0.0	0.0	0.0	6400.0	5100.0	4150.0	3350.0
	2750.0	2400.0	2100.0	1900.0	1700.0	1600.0	1520.0
	1450.0	1150.0	850.0	600.0	520.0	455.0	0.0
G 3	0.0	0.0	0.0	6520.0	5200.0	4320.0	3600.0
	3100.0	2700.0	2600.0	2300.0	2150.0	2000.0	1800.0
	1600.0	1300.0	950.0	725.0	620.0	560.0	0.0
G 4	0.0	0.0	0.0	6560.0	5900.0	5100.0	4200.0
	3750.0	3450.0	3300.0	3050.0	2650.0	2250.0	1950.0
	1660.0	1450.0	1050.0	900.0	730.0	580.0	0.0
G 5	0.0	0.0	0.0	6620.0	6080.0	5295.0	4495.0
	4090.0	3695.0	3395.0	3195.0	2895.0	2700.0	2500.0
	1870.0	1600.0	1270.0	1060.0	850.0	620.0	0.0
G 6	0.0	0.0	0.0	6700.0	6200.0	5400.0	4600.0
	4200.0	3740.0	3440.0	3240.0	3050.0	2720.0	2550.0
	1970.0	1670.0	1320.0	1160.0	890.0	740.0	0.0
G 7	0.0	0.0	0.0	6975.0	6885.0	5935.0	4935.0
	4170.0	3750.0	3470.0	3260.0	3150.0	2760.0	2580.0
	2090.0	1750.0	1325.0	1180.0	925.0	732.0	0.0
G 8	0.0	0.0	0.0	7030.0	6895.5	6010.0	5010.0
	4210.0	3850.0	3700.0	3375.0	3200.0	2950.0	2650.0
	2110.0	1760.0	1330.0	970.0	650.0	480.0	0.0
G 9	0.0	0.0	0.0	7105.0	6930.0	6070.0	5060.0
	4250.0	3900.0	3750.0	3400.0	3300.0	3000.0	2700.0
	2125.0	1765.0	1340.0	880.0	590.0	410.0	0.0
G 10	0.0	0.0	0.0	7600.0	7100.0	6140.0	5150.0
	4400.0	4100.0	3800.0	3450.0	3350.0	3050.0	2800.0
	1910.0	1600.0	1235.0	810.0	490.0	340.0	0.0
G 11	0.0	0.0	0.0	8100.0	7500.0	6300.0	5350.0

		4600.0	4450.0	4300.0	4000.0	3600.0	3150.0	3000.0
		1785.0	1440.0	940.0	725.0	405.0	255.0	0.0
G	12	0.0	0.0	0.0	9000.0	7700.0	6500.0	5450.0
		4700.0	4600.0	4400.0	4150.0	3700.0	3230.0	3100.0
		1685.0	1240.0	730.0	650.0	360.0	190.0	0.0
G	13	0.0	0.0	0.0	9700.0	7850.0	6600.0	5520.0
		4900.0	4675.0	4450.0	4250.0	3800.0	3280.0	3150.0
		1485.0	1140.0	630.0	575.0	310.0	176.0	0.0
G	14	0.0	0.0	0.0	10500.0	7900.0	6700.0	5820.0
		5000.0	4750.0	4475.0	4350.0	3900.0	3400.0	3250.0
		1285.0	950.0	590.0	510.0	290.0	168.0	0.0
PRESSURE ROW	6							
G	1	0.0	0.0	7600.0	6400.0	5100.0	4100.7	3300.0
		2700.0	2200.0	1800.0	1500.0	1200.0	1100.0	1000.0
		850.0	760.0	590.0	510.0	420.0	400.0	0.0
G	2	0.0	0.0	7800.0	6500.0	5270.0	4200.0	3400.0
		2900.0	2600.0	2350.0	2150.0	1900.0	1800.0	1700.0
		1500.0	1350.0	1000.0	700.0	550.0	470.0	0.0
G	3	0.0	0.0	7900.0	6600.0	5350.0	4350.0	3650.0
		3250.0	2900.0	2700.0	2500.0	2250.0	2050.0	1850.0
		1650.0	1400.0	1100.0	800.0	656.0	578.0	0.0
G	4	0.0	0.0	7950.0	6650.0	5950.0	4950.0	4400.0
		3800.0	3500.0	3400.0	3200.0	2800.0	2600.0	2200.0
		1700.0	1500.0	1300.0	1100.0	750.0	620.0	0.0
G	5	0.0	0.0	6986.0	6620.0	6100.0	5330.0	4530.0
		4120.0	3710.0	3450.0	3210.0	2930.0	2750.0	2600.0
		1950.0	1700.0	1410.0	1200.0	860.0	670.0	0.0
G	6	0.0	0.0	7208.0	6800.0	6300.0	5600.0	4700.0
		4250.0	3800.0	3600.0	3300.0	3100.0	2800.0	2650.0
		2100.0	1800.0	1500.0	1210.0	900.0	690.0	0.0
G	7	0.0	0.0	7460.0	7200.0	6900.0	6200.0	5300.0
		4400.0	3900.0	3700.0	3400.0	3200.0	2900.0	2700.0
		2130.0	1850.0	1550.0	1220.0	930.0	734.0	0.0
G	8	0.0	0.0	7696.0	7250.0	6910.0	6210.0	5320.0
		4405.9	3905.0	3750.0	3520.0	3250.0	3000.0	2750.0
		2128.0	1860.0	1560.0	980.0	660.0	490.0	0.0
G	9	0.0	0.0	8000.0	7500.0	6940.0	6080.0	5330.0
		4410.0	4200.0	3770.0	3600.0	3400.0	3050.0	2800.0
		2126.0	1863.0	1375.0	890.0	610.0	415.0	0.0
G	10	0.0	0.0	8200.0	7800.0	7200.0	6250.0	5335.0
		4600.0	4350.0	4100.0	3700.0	3500.0	3100.0	2900.0

	1915.0	1650.0	1240.0	820.0	510.0	345.0	0.0
G 11	0.0	0.0	9312.0	8500.0	7700.0	6400.0	5500.0
	4700.0	4525.0	4350.0	4200.0	3600.0	3200.0	3100.0
	1785.0	1445.0	950.0	735.0	410.0	265.0	0.0
G 12	0.0	0.0	10026.0	9500.0	7900.0	6600.0	5600.0
	4800.0	4700.0	4400.0	4250.0	3700.0	3260.0	3150.0
	1685.0	1245.0	740.0	660.0	370.0	210.0	0.0
G 13	0.0	0.0	10705.0	10200.0	8100.0	6700.0	5620.0
	5000.0	4800.0	4500.0	4300.0	3850.0	3300.0	3175.0
	1485.0	1145.0	640.0	585.0	330.0	186.0	0.0
G 14	0.0	0.0	12294.0	11000.0	8300.0	6800.0	5920.0
	5200.0	4970.0	4600.0	4400.0	3925.0	3410.0	3260.0
	1285.0	970.0	600.0	520.0	315.0	180.0	0.0

PRESSURE ROW 7

G 1	0.0	0.0	8092.0	6551.0	5400.0	4600.0	3900.0
	3300.0	2800.0	2400.0	2100.0	1750.0	1500.0	1300.0
	1100.0	950.0	800.0	700.0	600.0	500.0	0.0
G 2	0.0	0.0	8195.0	6900.0	5800.0	4900.0	4100.0
	3400.0	2900.0	2600.0	2350.0	2150.0	2000.0	1900.0
	1750.0	1542.0	1204.0	900.0	650.0	530.0	0.0
G 3	0.0	0.0	8271.0	7000.0	6000.0	5200.0	4500.0
	4100.0	3900.0	3700.0	3500.0	3350.0	3200.0	3100.0
	2900.0	2500.0	2000.0	1400.0	1100.0	610.0	0.0
G 4	0.0	0.0	8403.0	7100.0	6170.0	5200.0	4600.0
	4200.0	4000.0	3900.0	3800.0	3750.0	3625.0	3500.0
	3300.0	2800.0	2300.0	1600.0	1200.0	630.0	0.0
G 5	0.0	0.0	8522.0	7200.0	6320.0	5500.0	4900.0
	4500.0	4300.0	4100.0	3900.0	3825.0	3775.0	3725.0
	3600.0	3100.0	2400.0	1800.0	1300.0	700.0	0.0
G 6	0.0	0.0	8738.0	7429.6	6600.0	5800.0	5100.0
	4800.0	4500.0	4300.0	4200.0	4100.0	4050.0	4000.0
	3900.0	3200.0	2500.0	1500.0	1000.0	720.0	0.0
G 7	0.0	0.0	8985.0	8100.0	7100.0	6300.0	5420.0
	5100.0	4700.0	4500.0	4300.0	4200.0	4125.0	4075.8
	3600.0	2272.0	1850.0	1300.0	932.0	732.0	0.0
G 8	0.0	0.0	9217.0	8150.4	7135.4	6350.0	5500.0
	5150.0	4800.0	4700.0	4600.0	4450.0	4250.0	4000.0
	3500.0	1900.0	1700.0	990.0	665.0	495.0	0.0
G 9	0.0	0.0	9647.0	8204.2	7270.0	6400.0	5575.0
	5200.0	5100.0	5000.0	4650.0	4500.0	4300.0	4050.0
	3200.0	1910.0	1380.0	910.0	620.0	420.0	0.0

G	10	0.0	0.0	10049.0	8307.9	7437.3	6410.2	5650.0
		5300.0	5246.0	5100.0	4700.0	4550.0	4350.0	4100.0
		2500.0	1660.0	1245.0	840.0	515.0	350.0	0.0
G	11	0.0	0.0	10798.0	9362.0	7900.0	6700.0	5789.8
		5482.9	5282.2	5120.0	4800.0	4200.0	3800.0	3600.0
		2000.0	1460.0	970.0	750.0	415.0	270.0	0.0
G	12	0.0	0.0	11497.0	10088.0	8135.0	6900.0	5830.0
		5562.1	5300.0	5000.0	4900.0	4100.0	3500.0	3350.0
		1800.0	1250.0	760.0	680.0	380.0	220.0	0.0
G	13	0.0	0.0	12161.0	10778.0	8492.6	7000.0	5870.9
		5700.0	5400.0	4900.0	4500.0	4000.0	3450.0	3300.0
		1700.0	1160.0	680.0	600.0	345.0	196.0	0.0
G	14	0.0	0.0	13716.0	12391.0	9007.4	7300.0	6060.4
		5815.5	5500.0	4800.0	4430.0	3950.0	3420.0	3270.0
		1500.0	1000.0	620.0	550.0	330.0	190.0	0.0

PRESSURE ROW 8

G	1	0.0	8975.0	8100.0	6900.0	5800.0	4900.0	4200.0
		3700.0	3300.0	3050.0	2850.0	2650.0	2450.0	2200.0
		1300.0	1100.0	1050.0	850.0	700.0	550.0	0.0
G	2	0.0	9088.0	8200.0	7050.0	6000.0	5100.0	4400.0
		3800.0	3500.0	3300.0	3200.0	3100.0	3000.0	2850.0
		2600.0	2100.0	1500.0	1151.0	850.0	560.0	0.0
G	3	0.0	9171.0	8300.0	7100.0	6100.0	5200.0	4600.0
		4300.0	4100.0	3900.0	3750.0	3600.0	3550.0	3500.0
		3300.0	3000.0	2400.0	2000.0	1200.0	700.0	0.0
G	4	0.0	9315.0	8320.0	7300.0	6500.0	5700.0	5200.0
		5000.0	4900.0	4800.0	4700.0	4600.0	4400.0	4000.0
		3600.0	3200.0	2800.0	2300.0	1500.0	800.0	0.0
G	5	0.0	9445.0	8600.0	7500.0	6800.0	6200.0	5900.0
		5600.0	5400.0	5300.0	5250.0	5200.0	5150.0	5050.0
		4500.0	4400.0	3600.0	2500.0	1700.0	850.0	0.0
G	6	0.0	9683.0	8700.0	7800.0	6900.0	6500.0	6300.0
		6100.0	5800.0	5900.0	5700.0	5500.0	5300.0	5100.0
		4600.0	4200.0	3400.0	1900.0	1056.0	750.0	0.0
G	7	0.0	9700.0	9100.0	8200.0	7400.0	6700.0	6400.0
		6150.0	6000.0	5700.0	5600.0	5100.0	4700.0	4400.0
		4000.0	3544.0	2100.0	1384.0	934.0	733.0	0.0
G	8	0.0	10207.0	9120.0	8220.0	7500.0	6856.0	6507.2
		6175.0	6050.0	5750.0	5400.0	5150.0	4750.0	4300.0
		3700.0	2081.0	1800.0	1000.0	667.0	500.0	0.0

G 9	0.0	10678.0	9700.0	8300.0	7631.0	6900.0	6570.6
	6225.0	5675.0	5300.0	5200.0	4900.0	4600.0	4200.0
	3400.0	2100.0	1390.0	930.0	622.0	425.0	0.0
G 10	0.0	11119.0	10100.0	8757.0	7858.3	6969.5	6719.0
	6300.0	5637.2	5200.0	5000.0	4560.0	4360.0	4050.0
	2600.0	1550.0	1250.0	860.0	517.0	355.0	0.0
G 11	0.0	11939.0	10893.0	9637.0	8147.9	7083.0	7060.7
	6400.0	5600.0	5120.0	4950.0	4300.0	4000.0	3700.0
	2100.0	1300.0	1000.0	770.0	420.0	275.0	0.0
G 12	0.0	12705.0	11714.0	10459.0	8457.6	7261.5	7069.0
	6450.0	5575.0	5050.0	4910.0	4200.0	3800.0	3400.0
	1900.0	1270.0	900.0	700.0	400.0	230.0	0.0
G 13	0.0	13433.0	12493.0	11239.0	9146.3	7500.0	7084.7
	6475.0	5500.0	4930.0	4600.0	4100.0	3550.0	3310.0
	1800.0	1200.0	730.0	630.0	360.0	206.0	0.0
G 14	0.0	15137.0	14317.0	13065.0	9858.6	8000.0	7100.0
	6500.0	5400.0	4810.0	4500.0	4000.0	3500.0	3260.0
	1600.0	1150.0	650.0	590.0	350.0	200.0	0.0

PRESSURE ROW 9

G 1	9632.0	8569.0	7595.0	6521.0	5581.0	4700.0	4000.0
	3695.0	3250.0	3000.0	2800.0	2600.0	2460.0	2210.0
	1780.0	1300.0	1100.0	900.0	690.0	595.0	0.0
G 2	9749.0	8692.0	7629.0	6550.0	5770.0	5000.0	4320.0
	3820.0	3520.8	3320.0	3230.0	3150.0	3100.0	3050.0
	2900.0	2600.0	2100.0	1500.0	1000.0	600.0	0.0
G 3	9836.0	8784.0	7729.0	6800.0	6000.0	5150.0	4575.0
	4320.0	4150.0	4000.0	3800.0	3800.0	3700.0	3600.0
	3400.0	3100.0	2600.0	2100.0	1400.0	762.0	0.0
G 4	9900.0	9300.0	8350.0	7370.0	6670.0	6000.0	5700.0
	5400.0	5200.0	5100.0	5000.0	4950.0	4900.0	4800.0
	4500.0	3900.0	3300.0	2500.0	1650.0	829.0	0.0
G 5	10124.0	9450.0	8620.0	7520.0	6700.0	6300.0	6200.0
	5800.0	5700.0	5600.0	5500.0	5450.0	5325.0	5200.0
	4900.0	4500.0	3900.0	3000.0	2000.0	900.0	0.0
G 6	10372.0	9700.0	8900.0	8200.0	7800.0	7800.0	7500.0
	7400.0	6900.0	6800.0	6400.0	6000.0	5600.0	5300.0
	4800.0	4400.0	3800.0	2846.0	1600.0	755.0	0.0
G 7	10656.0	9750.0	9150.0	8350.0	7950.0	7700.0	7600.0
	7350.0	7100.0	6790.0	6300.0	5800.0	5400.0	5000.0
	4500.0	3601.0	2549.0	1450.0	935.0	734.0	0.0
G 8	10921.0	9928.0	8971.0	8300.0	8200.0	8100.0	7800.0

	7323.7	7000.0	6745.0	5964.0	5790.0	5300.0	4900.0
	4000.0	2752.0	2000.0	1012.0	670.0	530.0	0.0
G 9	11414.0	10448.0	9536.0	8700.0	8500.0	8150.0	7850.0
	7200.0	6771.0	6400.0	5892.0	5600.0	5000.0	4600.0
	3800.0	2200.0	1500.0	975.0	625.0	460.0	0.0
G 10	11876.0	10934.0	10064.0	9000.0	8700.0	8170.0	7950.0
	7000.0	6156.7	5800.0	5400.0	5000.0	4500.0	4200.0
	2900.0	1800.0	1260.0	880.0	530.0	360.0	0.0
G 11	12735.0	11840.0	11047.0	9832.0	8944.0	8210.6	8100.0
	6770.8	5800.7	5600.0	5240.0	4600.0	4300.0	3850.0
	2450.0	1600.0	1200.0	800.0	425.0	280.0	0.0
G 12	13537.0	12685.0	11964.0	10713.0	9060.0	8251.0	8120.0
	6326.8	5691.6	5200.0	5000.0	4400.0	4100.0	3500.0
	2100.0	1425.0	1100.0	750.0	410.0	240.0	0.0
G 13	14299.0	13489.0	12836.0	11550.0	10000.0	8265.0	8130.0
	5400.0	5300.0	5000.0	4800.0	4200.0	3800.0	3315.0
	1900.0	1400.0	900.0	680.0	380.0	226.0	0.0
G 14	16083.0	15369.0	14876.0	13507.0	10300.0	8300.0	8140.0
	5100.0	5000.0	4850.0	4700.0	4020.0	3700.0	3260.0
	1850.0	1500.0	800.0	650.0	370.0	220.0	0.0

PRESSURE ROW 10

G 1	8858.0	8031.0	7107.0	6000.0	5100.0	4346.0	3930.0
	3740.0	3540.0	3350.0	3170.0	3000.0	2840.0	2650.0
	2350.0	1750.0	1200.0	950.0	700.0	600.0	0.0
G 2	8993.0	8181.0	7258.0	6100.0	5400.0	4800.0	4300.0
	3840.0	3600.0	3400.0	3300.0	3225.0	3175.0	3150.0
	3050.0	2850.0	2450.0	1650.0	1100.0	700.0	0.0
G 3	9093.0	8291.0	7400.0	6420.0	5600.0	5000.0	4500.0
	4330.0	4180.0	4060.0	3960.0	3870.0	3780.0	3690.0
	3500.0	3200.0	2800.0	2200.0	1500.0	800.0	0.0
G 4	9267.0	8400.0	7665.0	7100.0	6500.0	5900.0	5500.0
	5350.0	5250.0	5175.0	5100.0	5025.0	4975.0	4900.0
	4700.0	4300.0	3700.0	2800.0	1700.0	819.0	0.0
G 5	9424.0	8657.0	7841.0	7200.0	6600.0	6300.0	6100.0
	5900.0	5800.0	5700.0	5600.0	5525.0	5475.0	5450.0
	5300.0	4900.0	4100.0	3200.0	1800.0	1000.0	0.0
G 6	9710.0	8973.0	8161.0	7700.0	7600.0	7520.0	7475.0
	7420.0	7000.0	6900.0	6700.0	6400.0	6100.0	5699.0
	5200.0	4600.0	3900.0	2900.0	1750.0	900.0	0.0
G 7	10036.0	9334.0	8527.0	8100.0	7800.0	7500.0	7425.0
	7350.0	7120.0	7000.0	6600.0	6200.0	5700.0	5350.0

	4800.0	3700.0	2850.0	2000.0	1500.0	800.0	0.0
G 8	10341.0	9671.0	8869.0	8500.0	8300.0	8200.0	8000.0
	7300.0	6900.0	6600.0	6300.0	5800.0	5400.0	5100.0
	4200.0	3312.0	2400.0	1875.0	1300.0	640.0	0.0
G 9	10909.0	10299.0	9505.0	8800.0	8700.0	8248.0	8100.0
	7250.0	6700.0	6500.0	6200.0	5400.0	5000.0	4850.0
	3850.0	2523.0	2000.0	1500.0	1000.0	465.0	0.0
G 10	11440.0	10885.0	10099.0	9200.0	9100.0	8300.0	8200.0
	7150.0	6100.0	6000.0	5900.0	5216.0	4792.0	4400.0
	2950.0	2122.0	1650.0	1100.0	800.0	365.0	0.0
G 11	12429.0	11977.0	11206.0	10010.0	9500.0	8333.7	8250.0
	7000.0	5750.0	5600.0	5500.0	4997.0	4400.0	4000.0
	2500.0	2015.0	1400.0	1050.0	600.0	290.0	0.0
G 12	13351.0	12997.0	12239.0	10947.0	10500.0	8419.4	8280.4
	6592.0	5500.0	5300.0	5047.0	4600.0	4100.0	3650.0
	2150.0	1900.0	1375.0	900.0	500.0	250.0	0.0
G 13	14228.0	13966.0	13221.0	11837.0	10800.0	8505.0	8300.0
	5870.0	5283.0	5100.0	4850.0	4300.0	3850.0	3320.0
	2000.0	1910.0	1200.0	850.0	450.0	240.0	0.0
G 14	16281.0	16234.0	15518.0	13919.0	11200.0	8623.0	8310.0
	5246.0	5000.0	4900.0	4730.0	4060.0	3800.0	3270.0
	1875.0	1920.0	1100.0	750.0	425.0	350.0	0.0
PRESSURE ROW 11							
G 1	8083.0	7488.0	6800.0	5800.0	4800.0	4000.0	3500.0
	3250.0	3100.0	3000.0	2900.0	2600.0	2300.0	2000.0
	1400.0	800.0	600.0	400.0	320.0	260.0	0.0
G 2	8250.0	7658.0	6900.0	6000.0	5200.0	4400.0	3900.0
	3600.0	3400.0	3250.0	3125.0	3000.0	2900.0	2875.0
	2600.0	2000.0	1400.0	900.0	600.0	450.0	0.0
G 3	8374.0	7784.0	7000.0	6150.0	5300.0	4800.0	4400.0
	4200.0	4100.0	3950.0	3850.0	3775.0	3725.0	3675.0
	3475.0	2975.0	2275.0	1675.0	1100.0	760.0	0.0
G 4	8589.0	8004.0	7381.0	6700.0	6200.0	5800.0	5460.0
	5250.0	5100.0	4975.0	4875.0	4800.0	4600.0	4300.0
	3800.0	3200.0	2650.0	1800.0	1300.0	800.0	0.0
G 5	8783.0	8202.0	7567.0	6900.0	6500.0	6200.0	5800.0
	5700.0	5600.0	5425.0	5375.0	5200.0	5000.0	4700.0
	4400.0	4000.0	3400.0	2600.0	1700.0	950.0	0.0
G 6	9136.0	8562.0	7906.0	7400.0	7300.0	7200.0	7000.0
	6900.0	6500.0	6100.0	5600.0	5100.0	4600.0	4200.0
	3850.0	3300.0	2800.0	2392.0	1500.0	860.0	0.0

G	7	9539.0	8973.0	8294.0	7700.0	7200.0	6800.0	6600.0
		6568.9	6200.0	5600.0	5100.0	4600.0	4200.0	4000.0
		3400.0	3000.0	2611.0	2100.0	1200.0	775.0	0.0
G	8	9916.0	9357.0	8656.0	7816.0	7700.0	7311.7	6586.0
		5976.0	5838.0	5173.0	4800.0	4295.0	3900.0	3600.0
		3000.0	2400.0	2300.0	1950.0	1000.0	631.0	0.0
G	9	10617.0	10073.0	9330.0	8500.0	7700.0	6800.0	6000.0
		5600.0	5400.0	5100.0	4700.0	4200.0	3600.0	3100.0
		2500.0	1800.0	1644.0	1350.0	800.0	458.0	0.0
G	10	11273.0	10741.0	9959.0	8600.0	7960.9	7569.8	5500.0
		5405.0	5319.0	5000.0	4722.0	4000.0	3400.0	3050.0
		2200.0	1450.0	1346.0	710.0	510.0	290.0	0.0
G	11	12494.0	11986.0	11132.0	8700.0	8227.3	7716.9	5327.0
		5000.0	4996.0	4798.0	4500.0	3800.0	3200.0	2617.0
		1889.0	1200.0	1100.0	550.0	400.0	235.0	0.0
G	12	13633.0	13148.0	12226.0	9215.0	8700.0	7747.0	6216.0
		5120.3	4944.0	4525.0	4180.0	3600.0	3000.0	2300.0
		1527.0	1100.0	900.0	393.0	330.0	200.0	0.0
G	13	14716.0	14252.0	13266.0	9890.0	9100.0	8000.0	6624.0
		5200.0	4586.0	4101.0	3825.0	3500.0	2893.0	2325.0
		1366.0	1150.0	925.0	575.0	350.0	210.0	0.0
G	14	17251.0	16835.0	15698.0	10510.0	9913.0	8833.0	7037.6
		5250.0	4400.0	4000.0	3900.0	3553.0	2969.0	2355.0
		1800.0	1462.0	1000.0	600.0	450.0	325.0	0.0

PRESSURE ROW 12

G	1	7118.0	6752.0	6200.0	5500.0	4700.0	3900.0	3400.0
		3200.0	3050.0	2800.0	2750.0	2250.0	1550.0	1000.0
		700.0	500.0	420.0	325.0	300.0	230.0	0.0
G	2	7306.0	6927.0	6336.0	5700.0	4900.0	4300.0	3850.0
		3550.0	3300.0	3100.0	2950.0	2800.0	2578.0	2100.0
		1600.0	1169.0	800.0	535.0	425.0	375.0	0.0
G	3	7446.0	7057.0	6500.0	5800.0	5000.0	4500.0	4250.0
		4100.0	4000.0	3900.0	3800.0	3600.0	3200.0	2600.0
		2000.0	1450.0	1150.0	900.0	780.0	700.0	0.0
G	4	7688.0	7284.0	6852.0	6391.0	6000.0	5700.0	5500.0
		5200.0	5100.0	4500.0	4600.0	4200.0	3800.0	3400.0
		3000.0	2550.0	2000.0	1400.0	1157.0	750.0	0.0
G	5	7907.0	7487.0	7032.0	6500.0	6150.0	5900.0	5600.0
		5400.0	5200.0	5000.0	4800.0	4600.0	4300.0	3900.0
		3500.0	3172.0	2600.0	1937.0	1531.0	825.0	0.0

G	6	8305.0	7858.0	7361.0	6817.0	6500.0	6200.0	6000.0
		5800.0	5600.0	5400.0	5000.0	4400.0	4000.0	3700.0
		3100.0	2600.0	2100.0	1800.0	1300.0	800.0	0.0
G	7	8759.0	8282.0	7736.0	7131.0	6574.8	6181.1	5814.9
		5500.0	5203.0	4892.0	4350.0	3727.0	3597.0	3400.0
		2866.0	2350.0	2000.0	1650.0	978.0	667.0	0.0
G	8	9184.0	8678.0	8087.0	7425.0	6800.0	6281.0	5758.0
		5296.0	5100.0	4646.0	4057.0	3551.0	3356.0	3000.0
		2598.0	1850.0	1571.0	1400.0	675.0	400.0	0.0
G	9	9975.0	9416.0	8740.0	7556.4	7052.0	6296.4	5100.0
		4800.0	4600.0	4300.0	3896.0	3300.0	3100.0	2700.0
		1966.0	1325.0	992.0	900.0	450.0	325.0	0.0
G	10	10713.0	10104.0	9349.0	7808.0	7305.0	6343.0	4935.0
		4661.3	4323.0	3685.0	3265.0	3179.0	2917.0	2423.0
		1558.0	1023.0	776.0	500.0	330.0	180.0	0.0
G	11	12089.0	11387.0	10485.0	8226.5	7564.8	6558.4	4995.0
		4500.0	3832.0	3199.0	2932.0	2905.0	2521.0	1904.0
		1049.0	521.0	349.0	260.0	200.0	140.0	0.0
G	12	13373.0	12584.0	11544.0	8596.8	7982.4	7060.1	5694.0
		4600.0	3742.0	2929.0	2614.0	2435.0	2085.0	1670.0
		851.0	341.0	255.0	234.0	175.0	110.0	0.0
G	13	14593.0	13721.0	12550.0	9487.0	8696.0	7889.0	6408.0
		4650.0	3470.0	2800.0	2400.0	2350.0	2000.0	1466.0
		846.0	600.0	400.0	300.0	280.0	150.0	0.0
G	14	17447.0	16381.0	14903.0	10262.0	9817.0	8841.0	7042.0
		4700.0	3636.0	2941.0	2570.0	2500.0	2200.0	2143.0
		1700.0	900.0	500.0	450.0	375.0	200.0	0.0

PRESSURE ROW 13

G	1	4731.0	4566.0	4300.0	4000.0	3700.0	3400.0	3250.0
		3150.0	2900.0	2300.0	1781.0	1200.0	900.0	700.0
		600.0	498.0	399.0	300.0	230.0	200.0	0.0
G	2	4930.0	4745.0	4451.0	4100.0	3900.0	3700.0	3600.0
		3500.0	3300.0	3000.0	2800.0	2300.0	1800.0	1500.0
		1200.0	900.0	650.0	455.0	350.0	300.0	0.0
G	3	5078.0	4877.0	4600.0	4450.0	4250.0	4100.0	4050.0
		4025.0	3800.0	3500.0	3100.0	2700.0	2300.0	2000.0
		1600.0	1300.0	1000.0	700.0	500.0	450.0	0.0
G	4	5336.0	5108.0	4866.0	4610.0	4400.0	4300.0	4250.0
		4150.0	3900.0	3550.0	3300.0	3000.0	2700.0	2400.0
		2100.0	1700.0	1400.0	1100.0	900.0	550.0	0.0
G	5	5568.0	5315.0	5046.0	4760.0	4700.0	4651.8	4451.3

		4208.6	3725.0	3600.7	3353.0	3200.0	3164.0	2741.0
		2398.0	1826.0	1617.0	1477.0	1125.0	575.0	0.0
G	6	5600.0	5500.0	5300.0	5100.0	4900.0	4700.0	4500.0
		4300.0	3900.0	3700.0	3100.0	2900.0	2700.0	2400.0
		2200.0	1800.0	1400.0	1100.0	800.0	460.0	0.0
G	7	5800.0	5600.0	5500.0	5451.0	5053.3	4761.9	4463.0
		4125.1	3602.0	3428.0	3177.0	2800.0	2500.0	2135.0
		1683.0	1363.0	875.0	676.0	491.0	284.0	0.0
G	8	6924.0	6200.0	5908.0	5558.0	5099.5	4848.0	4448.2
		4052.0	3713.0	3376.0	3121.0	2600.0	2393.0	1844.0
		1061.0	810.0	595.0	425.0	350.0	310.0	0.0
G	9	7763.0	6900.0	6476.0	5772.0	5382.9	4947.8	4413.0
		3903.0	3581.0	3166.0	2699.0	2000.0	1873.0	1528.0
		871.0	550.0	379.0	320.0	300.0	283.0	0.0
G	10	8547.0	7982.0	6686.0	6400.0	5776.0	5066.0	4385.0
		3851.2	3458.0	2768.0	2178.0	1772.0	1526.0	1227.0
		666.0	386.0	300.0	250.0	230.0	166.0	0.0
G	11	11650.0	9289.0	8298.0	6700.0	6700.0	5473.0	4476.0
		3860.0	3232.0	2374.0	1883.0	1569.0	1385.0	1133.0
		542.0	267.0	223.0	220.0	209.0	168.0	0.0
G	12	12289.0	10508.0	9489.0	7170.0	7134.0	5995.0	4637.0
		3901.6	3110.0	2213.0	1705.0	1447.0	1309.0	1015.0
		454.0	227.0	200.0	200.0	177.0	160.0	0.0
G	13	13179.0	11414.0	10337.0	8300.0	8223.0	7226.0	5831.0
		4035.0	2929.0	2100.0	1658.0	1534.0	1370.0	1200.0
		703.0	450.0	300.0	225.0	177.0	165.0	0.0
G	14	14766.0	13009.0	11908.0	8703.0	8615.0	7704.0	6241.0
		4273.7	3561.0	2500.0	2391.0	2296.0	2100.0	2000.0
		1650.0	758.0	450.0	425.0	300.0	205.0	0.0

PRESSURE ROW 14

G	1	3308.0	3249.0	3187.0	3117.0	3103.0	3046.0	2987.0
		2830.0	2206.0	1731.0	1395.0	1100.0	850.0	650.0
		500.0	420.0	360.0	300.0	240.0	180.0	0.0
G	2	3434.0	3363.0	3287.0	3204.0	3176.0	3087.0	2997.0
		2908.0	2700.0	2200.0	1999.0	1700.0	1500.0	1300.0
		1050.0	800.0	600.0	400.0	300.0	262.0	0.0
G	3	3528.0	3446.0	3361.0	3269.0	3200.0	3100.0	3000.0
		2950.0	2557.0	2400.0	2000.0	1800.0	1600.0	1400.0
		1200.0	1000.0	800.0	600.0	450.0	375.0	0.0
G	4	3690.0	3592.0	3490.0	3381.0	3250.0	3150.0	3010.0
		2960.0	2585.0	2500.0	2266.0	2053.0	1900.0	1700.0

G	6	8305.0	7858.0	7361.0	6817.0	6500.0	6200.0	6000.0
		5800.0	5600.0	5400.0	5000.0	4400.0	4000.0	3700.0
		3100.0	2600.0	2100.0	1800.0	1300.0	800.0	0.0
G	7	8759.0	8282.0	7736.0	7131.0	6574.8	6181.1	5814.9
		5500.0	5203.0	4892.0	4350.0	3727.0	3597.0	3400.0
		2866.0	2350.0	2000.0	1650.0	978.0	667.0	0.0
G	8	9184.0	8678.0	8087.0	7425.0	6600.0	6281.0	5758.0
		5296.0	5100.0	4646.0	4057.0	3551.0	3356.0	3000.0
		2598.0	1850.0	1571.0	1400.0	675.0	400.0	0.0
G	9	9975.0	9416.0	8740.0	7556.4	7052.0	6296.4	5100.0
		4800.0	4600.0	4300.0	3896.0	3300.0	3100.0	2700.0
		1966.0	1325.0	992.0	900.0	450.0	325.0	0.0
G	10	10713.0	10104.0	9349.0	7808.0	7305.0	6343.0	4935.0
		4661.3	4323.0	3685.0	3265.0	3179.0	2917.0	2423.0
		1558.0	1023.0	776.0	500.0	330.0	180.0	0.0
G	11	12089.0	11387.0	10485.0	8226.5	7564.8	6558.4	4995.0
		4500.0	3832.0	3199.0	2932.0	2905.0	2521.0	1904.0
		1049.0	521.0	349.0	260.0	200.0	140.0	0.0
G	12	13373.0	12584.0	11544.0	8596.8	7982.4	7060.1	5694.0
		4600.0	3742.0	2929.0	2614.0	2435.0	2085.0	1670.0
		851.0	341.0	255.0	234.0	175.0	110.0	0.0
G	13	14593.0	13721.0	12550.0	9487.0	8696.0	7889.0	6408.0
		4650.0	3470.0	2800.0	2400.0	2350.0	2000.0	1466.0
		846.0	600.0	400.0	300.0	280.0	150.0	0.0
G	14	17447.0	16381.0	14903.0	10262.0	9817.0	8841.0	7042.0
		4700.0	3636.0	2941.0	2570.0	2500.0	2200.0	2143.0
		1700.0	900.0	500.0	450.0	375.0	200.0	0.0
PRESSURE ROW 13								
G	1	4731.0	4566.0	4300.0	4000.0	3700.0	3400.0	3250.0
		3150.0	2900.0	2300.0	1781.0	1200.0	900.0	700.0
		600.0	498.0	399.0	300.0	230.0	200.0	0.0
G	2	4930.0	4745.0	4451.0	4100.0	3900.0	3700.0	3600.0
		3500.0	3300.0	3000.0	2800.0	2300.0	1800.0	1500.0
		1200.0	900.0	650.0	455.0	350.0	300.0	0.0
G	3	5078.0	4877.0	4600.0	4450.0	4250.0	4100.0	4050.0
		4025.0	3800.0	3500.0	3100.0	2700.0	2300.0	2000.0
		1600.0	1300.0	1000.0	700.0	500.0	450.0	0.0
G	4	5336.0	5108.0	4866.0	4610.0	4400.0	4300.0	4250.0
		4150.0	3900.0	3550.0	3300.0	3000.0	2700.0	2400.0
		2100.0	1700.0	1400.0	1100.0	900.0	550.0	0.0
G	5	5568.0	5315.0	5046.0	4760.0	4700.0	4651.8	4451.3

		4208.6	3725.0	3600.7	3353.0	3200.0	3164.0	2741.0
		2398.0	1826.0	1617.0	1477.0	1125.0	575.0	0.0
G	6	5600.0	5500.0	5300.0	5100.0	4900.0	4700.0	4500.0
		4300.0	3900.0	3700.0	3100.0	2900.0	2700.0	2400.0
		2200.0	1800.0	1400.0	1100.0	800.0	460.0	0.0
G	7	5800.0	5600.0	5500.0	5451.0	5053.3	4761.9	4463.0
		4125.1	3602.0	3428.0	3177.0	2800.0	2500.0	2135.0
		1683.0	1363.0	875.0	676.0	491.0	284.0	0.0
G	8	6924.0	6200.0	5908.0	5558.0	5099.5	4848.0	4448.2
		4052.0	3713.0	3376.0	3121.0	2600.0	2393.0	1844.0
		1061.0	810.0	595.0	425.0	350.0	310.0	0.0
G	9	7763.0	6900.0	6476.0	5772.0	5382.9	4947.8	4413.0
		3903.0	3581.0	3166.0	2699.0	2000.0	1873.0	1528.0
		871.0	550.0	379.0	320.0	300.0	283.0	0.0
G	10	8547.0	7982.0	6686.0	6400.0	5776.0	5066.0	4385.0
		3851.2	3458.0	2768.0	2178.0	1772.0	1526.0	1227.0
		666.0	386.0	300.0	250.0	230.0	166.0	0.0
G	11	11650.0	9289.0	8298.0	6700.0	6700.0	5473.0	4476.0
		3860.0	3232.0	2374.0	1883.0	1569.0	1385.0	1133.0
		542.0	267.0	223.0	220.0	209.0	168.0	0.0
G	12	12289.0	10508.0	9489.0	7170.0	7134.0	5995.0	4637.0
		3901.6	3110.0	2213.0	1705.0	1447.0	1309.0	1015.0
		454.0	227.0	200.0	200.0	177.0	160.0	0.0
G	13	13179.0	11414.0	10337.0	8300.0	8223.0	7226.0	5831.0
		4035.0	2929.0	2100.0	1658.0	1534.0	1370.0	1200.0
		703.0	450.0	300.0	225.0	177.0	165.0	0.0
G	14	14766.0	13009.0	11908.0	8703.0	8615.0	7704.0	6241.0
		4273.7	3561.0	2500.0	2391.0	2296.0	2100.0	2000.0
		1650.0	758.0	450.0	425.0	300.0	205.0	0.0

PRESSURE ROW 14

G	1	3308.0	3249.0	3187.0	3117.0	3103.0	3046.0	2987.0
		2830.0	2206.0	1731.0	1395.0	1100.0	850.0	650.0
		500.0	420.0	360.0	300.0	240.0	180.0	0.0
G	2	3434.0	3363.0	3287.0	3204.0	3176.0	3087.0	2997.0
		2908.0	2700.0	2200.0	1999.0	1700.0	1500.0	1300.0
		1050.0	800.0	600.0	400.0	300.0	262.0	0.0
G	3	3528.0	3446.0	3361.0	3269.0	3200.0	3100.0	3000.0
		2950.0	2557.0	2400.0	2000.0	1800.0	1600.0	1400.0
		1200.0	1000.0	800.0	600.0	450.0	375.0	0.0
G	4	3690.0	3592.0	3490.0	3381.0	3250.0	3150.0	3010.0
		2960.0	2585.0	2500.0	2266.0	2053.0	1900.0	1700.0

		1500.0	1300.0	1000.0	600.0	500.0	450.0	0.0
G	5	3837.0	3724.0	3606.0	3482.0	3300.0	3203.0	3025.0
		2970.0	2600.0	2560.0	2478.0	2201.0	2095.0	1800.0
		1488.0	1112.0	816.0	600.0	375.0	300.0	0.0
G	6	3838.0	3750.0	3700.0	3569.0	3377.0	3209.0	3035.0
		3000.0	2900.0	2500.0	2100.0	1700.0	1600.0	1400.0
		1000.0	800.0	600.0	450.0	300.0	178.0	0.0
G	7	3839.0	3811.4	3789.0	3687.9	3399.0	3200.0	3050.0
		2800.0	2700.0	2300.0	1800.0	1441.0	1300.0	1168.0
		769.0	517.0	400.0	400.0	210.0	175.0	0.0
G	8	3992.7	3908.7	3827.0	3715.3	3421.0	3227.5	3040.0
		2620.7	2183.0	1806.0	1466.0	1130.0	1000.0	930.0
		425.0	263.0	242.0	225.0	200.0	170.0	0.0
G	9	4300.0	4100.0	3947.0	3770.0	3465.0	3246.0	3062.0
		2630.0	2103.0	1549.0	1264.0	1032.0	850.0	644.0
		335.0	220.0	196.0	190.0	180.0	167.0	0.0
G	10	5530.0	5091.0	4433.0	4180.0	3670.0	3244.0	2715.0
		2697.5	2104.0	1673.0	1272.0	950.0	718.0	529.0
		299.0	222.0	192.0	190.0	175.0	164.0	0.0
G	11	6904.0	5218.0	5163.0	4629.0	4236.0	3578.0	2967.0
		2726.0	2288.0	1722.0	1299.0	1017.0	869.0	634.0
		431.0	286.0	220.0	210.0	185.0	162.0	0.0
G	12	7402.0	6681.0	6015.4	4734.0	4581.0	3906.0	3200.0
		2953.0	2525.0	1906.0	1476.0	1134.0	1000.0	732.0
		514.0	324.0	260.0	225.0	200.0	180.0	0.0
G	13	8573.0	7329.0	6303.0	5703.0	5380.8	5158.0	4356.0
		3567.0	2841.0	2050.0	1802.0	1377.0	1240.0	1103.0
		790.0	620.0	450.0	350.0	225.0	200.0	0.0
G	14	10140.0	9040.0	7881.0	6401.0	6089.0	5567.0	4749.0
		4406.0	3800.0	2600.0	2441.0	2109.0	1900.0	1800.0
		1562.0	1000.0	620.0	400.0	265.0	220.0	0.0

PRESSURE ROW 15

G	1	1211.0	1204.0	1202.0	1198.0	1107.0	1087.0	1066.0
		1000.0	907.0	791.0	692.0	607.0	533.0	467.0
		357.0	269.0	200.0	150.0	100.0	50.0	0.0
G	2	1300.0	1300.0	1294.0	1286.0	1133.0	1101.0	1069.0
		1030.0	922.0	813.0	762.0	687.0	642.0	598.0
		544.0	358.0	295.0	199.0	170.0	146.0	0.0
G	3	1400.0	1400.0	1362.0	1351.0	1191.0	1106.0	1070.0
		1040.0	927.0	820.0	785.0	713.0	678.0	642.0
		606.0	421.0	365.0	250.0	185.0	150.0	0.0

G	4	1550.0	1500.0	1500.0	1465.0	1344.0	1271.0	1070.0
		1050.0	930.0	850.0	800.0	760.0	720.0	675.0
		679.0	676.0	675.0	425.0	323.0	300.0	0.0
G	5	1600.0	1600.0	1587.0	1500.0	1400.0	1300.0	1150.0
		1079.5	940.0	900.0	850.0	800.0	760.0	700.0
		789.0	657.0	456.0	440.0	183.0	180.0	0.0
G	6	1665.0	1649.0	1640.0	1550.0	1458.3	1330.5	1194.4
		1155.3	950.0	910.0	870.0	810.0	780.0	725.0
		430.0	325.0	250.0	172.0	150.0	140.0	0.0
G	7	1838.0	1819.0	1740.0	1612.0	1531.3	1377.8	1250.0
		1204.7	960.0	920.0	900.0	830.0	800.0	750.0
		400.0	328.0	170.0	150.0	120.0	110.0	0.0
G	8	2058.7	1962.3	1826.5	1675.0	1604.0	1400.0	1317.7
		1254.0	980.0	925.0	905.0	850.0	820.0	770.0
		387.0	254.0	140.0	140.0	105.0	98.0	0.0
G	9	2500.0	2249.0	1997.0	1800.0	1750.0	1712.0	1399.0
		1261.0	1054.0	930.0	910.0	870.0	840.0	790.0
		375.0	250.0	131.0	130.0	103.0	97.0	0.0
G	10	3261.0	2878.0	2458.0	2098.0	1904.5	1753.5	1500.0
		1498.0	1420.0	1100.0	950.0	900.0	860.0	810.0
		568.0	388.0	160.0	110.0	100.0	99.0	0.0
G	11	3939.0	3176.0	3017.0	2671.0	2233.0	2000.0	1958.0
		1900.0	1716.0	1598.0	1200.0	1000.0	900.0	840.0
		780.0	505.0	189.0	120.0	110.0	107.0	0.0
G	12	4365.0	4000.0	3891.0	2939.0	2576.0	2300.0	2250.0
		2235.0	1960.0	1854.0	1500.0	1100.0	1000.0	900.0
		900.0	622.6	210.0	150.0	168.0	143.0	0.0
G	13	4041.0	4000.0	3881.0	3732.0	3215.0	2875.0	2580.0
		2357.0	2150.0	2015.0	1745.0	1300.0	1200.0	1000.0
		965.0	740.2	500.0	230.0	210.0	204.0	0.0
G	14	5101.0	5017.0	4900.0	3849.0	3300.0	3228.0	3200.0
		3200.0	3185.0	2594.0	2400.0	1500.0	1400.0	1200.0
		1486.0	1034.0	750.0	325.0	250.0	240.0	0.0

Appendix C

Program for Predicting The Non-aqueous CHF Data by Groeneveld's Table Look-up Method

This chapter includes only one program which can predict the non-aqueous CHF data by interpolation or extrapolation from the given conditions. While the CHF data to be read by this program is the same as shown in Fig. B.2.

```
      SUBROUTINE CALCHF(P,G,D,X,CHF,NFLG)
C*********************************************************************
C                                                                    *
C     Subroutine CALCHF                                              *
C                                                                    *
C     This subroutine is used to obtain the CHF from table of discrete *
C     values.  The table was presented by Groeneveld et al..         *
C                                                                    *
C*********************************************************************

C*********************************************************************
C                                                                    *
C     Variable declaration:                                          *
C                                                                    *
C     Character:                                                     *
C     GEOM    : a single character variable for channel geometry.    *
C     UNIT    : a single character variable for unit.                *
C     FLUID   : a single character variable for fluid type.          *
C     ORIENT  : a single character variable for channel orientation. *
C     STATE   : a single character variable for state of the system. *
C                                                                    *
C     Real:                                                          *
C     X       : provided quality.                                    *
C     D       : provided diameter.                                   *
C     G       : provided mass flux.                                  *
C     P       : provided pressure.                                   *
C     INTRP3  : the interpolated value.                              *
C     PX      : discrete value of quality.                           *
C     PG      : discrete value of mass flux.                         *
C     PP      : discrete value of pressure.                          *
C     CHFTAB  : a set of 4410 discrete values of CHF arranged in three-*
C               dimensional arrays.                                  *
C                                                                    *
C     Logical:                                                       *
C     NFLG    : Program termination flag.                            *
C     Flag    : Step termination flag.                               *
C                                                                    *
C*********************************************************************

      CHARACTER UNIT,GEOM,FLUID,ORIENT
      REAL PX(21),PG(14),PP(15),INTRP3,LAT
      LOGICAL FLAG,NFLG
      COMMON/CHOICE/UNIT,GEOM,FLUID,ORIENT
      COMMON/PROP/   VF,   VG,   VL,  RHOF,  RHOG,  RHOL,
     +               HF,   HG,   HL,  CPF,   CPG,   CPL,
     +               UF,   UG,   UL,  AKF,   AKG,   AKL,
     +               PRF,  PRG,  PRL, HFG,   PSAT,  TSAT,
     +                 SIGMA
      COMMON/CRIT/   TC,   PC,   VC,  W, WEIGH,  CO1,
     +               CO2,  CO3,  CO4,  BO,   TO,  TREF
      COMMON/ROWS/PX,PG,PP,IX,IG,IP

      NFLG = .FALSE.
      DEN = RHOF/RHOG
```

Figure C.1: Program for the non-aqueous CHF prediction by Groeneveld's table look-up method

```
C*********************************************************************
C                                                                    *
C     Calculate the equivalent pressure of water & Psi_k for         *
C     non-aqueous fluid                                              *
C                                                                    *
C*********************************************************************
      IF ((DEN .GE. 1.39) .AND. (DEN .LE. 10.75)) THEN
         TRY = -0.95*(ALOG10(DEN))**2.51
      IF (TRY .GE. 87.) THEN
         TRY = 86.99
      ELSE IF (TRY .LE. -87) THEN
         TRY = -86.99
      END IF
      PW = 17393.*EXP(TRY)+4792.8
      ELSE IF ((DEN .GT. 10.75) .AND. (DEN .LE. 84.6)) THEN
         TRY = -0.82*(ALOG10(DEN))**1.84
      IF (TRY .GE. 87.) THEN
         TRY = 86.99
      ELSE IF (TRY .LE. -87) THEN
         TRY = -86.99
      END IF
      PW = 25320.*EXP(TRY)+370.22
      ELSE IF ((DEN .GT. 84.6) .AND. (DEN .LE. 1624.5)) THEN
         TRY = -1.4*(ALOG10(DEN))**1.3
      IF (TRY .GE. 87.) THEN
         TRY = 86.99
      ELSE IF (TRY .LE. -87) THEN
         TRY = -86.99
      END IF
      PW = 53003.*EXP(TRY)+8.468
      ELSE
      NFLG = .TRUE.
      RETURN
      END IF
      PSI = G*0.008**0.5/SIGMA**0.5/RHOF**0.5
      PS = PW/22100
      IF ((PW .GE. 100) .AND. (PW .LE. 2000.)) THEN
        FUN = 7.7 - 59.6*PS + 693*PS**2 - 3449.3*PS**3
      ELSE IF ((PW .GT. 2000.) .AND. (PW .LE. 20500)) THEN
        FUN = 6.646 - 15.86*PS + 32.26*PS**2 - 51.45*PS**3
     +       + 44.23*PS**4 - 15.67*PS**5
      ELSE IF ((PW .GT. 20500.) .AND. (PW .LE. 21900)) THEN
        FUN = -32.4 + 75.63*PS - 43.167*PS**2
      ELSE
      NFLG = .TRUE.
      RETURN
      END IF
      GW = PSI*FUN/0.008**0.5
C*********************************************************************
C                                                                    *
C     Initialize the flag and range pointer.                         *
C                                                                    *
C*********************************************************************
```

```
      FLAG = .TRUE.
      IX = 20
      IG = 13
      IP = 14
C**********************************************************************
C                                                                     *
C     Locate the discrete value of quality bounding the input value.  *
C                                                                     *
C**********************************************************************
      DO 100 I=1,20
      IF((X .LE. PX(I+1)) .AND. FLAG)THEN
        IX = I
        FLAG = .FALSE.
      END IF
 100  CONTINUE
C**********************************************************************
C                                                                     *
C     Re-initialize the flag.                                         *
C     Locate the discrete value of mass flux bounding the input value. *
C                                                                     *
C**********************************************************************
      FLAG = .TRUE.
      DO 200 I=1,13
        IF((GW .LE. PG(I+1)) .AND. FLAG)THEN
          IG = I
          FLAG = .FALSE.
      END IF
 200  CONTINUE
C**********************************************************************
C                                                                     *
C     Re-initialize the flag.                                         *
C     Locate the discrete value of pressure bounding the input value. *
C                                                                     *
C**********************************************************************
      FLAG = .TRUE.
      DO 300 I=1,14
       IF((PW .LE. PP(I+1)) .AND. FLAG)THEN
         IP = I
         FLAG = .FALSE.
       END IF
 300  CONTINUE
C**********************************************************************
C                                                                     *
C     Calculate modification factor for tube diameter other than 0.008.*
C                                                                     *
C**********************************************************************
      IF(D .GT. 0.016)THEN
        CK1 = 0.7937
      ELSE IF(D .LT. 0.002)THEN
        CK1 = 1.5874
      ELSE
        CK1 = (0.008/D)**(1./3)
      END IF
      QC = INTRP3(X,GW,PW)*CK1*1000
      IF ((PW .GE. 100.) .AND. (PW .LE. 8000.)) THEN
```

```
    LAT = 2214181. - 4627523.*PS + 13275135.*PS**2-17924341.*PS**3
   ELSE IF ((PW .GT. 8000.) .AND. (PW .LE. 21000.)) THEN
     LAT = 3102130. - 11492443.*PS+34371536.*PS**2-57226128.*PS**3
  +       + 47189435.*PS**4 - 15650016.*PS**5
   ELSE IF ((PW .GT. 21000.) .AND. (PW .LE. 21900)) THEN
     LAT = -84338385. + 179793761.*PS - 95310141.*PS**2
   ELSE
   NFLG = .TRUE.
   RETURN
   END IF
   CHF = QC/GW/LAT*G*HFG
   RETURN
   END
   REAL FUNCTION INTRP3(X,G,P)
C***********************************************************************
C                                                                      *
C     Function INTRP3                                                  *
C                                                                      *
C     This function is used to set up the parameters for linear        *
C     interpolation in CHF evaluation.  The parameters are the slope,  *
C     and two boundary points.                                         *
C                                                                      *
C***********************************************************************

C***********************************************************************
C                                                                      *
C     Variable declaration:                                            *
C                                                                      *
C     Real:                                                            *
C     X        : provided quality.                                     *
C     G        : provided mass flux.                                   *
C     P        : provided pressure.                                    *
C     INTERP   : the interpolated value.                               *
C     PX       : discrete value of quality.                            *
C     PG       : discrete value of mass flux.                          *
C     PP       : discrete value of pressure.                           *
C     CHFTAB   : a set of 4410 discrete value of CHF arranged in three- *
C                dimensional arrays.                                   *
C                                                                      *
C***********************************************************************

      REAL INTERP,CHFTAB(21,14,15),PX(21),PG(14),PP(15)

C***********************************************************************
C                                                                      *
C     Call up two common blocks to pass some variables in and out the  *
C     subroutine.                                                      *
C                                                                      *
C***********************************************************************

      COMMON/TABLE/CHFTAB
      COMMON/ROWS/PX,PG,PP,IX,IG,IP

C***********************************************************************
```

```
C                                                                       *
C     Linear interpolate the pressure value.                            *
C                                                                       *
C************************************************************************

      PARAM = (P-PP(IP))/(PP(IP+1)-PP(IP))
      C1    = INTERP(CHFTAB(IX,IG,IP),CHFTAB(IX,IG,IP+1),PARAM)
      C2    = INTERP(CHFTAB(IX,IG+1,IP),CHFTAB(IX,IG+1,IP+1),PARAM)
      C3    = INTERP(CHFTAB(IX+1,IG,IP),CHFTAB(IX+1,IG,IP+1),PARAM)
      C4    = INTERP(CHFTAB(IX+1,IG+1,IP),CHFTAB(IX+1,IG+1,IP+1),PARAM)

C************************************************************************
C                                                                       *
C     Linear interpolate the mass flux value.                           *
C                                                                       *
C************************************************************************

      PARAM = (G-PG(IG))/(PG(IG+1)-PG(IG))
      C5    = INTERP(C1,C2,PARAM)
      C6    = INTERP(C3,C4,PARAM)

C************************************************************************
C                                                                       *
C     Linear interpolate the quality value.                             *
C                                                                       *
C************************************************************************

      PARAM = (X-PX(IX))/(PX(IX+1)-PX(IX))
      INTRP3 = INTERP(C5,C6,PARAM)
      RETURN
      END
      REAL FUNCTION INTERP(A1,A2,P)

C************************************************************************
C                                                                       *
C     Function INTERP                                                   *
C                                                                       *
C     This function is used to interpolate value linearly.              *
C     It requires the slope of the function and two boundary points.    *
C                                                                       *
C************************************************************************

C************************************************************************
C                                                                       *
C     Variable declaration:                                             *
C                                                                       *
C     Real:                                                             *
C     INTERP  : the interpolated value.                                 *
C     P       : slope of the function.                                  *
C     A1,A2   : the two bounds.                                         *
C                                                                       *
C************************************************************************

      INTERP = A1 + (A2-A1)*P
      RETURN
```

```
      END
                    SUBROUTINE READCHF
C******************************************************************
C                                                                 *
C     READ CHF DATA FROM CHFDA2.DATA                              *
C                                                                 *
C******************************************************************
      IMPLICIT REAL (A-H,O-Z)
      DIMENSION CHF(15,14,21),CHFTAB(21,14,15)
      COMMON/TABLE/CHFTAB

      OPEN(UNIT=1,FILE='CHFDA2 DATA')
      DO 1 I=1,15
         READ(1,4) K
 4       FORMAT(/,I1)
         DO 2 J=1,14
            READ(1,3) (CHF(I,J,K),K=1,21)
 3          FORMAT(3(T10,7F9.1,/))
 2       CONTINUE
 1    CONTINUE
      DO 100 I=1,15
         DO 200 J=1,14
            DO 300 K=1,21
               CHFTAB(K,J,I)=CHF(I,J,K)
 300        CONTINUE
 200     CONTINUE
 100  CONTINUE
      CLOSE(1)
      RETURN
      END
      BLOCK DATA TBCHF1
      REAL PX(21),PG(14),PP(15)
      COMMON/ROWS/PX,PG,PP,IX,IG,IP
      DATA PX/-.5,-.4,-.3,-.2,-.15,-.1,-.05,0.,.05,.1,.15,.2,.25,
     +       .3,.4,.5,.6,.7,.8,.9,1./
      DATA PG/0.,50.,100.,200.,300.,500.,750.,1000.,1500.,2000.,
     +       3000.,4000.,5000.,7500./
      DATA PP/100.,150.,200.,300.,450.,700.,1000.,1500.,2000.,
     +       3000.,4500.,7000.,10000.,15000.,20000./
      END
```